The interaction of *Salmonella* Typhimurium with host derived lipids

by

Jessica Louise Rooke

A thesis submitted to the University of Birmingham and the University of Melbourne for the jointly awarded degree of

DOCTOR OF PHILOSOPHY

Department of Microbiology & Immunology
The Peter Doherty Institute
University of Melbourne

Institute of Microbiology & Infection
College of Medical & Dental sciences
University of Birmingham

September 2018

Abstract

Autotransporters are some of the most abundantly secreted proteins in Gram-negative bacteria. Many of these proteins function as virulence factors. *S. enterica* serovar Typhimurium has five autotransporter proteins: SadA; ApeE; MisL; YaiU; and ShdA. Here, the outer membrane biogenesis and virulence properties of the *S.* Typhimurium autotransporters have been investigated. The outer membrane biogenesis of the multimeric autotransporter SadA was shown to be dependent upon BamA and BamD, which are essential components of the β-barrel assembly machinery complex, but the non-essential components, BamB, C and E, are not required. Contrary to a report in the literature, the translocation assembly module complex is also not required for SadA secretion.

ApeE is a classical autotransporter that has a GDSL lipase motif. ApeE was shown to have phospholipase B activity, with the ability to cleave acyl chains of phospholipids. The phospholipase activity of ApeE was inhibited by the serine lipase inhibitor methyl arachidonyl fluorophosphonate. Using an *in vivo* murine infection model, bacterial survival at 21 days post-infection in gallbladders of mice, and efficient faecal shedding, required a functional ApeE protein. ApeE was also required for *S*. Typhimurium to utilise lyso-phosphatidylcholine as a sole carbon source for growth. It is proposed that *Salmonella* survival in the mouse gallbladder depends on the ability of ApeE to hydrolyse bile phospholipids for use as a nutrient source *in vivo*.

Acknowledgements

First, I would like to thank my supervisor Professor Ian Henderson for all his help and guidance throughout these last 6 years, from undergraduate placement all the way through to the end of my PhD. I am looking forward to the new adventure in Brisbane with you and the Henderson lab! I would also like to thank Professor Jeffrey Cole for all his advice and guidance on writing, presentations and experiments. I don't think I will ever forget the difference between "may and might". I would also like to thank my University of Melbourne supervisor Professor Dick Strugnell. I am very grateful for my time in Melbourne, both experimentally and personally, and I thank you for all of your help. I would like to thank Professor Dan Slade for hosting me at Virginia Tech for a month, and teaching me how to become an enzyme Biochemist. Thank you for making me feel so welcome, for days out to go hiking and bouldering and for helpful scientific suggestions. I would like to Dr Amanda Rossiter, my mini boss for all of her help with the project and also Bio21 for all of the lipidomics analysis and to Dr Alan McNally for the phylogenetic analysis.

To Chris Icke and Emily Goodall, thank you for all of the fantastic times we have had over the last 3-4 years. To Chris for all of the out of tune singing, terrible jokes and general foolishness, I want to thank you for being an awesome friend (and housemate) and excellent colleague. To Emily, thank you for frequently housing me, for the time we stayed up late writing thesis with cups of tea and a fish finger sandwich! Thank you both, I can't wait for the new adventure in Brisbane! I'd also like to thank the rest of the Sweden crew (Charles Moore-Kelly and Richard Meek) for always being up for cake, pints and for providing joy, even during the most stressful times. I would like to say a huge thank you to Jack Bryant and Tamar Cranford-Smith for pushing me to go spinning, even on days when I didn't feel like it. Especially to Jack, who is always up for a coffee break. Thank you for all of your suggestion in the lab, for teaching me how to do TLCs and for generally being indispensable to the Henderson lab. I would also like to thank Georgia Isom, another long standing member of the grease crew, former housemate and long-time bestie. Thank you for all of your support scientifically (protein clustering analysis), and with my personal life, throughout all of these years that I have known you. Thank you to Irene Beriotto (and Georgia) for all of our trips over the years, and for being incredible friends. Both of you, and the original members of the magic rainbow 5, truly made the first years of my time in the Henderson lab unforgettable.

Finally, I would like to thank my Partner Karthik Pullela, who has supported me through this process from the opposite side of the world. Thank you for all of your patience, and kind words at the end of a very stressful day. I'd like to thank my family for their continued love and support. To Mom, Kev, Joe and Kate, thank you for all of the cups of tea (Kev), for the cupcakes (Kate), for sharing you "man cave" (Joe) and for gin (Mom). Thank you to Nan and Grandad for all of your support over the years (and for the recent trip to Spain!) I would also like to thank my Dad and Shirley for the many carveries that have sustained me over these few years.

Table of contents

List of Figures

List of Tables

List of Appendices

List of abbreviations

Abbreviation	Full name
4-mu	4-methylumbelliferone
4-muB	4-methylumbelliferyl butyrate
4-muH	4-methylumbelliferyl heptanoate
4-muO	4-methylumbelliferyl octanoate
4-muP	4-methylumbelliferyl palmitate
Acyl-CoA	Acyl co-enzyme A
AP	Alkaline phosphatase
APS	Ammonium persulphate
ATP	Adenosine triphosphate
Bam	β-barrel assembly machinery
BLAST	Basic local alignment sequencing tool
BSA	Bovine serum albumin
CAA	Casamino acids
CE	Cholesterol ester
CER	Ceramide
CIP	Calf intestinal phosphatase
CFU	Colony forming units
CGAT	Cholesterol: glycerophospholipid acyl transferase
CL	Cardiolipin
DG	Diacylglycerol
DIC	Differential interference contrast
DMSO	Dimethylsulfoxide
DOPC	Dioleoylphosphatidylcholine
DOPG	Dioleoylphosphatidylglycerol
ECL	Enhanced chemiluminescence
ECM	Extracellular matrix molecules
Fad	Fatty acid degradation
FP	Fluorophosphonate
GM1	Ganglioside 1
GM3	Ganglioside 3
GPC	Glycerophosphocholine
Hex1Cer	Hexosylceramide
HRP	Horse radish peroxidase
I.P	Intra-peritoneal
IFN-γ	Interferon γ
IL-18	Interleukin-18
IL-1β	Interleukin-1β
IL-8	Interleukin-8
indel	Insertion/deletion
iNTS	Invasive non-typhoidal *Salmonella*
IPTG	Isopropyl β-D-1-thiogalactopyranoside
LB	Lysogeny broth
LCFA	Long chain fatty acid
LCMS	Liquid chromatography mass spectrometry

LEE	Locus of Enterocyte Effacement
LPC	Lyso phosphatidylcholine
LPE	Lyso phosphatidylethanolamine
LPI	Lyso phosphatidylinositol
LPS	Lipopolysaccharide
Lyso-PC	Lyso phosphatidylcholine
Lyso-PG	Lyso phosphatidylglycerol
MAFP	Methyl arachidonyl fluorophosphonate
MHC-II	Major histocompatibility complex II
MOI	Multiplicity of infection
MOPS	3-(N-morpholino)propanesulfonic acid
NBP-BCIP	5-bromo-4-chloro-3'-indolyphosphate
NK cells	Natural killer cells
NTS	Non-typhoidal *Salmonella*
OD	Optical density
OMP	Outer membrane protein
PAMPs	Pathogen-associated molecular patterns
PBS	Phosphate buffered saline
PC	Phosphatidylcholine
PC-O	Ether linked phosphatidylcholine
PC-P	Plasminogen linked phosphatidylcholine
PE	Phosphatidylethanolamine
PE-O	Ether linked phosphatidylethanolamine
PE-P	Plasmalogen linked phosphatidylethanolamine
PG	Phosphatidylglycerol
P_i	Inorganic phosphate
PI	Phosphatidylinositol
PIK	Phosphatidylinositol kinase
PLA1	Phospholipase A_1
PLA2	Phospholipase A_2
PLB	Phospholipase B
PLC	Phospholipase C
PLD	Phospholipase D
PMA	Phosphomolybdic acid
PMSF	Phenylmethane sulfonyl fluoride
POTRA	Polypeptide transport associated
PRRs	Pattern recognition receptors
PS	Phosphatidylserine
PtdIns	Phosphatidylinositol
RF	Relative front
SCV	*Salmonella* containing vacuole
SDS	Sodium dodecyl sulphate
SDS-PAGE	Sodium dodecyl sulphate poly acrylamide gel electrophoresis
SIFs	*Salmonella* induced filaments
SLATs	*Salmonella* autotransporter mutant strain
SM	Sphingomyelin
SNP	Small nucleotide polymorphism
SPI	*Salmonella* pathogenicity island

T1SS	Type 1 Secretion system
T2SS	Type 2 Secretion system
T3SS	Type 3 Secretion system
T4SS	Type 4 Secretion system
T5SS	Type 5 Secretion system
T6SS	Type 6 Secretion system
TAA	Trimeric autotransporter adhesin
Tam	Translocation assembly module
T-bet	a T-box transcription factor
TBS	Tris buffered saline
TBST	Tris buffered saline Tween80
TCR	T cell receptor
TEMED	N,N,N',N'-tetramethylethane-1,2-diamine
TG	Triacylglycerol
TLC	Thin layer chromatography
TLR	Toll like receptor

CHAPTER 1

General Introduction

1.1 *Salmonella enterica*

1.1.1 *Salmonella enterica.*

The genus *Salmonella* contains two species: *S. bongori*; and *S. enterica. S. bongori* is mainly associated with causing disease in cold blooded animals, whereas *S. enterica* is known to colonise both warm blooded animals and plants. *S. enterica* is distributed into six subspecies, with subspecies 1 containing the majority of clinically relevant isolates. Phylogenetic analyses of *S. enterica* subspecies 1 revealed that there are two major lineages termed clades A and B, with clade A containing most of the strains known to cause disease in humans (Timme *et al*., 2013). In a recent phylogenetic study, whole genome sequencing of 445 *Salmonella* isolates revealed an average genome size of 4.73 megabases (Mb), with the distribution of bacteriophage species and conservation of major virulence factors shown to be largely clade specific (Worley *et al*., 2018), suggesting evolutionary constraints, such as the host, have had major impacts on the *S. enterica* genome.

Within *S. enterica* subspecies 1, there are >2500 different serovars, that are classified based on surface antigens, lipopolysaccharide (LPS) and flagella, and host specificity (Fierer and Guiney, 2001). Some serovars are capable of infecting multiple hosts such as *S. enterica* serovars Typhimurium and Enteritidis and are known as ‘generalists’. Other serovars infect a narrow range of hosts or are specific to just one. Examples of *S. enterica* serovars that are only able to invade a specific host are serovars Typhi and Paratyphi, which are thought to be human-specific.

S. enterica serovars Typhi and Paratyphi are the causative agents of typhoid and paratyphoid fever in humans, respectively (de Jong *et al*., 2012). These are systemic bacteraemia infections, also known as enteric fever, which are major causes

of death worldwide (Buckle *et al*., 2012). *S.* Typhi is restricted to a human host and has lost the ability to infect other animals, seemingly through the accumulation of mutations in more than 200 genes that might render them as pseudogenes (Baker and Dougan, 2007).

Examples of broad host range serovars are the non-typhoidal *Salmonellae* (NTS) serovars Typhimurium and Enteritidis. *S.* Typhimurium infection in humans causes acute gastroenteritis but can in rare circumstances, and predominantly in immunocompromised patients, cause systemic bacteraemia known as invasive NTS (iNTS) disease (Gordon, 2008). These iNTS infections are particularly problematic especially where they are associated with HIV or malaria co-infections in sub Saharan Africa. These coinfections lead to high mortality rates (MacLennan *et al*., 2010).

To understand the dynamics of *S. enterica* diseases in humans, a *S.* Typhimurium murine models of infection is commonly used (Strugnell *et al*., 2014) . The systemic disease cause by *S.* Typhimurium in mice is similar to that of typhoid fever in humans and thus a mouse model of *S.* Typhimurium infection is routinely used to try to elucidate the mechanisms of *S.* Typhi infection in humans (Santos *et al*., 2001). However, studies using the *S*. Typhimurium murine model of Typhoid fever must consider the differences between Typhimurium and Typhi. In a recent comparative genomic study, 600 genes were identified as unique to Typhi and 480 unique to Typhimurium (Sabbagh *et al*., 2010). One of the largest differences between the two serovars is the presence of the *Salmonella* Pathogenicity Island 7 (SPI7) loci in Typhi which, is absent in Typhimurium. The SPI7 loci encodes various factors important for *S.* Typhi infection such as the ViaB loci that encodes the Vi antigen (Parkhill *et al*., 2001). The Vi antigen forms a capsule that has immunosuppressive properties and

has been shown to mask Typhi from the innate immune response and thus permit systemic spread of Typhi in human hosts (Sharma and Qadri, 2004).

Even though there are marked differences between Typhi and Typhimurium, the *in vivo* and *in vitro* models are used provide important insight into *S. enterica* infections.

1.1.2 *S. enterica* lifecycle

The majority of human *S. enterica* infections are contracted via the consumption of contaminated food or water. The bacteria can survive the acidity of the stomach and pass into the intestine. Within the small intestines, and frequently within the Peyer's patches, *Salmonella* actively invade specialised microfold (M) cells (de Jong *et al*., 2012). M cells are characterised by irregular shape and dispersed microvilli at the apical surface and an invagination at the basal surface. This invagination forms a pocket like structure that can house immune cells such as lymphocytes and macrophages (Jepson and Clark, 2001). Genes located on the *Salmonella* pathogenicity island 1 (SPI1) locus encode a Type 3 secretion system (T3SS) apparatus and effector molecules that are required for invasion into non-phagocytic cells (Galan, 1999). T3SS proteins assemble to form a needle-like structure that spans the entire cell envelope and out of the bacterial cell (Figure 1.1). This needle injects protein 'effectors' into the host cell cytoplasm (Ehrbar *et al*., 2002). Once internalised, these effector proteins cause re-arrangement of host cell actin cytoskeleton causing an effect known as membrane "ruffling". The actin cytoskeleton rearrangements create an invagination at the host cell membrane that envelopes the invading *Salmonellae* into a vacuole known as the *Salmonella* containing vacuole (SCV) (Figure 1.2A). The re-arrangement of the actin cytoskeleton is essential for *Salmonella* replication inside the SCV (Meresse *et al*., 2001) and is partially mediated by the *S. enterica* SPI1

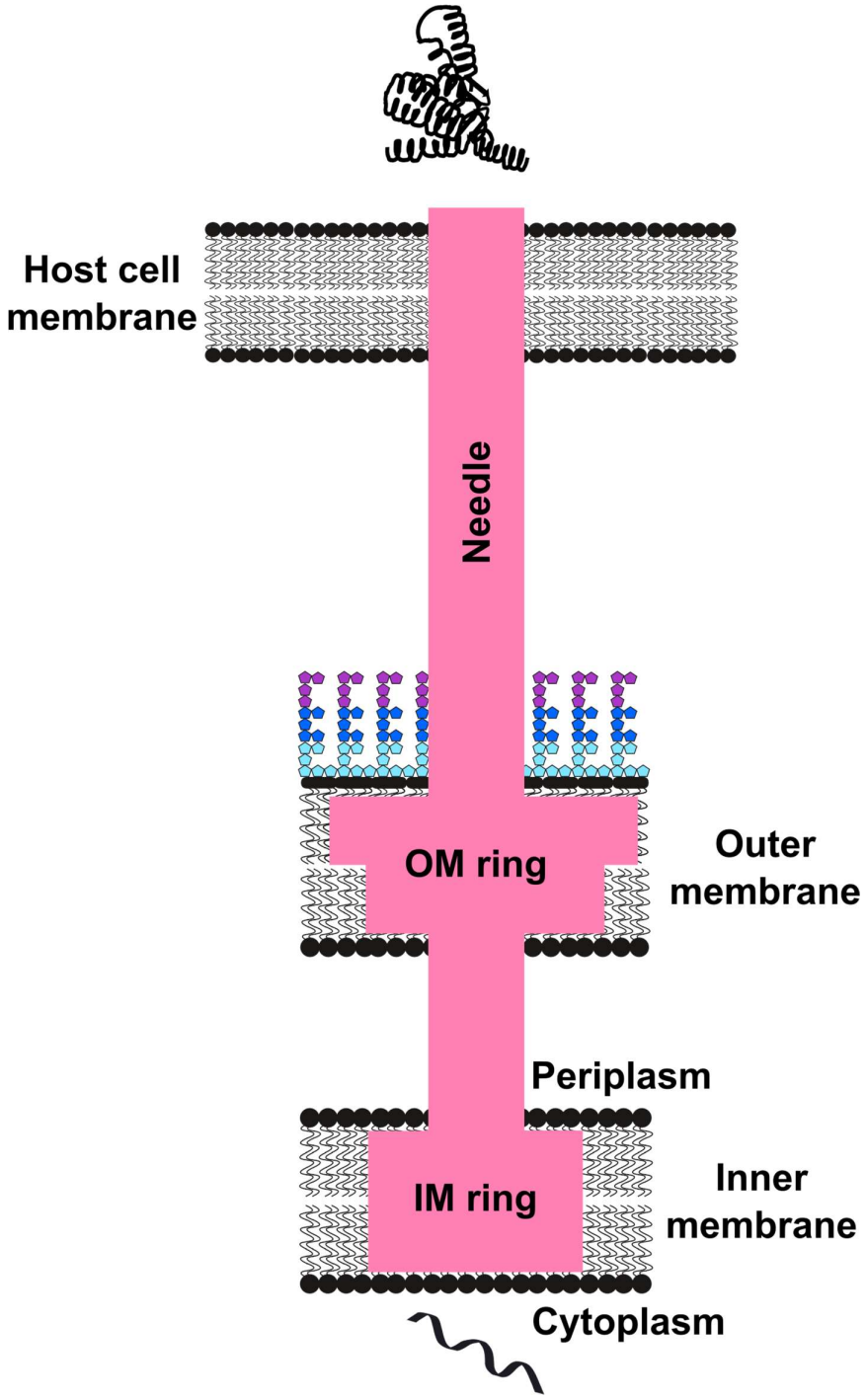

Figure 1.1. Type 3 secretion sytem overview. Type 3 secretion (T3SS) systems assemble into structures that span the inner and outer membrane, out of the bacterial cell and into the host cytosol. The T3SS transfers bacterial proteins synthesised in the cytoplasm directly into the host (reveiwed in (Coburn *et al*., 2007)).

effectors, SopB (Perrett and Zhou, 2013b), SipA (McIntosh *et al*., 2017) and SopE (Vonaesch *et al*., 2014).

Once inside the SCV, the *S. enterica* two-component regulatory system PhoPQ is activated by signals such as low Mg^{2+} concentrations (Groisman, 2001). PhoQ is a histidine kinase that, upon stimulation, phosphorylates the transcription factor PhoP, which subsequently alters the expression of over 200 genes (Groisman, 2001). The genes regulated by PhoPQ include those found on another SPI known as SPI2. Genes encoded on the SPI2 locus are involved in maintaining the SCV and limiting the impact of host innate defences on the replicating *Salmonellae*. Mutants of *phoPQ* are highly attenuated in murine models of infection (Miller *et al*., 1989), suggesting that this two-component regulatory system is important for *S. enterica* virulence.

Salmonella in the SCV can pass through the M cells exiting the basolateral surface where the bacteria encounter lymphocytes and macrophages. *Salmonella* can enter phagocytic cells such as macrophages and dendritic cells. Phagocytic cells are also known to phagocytose *Salmonella* as bacteria carrying null mutations in SPI1 (i.e. where there is no active host cell invasion) are still able to cause systemic disease (Vazquez-Torres *et al*., 1999). Post egress of the epithelial barrier, the resulting disease caused by *Salmonella* depends upon independent parameters such as the host immune system and the virulence of the infecting strain. Some infections result in self-limiting gastroenteritis while others may cause an invasive systemic disease. An understanding of the dynamics of human infections with *S. enterica* have come from studies in animal models, as well as clinical observations of human patients.

1.1.3 *S. enterica* acute infections

Many infections of *S. enterica* result in short term self-limiting gastroenteritis. In humans, serovars Typhimurium and Enteritidis are common causes of gastroenteritis (100 million+ cases annually) (Ao *et al*., 2015). These types of infections are typically limited to the gut as the host innate immune system is able to control the infection and prevent systemic spread of the bacteria. *S. enterica* gastroenteritis is characterised by fever, abdominal cramps and diarrhoea that resolves within a few days. The pathogenesis of the gastroenteritis is thought to be driven by release of the pro-inflammatory cytokine Interleukin 8 (IL-8) from intestinal epithelial cells that recruits neutrophils (McCormick *et al*., 1995) resulting in local inflammation of the intestines and diarrhoea (Zhang *et al*., 2003). These infections usually do not require medical intervention, unless the host is immunocompromised, very young or elderly.

1.1.4 Invasive systemic disease of *S. enterica*

Systemic infections of *Salmonella* occur when the bacteria pass through the epithelial layer at the Peyer's patches to invade the underlying phagocytes, usually macrophages, and these macrophages distribute *Salmonella* beyond the gastrointestinal tract (Vazquez-Torres *et al*., 1999). The serovars that cause systemic infections can be host-specific. *S.* Typhi and Paratyphi cause systemic infections in humans (McClelland *et al*., 2004) whereas *S. enterica* serovar Choleraesuis causes a systemic infection in pigs (Chiu *et al*., 2004).

Once the *Salmonella* are inside the phagocytes found at the basal surface of M cells, they can replicate inside the phagosome and SPI2 secreted effectors are thought to inhibit fusion of the bacteria-containing phagosome with toxic lysosomes (Santos *et al*., 2001). Within these specialised phagosomes, SPI2 effectors enable survival, replication and breakdown of the vacuole once the bacteria are ready to be released.

Phagocytes serve as cellular 'taxis', transporting *Salmonella* to secondary sites of infection such as the spleen, liver, gallbladder and bone marrow (reviewed by (Watson and Holden, 2010)). The bile within the gallbladder is continuously secreted into the intestines as part of normal gut function. When the gallbladder is infected with *Salmonella*, these bile secretions transport *Salmonella* from the gallbladder back into the intestine. Once in the intestine, the bacteria can be shed out of the host via contaminated faeces in a process described as faecal shedding. The lifecycle of *Salmonella* in the host is summarised in Figure 1.2.

1.1.5 Host immune responses to *S. enterica* infections.

Many studies have investigated the protective immune responses towards *S. enterica* infections using murine models of invasive disease (reviewed in (Tsolis *et al*., 2011)). It is important to note that wild-type *S*. Typhimurium, though causes a systemic disease in 'sensitive' mice, is invariably lethal, from doses as small as 10 organisms injected intravenously, or 10^4 bacteria given orally (Plant and Glynn, 1974). The sensitivity of mice to infection is dependent largely on the allele of *nramp-1* (also known as Slc11a1, *Lsh* and *Bcg*) carried by the mice (Govoni and Gros, 1998). The murine strain of choice to model *Salmonella* disease, C57BL/6, is $Nramp^{s/s}$, and hence carry the sensitive allele of Nramp-1 making them extremely sensitive to *S.* Typhimurium infections. For this reason, many studies use a growth attenuated mutant of *S.* Typhimurium, such as SL3261 (Hoiseth and Stocker, 1981) or BRD509 (Roberts *et al*., 2000) to understand the dynamics of *Salmonella* infection beyond the initial lethal stage.

Early immune responses to *S. enterica* infections are mainly driven by the recruitment of neutrophils to the sites of infection as part of the initial inflammatory response. Innate immune cell Pattern Recognition Receptors (PRRs) recognise

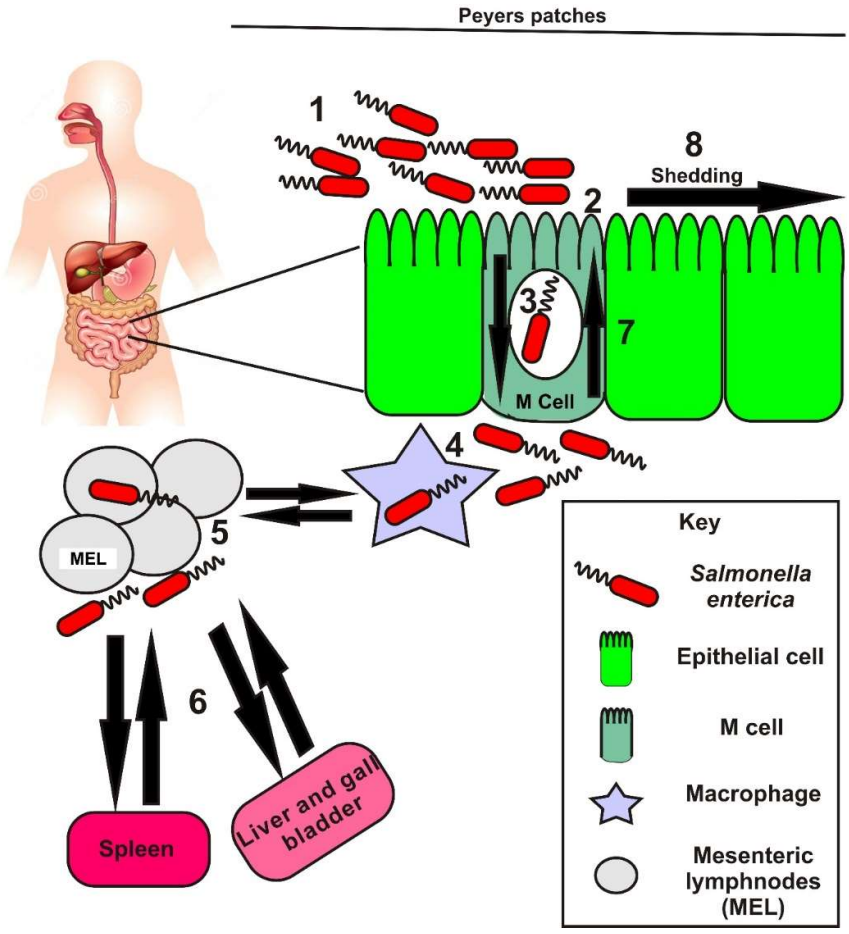

Figure 1.2. *S. enterica* infection. *S. enterica* are ingested usually via contaminated meat or vegetables and passes through the stomach to the small intestines (1). Here, the bacteria invade epithelial cells specifically in the Peyer's patches (2) (de Jong *et al*., 2012). *Salmonella* invade specialised epithelial cells known as M cells (3) and are released into the submucosa, encountering and invading macrophages (4). Once inside macrophages, *Salmonella* replicate inside a *Salmonella* containing vacuole (SCV) (Santos *et al*., 2001). *Salmonella* are transported to the mesenteric lymph nodes (MEL) (5) and from here disseminate into organs such as the spleen and liver (6) (Ibarra and Steele-Mortimer, 2009). The bacteria are shuttled between the livers and spleens to the MEL, back to Peyer's patches (7) and out of the host via faecal shedding (8).

conserved microbial signatures called Pathogen Associated Molecular Patterns (PAMPs) (reviewed by (Medzhitov, 2001)). These signatures are usually conserved features amongst microbial pathogens such as lipopolysaccharide (LPS), flagellin and DNA. One type of PRR are the Toll-like receptors (TLR). Different TLRs recognise different PAMPs. For example, TLR4 recognises LPS (Royle et al., 2003), whereas TLR5 recognises flagellin (Hayashi *et al*., 2001). The recognition of PAMPs by TLRs initiates a signalling cascade, which results in the production of pro-inflammatory cytokines (Weiss *et al*., 2004, Medzhitov, 2001). The production of pro-inflammatory cytokines is responsible for the recruitment of neutrophils and natural killer (NK) cells. These innate immune cells help to clear infections by ingesting invading pathogens (i.e. neutrophils) and the early production of interferon-γ (IFN-γ) (i.e. NK cells). The production of IFN-γ is essential for the maintenance and eventual clearance of *S.* infections, as transgenic mouse models that do not secrete IFN-γ succumb to the infection much more rapidly that wild-type mice (Kupz *et al*., 2014a).

Once *S. enterica* become intracellular, it is postulated that the bacteria become less visible to the host immune system. However, there are intracellular PRRs that can, when stimulated, activate caspase-1 (reviewed by (Bergsbaken *et al*., 2009)). The activation of caspase-1 induces production of IL-18 and IL-1β, which help to recruit IFN-γ producing cells including memory CD8+ T cells, NK cells and CD4+ T cells (Kupz *et al*., 2014b). Caspase-1 is also responsible for the initiation of a type of cell death known as pyroptosis (Bergsbaken *et al*., 2009).

The development of adaptive immunity and memory relies on the stimulation and activation of $CD4^+$ and $CD8^+$ T cells. The latter may be dispensable where CD4+ T cells are present, but become important where CD4+ T cells are depleted, as can happen in HIV/AIDS (Kupz *et al*., 2014a). At the basolateral surface of M cells in the

Peyer's patches, resident DC's regularly sample antigen and have also been shown to reach between epithelial cells to access bacteria present in the gut lumen (Lelouard *et al*., 2012). DC's can phagocytose *Salmonella* and subsequently degrade the bacteria to produce antigens which are presented on the surface of DCs via major histocompatibility complex II (MHC-II) molecules. Antigens presented on DC MHC-II might be recognised by naïve T-cells of the appropriate specificity via the surface T cell receptors (TCR) (Cheminay *et al*., 2005). Recognition of presented antigen by TCRs induces expression of the transcription factors including Tbet. Expression of T-bet, a T-box transcription factor, by CD4+ T cells 'polarises' the T cells to the Th1 phenotype and to secrete IFN-γ (Ravindran *et al*., 2005) (Figure 1.3).

1.1.6 Asymptomatic chronic carriage of systemic *Salmonella.*

Approximately 1-4% of typhoid fever patients become chronic carriers of *Salmonella*. In some instances, these patients do not present with typhoid fever and have no history of disease. These carriers shed the bacteria from their faeces into the environment and therefore serve as a source of *S.* Typhi. A very famous example of a chronic asymptomatic carrier of *S*. Typhi is "Typhoid Mary" who was an early 20th century cook in New York. Typhoid Mary is believed to infected over 100 individuals with typhoid fever, including the deaths of at least five, although never presenting with an episode of typhoid herself (Marineli *et al*., 2013).

The mechanism(s) employed by *S.* Typhi that enables chronic carriage has been studied, although the bacterial factors that facilitate chronic *Salmonella* carriage have not been fully elucidated. Studies from murine models of typhoid fever using *S.* Typhimurium indicate that one site for chronic carriage is the gallbladder. In murine models of *Salmonellosis*, mice can be induced to become chronic carriers (Crawford *et al*., 2010). Non-susceptible mouse strains (Nramp$^{R/R}$) fed a lithogenic diet of 1%

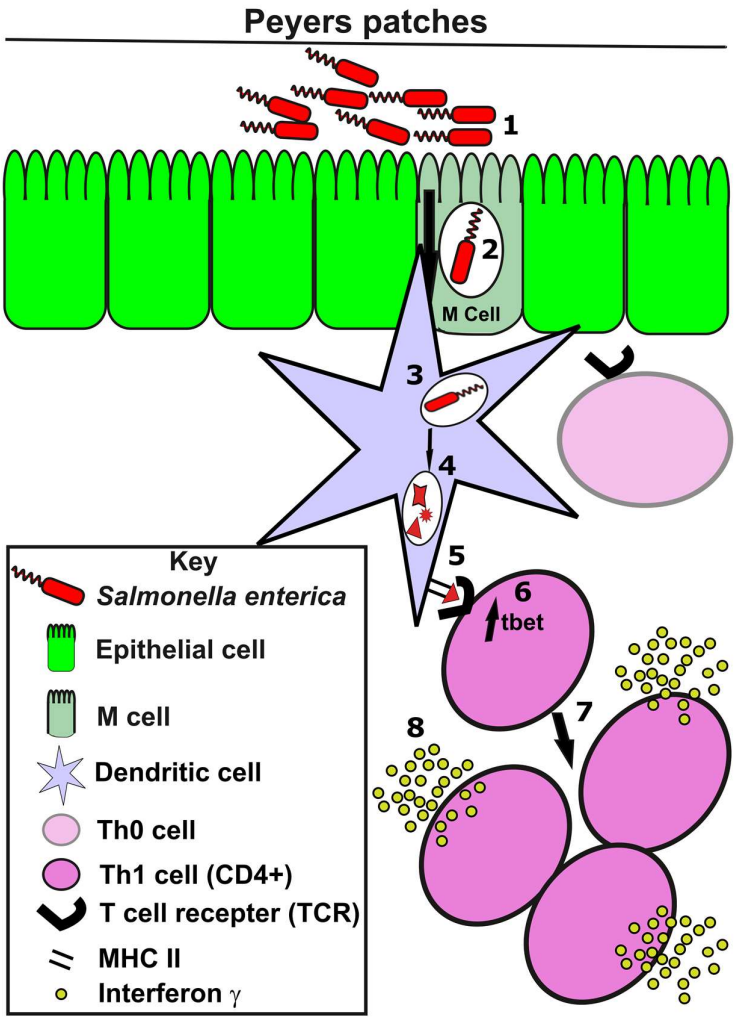

Figure 1.3. Adaptive immune response to *S. enterica* infections. (1) *S. enterica* traverse the epithelial barrier at the Peyers patches in a *Salmonella* containing vacuole (SCV) (2). Resident dendritic cells sample antigen at the Peyers patches (3) and can phagocytose *Salmonella.* Once inside the dendritic cell, the bacteria are processed to generate antigen (4). The processed antigen is displayed on MHC-II molecules (5). The antigens are recognised by naïve T cells expressing a T cell receptor that is complementary to the antigen. This binding induces the expression of T-bet (6), which is a transcriptopn factor that induces realease of inteferon γ (7).

cholesterol and 0.1% cholic acid induced gallstone formation (Crawford *et al*., 2010) and had higher *Salmonella* colonisation in the gallbladder than mice that did not have gallstones (Crawford *et al*., 2010). Approximately 90% of human typhoid carriers have gallstones and some chronic carriers subsequently develop gallbladder carcinomas (Koshiol *et al*., 2016). Other studies suggest that gallstones are correlated with *Salmonella* carriage and show that cholesterol gallstones can act as a surface for biofilm formation *in vivo* and *in vitro* (Prouty *et al*., 2002, Crawford *et al*., 2010).There is also evidence that *Salmonella* can replicate inside gallbladder epithelium and form biofilms on the epithelial cell layer (Gonzalez-Escobedo and Gunn, 2013). *Salmonella* can also live as planktonic cells in bile, and have adapted mechanisms to avoid bile salt induced death (Hernandez *et al*., 2012). The colonisation of the gallbladder by *Salmonella* is summarised in Figure 1.4.

The gallbladder contains bile, which is first synthesised by liver hepatocytes and then transported to intrahepatic bile ducts (Reshetnyak, 2013). Human bile is comprised of a mixture of compounds with the most abundant being bile salts (67%) and phospholipids (22%) (Reshetnyak, 2013). Phosphatidylcholine (PC) is a zwitterionic phospholipid that comprises approximately 95% of the bile phospholipid content (van Berge Henegouwen *et al*., 1987). The biosynthetic pathway to make PC does not exist in *S. enterica* (Sohlenkamp and Geiger, 2016). PC in bile has been shown to form mixed micelles with bile salts to solubilise cholesterol (Halpern *et al*., 1993). It is currently unknown whether colonisation of *S.* Typhi in humans causes gallstone formation, or if the gallstones develop independent of *S.* Typhi infection and the bacteria form opportunistic biofilms on gallstones in these patients. In a recent study, mice that developed *S.* Typhimurium biofilms on gallstones *in vivo* were subsequently treated or not with ciprofloxacin (Gonzalez *et al*., 2018). It was found that

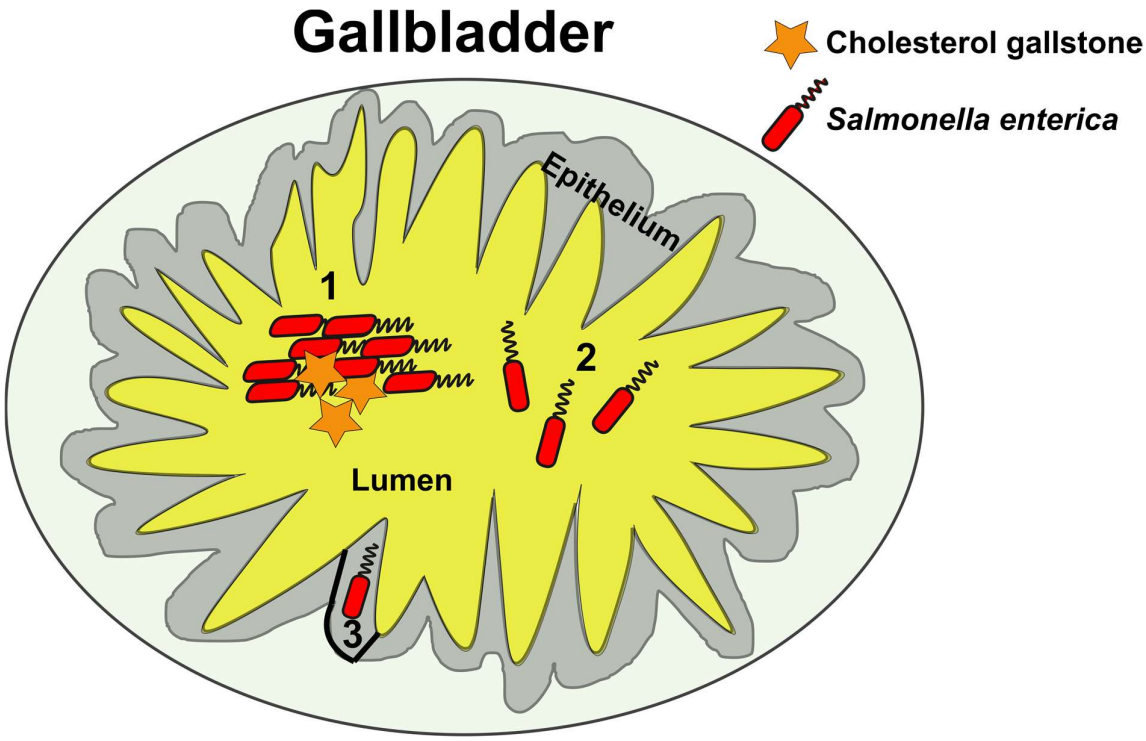

Figure 1.4. *S. enterica* lifecycle inside host gallbladders. There is considerable evidence that *S. enterica* can survive in bile as biofilm on cholesterol gallstones (1), as planktonic cells in bile (2) and within gallbladder epithelial cells (3).

S. Typhimurium biofilms on gallstones were less susceptible to ciprofloxacin treatment in mice than when no gallstone biofilm had formed, thus demonstrating the importance of biofilms for antibiotic resistance (Gonzalez *et al*., 2018). This ability to form drug-resistant biofilms is especially concerning given the rise of multi-drug resistant strains of *S.* Typhi, and the observation that antibiotic treatment does not always clear infection in chronic carriers (Gunn *et al*., 2014). Therefore, understanding the bacterial factors that mediate biofilm formation, survival in bile and faecal shedding is of great importance to understanding the mechanism(s) behind gallbladder chronic carriage.

Bile salts, which include compounds such a sodium deoxycholate and cholic acid, are like detergents that are capable of solubilising lipids in biological membranes and inducing DNA damage (Merritt and Donaldson, 2009). *S. enterica* have evolved mechanisms to overcome the bactericidal properties of bile salts, and *S*. Typhimurium can be adapted to 'bile stress' by growth in 5% deoxycholate (Hernandez *et al*., 2012). Not only has *S.* Typhimurium evolved mechanisms to overcome bile salt stresses, but it can replicate rapidly in whole mouse bile *in vitro* with a rate comparable to growth in rich LB medium (Menendez *et al*., 2009). Therefore, host bile contains all the required nutrients to permit efficient *Salmonellae* growth. Included in this nutrient requirement is a carbon source. A recent study investigating the metabolites that differed between naïve mice and those infected with *S*. Typhimurium, identified bile phospholipids as potential carbon sources *in vivo* and *in vitro* (Antunes *et al*., 2011). In particular, the hydrolysis of a bile phospholipid (lyso-phosphatidylcholine) permitted growth *in vitro* (Antunes *et al*., 2011). The bacterial factors that permitted growth on host phospholipids were not identified in this study. It must be noted that the decrease of metabolites *in vivo* by pathogens might be for a variety of reasons. For example,

phospholipids might be used as a carbon and/or phosphate source, therefore the exact function for the depletion of phospholipids in bile needs further investigation.

1.2 Pathogen interaction with host phospholipids

1.2.1 Host Phospholipids.

Phospholipids are fatty acid acyl chains connected to a phosphate based head group via 2 ester bonds at the sn-1 and sn-2 positions. The majority of lipid species in biological membranes are phospholipids. In eukaryotes, the major lipid species in the outer leaflet of cellular membranes are PC and sphingomyelin (SM) whereas the most abundant species in the inner leaflet are phosphatidylethanolamine (PE) and phosphatidylserine (PS) (Leventis and Grinstein, 2010, Yamaji-Hasegawa and Tsujimoto, 2006). PE, PC and SM are zwitterionic and have an overall neutral charge whereas PS is anionic and has an overall negative charge (Summarised in Figure 1.5). These lipids maintain structural integrity of the cellular membrane and are important in cell signalling. For example, if the membrane becomes damaged, PS becomes surface exposed on the outer leaflet and this signals to macrophages that the cell is damaged and induces phagocytosis (Birge *et al*., 2016). Another important class of phospholipid for signalling are the phosphatidylinositides (PtdIns), which are involved in regulating cell vesicular traffic (Roth and Sternweis, 1997). PtdIns lipids possess an inositol ring connected to 2 acyl chains at the sn-1 and sn-2 position (Figure 1.5). The inositol ring has 6 carbons that can be phosphorylated by specific PtdIns kinase (PIK) enzymes to generate mono, bi or tri phosphorylated PtdIns (De Matteis and Godi, 2004). These phosphorylated PtdIns lipids are important for various cellular functions such as

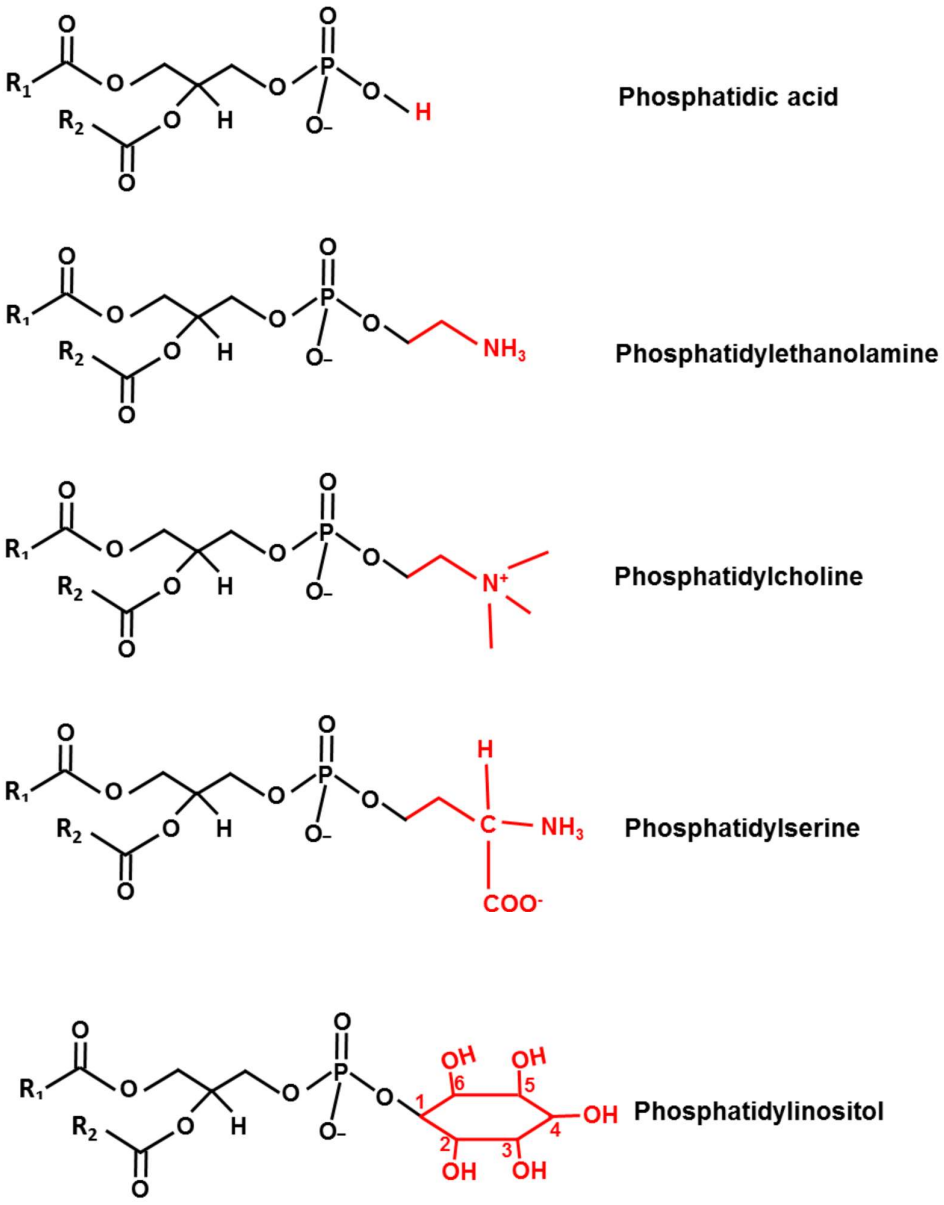

Figure 1.5. Chemical structure of host cellular lipids. Phospholipids are glycerol phosphate head groups attached to 2 acyl chains via 2 ester bonds. The head group (red) can be anionic or zwitterionic. The R_1 and R_2 acyl chains can vary in number of carbons and saturation.

induction of a phagosome-endosome fusion by phosphatidylinositol-3-phsophate (PI(3)P) (Simonsen *et al*., 1998).

1.2.2 Intracellular pathogens and host lipids

Pathogens have evolved secreted effectors that can interfere with host phospholipids. Some of these effectors are phospholipases, which exist in 4 classes (Figure 1.6). Phospholipase A_1 (PLA_1) enzymes cleave the ester bond at the sn-1 position, phospholipase A_2 (PLA_2) enzymes cleave the ester bond at the sn-2 position and phospholipase B (PLB) enzymes can cleave both ester bonds. Whereas phospholipases C and D (PLC and PLD respectively) cleave either before (PLC) or after (PLD) the phosphate bond and are also known as phosphatase enzymes. The roles of phospholipases in bacterial pathogenesis are summarised in Table 1.1. *S*. Typhimurium has a dedicated PtdIns phosphatase termed SopB, which is a SPI1 secreted effector that is required for *S.* Typhimurium intracellular growth (Hernandez *et al*., 2004). SopB has also been shown to reduce the negative charge of the SCV by depleting lipids such as PS and phosphatidylinositol-3-4-bisphosphate ($PI(3,4)P_2$), thereby inhibiting the SCV interaction with late endosome markers such as Rab35 (Bakowski *et al*., 2010). Rab35 is a eukaryotic GTPase involved in regulating the cytoskeleton (Chua *et al*., 2010). By inhibiting the interaction of the SCV with Rab35, SopB prevented the SCV fusing with the lysosome (Bakowski *et al*., 2010).

The hydrolysis of phospholipids by PLA_2 enzymes produces lyso-phospholipids (Figure 1.7). Lyso-phospholipids have one acyl chain connected to a phosphoryl head group via one ester bond at the sn-1 position. An example of a lyso-phospholipid is Lyso-phosphatidylcholine (Lyso-PC). Some PLA_2 enzymes have Glycerophospholipid: Cholesterol Acyl Transferase (GCAT) activity whereby the enzyme will hydrolyse the acyl chain from a host phospholipid (usually PC) and transfer this to cholesterol to form

Table 1.1. Bacterial effectors that interact with host lipids

Protein	Species	Function	Reference
SopB	*S.* Typhimurium	PtdIns phosphatase, recruits Rab5 to the SCV, causes accumulation of PI(3)P in the SCV.	(Mallo *et al*., 2008)
IgpD	*Shigella flexneri*	Phosphatase, converts PI(4,5)P_2 to PI(5)P	(Niebuhr *et al*., 2002)
FplA	*Fusobacterium nucleatum*	Phospholipase A_1, binds PtdIns	(Casasanta *et al*., 2017)
PlpD	*Pseudomonas aeruginosa*	Phospholipase A_1, binds PtdIns	(Salacha *et al*., 2010)
SseJ	*S.* Typhimurium	PLA_2, CGAT activity in the presence of RhoA GTPase	(Lossi *et al*., 2008)
ExoU	*P. aeruginosa*	PLA_2, major virulence factor, disrupts eukaryotic membranes	(Sato *et al*., 2003)
VipD	*Legionella pneumophila*	PLA_1, activated by Rab5, and cleaves PI(3)P to disrupt endosome fusion	(Gaspar and Machner, 2014)
PldA	*Helicobacter pylori*	PLA_1, haemolytic activity	(Dorrell *et al*., 1999)
SapM	*Mycobacterium tuberculosis*	Hydrolysis PI(3) to prevent phagosome-endosome fusion	(Vergne *et al*., 2005)

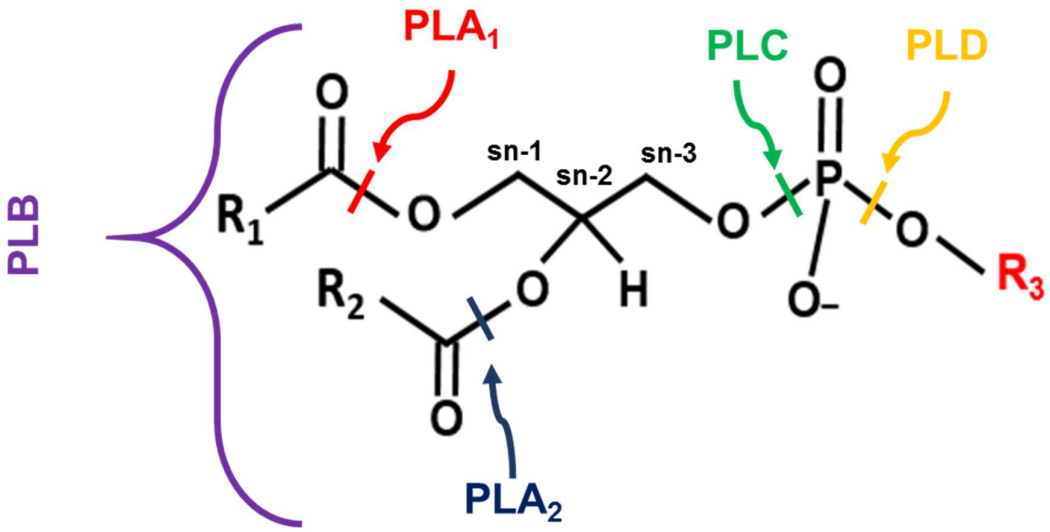

Figure 1.6. Phospholipase characterisation. Phospholipases exist in 4 classes. Phospholipase A_1 (PLA_1) enzymes cleave the ester bond at the sn-1 position, phospholipase A_2 (PLA_2) enzymes cleave the ester bond at the sn-2 position and phospholipase B (PLB) enzymes can cleave both ester bonds. Phospholipase C (PLC) enzymes cleave the phosphate bond before the phosphate and phospholipase D (PLD) enzymes cleave the phosphate bond after the phosphate.

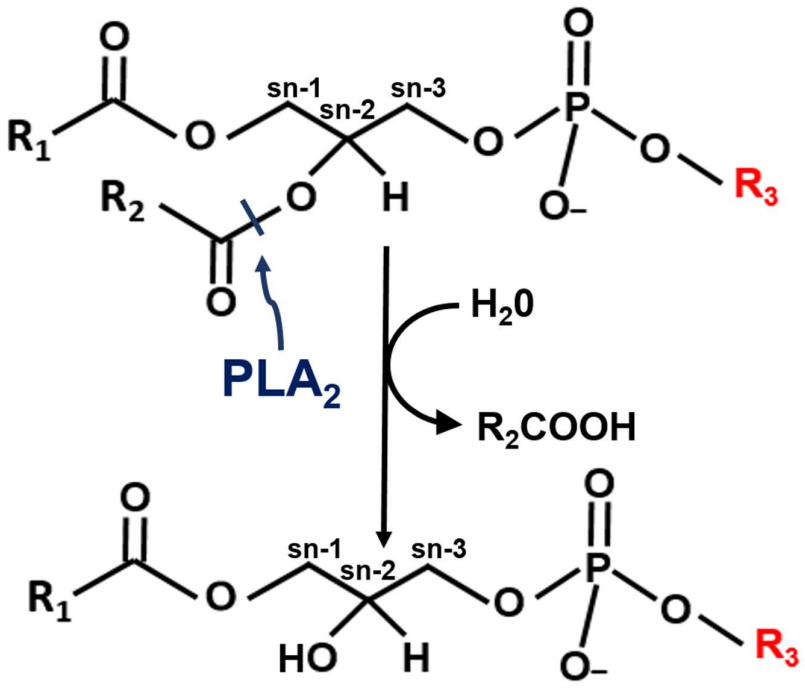

Figure 1.7. Lyso-phospholipid production. The hydrolysis of a phospholipid by a PLA_2 enzyme results in the production of a lyso-phospholipid and free fatty acid.

cholesterol esters (CE) and a lyso-phospholipid as a break down product. An *S*. Typhimurium SPI2 secreted effector termed SseJ has been experimentally proven to have PLA_2 and GCAT activity in the presence of RhoA GTPase (Lossi *et al*., 2008, Christen *et al*., 2009). SseJ is expressed inside the SCV and the GCAT activity of SseJ to generate CE is hypothesised to maintain fluidity of the SCV (Lossi *et al*., 2008).

1.3 *Salmonella* virulence factors

1.3.1 The *Salmonella* Outer Membrane.

Salmonella is a Gram-negative rod shape bacterium with a typical envelope comprising two membranes termed the outer membrane and the inner membrane. There are two cellular compartments of Gram-negative bacteria: the cytoplasm and the periplasm. The cytoplasm and the periplasm are separated by the inner membrane and the periplasm is separated from the external environment by the outer membrane. The inner membrane is a bilayer comprised of phospholipids and the outer membrane is an asymmetric bilayer with the inner leaflet comprised of phospholipids and the outer leaflet with lipid A/LPS (Figure 1.8). The major phospholipid species of *S. enterica* are PE, phosphatidylglycerol (PG), cardiolipin (CL) and acyl-PG (Olsen and Ballou, 1971) (Figure 1.8). Separating both membranes and maintaining the cellular shape and integrity is a thin layer of peptidoglycan that is made up of repeating units of alternating peptide cross-linked N-acetyl-glucosamine and N-acetyl-muranic acid (Quintela *et al*., 1997). The cell envelope of Gram negative bacteria provides protection to the extracellular environment as the outer membrane is intrinsically resistant to certain antibiotic stresses (Delcour, 2009). However, as the cell envelope is comprised of two

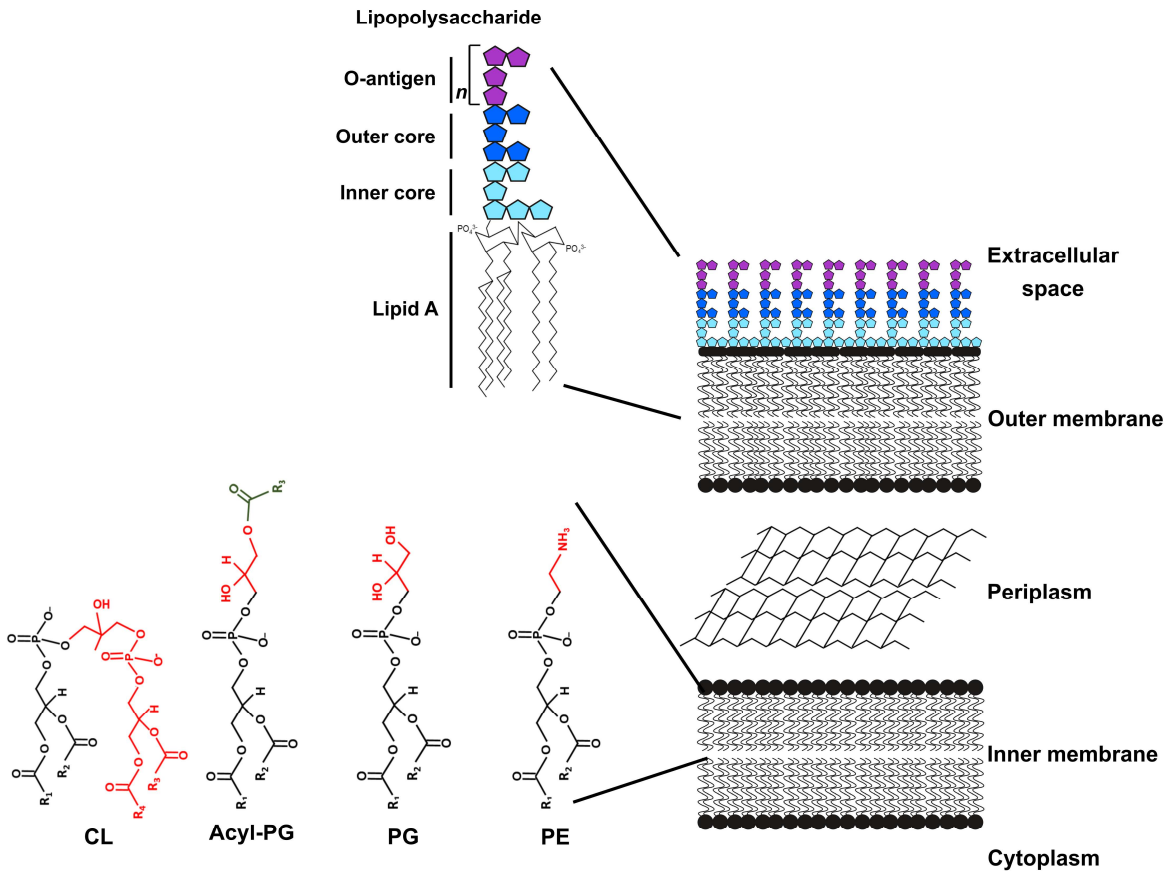

Figure 1.8. Outer membrane architecture of *S.* Typhimurium. The cell envelope of Gram-negative bacteria comprises the outer membrane (top), a layer of peptidoglycan and inner membrane (bottom). The outer membrane is an asymmetric bilayer with the outer leaflet comprised of lipopolysaccharide (LPS) and the inner leaflet comprised mainly of phospholipids. LPS is made up of Lipid A, which is attached to the inner core (3-deoxy-D-manno-oct-2-2-ulosonic acid and heptose). The inner core is linked to the outer core, which consists of hexose and hexosamine sugars. Attached to the outer core is the O-antigen polysaccharide (Caroff and Karibian, 2003). The inner membrane is comprised of the phospholipids cardiolipin (CL), acyl-phosphatidylglycerol (acyl-PG), phosphatidylglycerol (PG) and phosphatidylethanolamine (PE) (left to right).

membranes, and protein synthesis occurs in the cytoplasm, Gram negative bacteria have evolved protein secretion mechanisms to transport polypeptides that are synthesised in the cytoplasm through the cell envelope to their intended destination (Costa *et al*., 2015).

1.4 Protein secretion in Gram negative bacteria

1.4.1 Inner membrane translocation

The first barrier for secreted proteins, which are synthesised in the cytoplasm, is to cross the inner membrane. Broadly, there are two main systems that facilitate inner membrane translocation: the Sec pathway and the twin Arginine translocation (TAT) pathway with the Sec pathway involved in secreting unfolded proteins and the TAT pathway responsible for secreting folded proteins (Kudva *et al*., 2013). The Sec pathway is comprised of the SecYEG translocon, which is located at the inner membrane and forms a pore that opens laterally to secrete proteins through the inner membrane (du Plessis *et al*., 2009). The Sec pathway is responsible for the translocation of unfolded proteins and this translocation can occur post-translationally or co-translationally (Kudva *et al*., 2013). The co-translational pathway is usually involved in the secretion of integral inner membrane proteins that have a highly hydrophobic signal sequence (Chou and Kendall, 1990). This signal sequence is recognised by the signal recognition particle (SRP), which targets polypeptides exiting the ribosome (Luirink and Sinning, 2004, Jomaa *et al*., 2016). SRP directs the whole complex to SecYEG at the inner membrane and in conjunction with YidC, inserts the protein into the inner membrane (Sachelaru *et al*., 2017).

Proteins that are not intended for the inner membrane, such as lipoproteins or outer membrane proteins typically aren't targeted by SRP, and have a signal sequence that typically has a charged N region, hydrophobic H region and polar C region (Chou and Kendall, 1990). SecB transports the unfolded polypeptide to the SecYEG translocon at the inner membrane where the ATPase SecA, inserts into the SecYEG translocon and facilitates inner membrane translocation in an ATP dependent manner (Bechtluft *et al*., 2010). At the periplasmic face of the inner membrane, the signal sequence is cleaved (Dalbey *et al*., 1997).

1.4.2 Protein secretion overview

Gram-negative bacteria have evolved various methods to secrete proteins out of the cell. Some of these bypass both membranes and the periplasmic space, whilst others transport proteins sequentially from the cytoplasm, through the inner membrane, periplasm and outer membrane. At least six secretion systems to-date have been described in Gram- negative bacteria, Types 1-6 (Costa *et al*., 2015). These 6 systems encompass various methods to secrete a protein synthesised in the cytoplasm of the cell, through the periplasm and outer membrane into the extracellular space. The research presented in this dissertation will mainly focus on Type 5 secretion, however the others will be introduced briefly (Figure 1.9). Type 1 secretion systems are composed of 3 proteins: the ATP binding cassette transporter; membrane fusion protein; and outer membrane protein that come together to form a complex that is able to secrete proteins from the cytoplasm directly into the extracellular space. The most widely studied Type 1 protein is α- haemolysin (Thanabalu *et al*., 1998). Types 2, 3, 4 and 6 are multi-protein complexes. Type 2 secreted proteins are first exported from the cytoplasm to the periplasm in a Sec or Tat-depended manner and from the periplasm to the extracellular space via the secretory machinery

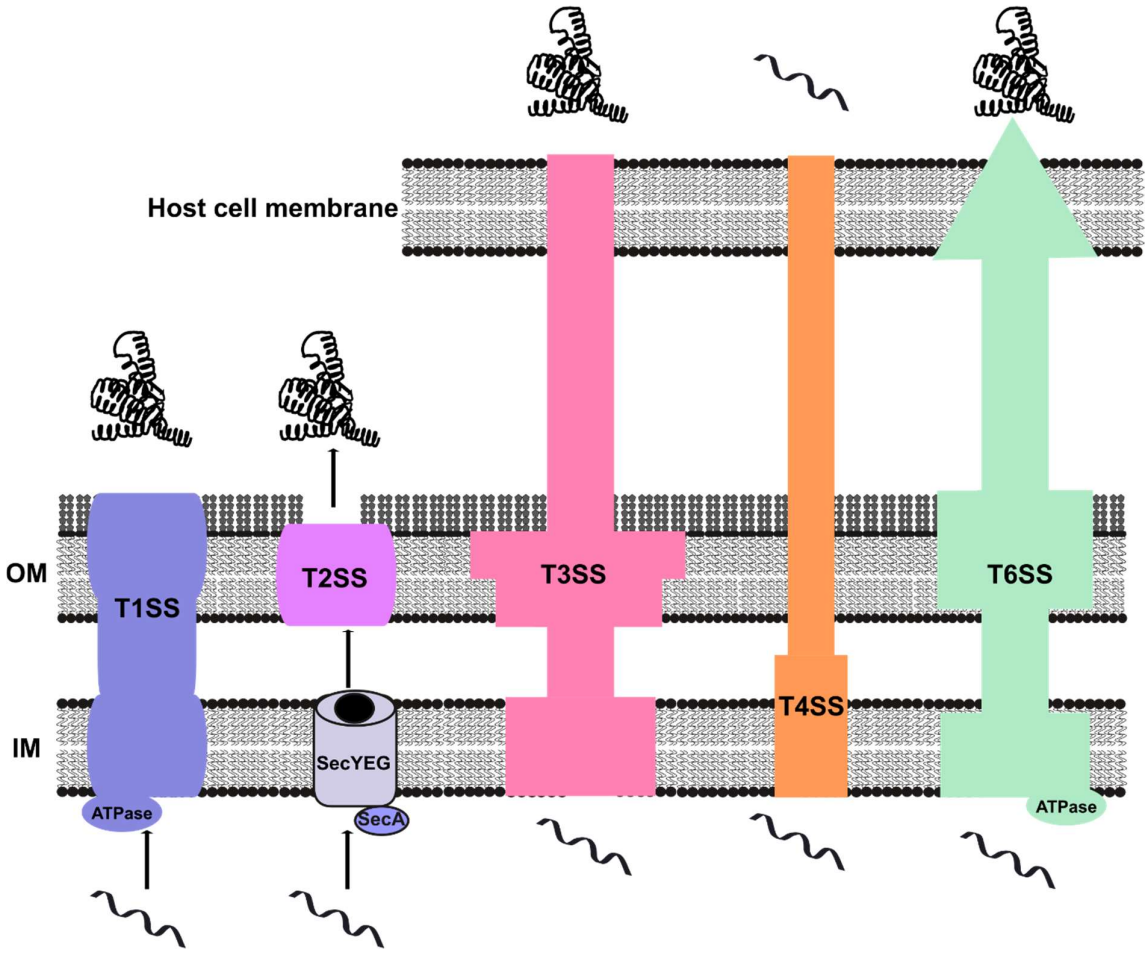

Figure 1.9 Overview of secretion systems in Gram negative bacteria. Schematic overview of the protein secretion systems in Gram negative bacteria. From left to right: Type 1 secretion system; type 2 secretion system; type 3 secretion system; type 4 secretion system; and type 6 secretion system. Types 1, 3, 4 and 6 transport substrates directly from the cytoplasm to the outside of the cell bypassing the inner and outer membranes (IM and OM respectively). For types 3, 4 and 6 secreted proteins, these are delivered straight into the host cell cytosol. Proteins secreted by the type 2 secretion system are first trsnslocated through the innner IM by the SecYEG translocon before passing though a channel in the outer membrane. Modified from (Depluverez *et al.*, 2016).

(Nivaskumar and Francetic, 2014). Type 3 secretion systems (T3SS) bypasses the inner membrane, periplasm and outer membrane and the complex extends away from the cell surface with a needle like projection that injects directly into host cells to allow transfer of proteins from the bacterial cytoplasm to the host cytosol with the most relevant examples including the T3SS from *Salmonella* (Kubori *et al*., 1998). The Type 4 secretion system might transfer DNA (as well as proteins) into either bacterial or eukaryotic cells (Alvarez-Martinez and Christie, 2009). Type 6 secretion systems translocate toxic proteins into recipient cells via a channel that spans both the inner and outer membranes (Zoued *et al*., 2014).

1.5 Type 5 secretion.

1.5.1 Type 5 protein overview and functions.

Type 5 secretion (T5SS) is the most abundant protein secretion system in Gram-negative bacteria (Henderson *et al*., 2004). Proteins that are members of Type 5 secretion are also termed autotransporters, with the two names used interchangeably. ‘Autotransporter’ arises from the misconception that Type 5 proteins contain all the information necessary for their own secretion. Several studies have now demonstrated that various chaperones are necessary for the sufficient secretion of Type 5 proteins (Jain and Goldberg, 2007, Ruiz-Perez *et al*., 2009, Rossiter *et al*., 2011), indicating that Type 5 proteins require more than their own domains for secretion. At the most basic level, Type 5 proteins are single polypeptides that have three domains: a signal sequence; a passenger domain; and a β-barrel domain (Henderson *et al*., 2004, Pohlner *et al*., 1987). The signal sequence is Sec-dependent and in around 10% of autotransporters, is unusually extended (50-60 residues)

(Henderson *et al*., 2004). The β-barrel domain is also known as the translocation domain that usually forms a 12 stranded β-barrel in the outer membrane. The passenger domain is thought to be secreted through the pore formed by the β-barrel domain to the cell surface where it may remain anchored, or be cleaved and released from the cell. The passenger domain is the functional moiety of Type 5 secreted proteins with the following functions reported to-date: proteinases (Henderson *et al*., 1999); lipases (Wilhelm *et al*., 1999); adhesins (Nummelin *et al*., 2004); biofilm inducers (Raghunathan *et al*., 2011); autoaggregation factors (Henderson *et al*., 1997); and host colonisation factors (Shaw *et al*., 2002) (Table 1.2).

1.5.2 Classes of Type 5 proteins

Type 5 proteins are further divided into five sub categories; type 5a (classical), type 5b (two-partner secretion), type 5c (trimeric autotransporter adhesin(TAA)), type 5d (fused two-partner) and type 5e (inverted) secretion (Leo *et al*., 2012). All sub-classes of type 5 secreted proteins have the following domains; a signal sequence, secreted passenger domain and a β-barrel translocation domain. However, the composition, order and size of these domains, differs between sub-classes (Figure 1.10). Type 5a proteins have an N-terminal signal sequence followed by the passenger domain and a C-terminal β-barrel domain encoded by the same open reading frame, which is translated into one polypeptide.

Type 5b proteins have the secreted domain and a β-barrel domain encoded on separate open reading frames. The secreted effector molecule is generally referred to as TpsA domain and the translocation domain as the TpsB (Jacob-Dubuisson *et al*., 2001). All Type 5a β-barrel domains to-date are composed of 12 β strands (Barnard *et al*., 2007, Clantin *et al*., 2007), but Type 5b TpsB proteins have 16 β strands and are related to members of the Omp85 family of proteins. TpsB proteins contain two

Table 1.2. Autotransporter characterisation and function

Organism	Protein	Class	Function	Reference
EAEC	Pet	5a	Serine protease autotransporter (SPATE), toxin, released from cell surface	(Navarro-Garcia *et al*., 2007)
Helicobacter pylori	VacA	5a	Cytoskeletal rearrangement and disrupting mitochondrial function	(Palframan *et al*., 2012)
E. coli	Antigen 43	5a	Promotes autoaggregation and biofilm formation , phase variable	(de Luna *et al*., 2008)
Bordetella pertussis	Pertactin	5a	Required or complete neutrophil clearance	(Inatsuka *et al*., 2010)
Pseudomonas aeruginosa	EstA	5a	Involved in biofilm formation and motility, GDSL lipase	(Wilhelm *et al*., 2007)
E. coli 0157:H7	EhaB	5a	Binding to ECM molecules laminin and collagen I and promotes biofilm formation	(Wells *et al*., 2009)
ETEC	EtpB	5b	β-barrel portion, responsible for secretion of EtpP (secreted effector).	(Fleckenstein *et al*., 2006)
E. coli	CdiB	5b	Contact-dependent inhibition, β-barrel portion, responsible for secretion of CdiA (secreted effector).	(Aoki *et al*., 2005)
Yersinia enterocolitica	YadA	5c	Promotes autoaggregation, binding to ECM molecules and resistance complement mediated killing	(Schindler *et al*., 2012)
EHEC	EhaG	5c	Binding to ECM molecules and host cell adhesion	(Totsika *et al*., 2012)
P. aeruginosa	PlpD	5d	Phospholipase	(Salacha *et al*., 2010)
Fusobacterium nucleatum	FplA	5d	Phospholipase, binds phosphatidylinositides	(Casasanta *et al*., 2017)
EPEC and EHEC	Intimin	5e	Binds to translocated Intimin receptor (TIR), a type III secreted protein, to promote a host cell adhesion, inverted AT.	(Leo *et al*., 2015)

Enteroaggerative *E. coli* (EAEC), Enterotoxigenic *E. coli* (ETEC), Enteropathogenic *E.* coli (EPEC), and Enteroheamorrhagic *E. coli* (EHEC)

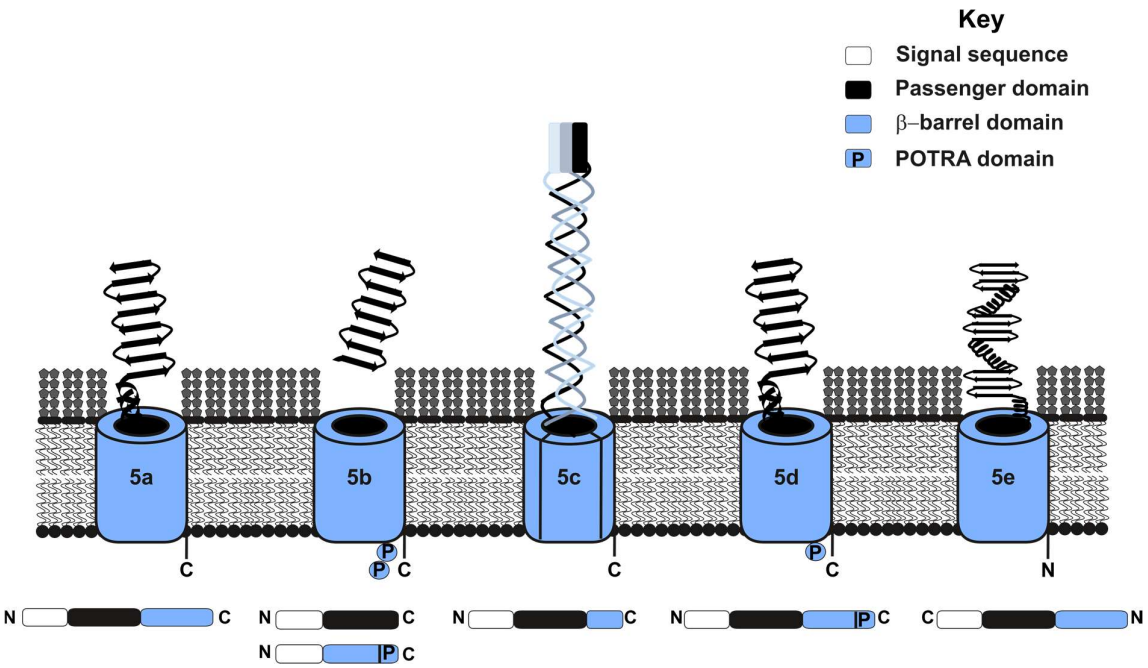

Figure 1.10. Type 5 secretion overview. Type 5 secreted proteins can be placed into subcategories 5a-5e (left to right) based on gene architecture and multimerisation. Briefly, Type 5a are classical autotransporters with an N-terminal signal sequence (white), passenger domain (black) and β-barrel domain (blue) encoded for on one open reading frame which is translated into one polypeptide. Type 5a autotransporters are inserted into the outer membrane with an embedded C-terminus and secreted N-terminus. Type 5b autotransporters (two partner secretion) have the passenger domain and β-barrel domain encoded for on separate genes. The β-barrel also contains two periplasmic POTRA (P) domains. Type 5c have all domains encoded for on one gene, but the β-barrel on encodes one third of a full barrel, therefore three 5c proteins form a homotrimer. Type 5d (fused two-partner secretion) have all domains encoded for on one open reading frame but the β-barrel also contains one POTRA domain. Type 5e have all domains encoded by one open reading frame, but is secreted such that the N-terminus is embedded in the outer membrane and the C-terminus is secreted and surface exposed.

polypeptide transport associated (POTRA) domains whereas the prototypical member of the Omp85 family, BamA, predominantly has 5 POTRA domains (Heinz and Lithgow, 2014). Trimeric, or Type 5c, proteins have all 3 domains encoded by one open reading frame, however the barrel portion only represents 1/3rd of the full β-barrel. Thus, three monomers of these proteins must aggregate to form a homotrimer in the outer membrane (Cotter *et al*., 2005). The archetypical Type 5c protein studied to date is YadA from *Yersinia enterocolitica*. YadA is believed to be the single most important factor for *Y. enterocolitica* virulence, with roles including complement resistance and the binding to extracellular matrix molecule (Schindler *et al*., 2012, Leo *et al*., 2010).

Type 5d proteins are also known as fused two-partner secretion because the protein has both passenger domain and β-barrel domain encoded by one open reading frame, but the β-barrel has 16 β-strands and a POTRA domain similar to Type 5b proteins. To-date, two Type 5d proteins have been characterised: PlpD from *Pseudomonas aeruginosa* and FplA from *Fusobacterium nucleatum* (Salacha *et al*., 2010, Casasanta *et al*., 2017). Both proteins were characterised as patatin-like lipases that bind to, and cleave, a variety of phospholipids (da Mata Madeira *et al*., 2016, Casasanta *et al*., 2017).

Type 5e proteins, again, have all three domains encoded for by one open reading frame but have a secreted C-terminus and embedded N-terminus and thus has been termed as ‘inverted autotransporters’ (Desvaux *et al*., 2004, Leo *et al*., 2012, Leo *et al*., 2014). The archetypal inverted autotransporter is Intimin, which is encoded by the *eae* gene at the Locus of Enterocyte Effacement (LEE) in Enteropathogenic *E. coli* (EPEC) (Jerse *et al*., 1990). The LEE encodes a T3SS that transports the Translocated Intimin Receptor (TIR) directly into host cells (DeVinney *et al*., 1999). The

attachment of Intimin to TIR enables host cell adherence and is important for infection (Lai *et al*., 2013, Ross and Miller, 2007).

1.5.3 Type 5 mode of secretion

Although previously believed to be a simple secretion system, recent studies have shown that other factors are needed for efficient secretion of Type 5 proteins. A simple summary of the secretion of Type 5a proteins is represented in Figure 1.11. Briefly, Type 5 proteins are synthesised in the cytoplasm and are directed to the SecYEG translocon, via the signal sequence, which facilitates translocation across the inner membrane (Hegde and Bernstein, 2006). Once in the periplasm, the signal sequence is cleaved by signal peptidases and the unfolded Type 5 protein is recognised by periplasmic chaperones such as SurA, Skp and DegP (Lazar and Kolter, 1996, Sklar *et al*., 2007b). These chaperones are believed to transport the protein to the β-barrel assembly machinery (Bam) complex at the outer membrane. The Bam complex is responsible for folding outer membrane proteins into the outer membrane, and is required to fold the β-barrel domain of the type 5 protein into a β-barrel structure into the outer membrane (Knowles *et al*., 2009), but the exact mechanism of Bam mediated outer membrane protein insertion is unknown. The passenger domain is thought to be secreted through the lumen of the newly formed barrel in the “hairpin model” of passenger domain secretion (Leyton *et al*., 2012). However, the evidence for this hypothesised secretion process is limited, with an alternative model proposing that BamA holds the autotransporter β-barrel in an open state to facilitate passenger domain surface exposure. The outer membrane biogenesis of autotransporters has been extensively reviewed (Leyton *et al*., 2012). Recent studies suggest that the Translocation machinery (Tam) complex facilitates secretion of the passenger domain (Selkrig *et al*., 2012). Once the passenger domain has reached the cell surface, it might

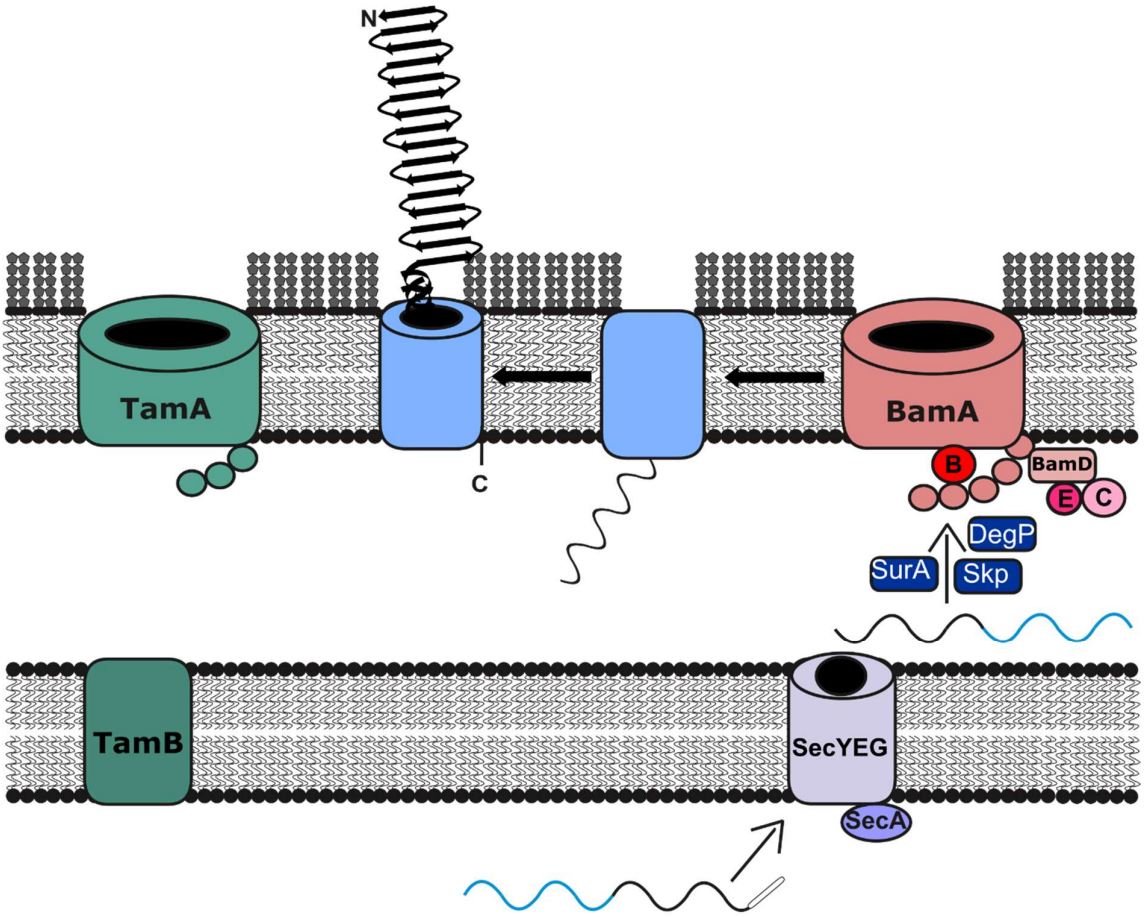

Figure 1.11. Type 5a protein outer membrane biogenesis. Type 5 proteins are synthesised in the cytoplasm and cross the inner membrane via the SecYEG translocon and once in the periplasm, the signal sequence is cleaved by signal peptidases. Periplasmic chaperones such as Skp, DegP and SurA transport the unfolded protein to the Bam complex, which, facilitates folding the β-barrel domain into the outer membrane. The passenger domain is believed to pass through the lumen of the barrel to be exposed on the cell surface with evidence suggesting that the Tam complex aids in passenger domain translocation.

remain attached the barrel, or it might be cleaved by external or internal peptidases to enter the extracellular milieu, or remain associated with the outer leaflet of the outer membrane as a cleaved or uncleaved domain.

1.5.4 The macromolecular complexes important for Type 5 outer membrane biogenesis.

Two protein complexes, Bam and Tam, are believed to have important roles in secretion of Type 5 proteins. The Bam complex differs between species of Gram-negative bacteria but always has an integral outer membrane protein known as BamA, which has homologues in mitochondria and chloroplasts. BamA is a member of the Omp85 family of proteins that are characterised as integral 16-stranded outer membrane β-barrel proteins with polypeptide transport associated (POTRA) domains. Mutagenesis evidence suggests that BamA is the most critical component of the Bam complex, which is essential to both cell viability and secretion of many Type 5 secreted proteins (Bodelon *et al*., 2009, Jain and Goldberg, 2007, Lehr *et al*., 2010, Rossiter *et al*., 2011).

In *Escherichia coli* and *S.* Typhimurium, the Bam complex comprises of five factors BamA-E. BamA and BamD are essential for cell viability in *E. coli* (Voulhoux *et al*., 2003, Malinverni *et al*., 2006). Both BamA and BamD are required for the outer membrane biogenesis of the Type 5a protein Pet (plasmid encoded toxin) from pathogenic *E. coli* (Rossiter *et al*., 2011). BamA forms a 16 stranded β-barrel outer membrane protein (OMP) with five POTRA domains (Albrecht *et al*., 2014, Werner and Misra, 2005). In association with BamA are four lipoproteins BamB-E that are localised to the inner leaflet of the outer membrane (Wu *et al*., 2005). BamB, C and E are non-essential factors that are not required for the secretion of Pet (Rossiter *et al*., 2011). The crystal structures of all the Bam complex proteins have been solved (Zhang *et al*.,

2011, Noinaj *et al*., 2011, Dong *et al*., 2012, Albrecht *et al*., 2014) as well as two structures for the whole Bam complex (Han, 2016). The solved crystal and cryo-electron microscopy (cryo-EM) structures of the Bam complex indicated that POTRA domains of BamA interact with the Bam lipoproteins forming a ring structure that protrudes into the periplasm (Figure 1.12A-B) (Han *et al*., 2016, Iadanza *et al*., 2016). The Bam lipoproteins form sub complexes within the Bam complex known as BamAB and BamCDE (Han *et al*., 2016). These two complexes interact to maintain the stability of the complex. The mechanism for Bam-mediated insertion of outer membrane proteins into the outer membrane is currently unknown. However, one hypothesis is that BamA opens laterally between β-strands 1 and 16 and the unfolded outer membrane protein uses the BamA structure as a template for β-barrel formation (Iadanza *et al*., 2016).

The Tam complex was described more recently (Selkrig *et al*., 2012, Fierer and Guiney, 2001) and in *E. coli* consists of factors TamA and TamB. TamA is another member of the Omp85 family of proteins and is an integral outer membrane protein with three POTRA domains. TamB is an inner membrane protein that interacts with TamA. Recent studies have suggested the Tam complex is required for efficient translocation of the passenger domains of various Type 5 proteins, such as Antigen 43 (Selkrig *et al*., 2012) and *E. coli* fimbrial proteins (Stubenrauch *et al*., 2016). TamA and B are not essential for bacterial viability though the structural relationships with the Bam complex suggest that important, yet to be discovered, roles for Tam may exist. In this study, the role for TamA and B for secreting and folding complex multimeric Type 5 proteins will be investigated.

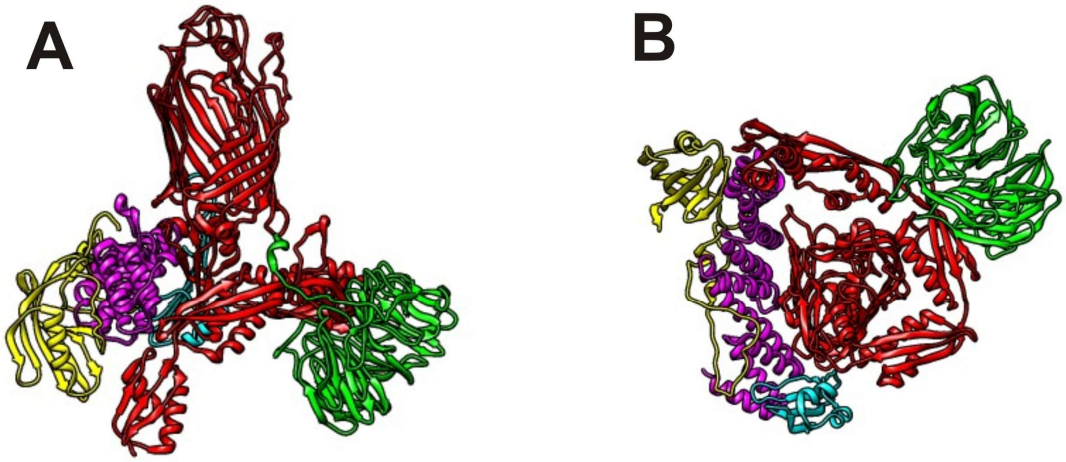

Figure 1.12. Solved cryo-EM structure of the Bam complex. (A) The cryo-EM structure of the Bam complex with the lateral gate between β stands 1 and 16 of BamA (red) facing forwards. To the right of BamA is BamB (green). To the left of BamA in a complex is BamD (pink), BamC (yellow) and BamE (blue). (B) View of the Bam complex from underneath, showing the POTRA domains of BamA interacting with the Bam lipoproteins to form a ring like structure (Iadanza *et al*., 2016).

1.6 *Salmonella enterica* autotransporter proteins.

S. Typhimurium SL1344 has four characterised Type 5 secreted proteins: 3 type 5a proteins (MisL (Dorsey *et al*., 2005), ShdA (Kingsley *et al*., 2002), and ApeE (Carinato *et al*., 1998)) and 1 type 5c (SadA (Raghunathan *et al*., 2011)). Some of these proteins have been investigated for their role in *S*. Typhimurium virulence, but for the most part, their contribution to virulence have not been extensively studied. ShdA and MisL were shown to bind to extracellular matrix molecules and be required for faecal shedding in mice (Dorsey *et al*., 2005, Kingsley *et al*., 2000), and SadA was shown to promote biofilm formation and to be partially required for pathogenesis (Raghunathan *et al*., 2011). ApeE has not been investigated in an infection setting to date. Both SadA and ApeE will be discussed in detail below.

1.6.1 The *Salmonella* and *Yersinia* trimeric autotransporters, SadA and YadA.

As described (section 1.5.2), the archetypal and most widely studied Type 5c protein is YadA from *Yersinia spp*. YadA is an important virulence factor that is important in bacterial attachment to host cells (Roggenkamp *et al*., 1996). Interestingly, YadA is mutated and not expressed in *Yersinia pestis* but is believed to be the major virulence factor in *Y. enterocolitica* and *Y. pseudotuberculosis* (Pepe *et al*., 1995). YadA forms a trimer of around 180 kDa with the monomer of 55 kDa.

SadA, from *S.* Typhimurium, was previously characterised as an important factor for adhesion and biofilm formation *in vitro* and *in vivo*. When overexpressed in *E. coli* K-12, SadA forms a trimer of approximately 500 kDa in size that promotes biofilm formation and autoaggregation *in vitro* (Raghunathan *et al*., 2011). SadA is not as important for *S.* Typhimurium virulence in a murine model of infection, in contrast with the role of YadA in *Yersinia* spp. infections. Although, evidence using a transposon

directed insertion site sequencing (TraDIS) method identified transposon insertions in *sadA* as less fit in a pig/ chicken model of infection suggesting that SadA might be a host-dependent virulence factor of *S.* Typhimurium (Chaudhuri *et al*., 2013). The structures of both YadA and SadA are summarised in Figure 1.13 (Hartmann *et al*., 2012). Both structures have been assembled to represent relative size difference, whereby SadA (left) forms a trimer that is much larger than that of YadA (right). Trimeric autotransporters are known to have different domains in their passenger domains: head; necks; and stalks (Figure 1.13 far right). YadA has one neck, head and stalk whereas SadA has interspersed head and neck domains throughout the structure of the passenger domain (Hartmann *et al*., 2012).

The outer membrane biogenesis of YadA has been shown to be dependent upon BamA (Lehr *et al*., 2010) but the requirement of the other Bam or Tam complex proteins have not been fully studied. The outer membrane biogenesis of SadA has also not been fully elucidated. A small lipoprotein termed SadB has been shown to assist in the trimer stability of SadA (Grin *et al*., 2014), whereby SadA is not detectable in the outer membrane in the absence of SadB. However, the requirement of Bam and Tam complexes have not been studied.

1.7 GDSL lipase autotransporters

1.7.1 Overview of GDSL lipase/esterases.

GDSL lipases are a group of proteins that carry a common sequence motif comprising glycine-aspartic acid-serine-leucine where the serine in this motif forms part of the catalytic triad in the active site of the enzyme (Upton and Buckley, 1995). The definition was broadened to include a class of lipases known as the SGNH

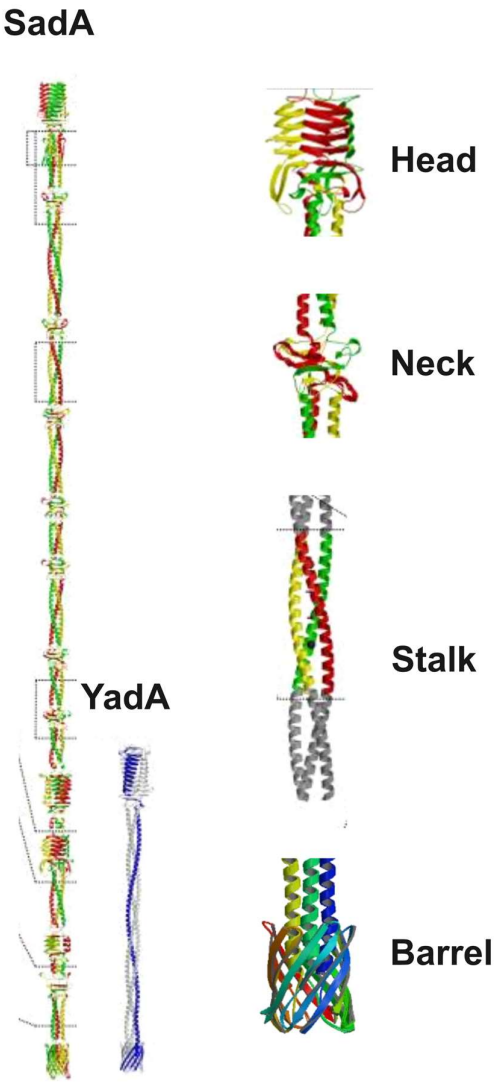

Figure 1.13. Comparison of the protein structures of SadA and YadA. Modified from Hartmann (2012). The crystal structures of fragments of trimeric autotransporters were reconstructed and arranged based on relative size. SadA (left) forms a structure that extends approximately 108 nm away from the bacterial cell surface. YadA (right) forms a trimer that extends approximately 35 nm from the cell. Both SadA and YadA have the domains associated with trimeric autotransporters, such as β-barrel, stalk neck and head domains. However, YadA has only one of each, whereas SadA has dispersed head and neck domains along the stalk.

hydrolase family (Akoh *et al*., 2004) as members of the GDSL/SGNH lipase family typically show low sequence identity, but have 5 conserved blocks, termed blocks I-V, that are important for lipase activity (Upton and Buckley, 1995). Block I contains the catalytic Serine and this is usually found at the N-terminus of the protein. Block II contains a Glycine that forms part of the oxyanion hole, block III contains Asparagine which also contributes towards the oxyanion hole and block V contains the catalytic Histidine. The lipase activity of these enzymes follows a classical nucleophilic attack on the ester bond mediated by the active site serine (Akoh *et al*., 2004).

GDSL lipase proteins exist throughout the tree of life. They are especially prevalent in plants and are involved in the breakdown and synthesis of waxy cuticles (Volokita *et al*., 2011, Akoh *et al*., 2004). These proteins also exist in bacteria, with many being involved in pathogenesis. For example, the *Salmonella* GDSL lipase protein SseJ is responsible for the degradation of *Salmonella* Induced Fibres (SIFs) within the SCV, and has shown *in vitro* phospholipase activity in the presence of an unknown eukaryotic factor (Ruiz-Albert *et al*., 2002, Lossi *et al*., 2008).

Some GDSL proteins are autotransporters. This class of autotransporters have the classical conserved blocks of GDSL lipases in the secreted passenger domain and the catalytic Serine is located at the extreme N-terminus of the secreted passenger domain (Wilhelm *et al*., 2011). These autotransporters usually fall into the Type 5a autotransporters, but differ from the majority as the passenger domains adopt a globular fold rather than the right handed β-helical fold characteristically associated with Type 5a proteins (Wilhelm *et al*., 2011, Cai *et al*., 2017, van den Berg, 2010). An example of this unusual passenger domain conformation is exemplified by comparing the solved crystal structures of the *P. aeruginosa* GDSL autotransporter EstA with the crystal structure of other Type 5a autotransporters (Figure 1.14). *S. enterica* has a

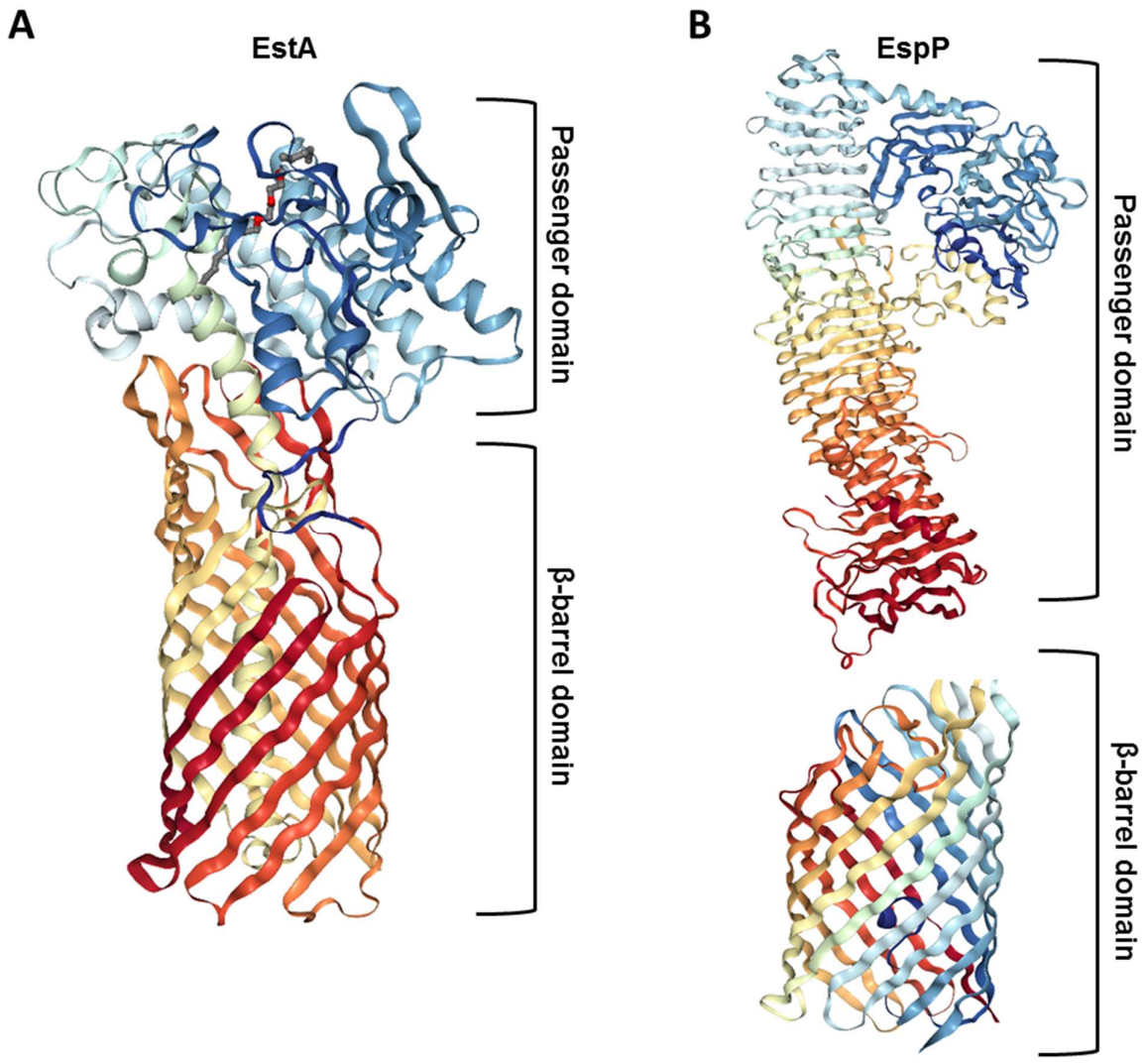

Figure 1.14. Comparison of the protein structures of EstA and EspP. (A) The solved crystal structure (2.5 Å resolution) of EstA from *P. aeruginosa* (protein database (PDB) 3KVN) (van den Berg, 2010). The structure shows that the β-barrel domain forms a regular autotransporter β-barrel but the passenger domain is rich in alpha helices. (B) The solved crystal structure (2.5 Å resolution) of the passenger domain of EspP (PDB 3SZE) (Khan *et al*., 2011) and the β-barrel domain (2.7 Å resolution) (PDB 2QOM) (Barnard *et al*., 2007). The passenger domain of EspP shows the classical right handed β-helical fold of T5aSS proteins.

homologue of EstA, known as ApeE, which shares 27% sequence identity overall, and both have conserved blocks of hydrolase activity (Schultheiss *et al*., 2008).

1.7.2 The *Salmonella* GDSL lipase autotransporter, ApeE.

ApeE is a classical Type 5a autotransporter that was first characterised as a napthyl esterase with no homologue in *E. coli* (Carinato *et al*., 1998). ApeE was shown to be able to cleave methylumbelliferyl caprylate (C8), which is a chromogenic substrate found in *Salmonella* isolation agar (Carinato *et al*., 1998). When the genetic locus encoding a high affinity phosphate transporter was knocked out, *apeE* was constitutively expressed, suggesting that *apeE* was under the regulatory control of the two component regulatory system that responds to phosphate limitation, termed PhoBR (Conlin *et al*., 2001).

ApeE has a GDSL lipase motif at the extreme N-terminus of its passenger domain, with the catalytic Serine (position 25) as part of the motif. The Aspartic acid and Histidine that form the catalytic triad are found at positions 326 and 329 respectively (Schultheiss *et al*., 2008). Previous work in our laboratory showed that ApeE was required for long term survival on tomatoes (Morris, 2013). ApeE was responsible for the degradation of tomato cutin, which is a polyester of hydroxylated palmitic (C_{16}) and oleic (C_{18}) fatty acids (Girard *et al*., 2012). Expression of *apeE* also enabled *S.* Typhimurium to grow utilising Tween80 as a sole carbon source in M9 minimal medium and this hydrolysis was abolished upon changing the active site Serine to an Alanine (Morris, 2013). To date, the role of ApeE during *S*. Typhimurium infections in animal models has not been fully investigated.

1.8 Aims and objectives

The overall aim of this study was to deepen the understanding of *S.* Typhimurium autotransporters. While the secretion of classical, Type 5a, autotransporters has been studied, the biogenesis of trimeric autotransporters has not been fully investigated, although a small lipoprotein termed SadB has been shown to assist in the trimer stability of SadA (Grin *et al*., 2014). In this study, the roles of the Bam and Tam complex components for the outer membrane biogenesis of both SadA and YadA were investigated.

The roles of the *Salmonella* autotransporters during infection have been partially investigated previously (Raghunathan *et al*., 2011, Dorsey *et al*., 2005, Kingsley *et al*., 2000, Chaudhuri *et al*., 2013), however, the combined role of these proteins for virulence in a murine model of infection has yet to be fully investigated. ApeE has not been investigated for a role for virulence, and even though attempts have been made to characterise ApeE, the biological substrates, enzyme activity and interaction with the host has largely eluded researchers. This study aims to investigate all of these outstanding gaps in the knowledge of ApeE, and to address whether or not ApeE is required for *Salmonella* pathogenesis.

Thesis objectives:

1. Chapter 3 will determine the roles of the Bam and Tam complexes in secreting trimeric autotransporters.
2. Chapter 4 will determine the contribution of the *Salmonella* autotransporter proteins to virulence, focusing on their conservation to identify factors that may be important for colonisation of certain bodily organs.

3. Chapter 5 will establish the biochemical conditions and kinetics of ApeE lipase activity *in vitro*.
4. Chapter 6 will determine the biological substrates of ApeE, focusing on phospholipid substrates. This chapter will also explore the advantage of ApeE mediated hydrolysis of phospholipids as a carbon and/or phosphate source for *S*. Typhimurium growth *in vitro*.
5. Chapter 7 will investigate whether ApeE contributes towards the virulence of *S.* Typhimurium in a murine model of infection.

CHAPTER 2

Materials and Methods

2.1 Culture media, growth conditions and strains

2.1.1 Bacterial strains and plasmids.

All bacterial strains and plasmids used in this study are described in Tables 2.1 and 2.2 respectively.

2.1.2 Standard laboratory growth conditions.

All bacteria were cultured in liquid Lysogeny broth (LB) at 37°C with shaking unless stated otherwise. To generate LB agar, 1.5% (w/v) technical agar was added to LB before autoclaving. If needed, the culture medium was supplemented with 100 µg/ml ampicillin, 100 µg/ml carbenicillin, 50 µg/ml kanamycin or 33 µg/ml chloramphenicol. For overnight liquid growth, 5 ml of LB was inoculated with a single colony, and grown for 16 h at 37°C with shaking. For larger growth volumes, overnight cultures were inoculated into fresh media at a 1:100 dilution and grown under the specific conditions required for the experiment.

2.1.3 M9 minimal medium preparation.

M9 minimal medium was made using 5 x M9 salts (Sigma Aldrich) and supplemented with 200 mM $MgSO_4$, 1 mM $CaCl_2$ and 30 µg/ml L-histidine. The desired carbon source was added and this was either 0.4% (w/v) glucose, 1 mg/ml lyso-phosphatidylcholine (Sigma Aldrich), lyso-phosphatidylglycerol (Avanti) or 50 µg/ml glycerophosphocholine (Sigma Aldrich). To make M9 minimal agar, 1.5% (w/v) technical agar was added to M9 liquid medium before autoclaving. Cultures were grown at 37°C with aeration unless stated otherwise.

Table 2.1 Strains used in this study

Name	Description	Reference
S. Typhimurium SL1344	*Salmonella enterica* serovar Typhimurium	(Wray and Sojka, 1978)
SL1344 *apeE::aph*	*apeE* gene replaced with the kanamycin resistance cassette	(Morris, 2013)
SL1344 *fadD::aph*	*fadD* gene replaced with the kanamycin resistance cassette	This study
SL1344 *fadL::aph*	*fadL* gene replaced with the kanamycin resistance cassette	This study
SL1344 Δ*glpT*	*glpT* gene deletion	This study
SL1344 *glpQ::aph*	*glpQ* gene replaced with the kanamycin resistance cassette	This study
SL1344 *ugpQ::aph*	*ugpQ* gene replaced with the kanamycin resistance cassette	This study
SL1344 Δ*ugpQ glpQ::aph*	*ugpQ* gene deletion with *glpQ* gene replaced with the kanamycin resistance cassette	This study
SL1344 *mlrA::aph*	*mlrA* gene replaced with the kanamycin resistance cassette	This study
S. Typhimurium SL3261	Δ*aroA* derivative of SL1344	(Hoiseth and Stocker, 1981)
SL3261 *apeE::aph*	*apeE* gene replaced with the kanamycin resistance cassette	This study
SL3261 SLATs	5 autotransporter deletion strain: Δ*misL* Δ*yaiU* Δ*apeE* Δ*sadA shdA::aph*	(Morris, 2013)
E. coli HB101	Laboratory non-aggregating *E. coli* strain	(Boyer and Roulland-Dussoix, 1969)
E. coli BL21 DE3	*E. coli* DE3 T7 express, protein expression strain	Invitrogen

Table 2.1 Strains used in this study continued

Name	Description	Reference
E. coli BL21 LOBSTRIL	BL21 DE3 with *arnA*(H359S, H361S, H592S, H593S)	(Andersen *et al*., 2013)
E. coli DH5α	Highly efficient competent cells, derived from DH5α	New England Biolabs
E. coli BW25113	K-12 derivative	(Baba *et al*., 2006)
JWD3	*E. coli* K-12 BamA depletion strain.	(Lehr *et al*., 2010)
JCM290	*E. coli* K-12 BamD depletion strain.	(Malinverni *et al*., 2006)
E. coli HB101 *bamB::aph*	Part of the *bamB* gene replaced with a kanamycin cassette	(Rossiter *et al*., 2011)
E. coli HB101 *bamC::aph*	Part of the *bamC* gene replaced with a kanamycin cassette	(Rossiter *et al*., 2011)
E. coli HB101 *bamE::aph*	Part of the *bamE* gene replaced with a kanamycin cassette	(Rossiter *et al*., 2011)
E. coli BW25113 *tamA::aph*	*tamA* gene replaced by kanamycin cassette	(Morris, 2013)
E. coli BW25113 *tamB::aph*	*tamB* gene replaced by kanamycin cassette	(Morris, 2013)

Table 2.2 Plasmids used in this study

Plasmid	Description	Reference
pET26B+	T7 expression vector, kanamycin resistance	Novagen
pJR01	*sadA* gene cloned in between the NdeI and EcoRI sites of pET26b(+)	This study
pDJSVT87	pACYCDuet-1 with *E. coli* OmpA signal sequence (residues 1-27) followed by a poly His tag and multiple cloning site.	(Casasanta *et al.*, 2017)
pJR02	*apeE* gene cloned between the KpnI and XhoI sites of pDJSVT87	This Study
pJR03	$apeE_{S35A}$ gene cloned between the KpnI and XhoI sites of pDJSVT87	This study
pET22b+	T7 expression vector, ampicillin resistance	Novagen
pJR04	Passenger domain of *apeE* cloned with an N-terminal 6-His tag between NdeI and XhoI sites of pET17b+	This study
pJR05	Passenger domain of *apeE* S35A cloned with an N-terminal 6-His tag between NdeI and XhoI sites of pET17b+	This Study
pQE60*	pQE60 with added NdeI restriction site in the multiple-cloning site and previously existing NdeI site removed	(Raghunathan *et al.*, 2011)
pQE60-*apeE*	*apeE* cloned between NdeI and HindIII sites in pQE60	(Morris, 2013)
pQE60-*apeE* S35A	$apeE_{S35A}$ cloned between NdeI and HindIII sites in pQE60	(Morris, 2013)
pDR03	*sadA* and *sadB* genes cloned into NdeI and HindIII sites in pQE60	(Raghunathan *et al.*, 2011)
pIBA2-YadA	*yadA* gene in anhydrous tetracycline-inducible expression vector pASK-IBA2	(Grosskinsky *et al.*, 2007)
pKD46	Plasmid expression λ-red recombinase, temperature sensitive	(Datsenko and Wanner, 2000)
pCP20	Plasmid encoding Flp recombinase, temperature sensitive	(Datsenko and Wanner, 2000)

2.1.4. MOPS minimal medium preparation

3-(N-morpholino)propanesulfonic acid (MOPS) minimal media was made up of components described in Table 2.3. The MOPS mix was made without a carbon or phosphate source, as these were added in when needed. All MOPS minimal media was supplemented with 30 µg/ml L-Histidine. 0.4% Glucose (w/v) or 0.5 mg/ml glycerophosphocholine were added as a carbon source. For a phosphate source, either 1.32 mM K_2HPO_4 or 0.5 mg/ml glycerophosphocholine (Sigma Aldrich) was added. All media was filter sterilised using 0.22 µM sterilisation units before use.

2.1.5 Microtitre plate growth assays.

Growth curves were achieved using 96 well microtitre plates (Corning). Bacterial strains from overnight cultures (approximately 10^9 cfu) were washed twice in either sterile phosphate buffered saline (PBS) or MOPS mix and were resuspended finally in 1 ml. Minimal media (MOPS or M9 based) was added to 96 well plates and bacterial strains were inoculated into the growth media to a starting OD_{600nm} of 0.02 in 200 µl. The outside wells of the plate were never used and all experiments contained wells with media only to account for background OD_{600nm} measurements. The plates were incubated at 37°C for 24 h with the OD_{600nm} measured every 15 min, with shaking in a Clariostar plate reader. The data were analysed using Microsoft excel, and Graphpad Prism.

2.1.6 Spot plating of bacterial dilution series onto agar plates.

Approximately 10^9 cfu from overnight cultures were washed twice in sterile PBS and finally resuspended in 1 ml PBS. The strains were diluted 1:10 into sterile PBS. 1.5 µl of each dilution was spot plated onto M9 minimal agar. The plates were incubated at 37°C for 16-30 h.

Table 2.3 MOPS minimal media composition

Component	Concentration (mM)
MOPS	40
Tricine	4
$FeSO_4$	0.01
NH_4Cl	9.5
K_2SO_4	0.28
$CaCl_2$	$5.0x10^{-4}$
$MgCl_2$	0.525
NaCl	50
$(NH_4)_6Mo_7O_{24}$	$7.2x10^{-8}$
H_3BO_3	$1.0x10^{-6}$
$MnCL_2$	$2.4x10^{-8}$
$ZnSO_4$	$2.4x10^{-8}$

2.1.7 Repression of gene expression.

E. coli strains containing genes under the control of the arabinose promoter were grown overnight in 5 ml of LB supplemented with 0.05% L-arabinose and sub-inoculated into fresh LB also containing 0.05% L-arabinose to maintain gene expression. To repress gene expression, the strains were grown overnight in 5 ml supplemented with 0.05% L-arabinose to maintain expression and then sub-cultured into fresh LB supplemented with 0.05% fructose to repress expression. In both cases fresh cultures were inoculated with a 1:100 dilution of overnight culture and grown at 37°C for 3 h. LB agar was supplemented with 0.2% L-arabinose to grow the strains under replete conditions on agar plates.

2.2 Bacterial transformation

2.2.1 Chemical competent transformations.

A single colony of the appropriate strain was inoculated into 5 ml LB and grown overnight at 37°C. The following day, a 1:100 dilution of overnight culture was added to fresh LB and grown to mid-exponential phase at an OD_{600nm} of ~0.5. The cells were chilled on ice for 30 min and centrifuged for 10 min at 6,000 *g* at 4°C. The pellet was re-suspended in ¼ volume of ice cold 0.1 M $CaCl_2$ and placed on ice for 30 min. The cells were centrifuged again and re-suspended in $1/10^{th}$ volume of 0.05 M calcium chloride 10% glycerol (v/v) and stored on ice for at least 30 min before use. For transformation, purified vector DNA was mixed with 50 µl of competent cells in a 1.5 ml microcentrifuge tube and incubated on ice for 30 min. The mixture was heat shocked for 90 s using a 42°C water bath and placed on ice for 5 min. 900 µl of LB was added and the cultures were aerated at the appropriate temperature for 1 h. The cells were

pelleted at 6,000 *g* for 5 min and re-suspended in 100 µl of LB. The transformation was plated onto LB agar with the appropriate antibiotic(s) and supplements.

2.2.2 Electroporation

An overnight culture was diluted 1:100 into 100 ml of fresh LB and grown to an OD_{600nm} of ~0.6. Cultures were placed on ice for 30 min and centrifuged at 6,000 *g* for 10 min at 4°C. The pellet was washed three times by resuspension and centrifugation with decreasing volumes of ice cold H_2O and were finally re-suspended in 1 ml of H_2O. For transformation, 50 µl of cells were mixed with appropriate concentrations of purified plasmid or linear DNA. The mixture was transferred to a 2 mm electroporation cuvette (Cell Projects) and pulsed at 2,200 V, with the immediate addition of either 1 ml SOC medium (New England Biolabs) or fresh LB. The cells were recovered in a 15 ml centrifuge tube to recover for 1-2 h in a shaking incubator at either 37°C or 30°C with aeration. The transformation was then plated onto LB agar with the appropriate antibiotic and incubated overnight at an appropriate temperature, usually 37°C.

2.3 Molecular biology techniques

2.3.1 Preparation of DNA

Plasmid DNA was extracted using the Qiagen mini prep kit following the manufacturer's instructions. Genomic DNA was extracted using the genome extraction kit by Stratec RTP Bacteria DNA Mini kit following the protocol for Gram-negative bacteria. All DNA samples were double eluted in nuclease free water (Ambion).

2.3.2 Polymerase chain reaction

Primers used in this study are described in Table 2.4. Fragments used for cloning and chromosomal mutations were amplified using either Phusion High-Fidelity

Table 2.4 Primers used in this study

Key	Primer name	Sequence (5'-3')	Description
P1	apeE_N_his_cyto_ndeI_F	TTAACATATGGGCCATCATCATCATCATCATCATCATCACAGCAGCGGCCATATCGAAGGTCGTTTTGACTCTCTTACGGTG	Forward primer to clone the passenger domain of *apeE* with an Nde1 restriction site and N-terminal poly-Histidine tag
P2	apeE_cyto_xhoI_R	AACGCTCGAGTCAACCAACAGGATTTTCCCCCTG	Reverse primer to clone the passenger domain of *apeE* with a XhoI restriction site
P3	T7_F	TAATACGACTCACTATAGGG	Forward primer to check pET based vectors constructs.
P4	T7_R	GCTAGTTATTGCTCAGCGG	Reverse primer to check pET based vectors constructs.
P5	apeE_16b_kpn1_F	TTAAGGTACCTTTGACTCTCTTACGGTG	Forward primer for cloning the passenger domain and β-barrel of *apeE* into pDJSVT87 with a KpnI restriction site
P6	apeE_16b_xho1_R	AACGCTCGAGTCAAAATCGGGCGCTAAAC	Reverse primer for cloning the passenger domain and β-barrel of *apeE* into pDJSVT87 with a XhoI restriction site
P7	apeE_check_F	TAATAATTTGCAGCCACAGGC	Forward primer for amplifying the *apeE* locus
P8	apeE_check_R	CTGTTAGTGAACATCCGGCT	Reverse primer for amplifying the *apeE* locus
P9	fadD_KO_F	CCTTATGGCTATGGCGGTTGG	Forward primer for amplifying the *fadD* locus
P10	fadD_KO_R	CCTACGCTTCTCTCCATAGAACG	Reverse primer for amplifying the *fadD* locus
P11	fadL_KO_F	GGCATTCGCCTCTCCAGTCG	Forward primer for amplifying the *fadL* locus
P12	fadL_KO_R	CGTGGTTGACCTGGCCAATG	Reverse primer for amplifying the *fadL* locus
P13	glpQ_KO_F	TAATGTTGATCGGTCTGCACG	Forward primer for amplifying the *glpQ* locus

Table 2.4 Primers used in this study continued

Key	Primer name	Sequence (5'-3')	Description
P15	ugpQ_KO_F	TACCGATAGGTGCGGACTATC	Forward primer for amplifying the *ugpQ* locus
P16	ugpQ_KO_R	GCAGTTGAATGCCAATACGCA	Reverse primer for amplifying the *ugpQ* locus
P17	mlrA_KO_F	AGCCACGCAATGACCAGAAACACG	Forward primer for amplifying the *mlrA* locus
P18	mlrA_KO_R	GCCAGTACGTTAGGCACGCCGATC	Reverse primer for amplifying the *mlrA* locus
P19	Kan_internal_F	CCTGCAAAGTAAACTGGATG	Forward primer that anneals to the *aph* gene
P20	Kan_internal_R	CATGCTCTTCGTGCAGATCA	Reverse primer that anneals to the *aph* gene
P21	glpT_KO_F	GTTTGCGAGTCGCGAGTTTTC	Forward primer for amplifying the *glpT* locus
P22	glpT_KO_R	GGTCAGCGACGTCAGTCACC	Reverse primer for amplifying the *glpT* locus

DNA Polymerase (New England Biolabs) with the use of 5x GC buffer and 3% (v/v) DMSO or Q5® hot start mastermix (New England Biolabs). Unless otherwise specified the thermocycling conditions for Phusion PCR were as in Table 2.5 and Q5 PCR are described in 2.6. PCR products amplified by Phusion were purified using the Qiagen QIAquick PCR purification kit. For colony PCR, MyTaq Red Mix (Bioline) was used. A small amount of bacterial colony was added to 10 µl of nuclease free water (Ambion) and boiled for 5 min at 98°C before addition of the Mytaq Red Mix and primers. The annealing temperature of 55°C was used (unless otherwise specified) for thermocycling reactions.

2.3.3 Agarose gel electrophoresis

Separation of DNA fragments was achieved using 1% (w/v) agarose (Bioline) gels in 1 x TAE buffer (50 x TAE buffer: 2 M Tris, 1 M acetic acid, 0.05 M EDTA in water) with Midori Green (Nippon Genetics) as the DNA dye. Samples were loaded using 5 x DNA loading buffer Blue (Bioline), with the exception of PCR products from MyTaq Red Mix, which includes a dye. Samples were separated using 1% (w/v) agarose using 1 x TAE buffer at 100 – 120 V until the loading dye had run sufficiently. All gels were loaded with Hyperladder 1 kb (Bioline) as a marker. Analytical gels were viewed under UV light (300 nM) in a Gel Doc (Bio-Rad), and preparative gels were viewed in a blue light LED illuminator (Geneflow).

2.3.4 Cloning

Plasmids used for cloning were digested with two restriction enzymes. For cloning into the expression vector pET22b+, *Nde*I and *Xho*I FastDigest enzymes (Thermo Scientific) were used for double restriction digest and for cloning using pDJSVT87 *Kpn*I and *Xho*I FastDigest enzymes (Thermo Scientific) were used. The

Table 2.5 Conditions for Phusion PCR

Step	Temperature (°C)	Time	Number of cycles
Initial Denaturing	98	30 s	X 1
Denaturing	98	10 s	
Annealing	45-72	30 s	X 30
Extension	72	30 s	
Final extension	72	10 min	X 1

Table 2.6 Conditions for Q5® hot start PCR

Step	Temperature (°C)	Time	Number of cycles
Initial Denaturing	98	30 s	X 1
Denaturing	98	10 s	
Annealing	45-72	30 s	X 30
Extension	72	30 s	
Final extension	72	10 min	X 1

PCR fragment to be cloned into each vector were digested with corresponding enzymes. 1,000 ng of plasmid DNA or linear DNA were used for the digestion reaction and were incubated at 37°C for an appropriate time and the digested products were separated by agarose gel electrophoresis. Bands at the appropriate size were excised from the agarose gel and the DNA extracted using the Qiagen QIAquick Gel Extraction kit. To prevent vector re-ligation, the digested vector DNA was treated with Calf Intestinal Phosphatase (CIP) for 30 min. Both vector and insert DNA was quantified using a Qubit fluorometer (Thermo Fisher) following manufacturer's guidelines. The quantified insert was ligated into the vector at a 3:1 ratio with at least 50 ng of vector DNA, using T4 ligase (NEB). After incubation at 16°C overnight, half of the ligation mixtures were transformed into NEB 5-alpha Competent *E. coli* (High Efficiency) and plated onto Luria agar with appropriate antibiotics.

2.3.5 Datsenko and Wanner method for gene inactivation

A modified version of Datsenko and Wanner (2000) was used to generate chromosomal deletions on the *S.* Typhimurium SL1344 or SL3261 chromosome. A collection of single gene disruptions in *S. enterica* Typhimurium ACTT 14028S (Porwollik *et al*., 2014) were used as the template for all knockout gene fragment PCR. Primers were designed to anneal ~200 bp up and downstream of the genes of interest. The resulting PCR fragment would contain the kanamycin (*aph*) resistance cassette flanked by ~200 bp of homology to the 3` and 5` ends of the gene of interest. The linear fragment was purified using the Qiagen PCR purification kit and the DNA quantity determined using a Qubit fluorometer (Thermo Fisher) following the manufacturer's instructions.

The intended recipient strain was made electrocompetent and transformed with the temperature sensitive λ recombinase vector pKD46. The transformed strain was grown in 100 ml LB supplemented with 100 µg/ml carbenicillin and 0.2% L-arabinose to induce production of the λ recombinase at 30°C until OD_{600nm} of 0.6 and then the cells were made electrocompetent. One µg of purified linear fragment DNA was electroporated into the intended recipient strain and plated onto agar plates containing 50 µg/ml kanamycin and incubated overnight at 37°C. Colonies were screened on agar containing 50 µg/ml kanamycin and separately onto agar plates containing 100 µg/ml carbenicillin and the mutation confirmed by colony PCR. A change in band size to reflect insertion of the kanamycin resistance cassette confirmed gene deletion.

2.3.6 Kanamycin cassette removal

To generate deletion strains without the kanamycin resistance cassette, confirmed mutants were made electrocompetent and were transformed with a plasmid expressing the yeast Flp recombinase, pCP20. Cells were recovered at 30°C and to remove the kanamycin resistance cassette, single colonies were inoculated into 5 ml of LB broth and incubated for 6 h at 37-42°C. Cultures were patch plated onto plain LB agar plates and agar plates supplemented with kanamycin and carbenicillin. Loss of the kanamycin cassette and pCP20 was confirmed by patch plating and PCR.

2.4 DNA sequencing

2.4.1 Genome sequencing

Strains for sequencing were sent to MicrobesNG sequencing service, University of Birmingham, which uses an Illumina MiSeq or HiSeq platform. Single nucleotide polymorphisms (SNP) and short insertion/deletions (indel) calling compared to the

chosen reference strain and aligned reads were browsed manually using Artemis Comparison Tool.

2.4.2 Plasmid sequencing

Plasmids were sequenced using the Functional Genomic Unit, University of Birmingham or Source Bioscience. In a 10 µl sequencing reaction there was 200-500 ng of vector DNA and 3.2 pmol of sequencing primer. The service uses the capillary sequencer ABI 3730.

2.5 Protein analysis

2.5.1 SDS-PAGE analysis

Protein samples were analysed on Tris-glycine gels with 10% resolving and 6% acrylamide stacking gels made in 1 mm gel casts (BioRad) unless stated otherwise. The resolving gel contained 10% acrylamide (Protogel) resolving buffer (0.75 M Tris pH 8.8, 1% (v/v) SDS, 0.5% (v/v) ammonium persulphate (APS) and 0.05% (v/v) of TEMED). The stacking gel contained 6% acrylamide (Protogel), stacking buffer (0.25 M Tris, pH 6.8), 1% (v/v) SDS, 0.5% (v/v) APS and 0.05% (v/v) TEMED). Protein samples were loaded in 2 x Laemmli sample buffer (Sigma Aldrich). Protein samples were separated at 100 V until the loading dye reached the resolving gel and then the voltage was increased to 120-130 V until the samples had reached the bottom of the gel. Gels were stained with R-250 Coomassie Brilliant Blue (Thermo Fisher Scientific) for 30 min and de-stained with de-stain solution (10% (v/v) glacial acetic).

2.5.2 Western immunoblotting

Protein samples were separated by 10% SDS-PAGE gels and transferred to a nitrocellulose membrane using iBlot (Invitrogen) dry transfer system. Membranes were

blocked for 1 h in either 5% (w/v) skimmed milk in Tris buffered saline (TBS), pH 8.4 or 3% bovine serum albumin (BSA) (Sigma Aldrich). After blocking, membranes were incubated for either 1 h or overnight with primary antibody diluted in either milk solution or 3% (w/v) BSA. Antibodies were diluted to appropriate dilutions; anti-His tag antibodies were used at a 1:10,000 dilution and anti-ApeE antibodies were used at a 1:5,000 dilution. After incubation, membranes were washed 3 times with TBST (1 x TBS 1% (v/v) Tween80). Secondary antibody diluted in either 5% (w/v) skimmed milk solution or 3% (w/v) BSA and incubated with the membrane for 30-60 min at room temperature. Anti-rabbit and anti-mouse IgG alkaline phosphatase conjugated antibodies raised in goats (Invitrogen) were used at a 1:10,000 and 1:30,000 dilution respectively. Anti-mouse IgG horse radish peroxidase (HRP) conjugated antibody was used at a 1:30,000 dilution. Immunoblots using alkaline phosphatase conjugated antibodies were detected using the substrate NBP-BCIP (nitroblue tetrazolium chloride–5-bromo-4-chloro-3′-indolylphosphate) (Sigma Aldrich). HRP immunoblots were developed using ECL Prime Western Blotting Detection Reagent (Amersham), and exposed to Hyperfilm ECL (Amersham) for between 5 s and 5 min.

2.5.3 Gene overexpression for protein analysis

For the expression of proteins for phenotypic and whole cell lipase activity assays, T7 vectors were induced with 0.5 M Isopropyl β-D-1-thiogalactopyranoside (IPTG), and pASK plasmids were induced with 200 pM of anhydrous tetracycline. Under all induction conditions, overnight cultures were inoculated 1:100 into fresh LB and incubated at 37°C until an OD_{600nm} 0.4-0.6. At mid-exponential phase (OD_{600nm} 0.4-0.6) induced was added at the appropriate concentrations. The induced cultures were incubated at 37°C for 3 h to allow protein expression.

2.5.4 Gene overexpression for protein purification.

For expression of proteins for protein purification, the genes were cloned into pET22b+ and included a modified N-terminal poly histidine tag instead of a C-terminal tag. The cloned plasmids were transformed into either BL21 DE3 or BL21 LOBSTRIL (Andersen *et al*., 2013). Transformants were incubated overnight at 37°C with 100 µg/ml carbenicillin. The following day, 2 L of 2 x LB was inoculated with a 1:100 dilution of overnight cultures and grown at 37°C with aeration until OD_{600nm} of ~0.6. The cultures were cooled to 16°C before induction with 50 µM isopropyl β-D-1-thiogalactpyranoside (IPTG) and growth for 16 h.

2.5.5 Protein purification

2 L of induced cultures were pelleted by centrifugation at 5,000 *g* for 15 min. The supernatant was discarded and the pellet re-suspended in lysis buffer (10 mM Tris, 20 mM imidazole, 400 mM NaCl, 1 mM PMSF pH 7.5) and the cells were lysed using an Emulsiflex-C3 (Avestin, Germany) by passing the resuspended cells through the machine 5 times. Once cells were lysed, the cellular debris were removed by centrifugation at 6,000 *g* and the insoluble fraction subsequently removed by centrifugation at 50,000 *g*. The soluble fraction was either mixed with 5 ml of $NiCl_2$ charged chelating sepharose beads (GE healthcare, USA) or applied to a 1 ml His-trap column coated in Nickel-agarose beads overnight using a peristaltic pump. The columns were washed with 100-300 ml of wash buffer (20 mM Tris, 50 mM imidazole, 400 mM NaCl pH 7.5) before being eluted in 10 ml of elution buffer (20 mM Tris, 250 mM imidazole, 400 mM NaCl pH7.5). Purification fractions were analysed by SDS-PAGE and the purified protein was stored in a buffer containing 10 mM Tris, 250 mM NaCl pH 7.4.

2.5.6 Bio-rad protein assay

Standard protein concentrations of BSA (0.05-0.5 mg/ml) were added in duplicate to 96 well microtitre plates. Test proteins samples were also added in duplicate to a 96 well microtitre plate at appropriate concentrations to be within the range of the BSA standards. Bio-rad protein (Coomassie® brilliant blue G-250) was diluted 1:4 in distilled H_2O. The reagent was added to BSA standards and test samples and incubated at room temperature for 5 min. The OD_{595nm} was measured in a Clariostar plate reader. The protein concentrations in the test sample was calculated from the standard curve generated from the absorbance of the BSA standards.

2.6 Cellular fractionation methods

2.6.1 Whole cell protein extraction

Whole cell protein fractions were prepared using 1 ml of overnight culture centrifuged at 13,000 *g* for 5 min and re-suspended in 2 x Laemmli sample buffer (Sigma Aldrich). This mixture was boiled for 5 min at 100°C and centrifuged at 13,000 *g* for 2 min prior to loading onto SDS-PAGE gels.

2.6.2 Outer membrane protein preparation

Outer membrane protein fractions were prepared as previously described (Parham *et al*., 2004). Briefly, 50 ml of cultures were grown to an OD_{600nm} 1.0 (including 3 h of induction if needed). The pellet was resuspended in 20 ml 10 mM Tris-HCl pH 7.0 and sonicated to lyse cells. The supernatant was centrifuged at 50,000 x *g* for 45 min at 4°C to pellet whole membrane fractions. The membrane pellet was re-suspended in 10 mM Tris-HCl pH 7.0, 0.2% (v/v) Triton X-100 and left at room temperature for 15 min with shaking to solubilise the inner membrane. The membranes

were centrifuged at 50,000 *g* for 45 min at 4°C. The resulting pellets containing outer membrane fractions and were washed three times in 10 mM Tris-HCl pH 7.0 before final resuspension in 100 µl 10 mM Tris-HCl pH 7.0 and analysis by SDS-PAGE and Western Immunoblotting.

2.6.3 Lipopolysaccharide isolation

Strains of interest were inoculated in 5 ml of LB and grown overnight at 37°C. The equivalent of 1 ml of OD_{600nm} 1.0 cells were centrifuged at 10,000 *g* and resuspended in 100 µl of lysis buffer containing 1 M Tris, pH 6.8, 2% (w/v) SDS, and 4% (v/v) 2-mercaptoethanol. The cell suspension was boiled at 100°C for 10 min. Proteinase K (Qiagen) was added at a final concentration of 25 µg/ml and the lysate incubated for 1 h at 60°C. Samples were boiled for 10 min at 98°C. Lipopolysaccharide isolations were separated on SDS-PAGE gels and visualized using SilverQuest kit (Invitrogen) following manufacturers guidelines.

2.6.4 Cell phospholipid extraction

Cell phospholipids were extracted using a modified Bligh-Dyer method. Overnight cultures were centrifuged at 3220 *x g* for 10 min at 4°C. The pellets were resuspended in 1 ml HPLC grade H_20 and transferred to a fresh glass tube. To generate a one-phase solution, a mixture of chloroform: methanol (1:2) v/v was added to the cell suspension and vortexed vigorously. The single phase solution was incubated at 50°C for 30 min. To generate a two-phase solution, 1.25 ml of chloroform followed by 1.25 ml of H_20 was added and subsequently vortexed. The two phase solution was centrifuged at 1000 rpm in an IEC table-top centrifuge for 5 min at room temperature. The lower organic phase was removed by applying gentle positive-pressure through the top phase and extracting the bottom phase. The organic phase

was dried at 60°C under nitrogen flow. The phospholipid pellets were resuspended in chloroform prior to analysis by thin layer chromatography.

2.7 Lipid analysis

2.7.1 Bligh-dyer method of lipid extraction from liquid

Lipids were extracted from various solutions. After 24 h of bacterial growth in M9 minimal media supplemented with either 1 mg/ml of Lyso-PC or Lyso-PG, bacteria were pelleted by centrifugation at 6,000 *g* for 10 min and the culture medium filter sterilised using 0.2 µM filter units. 1 ml of culture medium was used for lipid extraction. For determining the interaction of ApeE with bile, purified ApeE was added to a final concentration of 2 µM to a solution of 5% ox bile (Sigma Aldrich) in water (w/v) and incubated for 12-36 h at 37°C. After incubation, 1 ml of solution was used for lipid extraction.

To the 1 ml of solution, 3.75 ml of 1:2 (v/v) solution of chloroform: methanol was added and the mixture vortexed vigorously. 1.25 ml of chloroform was added followed by vortexing and the addition of 1.25 ml of dH_2O and a final vortex. The tubes were centrifuged at 1000 rpm in an IEC table-top centrifuge for 5 min at room temperature to generate a bottom organic phase containing lipids and an aqueous top phase. Using a glass Pasteur pipette, the bottom organic phase was removed by applying gentle positive-pressure through the top phase and extracting the bottom phase. Some samples were washed with authentic upper phase at this step and the authentic upper phase was generated by following the same protocol mentioned above but using dH_2O instead of sample. The final bottom phase was dried at 60°C under Nitrogen flow. The pellets were resuspended in 100 µl of chloroform and stored at -80°C until required.

2.7.2 One direction Thin Layer Chromatography (TLC)

Silica gel 60 TLC plates (Merck Millipore) were cut 10 cm by 10cm (length x width). This size allowed for 1 cm gaps between samples and the edges of the plate. 10 µl of lipid samples were spotted onto the plate using 5 µl microcapillary tubes (Sigma Aldrich). The plates were placed in a humid chamber with an equilibrated solvent system, which depended on the lipid species being separated. For separating bile lipids, a solvent system of either chloroform: methanol: water (65:25:4) or chloroform: methanol: ammonium hydroxide (65:25:4) was used. For separating membrane lipids, a solvent system of chloroform: methanol: acetic acid (65:25:10) was used. The TLC plate remained in the solvent until the solvent front was ~1 cm from the top of the plate. The plate was left to dry thoroughly for 30 min at room temperature and stained with phosphomolybdic acid (PMA). The stained plate was heated with a hair-dryer to activate phosphomolybdic acid until lipid species became visible.

2.7.3 PIP strip™ phospholipid binding assay

PIP strip™ (Thermo Fisher) phospholipid arrays were used to determine the binding affinity of ApeE to a variety of phospholipids. These purchased PIP strips™ had 200 pmol of a variety of Phospholipid species spotted onto Polyvinylidene fluoride (PVDF) membrane. The PIP strips™ were incubated with a 3% BSA solution in TBST (w/v) for 3 h at room temperature. Purified ApeE (50 µg/ml) was diluted into 3% (w/v) BSA TBST and this was incubated with the PIP strip™ for 16 h at 4°C. After incubation, the BSA-protein solution was removed and the membranes washed vigorously in 3% (w/v) BSA TBST. Primary anti-ApeE antibody was diluted in 3% (w/v) BSA TBST 1:2,000 and this was incubated with the PIP strip™ for 1 h at room temperature. Following incubation, the membrane was washed vigorously in 3% (w/v) BSA TBST. The secondary goat anti-rabbit IgG antibody was diluted 1:1,000 into 3% (w/v) BSA

TBST and this was incubated with the membrane for 30 min at room temperature. The membranes were developed upon the addition of the alkaline phosphatase substrate NBP-BCIP. The reaction was stopped by the addition of distilled H_2O.

2.7.4. Targeted lipidomics by liquid chromatography mass spectrometry

Bile from mice was extracted and snap frozen in liquid nitrogen. The samples were processed and analysed by liquid chromatography mass spectrometry (LCMS) using an Agilent 6490 as a service by Metabolomics Australia, Bio21. Briefly, the frozen bile samples were thawed and resuspended in 95 µl of chilled chloroform: methanol (2:1) and vortexed for 30 s. The samples were centrifuged at 15, 000 rpm for 10 min. The supernatant was evaporated under a speedvac. The dried sample was reconstituted in water-saturated butanol and methanol (ratio 9:1) before MS analysis.

2.8 Lipase kinetic assays

2.8.1 Continuous enzyme kinetics

Purified proteins were quantified using a Bradford assay and diluted to 10 nM in appropriate buffer for each kinetic experiment. Lipase substrates 4-methylumbelliferyll heptanoate (4-muH), 4-methylumbiferyll butyrate (4-muB), 4-methylumbelliferyll palmitate (4-muP) and 4-methylumbelliferyll oleate (4-muO) (Santa cruz Biotechnology, USA). Each lipase substrate was stored as a stock solution of 50 mM in either DMSO (4-muH, 4-muB and 4-muO) or chloroform (4-muP). For continuous lipase enzyme kinetics, each lipase substrate was diluted in DMSO or chloroform to generate a range of substrate concentration from 0-200 µM in a buffer of 20 mM Tris, or 20 mM HEPES, 50 mM NaCl, 0.05% BOG at various pH. Each concentration of substrate had the same volume of DMSO/chloroform (0.4%). 90 µl of

each dilution were added to black 96 well microtitre plates in duplicate and for each assay, buffer only was added to each substrate dilution as well as a no substrate control. For test wells, 10 µl of the 10 nM stock solution of purified protein was added to substrate. Upon cleavage of the ester bond, the fluorescence molecule was (4-methylumbeliferone) realised. The fluorescence intensity was recorded using an emission= 449 nm and excitation= 360 nm every 2 min for 20 min on a SpectraMax M5e 644 plate reader.

To determine the concentration of product produced upon ester bond cleavage, standard curves of the fluorescence intensity of 4-methylumbeliferone (Sigma Aldrich) in each buffer system used was generated. Concentrations ranging from 0-10 µM of 4-methylumbeliiferone (Sigma Aldrich, USA) were added to 96 well black microtitre plates an endpoint reading was taken using a SpectreMax M5^{e} plate reader. The steady-state kinetic parameters for each substrate and buffer condition were determined using GraphPad prism version 7.04 by fitting the initial rate data (n=2) to the Michaelis-Menten equation: $\boldsymbol{v = V_{max}[S] / (K_M + [S])}$

2.8.2 IC_{50} inhibitor determination

The IC_{50} of enzyme inhibitors is the concentration of inhibitor added that results in the inhibition of enzyme by 50%. A known inhibitor of phospholipases, Methyl Arachidonyl fluorophosphonate (MAFP) (Cayman Chemical, USA), was used as a potential ApeE inhibitor. MAFP was diluted in reaction buffer (50 mM HEPES, pH 8.0, 50 mM NaCl, 0.05% BOG) at concentrations in the range 0-50 nM. Each dilution of MAFP was added to wells on a 96 well black microtitre plate. ApeE was added to a final concentration of 1 nM and the mix was incubated at RT for 30 min. To start the reaction, 10 µM of 4-muH was added. Fluorescence was monitored for 20 min at 26°C

with readings taken every 2 min (Ex = 360 nm, Em 449 nm) using a SpectreMax M5^{e} plate reader. Raw data (n=2) for the reactions was analysed using Graphpad prism.

2.8.3 ActivX TAMRA-fluorophosphonate serine hydrolase labelling.

ActivX TAMRA-fluorophosphonate (TAMRA-FP) was incubated with purified protein at room temperature for 20 min. TAMRA FP binds to active site serines and fluorescence was detected. After incubation, protein and TAMRA-FP samples were analysed by SDS-PAGE. TAMRA-FP was visualised using a G:Box XX6 system using the TAMRA fluorescence filter to detect TAMRA fluorescence.

2.8.4 Determining cell surface lipase activity.

Overnight cultures were diluted to an OD_{600nm} of 0.2 and washed twice with sterile PBS, and finally resuspended in 900 µl of PBS. For MAFP inhibition, 10 µM of MAFP was added to the cells for 60 min at room temperature. Samples with no MAFP added were also incubated at room temperature for 60 min. After incubation, the cells were washed twice with sterile PBS and resuspended in reaction buffer (20 mM HEPES, 50 mM NaCl, 0.1% BOG pH 8.0). Approximately $2x10^{6}$ cells were added to a 10 µM 4-muH in black 96 well plates. The fluorescence (Ex = 360 nm, Em 449 nm) was measured using a SpectreMax M5^{e} plate reader every 2 min for 20 min at 26°C.

2.8.5 Phospholipase A1 and A2 activity determination.

The phospholipase activity characterisation was achieved using EnzChek® phospholipase A_1 and A_2 kits (Invitrogen). A_1 and A_2 specific phospholipase substrates (PED-A1 and BODIPY® PC-A2 respectively) were incorporated into liposomes containing dioleoylphosphatidylglycerol (DOPG) and dioleoylphosphatidylcholine (DOPC) in reaction buffer 50 mM Tris-HCl, 100 mM NaCl, 1 mM $CaCl_2$, pH 8.9. The liposome mix was diluted 1:2 with either buffer only control or with protein in a black

96 well microtitre plate, resulting in final concentrations of A_1 or A_2 substrate of 1.65 µM and DOPG and DOPC at 16.5 µM. Purified protein was added at a concentration of either 1 or 10 µM. Fluorescence was measured using a Clariostar plate reader for 30 min every 2 min at 26°C. The excitation and emission wavelengths were 505 nm and 460 nm respectively.

2.9 *in vitro* infection techniques

2.9.1 Cell line maintenance.

Raw264.7 immortalised macrophage cells lines were maintained in full RPMI medium2 (RPMI, 10% foetal calf serum, 1% penicillin/streptomycin) at 37°C at 5% CO_2. HeLa cells were maintained in full RPMI as above, and supplemented with 2 mM L-glutamine at 37°C with 5% CO_2. Cells were maintained in 75 ml tissue culture flasks with fresh medium added every 2-3 days. At 80% confluency, the cells were used for infection assays.

2.9.2 Cell invasion and replication experiments.

Tissue culture cells ($5x10^5$) were seeded into tissue culture treated 12 well plates. Overnight cultures of bacterial strains were diluted 1:100 in fresh LB broth and grown until OD_{600nm} of 1.0. The cells were washed twice in sterile PBS and added to the tissue culture cells to a multiplicity of infection of 10. The cultures were incubated at 37°C for 1 h before washing and the addition of gentamicin (100 µg/ml) to kill non-intracellular bacteria. After varying incubation times, the tissue culture cells were lysed by the addition of 0.1% (v/v) Triton X-100 in PBS. Bacteria were enumerated by plating serial dilutions onto agar plates.

2.9.3 Serum bactericidal assays

Strains of interest were inoculated into 5 mL of LB and incubated overnight at 37°C. The following day, cultures were inoculated into fresh LB at a 1:100 dilution and grown until OD_{600} of 0.6. Approximately 10^9 bacterial cells were pelleted at 6,000 *g* for 5 minutes and washed twice with PBS and then diluted 1:10 into fresh PBS to generate the starting inoculum. 5 µL of starting inoculum was added to 45 µL of healthy human serum at either 100% or 50% (v/v) in PBS and incubated at 37°C. At regular intervals up to 180 minutes post inoculation, colony forming units (CFU's) were enumerated. As a control, complement factors in healthy serum were heat inactivated at 60°C for 1 hour. The serum bactericidal activity was plotted as the Log_{10} change in cfu in comparison to the starting inoculum.

2.10 Animal models of infection

2.10.1 Infection of C57BL/6 mice with *S.* Typhimurium

All animal experiments were ethically approved and carried out by personal licence number (I6237A091) (Jessica Rooke), under the project license (30/2850**)** at the Biomedical services unit and University of Birmingham. C57BL/6 mice (6 to 8 weeks old) infected either by I.P. (intra-peritoneally) with 5 x 10^5 organisms or orally with 10^7 organisms of appropriate *S*. Typhimurium strains. At experimental time-points, mice were humanely culled and the spleens, livers, gallbladders, faeces and blood collected. Livers and spleens were washed in sterile PBS and weighed. Spleens and livers were added to 5 ml of sterile PBS in stomacher bags (Starstedt, Australia) and homogenised using a stomacher®80 machine. Whole gallbladders were homogenised into 200 µl of sterile PBS. Serial dilutions of homogenised organs were plated onto

appropriate agar plates to determine the colony forming units (cfu). Data were represented as cfu/organ. 100 µl of blood was plated directly onto selective agar plates. To determine the bacterial burdens in murine faeces, samples were collected and weighed and homogenised in sterile PBS. The cfu/100 mg of faeces were determined by plating serial dilutions of faecal samples.

2.11 Microscopy

2.11.1 Immunofluorescence

Overnight cultures were diluted 1:100 into 5 ml of fresh LB and grown to an OD_{600nm} 1.0. 1 ml of culture was centrifuged at 10,000 *g* and resuspended in 1 ml PBS. The cells were fixed in 4% (v/v) paraformaldehyde and 10 µl spots were added to poly-l-lysine coated microscope cover slips. These slips were blocked with either 0.5% (w/v) BSA in PBS or 0.2% gelatin pH 7.5 before incubation for 1 hour in primary antibody diluted in either 0.5% BSA or gelatin. Either a 1:5,000 dilution of anti-YadA, 1:1,000 dilution of anti-SadA or 1:10,000 anti-polyhistidine tag were used. Cover slips were washed three times in PBS and then incubated in secondary antibody diluted in either 0.5% (w/v) BSA or gelatine. A 1:5,000 dilution of anti-mouse IgG Alexa Fluor 488 was used. Cells were imaged using fluorescence microscopy

2.12 Phenotypic screens

2.12.1 Microtitre plate biofilm assay

The ability of the strains to form biofilms was determined using a microtitre plate biofilm assay. Overnight cultures were inoculated into fresh M9 minimal medium to a

starting OD_{600nm} 0.02. These cultures were added in equal volumes to a 96 well microtitre plate and was incubated at 37°C overnight either in the Clariostar or static incubator. Following incubation, the cultures were removed from the plate and 150 µl of 0.1% crystal violet stain was added to each well for 30 min. After incubation of the stain, the plate was washed 3 times with distilled water and left to air dry. Bacteria adhered to the microtitre plate wells forming biofilms would retain the crystal violet stain after washing. Once the wells were dry, 150 µl 80:20 ethanol: acetone solution was added to de-stain the wells. The OD_{600nm} of the plate was determined using the Clariostar plate reader.

2.12.2 Extracellular matrix molecule binding assay

Bacterial adherence to extracellular matrix molecules was measured via growth. Overnight cultures were inoculated 1:100 into fresh LB and were grown to OD_{600nm} 1.0 at 37°C and expression of plasmids was achieved using the appropriate inducer for 2 h. 10^9 bacterial cells were washed in PBS and resuspended in 1 ml of PBS. Cells were added to microtitre plates coated with 20 µg/ml of collagen I isolated from rat tails (Sigma-Aldrich). BSA-coated wells (50 µg/ml) were used as a control. After 1 h incubation the wells were washed with PBS to remove non-adherent bacteria. Adherent cells were incubated in LB for a further 5 h prior to enumeration by direct colony counting on agar plates.

2.12.3 Autoaggregation assay

Aggregation of the strains was determined using an aggregation settling assay. Overnight cultures were inoculated 1:100 into fresh LB and grown until OD_{600nm} 0.6, at which point *yadA* expression was induced by anhydrous tetracycline. The cultures were grown and standardised to a final OD_{600nm} 1.0 and mixed vigorously for 15 s prior

to the start of the assay. Every 30 min, a 150 µl sample was taken approximately 0.1 cm from the liquid surface and transferred into a microtitre plate maintained on ice. At the end of the experiment, the OD_{600nm} values were measured using a Clariostar microtitre plate reader.

2.13 Bioinformatic analyses

2.13.1 Protein Clustering.

A representative set of 1,999 Lipase_GDSL proteins selected using the CD-HIT Suite at a cut-off of 30% protein identity were used in all-against-all searches in BLASTP with an e-value threshold of 1e-4 and 1e-20. Information about each protein (phylum, architecture, etc) was incorporated into the BLAST results based on the previous architecture designations and information from UniProt. Cluster diagrams were constructed using Cytoscape (v.3.3.0) (Shannon *et al*., 2003), where each node represents a single protein sequence and each line (or edge) represents a match below the e-value threshold.

2.13.2 Identification of homologues and phylogenetic tree construction

BLASTP was used to search all genome sequences of Gram negative bacteria using the protein sequence of ApeE. Putative ApeE homologs were verified by SMART sequence analysis to determine the proteins included an N-terminal signal sequence, Pfam: Autotransporter domain and a Pfam: Lipase_GDSL domain. Protein sequences were aligned using ClustalX (Thompson *et al*., 1997). Phylogenetic distances were estimated using the neighbour joining method of Saitou and Nei applying a distance matrix. The phylogenetic tree was drawn in MEGA 4 with incorporation of bootstrap values that were obtained involving 1000 replicates.

2.14 Statistics

Graphpad prism (version 7.04) was used for all statistical analyses. Statistical significance was determined by $p<0.05$ and the statistical analysis depended upon the comparison for each experiment. The most common statistical tests were Mann-Whitney non-parametric U tests, 1 way and 2 way anova and Student's T-test. Multiple comparisons were corrected using Graphpads inbuilt correction system for multiple comparisons. The details for the statistical analyses for each experiment are stated in the results.

CHAPTER 3

Investigating the mechanism of trimeric autotransporter biogenesis

3.1 Introduction

In *Escherichia coli,* the β-barrel assembly (Bam) complex is comprised of five factors, BamA-BamE (Rossiter *et al*., 2011, Jain and Goldberg, 2007, Voulhoux *et al*., 2003). BamA is an essential outer membrane protein (Knowles *et al*., 2008, Werner and Misra, 2005). Four periplasmic lipoproteins, BamB-BamE, form a non-covalent interaction with BamA to create the complex (Knowles *et al*., 2011, Wu *et al*., 2005). Like BamA, BamD is essential for viability (Malinverni *et al*., 2006). The remaining components are not critical for viability but their loss compromises the integrity of the outer membrane and the biogenesis of outer membrane proteins (Malinverni *et al*., 2006). Recent studies to assess the contribution of individual complex proteins to the biogenesis of T5aSS autotransporters in *E. coli* have shown that BamA and BamD are essential for their secretion (Rossiter *et al*., 2011). In contrast, BamB, BamC and BamE were not essential for the secretion or folding of the proteins (Rossiter *et al*., 2011). Furthermore, recently it was reported that the Translocation Assembly Machinery (Tam) complex was also required for efficient secretion of a folded protein via the T5aSS (Selkrig *et al*., 2012). The Tam complex consists of the integral outer membrane protein TamA and the integral inner membrane protein TamB. TamA shares structural similarity with BamA. However, the precise contribution of the Tam complex to the biogenesis of the T5aSS is yet to be elucidated.

In contrast to the T5aSS, the mechanisms for secretion of the other subclasses is less well understood. Proteins belonging to the T5cSS, or the Trimeric Autotransporter Adhesin (TAA) family, have key differences when compared to members of the T5aSS (Hernandez Alvarez *et al*., 2008, Linke *et al*., 2006). TAAs are defined by the presence of a short 70-100 amino acid C-terminal translocation domain, and thus the protein must form a homotrimer in order to generate a complete β-barrel

(Wells *et al*., 2010, Wells *et al*., 2007, Cotter *et al*., 2005). Consequently, unlike the passenger domains of the T5aSS, which predominantly adopt a monomeric β-helical conformation, the TAA passenger domains form a trimeric structure composed of oligomeric coiled-coil regions interspersed with distinct head and neck motifs (Linke *et al*., 2006). The molecular organisation of these proteins presents logistical challenges for the bacterium. For example, the trimer must assemble in a manner that is consistent with the secretion of large passenger domains (up to 5 MDa) to the bacterial cell surface; at the outer membrane each monomer must be maintained in a conformation that is consistent with pairing to its sister monomers; and monomers must be inserted into the outer membrane whilst being prevented from pairing with the nascent β-strands of non-partner proteins.

Previously, using the archetypical and widely studied TAA protein, YadA from *Yersinia,* it was demonstrated that BamA is essential for the assembly of a folded functional trimer into the outer membrane (Lehr *et al*., 2010). It was hypothesised that the other components of the Bam complex and/or the components of the Tam complex would play important roles in co-ordinating the assembly of the TAA homotrimer into the outer membrane. Here we tested this hypothesis by determining the impact that loss of each Bam and Tam component had on the assembly and function of two different TAAs.

3.2 Results

3.2.1 The requirement of BamA and BamD for the secretion of SadA and YadA.

Previously, it was determined that BamA was required for the biogenesis of the trimeric autotransporter YadA (Lehr *et al*., 2010). To determine if this observation was

true for other TAAs, the role of BamA for the biogenesis of a sequence divergent TAA, SadA, was investigated. An expression vector encoding full-length SadA (pDR03) was transformed into the BamA depletion strain *E. coli* JWD3 (Lehr *et al*., 2010). Overnight cultures of either HB101 wild-type, JWD3 with empty vector (EV) or pDR03 were inoculated 1:100 into fresh media. The expression of *bamA* in the BamA depletion strain JWD3, was either depleted with fructose or induced with arabinose for 3 h. After growth, outer membrane fractions were isolated using a TritonX-100 extraction method. The samples were analysed by SDS-PAGE and Western Immunoblotting using primary anti-SadA, BamA and OmpF/C antibodies. OmpF/C protein levels are known to be reduced under BamA depletion conditions. SadA could be detected in wild-type strains of *E. coli* and in *E. coli* JWD3 under BamA replete conditions (Figure 3.1A). In contrast, SadA levels were severely diminished from BamA-depleted cells (Figure 3.1A). The levels of OmpF/C were also depleted in the absence of BamA (Figure 3.1A).

BamD is the second component of the BAM complex that is vital for cell viability (Malinverni *et al*., 2006). To determine whether BamD is required for TAA secretion a similar method was followed. The BamD depletion strain (JCM290) was transformed with either EV or pDR03. Depletion of BamD was achieved as previously described for the BamA depletion described above. Outer membrane proteins were isolated from each strain and analysed by SDS-PAGE and Western immunoblotting with primary antibodies towards SadA, BamD and OmpF/C. The secretion of SadA to the outer membrane was investigated in a BamD depletion strain (JCM290). Similar to BamA, when BamD is depleted from the cell, the protein levels of SadA and OmpF/C are considerably depleted in the outer membrane (Figure 3.1B).

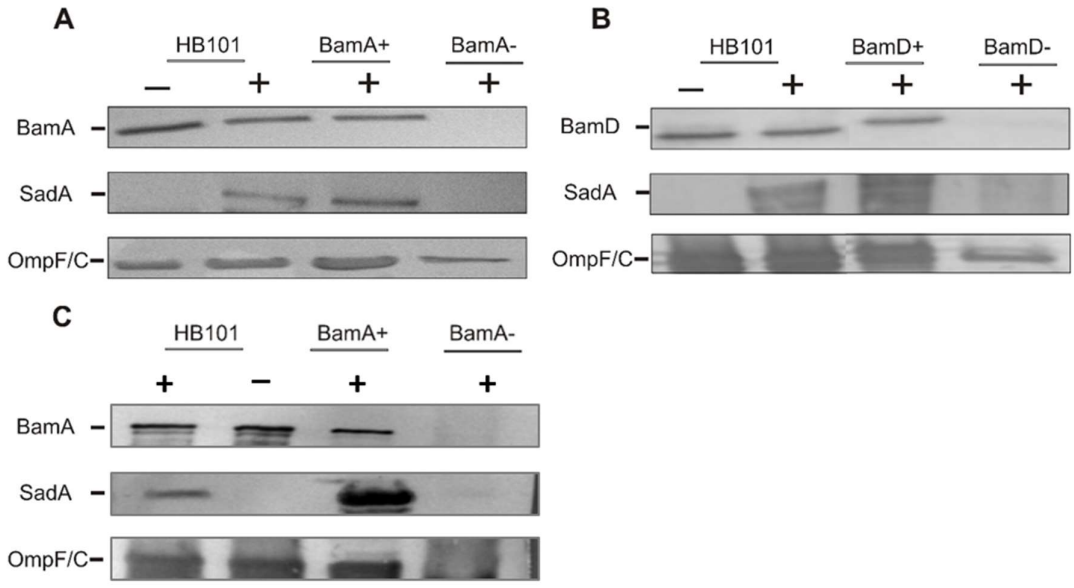

Figure 3.1. Western blot analysis of the BamA and BamD requirement for SadA and YadA outer membrane biogenesis (A) Western blot analysis of outer membrane fractions of HB101 and BamA depletion JWD3 strain (+/- depletion) with either empty vector (-) or pDR03 (SadA) (+) plasmids. Fractions were probed with anti-BamA, SadA, and OmpF/C. Bands indicate presence of the protein in the outer membrane. (B) Similar western blot analysis of HB101 and BamD depletion JCM290 strain (+/- depletion) with EV or SadA+ plasmids. Fractions were probed with anti-BamD, SadA, BamB and OmpF/C. SadA is not detectable in the outer membrane in the absence of BamA and BamD. (C) Western blot analysis of outer membrane fraction of HB101 and JWD3 depletion strain (+/- BamA) with either empty vector (-) or YadA (+).

To further confirm the observations that BamA is essential for the secretion of TAAs, a second trimeric protein (YadA) was investigated for secretion under BamA depletion conditions. HB101 and JWD3 were transformed with an expression vector cloned with *yadA* (pIBA2-YadA). After growth in the absence or presence of arabinose, the outer membrane proteins were isolated as previously described. The proteins were analysed by SDS-PAGE and Western immunoblot using antibodies against YadA, BamA and OmpF/C. Under replete conditions, YadA was detected in the outer membranes of both HB101 and JWD3. Upon depletion of BamA, YadA is no longer detectable in the outer membrane (Figure 3.1C).

These results reinforce previous observations that BamA is required for the biogenesis of TAAs and demonstrate for the first time that BamD is essential for TAA biogenesis.

3.2.2 The requirement of the non-essential Bam complex components for OM localisation of TAA's.

Given the complex requirements for the assembly of a trimeric protein into the outer membrane, it was hypothesised that the nonessential components of the BAM complex (BamB, BamC, and BamE) might play a role in TAA biogenesis. To investigate this, *E. coli* HB101 and its isogenic *bamB*, *bamC*, and *bamE* deletion mutants (Rossiter *et al*., 2011) were transformed with pDR03 or pIBA2-YadA, which encode SadA or YadA, respectively. Each mutant was also transformed with the respective empty vector. Overnight cultures of each strain were diluted 1:100 and grown until an OD_{600nm} of 1.0 at 37°C. Outer membrane protein fractions were isolated from these cultures using a TritonX-100 detergent extraction method and separated by SDS-PAGE. The absence of each Bam component from the respective mutant was confirmed by Western immunoblot analysis (Figure 3.2A). Western immunoblotting using polyclonal

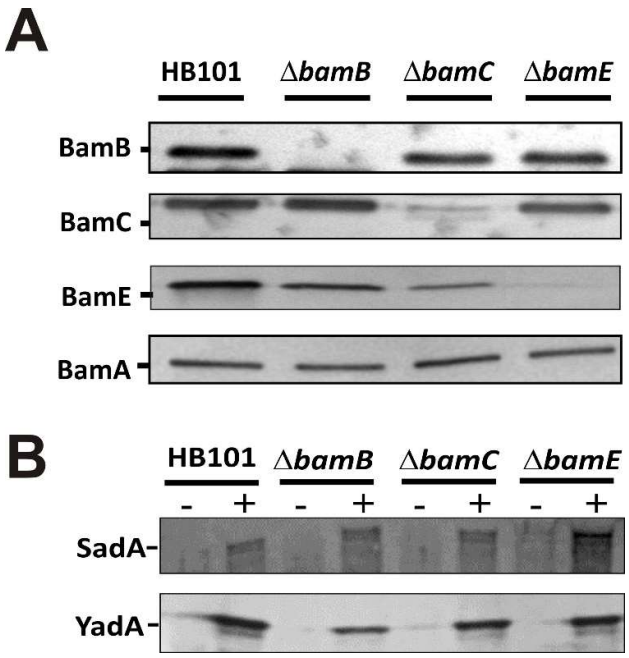

Figure 3.2. Western blot analysis of BamB, C and E requirement for outer membrane localisation of trimeric autotransporters. (A) Western blot analysis of wild-type HB101 and *bamB, C* or *E* mutant strains confirming the loss of each protein in the corresponding mutant. Outer membrane fractions were probed with either Bam A, B, C, E specific antibodies. (B) Outer membrane fractions of wild-type and *bam* mutant strains expressing either an empty vector control (-) or SadA/Yada (+) analysis by Western blot. Protein fractions were probed using either YadA or SadA specific antibodies confirming the presence of the proteins in the outer membrane.

rabbit antisera to SadA or YadA revealed the accumulation of each protein in the outer membrane was unaffected by the absence of BamB, BamC or BamE (Figure 3.2B). These observations indicate BamB, BamC and BamE are not required for the translocation of TAAs to the outer membrane.

3.2.3 Outer membrane localisation of trimeric autotransporters in Tam complex mutants.

Earlier studies demonstrated that the Tam complex is required for the correct biogenesis of T5aSS proteins (Selkrig *et al*., 2012). Therefore, it was hypothesised that the TAAs proteins would also require the assistance of the Tam complex for biogenesis. To test this, the loss of TamA and TamB from the corresponding gene deletion strains were confirmed by Western blot analysis of whole cell protein fractions using TamA and B specific primary antibodies (Figure 3.3A). The confirmed *tamA* and *tamB* mutants were transformed with either the empty vectors or pDR03 or pIBA2-YadA. Cultures and outer membrane proteins were prepared as previously described and the outer membrane localisation of SadA and YadA was monitored by Western blot. In the absence of TamA or TamB, both YadA and SadA are incorporated into the outer membrane at levels similar to the wild-type parental strain, suggesting that the Tam complex is not required for the localisation of TAAs to the outer membrane (Figure 3.3B).

3.2.4 Surface exposure of TAA's in Bam and Tam mutants.

Previously studies observed that intermediates of the T5aSS are localised to the outer membrane but are unable to translocate their cognate passenger domains to the cell surface (Leyton *et al*., 2011). Furthermore, the translocation of the TAA

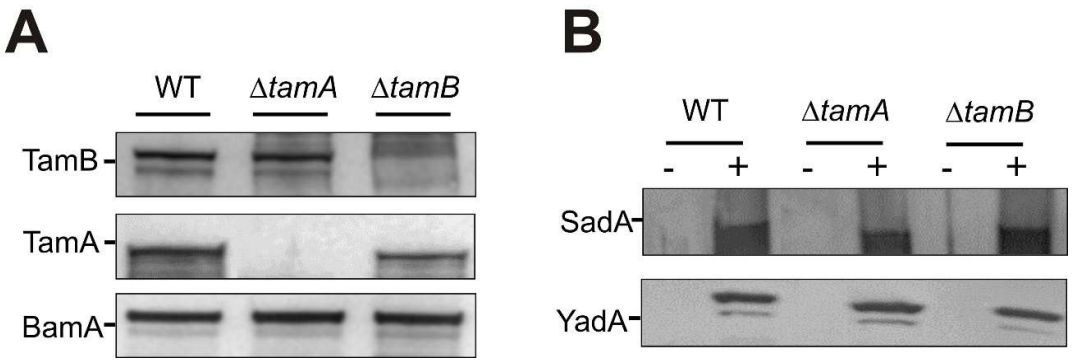

Figure 3.3. Requirement of TamA and B for outer membrane insertion of trimeric autotransporters. (A) Western blot analysis of wild-type HB101 and *tamA* and *tamB* mutant outer membrane fractions confirming the loss of each protein in the corresponding mutant using antibodies specific to TamA and B. BamA specific antibodies were used as a positive control. (B) Western blot analysis of wild-type HB101 and *tamA* and *tamB* mutant outer membrane fractions expressing either empty vector (-) or YadA/SadA (+) using YadA or SadA specific antibodies to confirm the presence of the proteins in the outer membrane.

passenger domains to the cell surface must be co-ordinated in a manner that prevents misfolding before secretion and does not sterically hinder the secretion of their sibling passenger domains. Therefore, it was hypothesised that whilst the non-essential Bam components and the Tam components were not required for localisation to the outer membrane, they might be responsible for holding the C-terminal translocation unit and/or passenger domains in a conformation that permits secretion of the passenger domain to the cell surface. To test this hypothesis, the surface exposure of YadA in the Bam and Tam mutants was monitored by immunofluorescence microscopy using antibodies against YadA and the secondary antibody anti-IgG conjugated with Alexafluor488. YadA was detected on the surface of the parental and non-permeablised *bam* (Figure 3.4A) and *tam* mutants (Figure 3.4B). These data suggest that neither the non-essential Bam nor the Tam complexes are required for surface exposure of trimeric autotransporters.

3.2.5 The function of Trimeric autotransporters in Bam and Tam mutants.

Although the Tam and the non-essential Bam components are not required for localisation to the outer membrane or for surface localisation of the passenger domain, they might be required for the correct folding of TAA passenger domains on the cell surface. In order to determine whether these components play a role in folding, the function of the TAA proteins in the mutant backgrounds were tested.

As YadA is known to mediate binding to collagen I and to promote autoaggregation (Nummelin *et al*., 2004), the *E. coli bamB*, *bamC* and *bamE* mutants expressing YadA were tested in a growth-based collagen binding assay. Strains were incubated in wells coated with collagen I prior to vigorous washing. LB medium was added to the wells and the plates were incubated at 37°C for 2 hours. Strains that had adhered to collagen I would have more bacterial cells in the wells and would therefore

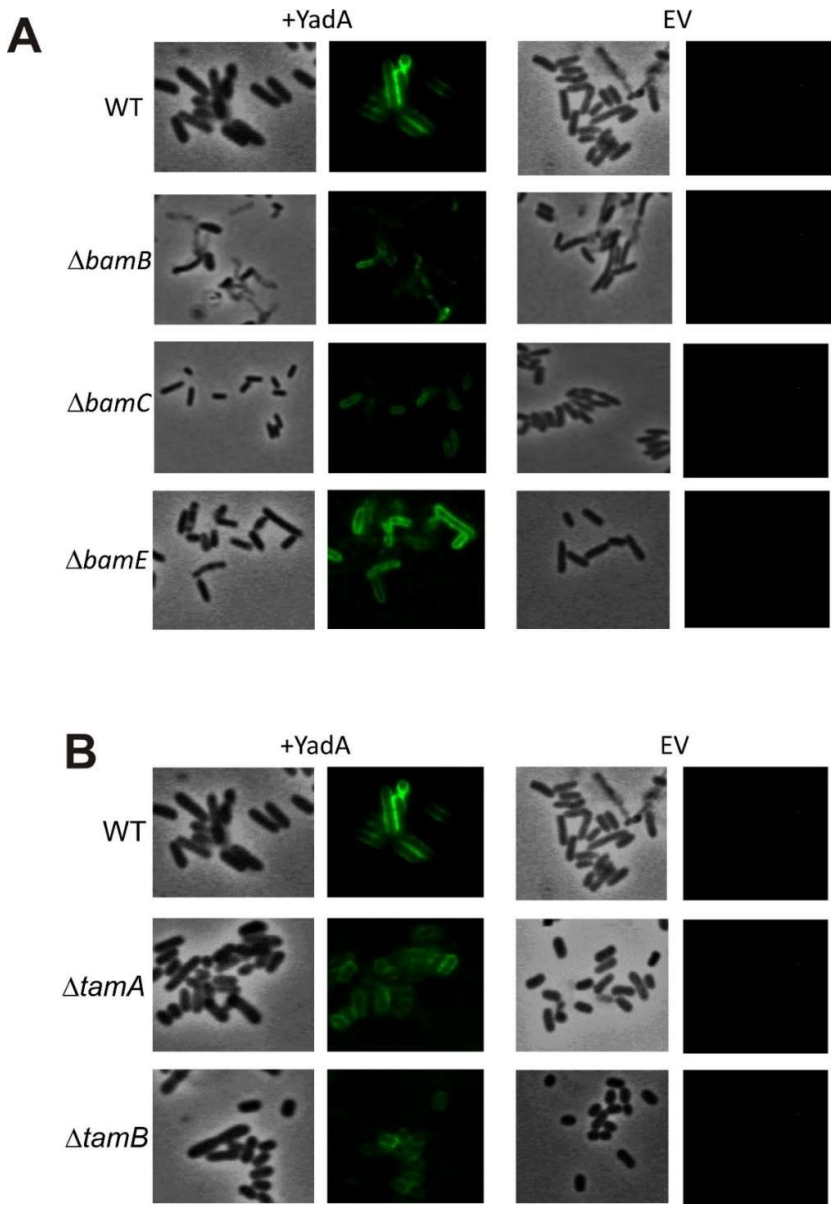

Figure 3.4. Immunofluorescence of YadA surface exposure in Bam and Tam mutants (A) Immunofluorescence imaging of wild-type, and *bamB*, *C* and *E* mutant PFA fixed cells containing either empty vector (EV) or YadA plasmid (+YadA). (B) Immunofluorescence microscopy using antibodies raised to YadA. Shown are microscope images of light and fluorescent images of cells expressing *yadA* (+Yada) and those with empty vector (EV).

show higher growth, which was measured as colony forming units (cfu) per ml. Expression of YadA in all strains promoted significant increases in binding collagen I compared to the empty vector control, regardless of *bam* mutation (Figure 3.5A). Similarly, induction of YadA expression in all strains led to significant autoaggregation, in contrast to empty vector control strains, which had no discernible aggregation (Figure 3.5B).

Previously, it was demonstrated that SadA could promote biofilm production *in vitro* (Raghunathan *et al*., 2011). Thus, the ability of wild-type and Bam mutant strains, either expressing or not expressing SadA, for their ability to form a biofilm on polystyrene plates was investigated. Strains were inoculated into M9 minimal medium and incubated overnight at 37°C. The next day, the plates were washed vigorously and stained with crystal violet. The crystal violet was removed and the plates were destained with an ethanol: acetone (80:20) solution. The OD_{620nm} was measured and biofilm was determined by increased OD_{620nm} measurement. All strains expressing SadA had significantly ($P < 0.001$) higher biofilm formation than those strains with the empty vector (Figure 3.6).

To investigate whether TamA and TamB were required for folding of TAA passenger domains, the *tam* mutants described above were monitored for YadA function. In order to determine whether YadA was functional when expressed in a *tam* mutant, the ability of YadA to bind collagen I was tested. In both *tamA* and *tamB* mutants, YadA promoted binding to collagen I (Figure 3.7). These data suggest that TAAs are secreted, folded and function even in the absence of BamB, C or E and the Tam complex.

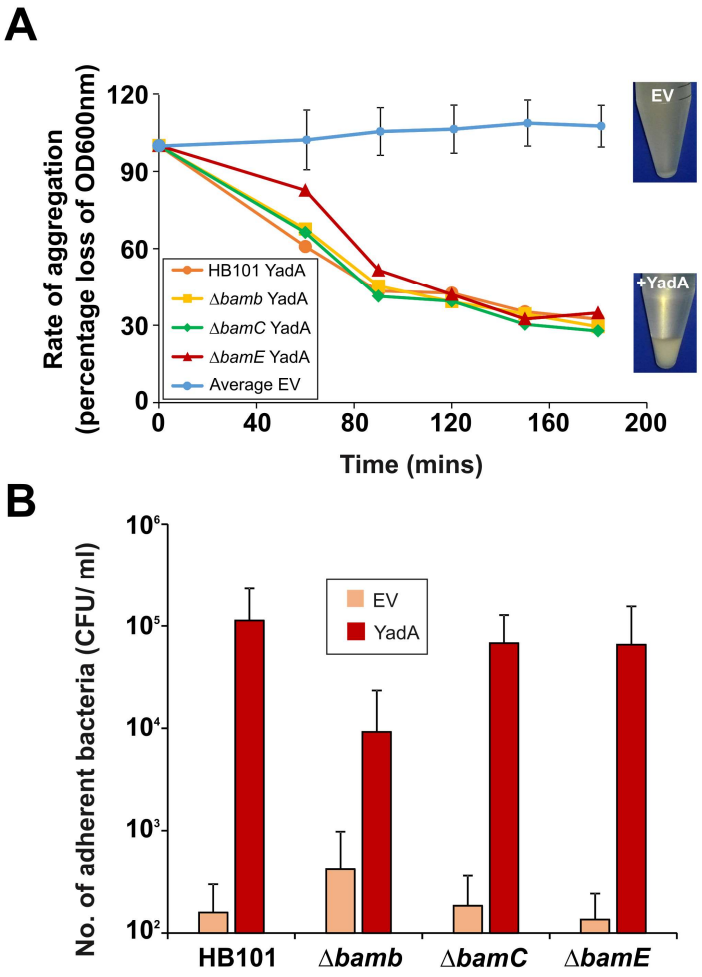

Figure 3.5. The function of Trimeric autotransporters in the absence of the non-essential Bam components. (A) Collagen I binding by wild-type and Bam mutant HB101 strains containing either EV or YadA+ plasmid. Adhesion was examined via measuring growth in microtitre plates after binding and washing. Significance ($p<0.05$) was determined by a Students T-test. Error bars represent standard deviation of at least 8 technical replicates and 3 separate experiments. (B) Aggregation of wild-type and mutant HB101 strains containing either EV or YadA+ plasmid. The pellet formed by autoaggregation can be visibly compared after three hours (insets). Significance ($p<0.05$) was determined by a Students T-test and error bars represent standard deviation of 3 separate experiments.

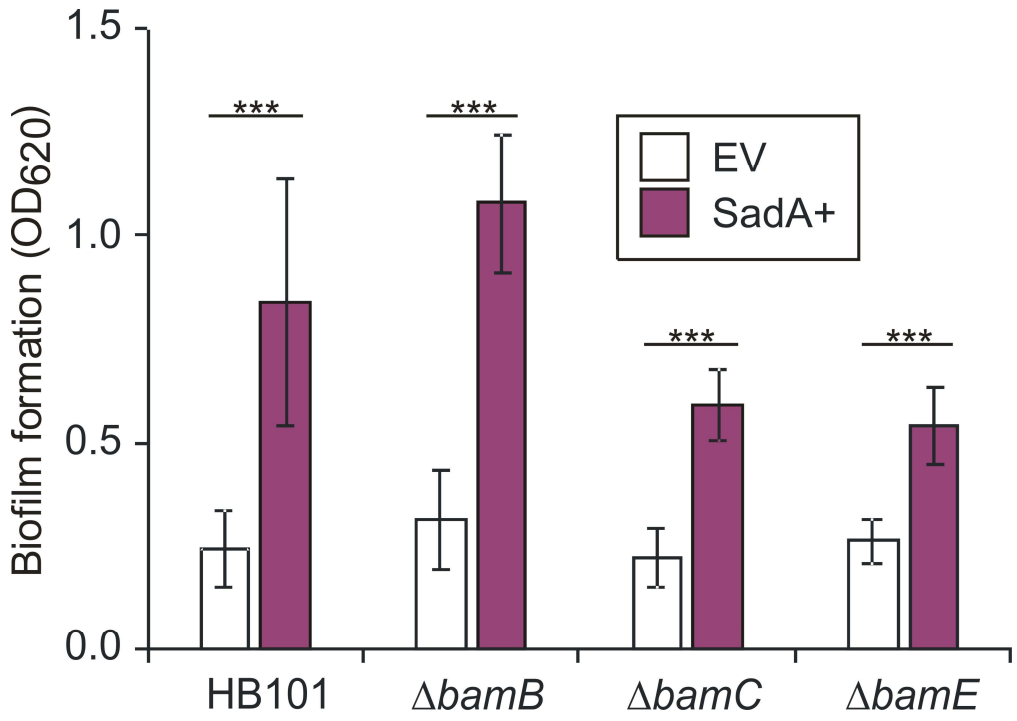

Figure 3.6 Biofilm formation mediated by SadA in the absence of the non-essential Bam components. Biofilm formation by wild-type and mutant HB101 strains containing either EV or SadA expressing plasmid. Biofilm formation was examined in polystyrene microtitre plates. Significance ($p<0.05$) was determined by a Students T-test (*** $p<0.001$). Error bars represent standard deviation of at least 12 technical replicates and 3 separate experiments.

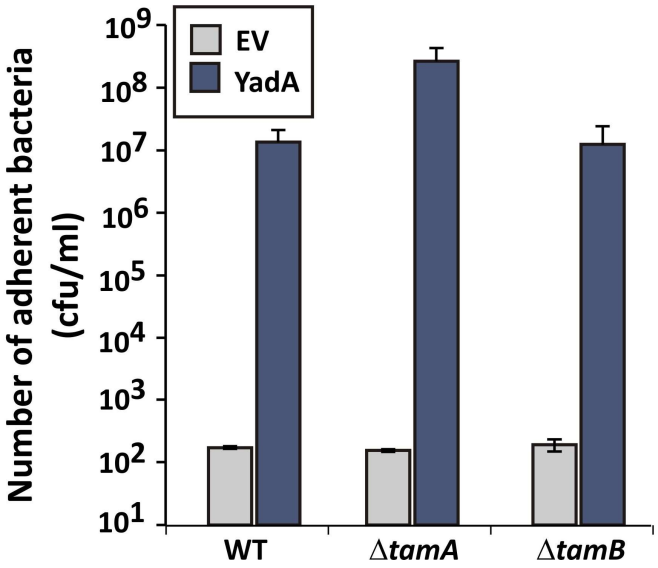

Figure 3.7. Collagen I binding assay of YadA secreted in the absence of TamA and B (A) Collagen I binding by wild-type (WT) and mutant *tamA* and *tamB* strains containing either EV or YadA+ plasmid. Adhesion was examined via measuring growth in microtitre plates after binding and washing. Significance ($p<0.05$) was determined by a Students T-test. Error bars represent standard deviation of 3 separate experiments.

3.3. Discussion

The proteins SadA and YadA are both trimeric autotransporter adhesins, however they vary greatly in sequence homology, length and function. YadA is the prototypical TAA, its trimeric structure composed of a β-barrel in the outer membrane, with a single stalk, neck and head domain extending 35 nm into the extracellular environment. In contrast, SadA extends 108 nm and is composed of multiple stalk, neck and head domains alternatingly dispersed (Hartmann *et al*., 2012). Here, it was found that despite these size and structural differences that both BamA and BamD are required for the secretion and function of SadA and YadA. This is agreement with studies on other outer membrane proteins (Rossiter *et al*., 2011), and is further evidence that BamA and BamD work in unison to assemble proteins into the outer membrane (Hagan *et al*., 2010, Malinverni *et al*., 2006). In contrast, both SadA and YadA were functionally assembled into the outer membrane in BamB, BamC and BamE mutant strains. These three lipoproteins have been shown to be non-essential in *E. coli* and although been shown to be required for the secretion of some outer membrane proteins (Charlson *et al*., 2006, Hagan *et al*., 2010), are also not required for others (Sklar *et al*., 2007a, Volokhina *et al*., 2009). The ability of SadA to induce biofilm formation was the same in the wild-type and a BamB mutant. This is unsurprising as other proteins (such as Pet, TolC) have been shown to be functionally assembled in BamB mutants. Additionally, TAA proteins such as NhhA exist in bacterial species (*Neisseria meningitidis*) that don't have a BamB homolog, suggesting it is not required for proper assembly of this protein class (Volokhina *et al*., 2009).

TamA and B have been implicated in the secretion of classical autotransporters. Here, we observe that TamA and B are not required for the biogenesis of TAA proteins, suggesting TamA and B involvement in type 5 secretion may be specific to a subset of

type 5 proteins. TamA and B were recently implicated in the efficient biogenesis of *E. coli* fimbrial proteins (Stubenrauch *et al*., 2016), thereby demonstrating that the exact role of the Tam complex for proteins destined to insert in the outer membrane is an area of research that is still ongoing.

The assembly of trimeric proteins are poorly understood and it is unknown whether the trimers form prior to insertion or whether monomers are held in the membrane by some factor and are assembled when three monomers are available. Here, we show that the non-essential components of the Bam complex and both TamA and B are not required for TAA assembly. However, this does not rule out the possibility that the accessory Bam components and perhaps the Tam complex are involved in efficient outer membrane biogenesis of trimeric autotransporters and other outer membrane proteins.

CHAPTER 4

Characterisation of *Salmonella* autotransporters

4.1. Introduction

The major virulence factors of *Salmonella enterica* are the two Type 3 secretion systems encoded for on *Salmonella* pathogenicity islands (SPI) 1 and 2. These Type 3 secretion systems have been experimentally proven to be important for *S.* Typhimurium intracellular entry and survival (Johnson *et al*., 2018a). However, an understudied area of *S. enterica* pathogenicity is that of the contribution of a family of *Salmonella* Type 5 secretion proteins, also termed autotransporters.

Autotransporter proteins are among some of the most abundant outer membrane proteins in Gram negative bacteria, which typically play roles in bacterial virulence (Henderson *et al*., 2004). *S.* Typhimurium has 4 characterised autotransporters termed ApeE (Carinato *et al*., 1998), SadA (Raghunathan *et al*., 2011), MisL (Dorsey *et al*., 2005) and ShdA (Kingsley *et al*., 2002). As there are multiple autotransporters in *Escherichia coli* with overlapping roles (Wells *et al*., 2010), it might be difficult to determine the contribution of the *S*. Typhimurium autotransporters by only deleting one gene. Therefore, to determine the contribution of the *S.* Typhimurium autotransporters to virulence initially, a multiple autotransporter mutant was constructed that had multiple autotransporters deleted from the chromosome. This multiple autotransporter deletion strain was investigated for pathogenesis using a murine model of infection. To understand which autotransporter might be important for virulence in this model, the conservation of each protein was compared amongst clinically relevant serovars of *Salmonella.*

This chapter aims to investigate the contribution of the *S.* Typhimurium autotransporters to virulence using a murine model of infection. This chapter will also investigate the conservation of these proteins using a variety of bioinformatics techniques.

4.2. Results

4.2.1. Characterisation of autotransporters within *Salmonella.*

There were 4 characterised autotransporters in *S.* Typhimurium SL1344 and previous bioinformatics analysis in our laboratory identified a 5th SL1344 autotransporter termed YaiU (Morris, 2013). To further characterise the SL1344 autotransporters, the protein sequences were analysed for predicted functional domains, extended signal peptide and size by a BLASTp protein sequence of each autotransporter protein sequence using the Uniprot database. MisL, and YaiU are Type 5a autotransporters predicted to have a Pertactin-like domain and to be around 105 kDa in size (Table 4.1). ShdA was predicted to be approximately 224 kDa and contain an AIDA-1 motif (Table 4.1). SadA was predicted to form a trimer with a molecular weight of 482 kDa and to contain a YadA head motif (Table 4.1). ApeE was predicted to contain a GDSL lipase motif and have a molecular weight of 72 kDa. YaiU and ShdA had extended signal peptides that are present in approximately 10% of autotransporters (Leyton *et al*., 2012). The predicted structures of each autotransporter was described in Figure 4.1, which shows relative size and predicted passenger domain structure (Figure 4.1) Autotransporters are often involved in bacterial pathogenesis, and the conserved motifs of the *S.* Typhimurium autotransporters would suggest that these proteins are no different.

4.2.2. The role of the *Salmonella* autotransporters in chronic infection.

To investigate the role of the *Salmonella* autotransporter proteins in chronic systemic infections of *Salmonella*, the model organism *S*. Typhimurium SL3261 was used. SL3261 is an attenuated *S.* Typhimurium strain that is an aromatic amino acid auxotroph that is less lethal in mice than SL1344.

Table 4.1. *S*. Typhimurium autotransporter summary

Name	Type	Size (kDa)	Signal peptide	Conserved domains	Upregulated in macrophages?*
MisL	5a	105	27	Pertactin like pectin lyase fold	No
YaiU	5a	107	50	Pertactin like pectin lyase fold	1.68 fold
ShdA	5a	224	60	AIDA-1 like motif	No
SadA	5c	482	27	Trimeric autotransporter adhesin, YadA motif	No
ApeE	5a	72	25	GDSL lipase/esterase motif	2.58 fold

*(Srikumar *et al*., 2015)

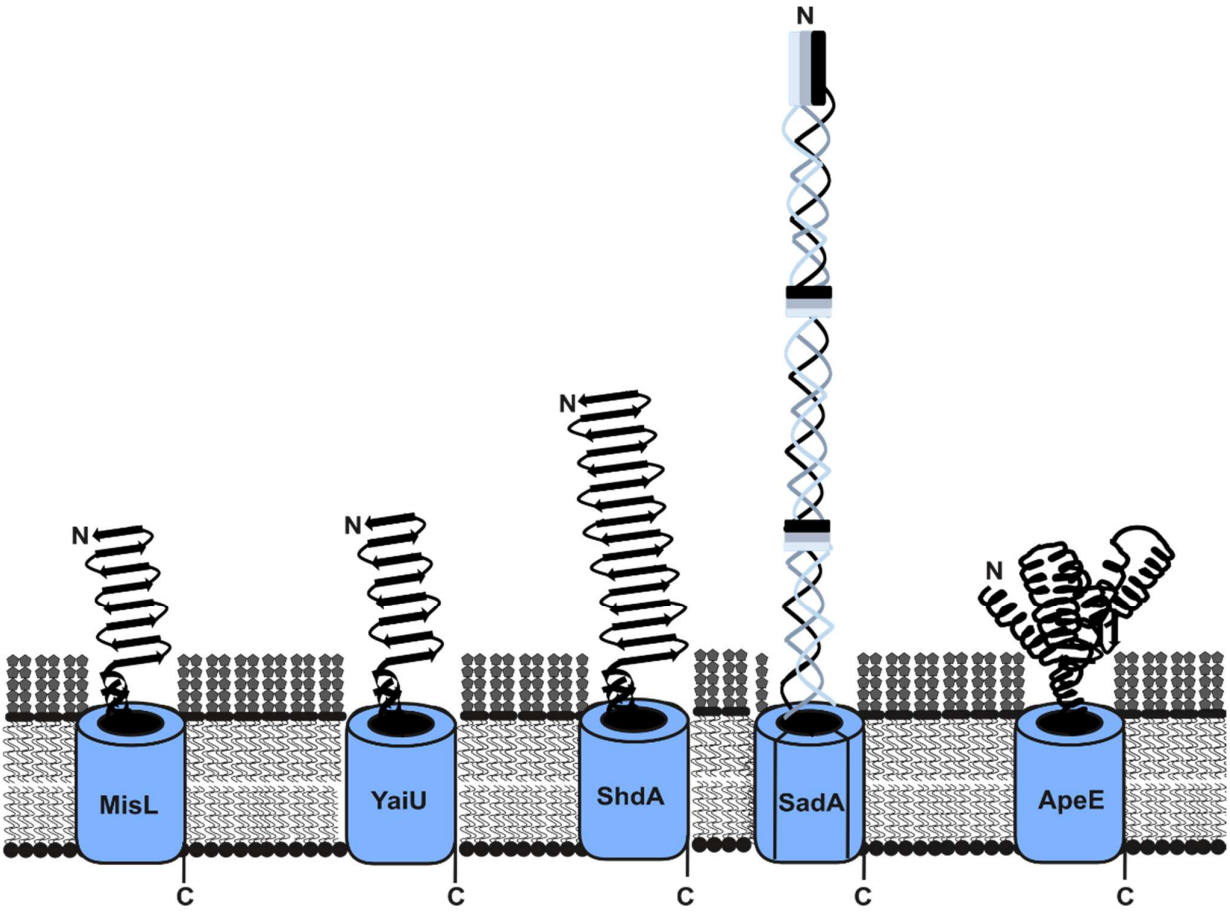

Figure 4.1. Schematic of the *S.* Typhimurium SL1344 autotransporters. For each autotransporter protein, the predicted domain structure was determined using Pfam and UniProt.

(Hoiseth and Stocker, 1981) and can therefore be used to study long-term *Salmonella* infections. Previous work in our laboratory constructed a multiple autotransporter mutant strain in SL3261 which was genetically Δ*misL* Δ*yaiU* Δ*sadA* Δ*apeE shdA::aph* termed the *Salmonella* autotransporter knockout (SLATs) strain (Morris, 2013) . C57BL/6 mice were infected intraperitoneally (I.P.) with ~10^5 cfu's on day 1 of infection with either SL3261 wild-type or SL3261 SLAT's. At days 7, 21 and 35 post infection, the spleens, livers, gallbladders and blood of each mouse was harvested and processed to elucidate the colony forming units (cfu) per organ (bacterial burdens) of the different sites tested. On each day, the SLAT's strain had fewer bacterial cfu/ organ than the wild-type (Figure 4.2). In the spleen and liver, there were significant differences in bacterial burdens between mice infected with SL3261 wild-type and the SLATs mutant, at every time point tested (Figure 4.2A and B). In the blood, there were significant differences in bacterial burdens between mice infected with SL3261 and those infected with the SLATs strain at days 7 and day 21 (Figure 4.2C). By day 35 none of the mice from either group had detectable bacteria in the blood (Figure 4.2C). In the gallbladder, at 21 days post infection, there were significant differences in bacterial burdens between mice infected with the wild-type and mutant bacteria (Figure 4.2D). These data indicated that the *Salmonella* autotransporters were cumulatively important for systemic infection in mice. The attenuation observed in the gallbladder was of particular interest, as the gallbladder might be the site that harbours chronic infections of *Salmonella* (Sinnott and Teall, 1987).

4.2.3. Distribution and conservation of Autotransporters in *Salmonella.*

To try to understand which of the *S*. Typhimurium SL1344 autotransporters might be important for the lifecycle of *Salmonella* and thus might be important for gallbladder colonisation, the conservation of each protein was determined amongst

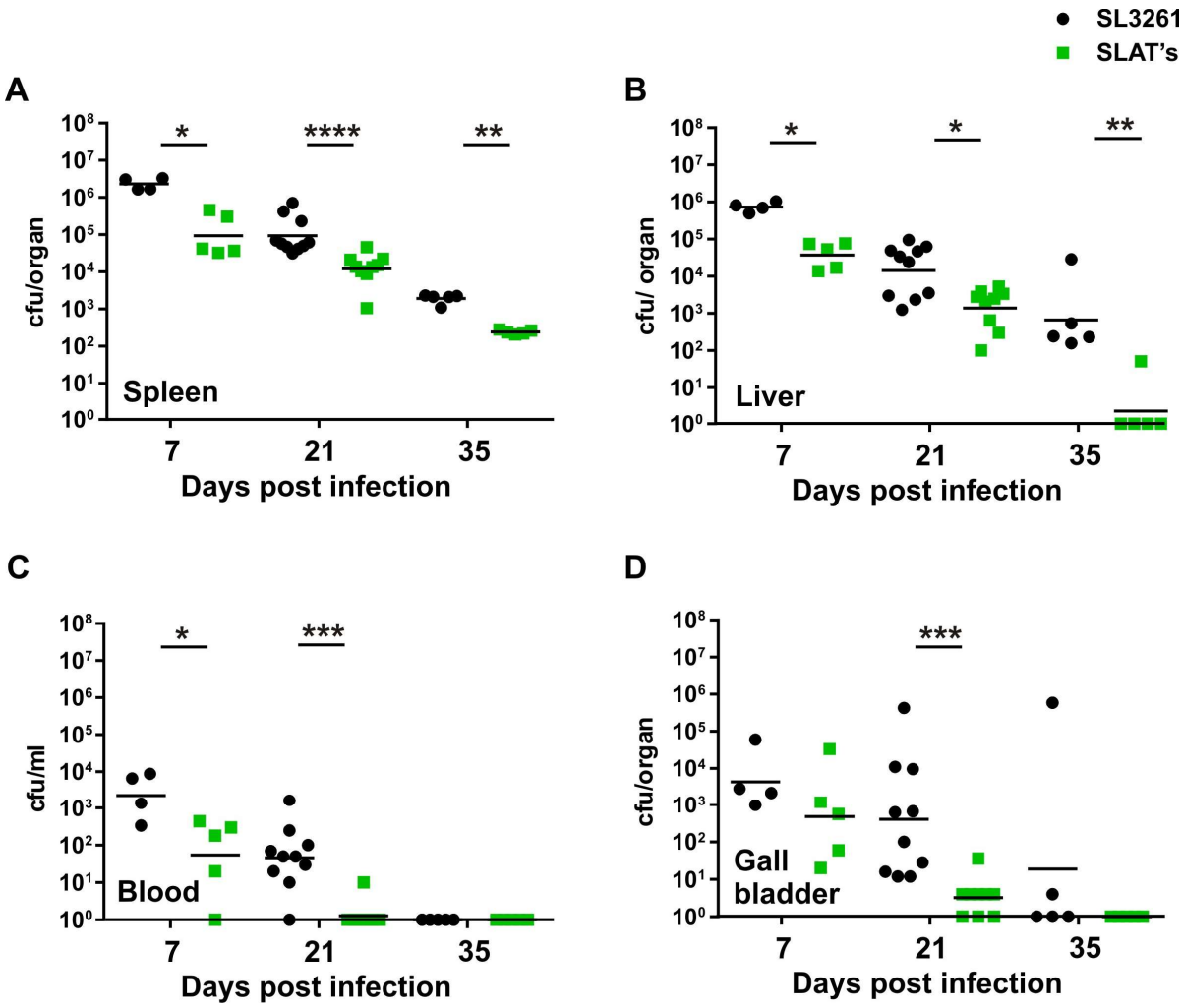

Figure 4.2. Dynamics of a 35 day infection period of mice infected with either SL3261 or SLATs. Bacterial burdens of mice infected with either SL3261 (black circles) or SLATs (green squares) over a 35 day infection period. Mice were infected with 10^5 cfu of either SL3261 or SLATs and on days 7, 21 and 35 post infection, burdens were enumerated by plating serial dilutions of homogenised organs onto agar plates. The data here represents the burdens of the spleen (A) liver (B), blood (C) and gallbladder (D). Statistical significance ($p<0.05$) was determined using a Mann-Whitney non-parametric U-test (*$p<0.05$, **$p<0.01$, ***$p<0.001$ and ****$p<0.0001$).

host restrictive and broad host range serovars of *S. enterica*. The protein sequence for each autotransporter was BLASTp searched against a selection of *S. enterica* reference genomes. The genomes of host restricted serovars tested for autotransporter protein sequence conservation were as follows: *S.* Typhi (human); *S*. Choleraesuis (Pig); *S*. Gallinarum (Chicken) and; *S.* Paratyphi A (Human) and the broad host range serovars tested were *S.* Typhimurium, and *S*. Enteritidis. The percentage identity of each autotransporter protein found in the reference genomes for each serovar are reported in Table 4.2. ApeE, and YaiU were highly conserved in each strain tested (Table 4.2). ShdA was conserved with high percentage identity in serovars Enteritidis, Choleraesuis and Typhimurium but not in Typhi, Paratyphi A or Gallinarum. As ShdA is not highly conserved in host specific serovars, it was hypothesised that it might not play a role in chronic gallbladder colonisation.

The role of SadA and MisL during murine infections have been established previously (Raghunathan *et al*., 2011, Dorsey *et al*., 2005). In these studies, no role for these proteins in colonisation of the host gallbladder was discovered and here, it was hypothesised that these proteins might not contribute to gallbladder colonisation. Whilst YaiU has not been investigated for a role during infection, the protein is predicted to be a similar autotransporter to MisL, with a Pertactin like pectin lyase fold and a similar size (Table 4.1), and therefore might have a similar function. The last protein that was highly conserved in all strains tested was ApeE, which is a GDSL lipase autotransporter. ApeE had not been investigated for a role during infection previously. However, as ApeE was a known lipase, it might interact with host lipids that are highly abundant in host gallbladder (Boyer, 2013).

Table 4.2 Autotransporter protein conservation in different serovars of *S. enterica*

	% identity				
***S. enterica* serovar:**	**ApeE**	**ShdA**	**MisL**	**YaiU**	**SadA**
Typhi CT18	97.8	16.4	ND*	98.7	99.8
Typhimurium LT2	100	100	100	100	100
Enteritidis PT4	97.5	97.3	99.1	98.9	99.8
Gallinarum 287/91	97.8	36.4	99.1	98.4	99.8
Choleraesuis SC-B67	98.8	96.6	98.5	98.9	100
Paratyphi A ATCC 9150	99.3	35.5	97.0	98.9	ND*

Non detected (ND)*

4.2.4. Phylogeny of ApeE.

As ApeE was conserved amongst clinically relevant *S. enterica,* the conservation and distribution of ApeE was investigated further. All proteins containing a Pfam: Lipase_GDSL domain were subjected to further bioinformatic studies. Analysis of protein domain organisation revealed that single Lipase_GDSL domain-containing proteins are the most common and these are widespread in bacteria, plants, fungi, archaea and animals (Figure 4.3). The ApeE-like autotransporter architecture was identified as the second most common protein architecture (Figure 4.3). Phylogenetic analysis of this constrained cluster showed a clear two clade split between plants and all other GDSL lipases (Figure 4.4). Annotation of the tree with taxonomic information and presence of an autotransporter domain shows there has been frequent horizontal gene transfer of GDSL lipases between fungi, Cyanobacteria and Proteobacteria, leading to a relatively recent expansion event of autotransporter-associated GDSL lipases in Proteobacteria. The structure of the network indicated that this cluster of GDSL lipases is evolutionarily constrained, most likely due to functional properties, given their lack of diversity compared to GDSL lipases from across other domains of life (Figure 4.3). These ApeE homologues in Proteobacteria are present in species most commonly associated with disease of plants (Coleman, 2016, Helfer, 2014, Sundin *et al*., 2016). However, as ApeE was highly conserved in the human pathogens Typhi and Paratyphi A, it was hypothesised that its function might be diverse and important for various aspects of *S. enterica* life cycle.

4.2.5. Demonstration that ApeE is a surface exposed Autotransporter.

ApeE was predicted to localise to the outer membrane of *S.* Typhimurium. To determine whether ApeE was localised in the outer membrane, cultures of SL1344, *apeE::aph* and *apeE::* + pApeE were grown overnight at 37°C for approximately 16 h.

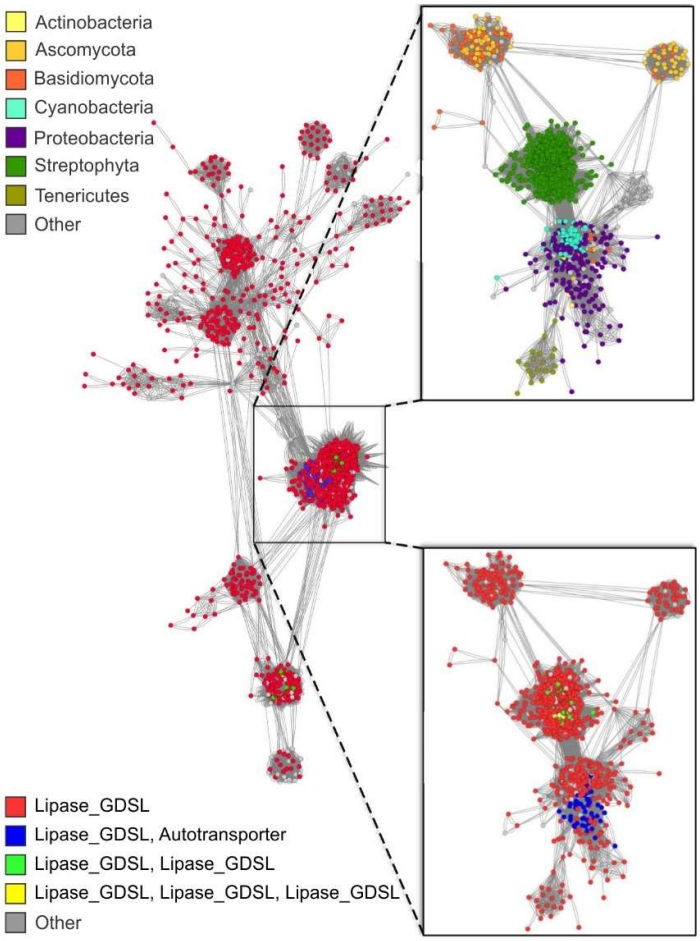

Figure 4.3. Network clustering analysis of GDSL lipase proteins. A network clustering analysis of all Lipase_GDSL domain-containing proteins coloured for protein architecture (main, lower inset) or phyla of origin (top inset).

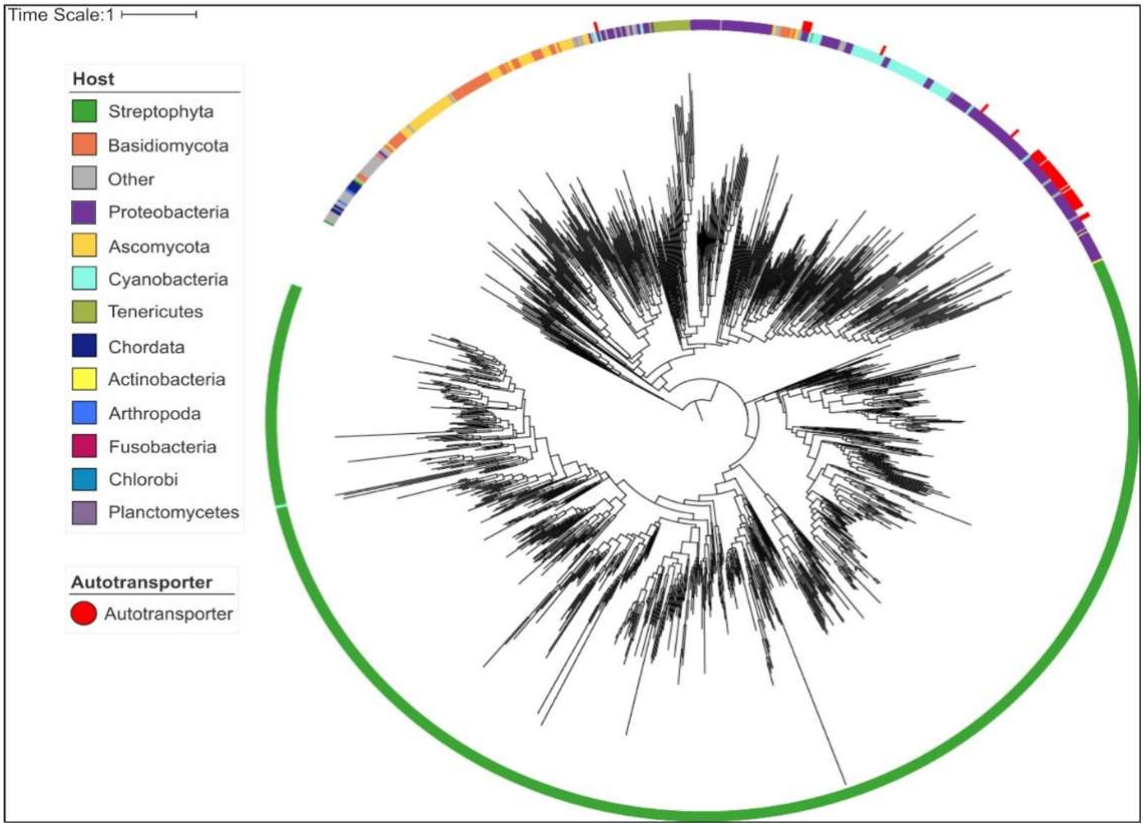

Figure 4.4. Phylogenetic tree of GDSL lipase proteins. Individual proteins are coloured for phyla of host organism origin. Proteins with an autotransporter protein structure are highlighted in red.

The outer membrane proteins were extracted via a Triton X-100 method. The proteins were analysed by SDS-PAGE and Western immunoblot using anti-ApeE primary antibodies. ApeE was detected as a faint band at approximately 69 kDa (Figure 4.6A) in the SL1344 wild-type and complemented strain. No ApeE band was detected in the outer membrane of the *apeE* mutant. All samples had comparable levels of protein when analysed by SDS-PAGE (Figure 4.5A). Therefore it was concluded that ApeE is localised to the outer membrane of *S.* Typhimurium.

To date, no crystal or other structure of the ApeE protein has been solved. To guage what the tertiary structure of ApeE might resemble, the protein sequence was submitted to structural modelling using Phyre2 (Kelley, 2015). The predicted structure was modelled (with 100% confidence) to the solved structure of the ApeE homologue EstA (van den Berg, 2010), which shares 27% protein identity with ApeE. The model predicted that ApeE would form a 12 stranded β-barrel with a passenger domain that had mostly alpha helices (Figure 4.5B), which is a known feauture of GDSL lipase autotransporters (van den Berg, 2010).

To understand whether ApeE was surface localised, recombinant plasmids expressing either ApeE or a serine point mutant $ApeE_{S35A}$ were transformed into *E. coli* BL21. Many non-native autotransporters have been expressed in laboratory strains of *E. coli* (Raghunathan *et al*., 2011, Casasanta *et al*., 2017) to determine function and cellular localisation as these strains of *E. coli* typically do not contain as many interferring surface molecules such as O-antigen (Raghunathan *et al*., 2011). Plasmid constructs were designed to express the *apeE* native passenger domain (pJR02), or serine point mutant (pJR03) and native β-barrel with an *E. coli* OmpA signal sequence. An N-terminal poly-histidine tag had been engineered to this gene such that it remains attached to the protein post-signal sequence cleavage. This construct enables

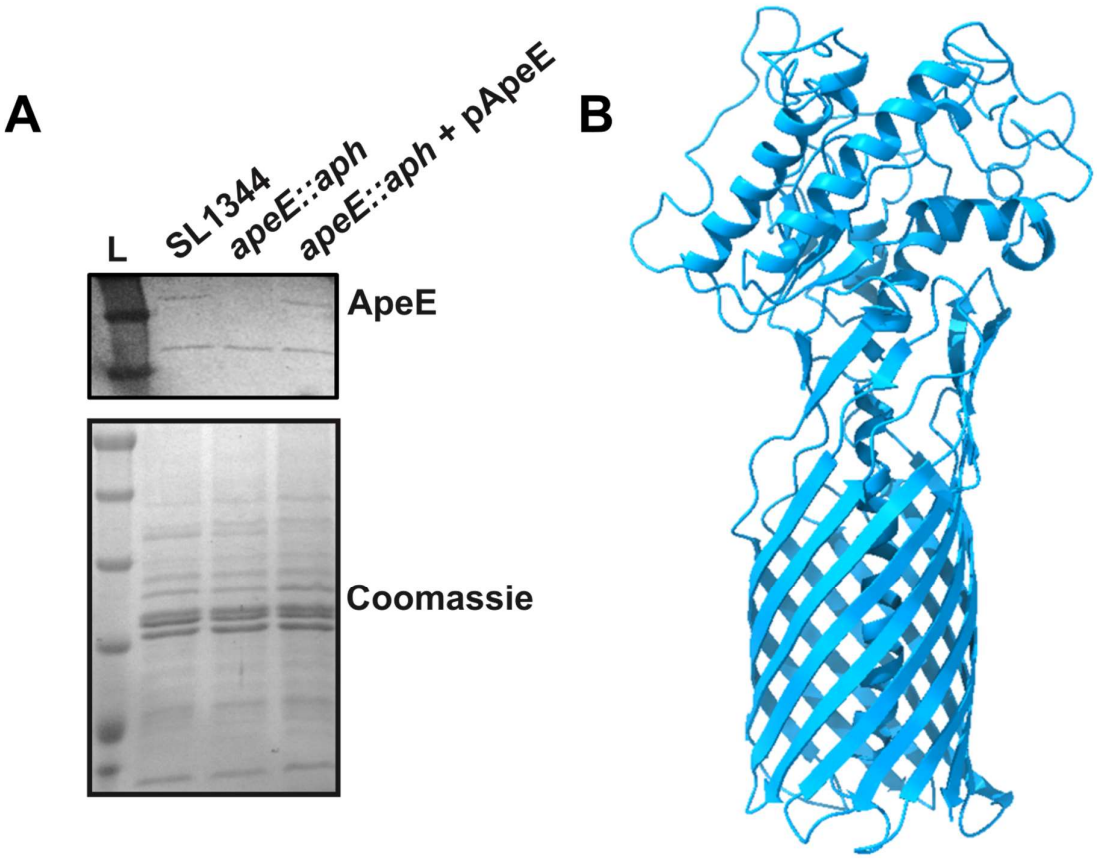

Figure 4.5. Outer membrane localisation and predicted structure of ApeE. (A) Outer membrane proteins from *S.* Typhimurium, *apeE::aph* and *apeE::aph* + pApeE were extracted using TritonX-100. The proteins were analysed by SDS-PAGE and Western immunoblot with primary anti-ApeE antibodies. The blots were developed upon the additon of the substrate NBP-BCIP and the SDS-PAGE gels were stained with Coomassie. (B) The protein sequence of ApeE was submitted to structural modelling using Phyre2. The structure was modelled with 100% confidence based on the solved cystal structure of the outer membrane esterase, EstA, from *P. aeruginosa.*

efficient surface display of lipase autotransporters on the surface of *E. coli* (Casasanta *et al.*, 2017). The recombinant plasmids were transformed into *E. coli* BL21 chemically competent cells.

First, the expression and surface display of the recombinant ApeE proteins in *E. coli* BL21 was determined. Whole cell protein fractions were analysed by SDS-PAGE and Western immunoblotting. Blots were probed with anti-his tag primary antibodies. The Western blot showed that both the ApeE and ApeE$_{S35A}$ construct were produced and recognised by the anti-his tag antibodies, and that the empty vector was not producing protein detected by these antibodies (Figure 4.6A). Similar levels of protein were detected by SDS-PAGE in each sample. A band corresponding in size to the full length ApeE was clearly visible in samples from *E. coli* expressing *apeE* or *apeE$_{S35A}$* (Figure 4.6A).

To determine whether the proteins produced were surface exposed, fixed bacterial cells were visualised using immunofluorescence. If the ApeE produced was surface exposed, anti-His-tag antibodies would detect the protein at the cell surface, and a secondary antibody with a green fluorescent tag could be imaged. Induced overnight cultures of either BL21 empty vector, +ApeE or +ApeE$_{S35A}$ were fixed in paraformaldehyde prior to loading onto poly-L-lysine coated cover slips. The cover slips were probed with anti-poly His-tag antibodies followed by anti-mouse-AlexaFluor488 antibodies. The cover slips were loaded onto microscope slides, and then imaged on a fluorescence microscope using the gfp or DIC bright field filter. All strains could be seen using the DIC filter, but only strains expressing ApeE or ApeE$_{S35A}$ could be detected with the gfp filter (Figure 4.6B). These data suggest that the ApeE produced from these constructs is surface exposed.

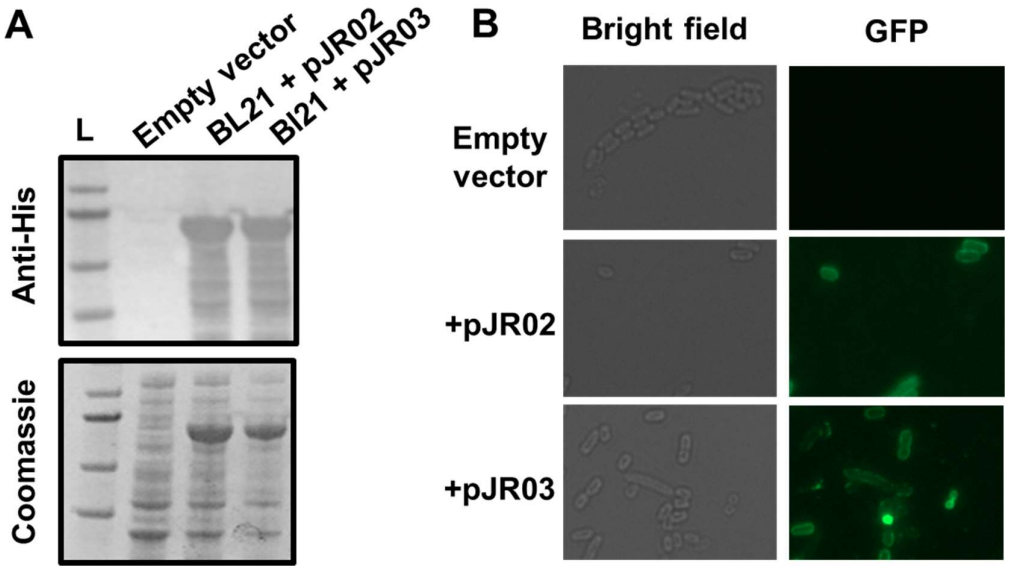

Figure 4.6. Expression and surface display of full length ApeE in *E. coli* BL21. (A) Analysis of whole cell protein fractions of either BL21 + pDJVTS87 (empty vector), BL21 + pJR02 (+ApeE) or BL21 + pJR03 (+ApeE$_{S35A}$). The samples were separated by SDS-PAGE gel electrophoresis and then probed by Western Immunoblotting with anti-his tag antibodies or stained with coomassie. (B) Immunofluorescence of either BL21 + pDJVTS87 (empty vector), BL21 + pJR02 (ApeE) or BL21 + pJR03 (ApeE$_{S35A}$). The cells were probed with anti-his tag antibody and subsequently probed with anti-mouse antibody conjugated to Alexafluor 488. The cells were imaged using DIC (bright field) or gfp filter.

4.3. Discussion.

In this chapter, the role of five of the *S*. Typhimurium autotransporters for virulence was investigated in a chronic infection model. The strain lacking five autotransporters (SLATs) was attenuated for growth in the spleens, livers, blood and gallbladders of mice on various days after infection. The attenuation observed is not similar to the studies investigating the roles of the individual SadA, MisL or ShdA mutants for *S.* Typhimurium virulence (Raghunathan *et al*., 2011, Dorsey *et al*., 2005, Boyen *et al*., 2006). It could be that upon deletion of all 5 putative autotransporters, there is an additive effect and that the autotransporters of *S.* Typhimurium work together to enable bacterial survival in the host. It is also plausible that this strain is more susceptible to the host immune response as other autotransporters have been implicated in mediating the host immune system (Schindler *et al*., 2012). It is also unsurprising given the predicted function of these autotransporters using pfam. These predicted functions included functions such as adhesins and lipases, both of which have been previously implicated during infections (Henderson *et al*., 2004). A study investigating the genes of *S.* Typhimurium that were required for colonisation of pigs, cattle, chicks and mice using transposon mutagenesis combined with genome sequencing determined that the autotransporters were each required for the colonisation of at least 1 animal (Chaudhuri *et al*., 2013). Nearing the end of this study, and as bioinformatic databases became more robust and readily available, two other SL1344 putative autotransporters were identified using the Uniprot Knowledge database. It would be interesting to see if these newly identified autotransporters also contributed to *S.* Typhimurium virulence.

The conservation of each protein in clinically relevant strains were tested to investigate which of the deleted autotransporters might be mediating the severe

attenuation observed in this study, it was determined that ApeE was highly conserved, and was not present in closely related *Enterobacteriaceae* such as *E. coli.* Immunofluorescence microscopy revealed that the passenger domain of ApeE is surface exposed. This is in contrast to a study that tested the surface exposure of ApeE using Proteinase K digestion (Schultheiss *et al*., 2008). In the study by Schultheiss (2008), ApeE was resistant to Proteinase K and the authors concluded that the functional motif of ApeE was therefore located at the periplasmic side of the outer membrane (Schultheiss *et al*., 2008). The results in this study do not confirm this conclusion, rather they contradict it and suggest that the functional motif of ApeE is likely to be surface exposed, and this fits with other models of autotransporter surface localisation (Rutherford and Mourez, 2006). As ApeE was shown to be surface exposed in this study, it is plausible that ApeE might be interacting with the host in some way.

An important aspect of the *S. enterica* pathogenesis in human patients of typhoid fever is asymptomatic carriage, which is usually associated with gallbladder colonisation and faecal shedding (Sinnott and Teall, 1987). Interestingly, the SLATs strain showed high growth attenuation in the gallbladders of mice at day 21 of infection, suggesting one or more of the autotransporters might be important for long-term survival in murine gallbladders. The next chapters will explore the mechanism behind the SLATs attenuation observed in the gallbladders.

CHAPTER 5

Biochemical characterisation of ApeE

5.1 Introduction

ApeE was first described as a *S. enterica* serovar Typhimurium outer membrane esterase (Carinato *et al*., 1998). These investigators demonstrated that ApeE was an esterase with activity against the synthetic substrate methylumbelliferyl caprylate, a C8 fluorogenic substrate useful in distinguishing *Salmonella* species from other members of the *Enterobacteriaceae*. In the literature, ApeE has been proven to be under the control of the PhoBR two-component regulatory system, which responds to phosphate limitation (Conlin et al., 2001, Jiang et al., 2018). PhoR is a histidine kinase that phosphorylates PhoB in response to low inorganic phosphate (P_i) conditions (Santos-Beneit, 2015). PhoB then affects the expression of downstream genes, including a locus that encodes a high affinity phosphate transporter, that when deleted, results in the constitutive expression of *apeE* (Conlin *et al*., 2001). In addition, in a recent publication, ApeE was determined to be one of the most abundant proteins in response to phosphate limitation (Jiang *et al*., 2018). Previous data from our laboratory revealed that ApeE can hydrolyse the synthetic sorbitan oleic acid ester, Tween80.

Despite these observations, the precise contribution of ApeE to *Salmonella* pathogenesis and the identification of natural substrates for ApeE have eluded researchers. In this chapter, studies were conducted to resolve the substrate specificity of ApeE and its enzyme kinetics, with a view to understanding how ApeE might be interacting with the host. This might assist the elucidation of the overall function of ApeE.

5.2 Results

5.2.1 Purification of the ApeE$_{25\text{-}385}$ and ApeE$_{25\text{-}385\ S35A}$ proteins.

To biochemically characterise ApeE, the enzyme needed to be purified. As full length ApeE contains an outer membrane β-barrel, and is therefore insoluble, a soluble truncated version of the protein was required for enzyme activity assays. The region of *apeE* encoding the passenger domain was cloned into the expression plasmid pET22b+ such that the expressed protein contained an N-terminal His tag. In addition, a similar plasmid vector was constructed but with a mutation to abolish the active site serine (S35A). These recombinant plasmids were transformed into *E. coli* BL21 LOBSTRIL; this derivative of BL21 has been modified so that genes encoding histidine rich-proteins were mutagenised in order to reduce non-specific binding to the nickel-agarose purification columns (Andersen *et al*., 2013).

For protein purification, 2 L cultures of *E. coli* BL21 LOBSTRIL, encoding either *apeE*$_{25\text{-}385}$ or *apeE*$_{25\text{-}385\ S35A}$ were induced with 50 μM IPTG for 16 h at 16°C. The following day, the cell pellets were lysed to produce a soluble fraction, which was purified by nickel affinity chromatography. Samples from each fraction representing each step of the purification of both ApeE$_{25\text{-}385}$ and ApeE$_{25\text{-}385\ S35A}$ were analysed by SDS-PAGE (Figure 5.1). For each purification, truncated ApeE could be seen as an approx. 40-kDa band in the lysate and in the final eluted sample (Figure 5.1). The gel indicated that the proteins were sufficiently pure to be used for the subsequent assays and the proteins were buffer-exchanged into 10 mM Tris pH 7.4 150 mM NaCl for enzyme kinetic experiments.

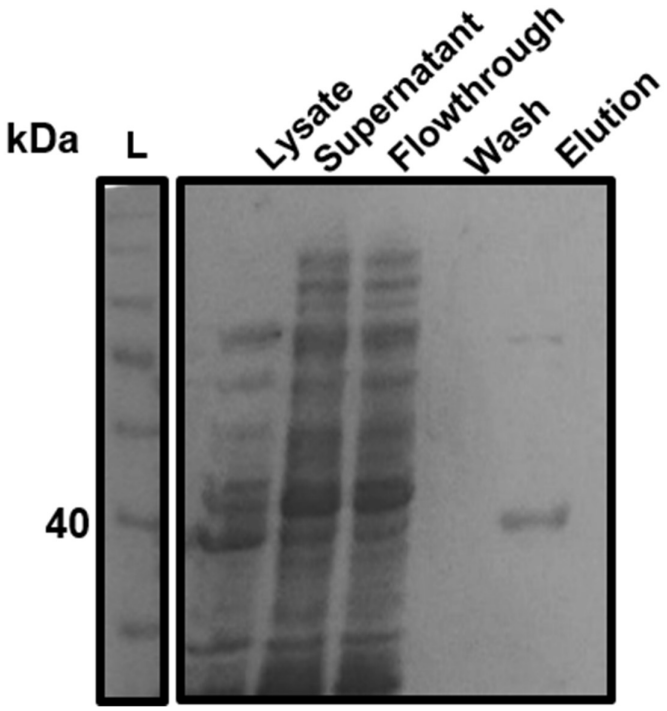

Figure 5.1. Purification of ApeE$_{25\text{-}385}$ and ApeE$_{25\text{-}385\ S35A}$. Example of SDS-PAGE analysis of the different fractions produced during purification of ApeE$_{25\text{-}385}$ To purify ApeE$_{25\text{-}385}$, 2 L cultures of BL21 LOBSTRIL, expressing either *apeE$_{25\text{-}385}$* or *apeE$_{25\text{-}385\ S35A}$* were induced at an OD$_{600nm}$ of about 0.6 with 50 µM IPTG for 16 h at 16°C. The following day, the cell pellets were lysed using a C3 cell disrupter to produce a lysate and from this lysate the soluble fraction was isolated (supernatant) and subsequently added to nickel-agarose beads for 30 min before being loaded onto a column. The flow-through was collected and the beads were washed with 300 mL of wash buffer prior to elution in 10 mL of elution buffer.

5.2.2. Lipase characterisation of ApeE using artificial fluorescent substrates.

Before embarking on biochemical characterisation of ApeE, it was essential to establish whether the purified protein was active. Previous work characterising the lipase activity of an *F. nucleatum* GDSL lipase autotransporter protein reported that 4-methylumbeliferylheptanoate (4-muH) was a good substrate for assessing lipase activity (Casasanta *et al*., 2017). Therefore, the purified ApeE proteins were tested for lipase activty against substrate 4-muH. Purified protein or buffer-exchange solution were added to black 96 well plates containing only reaction buffer or 50 μM 4-muH. If lipase activity was present, the breakdown product of 4-muH (4-mu) would fluoresce. Therefore, increased fluorescence was a proxy for increased lipase activity in the experiment. Fluorescence was measured every 2 min for 20 min at 26°C. The fluorescence was corrected for background fluorescence during analysis. As expected, samples that contained $ApeE_{25\text{-}385}$ had fluorescence outputs that were sigificantly highed than the fluorescence signal detected from lipase null mutant $ApeE_{25\text{-}385\ S35A}$ (Figure 5.2).

5.2.3. The effect of pH on ApeE activity.

For enzyme kinetic studies, it was important to determine the pH at which ApeE was most active as a lipase. To determine the effect of pH on ApeE activity, the purifed $ApeE_{25\text{-}385}$ was incubated with 200 μM of 4-muH in buffers ranging from pH 6.0-10.5. The fluorescence was measured every 2 min for 20 min at 26°C. The pH at which ApeE had the highest acitivty was 8.0 (Figure 5.3). At pH 6.0, little lipase activity could be detected (Figure 5.3). Above pH 8.5, the buffer alone started to hydrolyse the probe (data not shown) and therefore the activity of ApeE at these higher pH's are not likely

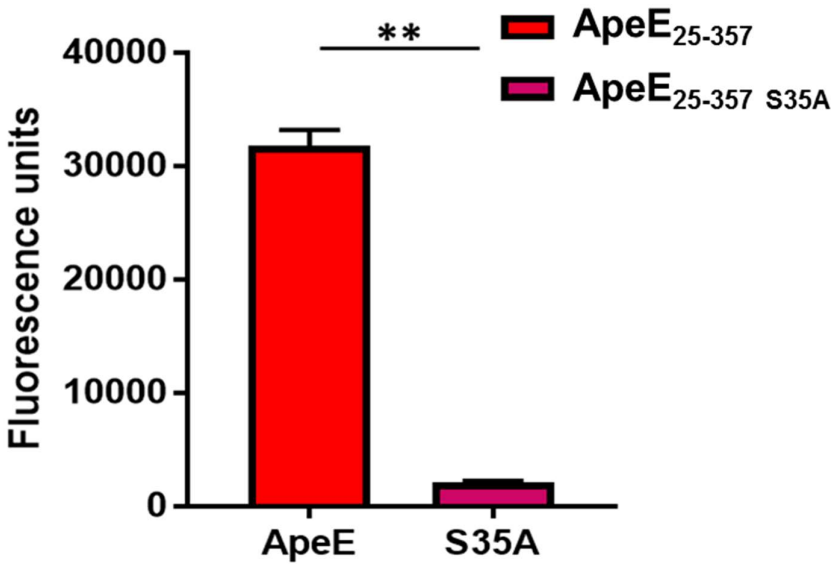

Figure 5.2. Lipase activity of purified ApeE against 4-muH. The activity of $ApeE_{25\text{-}385}$ (red) and $ApeE_{25\text{-}385\ S35A}$ (purple) on the artificial substrate 4-muH at 20 min. The fluorescence units measured are arbitrary and correspond to ester bond cleavage of the substrate. Statistical significance ($p<0.05$) was determined using a 2-tailed Students *t*-test (** $p<0.01$) and error bars represent the standard deviation.

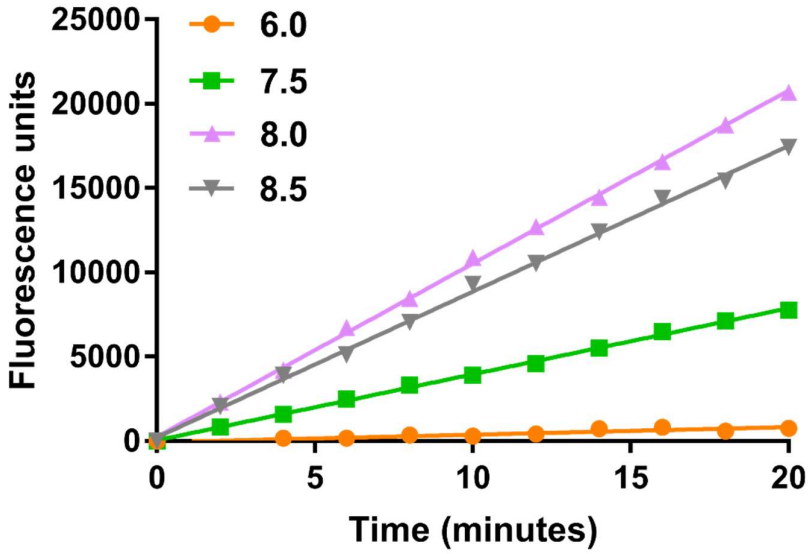

Figure 5.3. The effect of pH on the hydrolyisis of 4-muH by ApeE. To each pH buffer containing 200 μM 4-muH, 1 nM of purifed $ApeE_{25\text{-}385}$ was added. The fluorescence was measure every 2 min for 20 min at 26°C.

to be accurate. As a result, subsequent experiments investigating the effect of pH on ApeE activity used pH buffers ranging from 7.5-8.5.

A previous study establishing the enzyme activity of a lipase autotransporter reported an enzyme concentration of 1 nM to be optimum for kinetic experiments (Casasanta *et al*., 2017). To establish the optimum substrate concentration to determine the kinetic activity of ApeE, the pH 8.0 buffer was used. A concentration range of 4-muH between 0-15 μM was determined to show excess substrate and be suitable for kinetic experiments. The catalytic efficiency of ApeE in the pH buffer ranging from 7.5-8.5 was tested. In each pH buffer, 4-muH ranging in concentration from 0-15 μM was incubated with purified $ApeE_{25-385}$ and the fluoresence was measured every 2 min for 20 min at 26°C. The reaction was analysed at the intial rate of reaction, and for each condition, the concentration of product form per second was calculated to determine enzyme velocity. By fitting the rate data to the Michaelis-Menton equation, the paramters of ApeE enzyme kinetics were determined. ApeE had the most efficient catalytic activity (k_{cat}/K_m) at pH 8.0 (Figure 5.4) and the kinetics of ApeE lipase activty followed Michaelis-Menten kinetics. The pH 8.0 buffer was used for subsequent experiments.

5.2.4. Effect of the length of substrate acyl chain on ApeE activity.

To determine the substrate specificity of ApeE, the effect of varying the acyl chain on the lipase activity of ApeE was determined. Using the conditions established previously, four different substrates described in Table 5.1 were tested, with acyl chains ranging from C_4 to C_{18}. To initiate the reaction, 1 nM of purified $ApeE_{25-385}$ was added to 200 μM of substrate, and the fluorescence intensity was measured every 2 min for 20 min at 26°C. The substrates hydrolysed by ApeE were 4-muH and 4-muB (acyl chain lengths of 7 and 4 respectively), with an acyl chain length of 7 being optimal

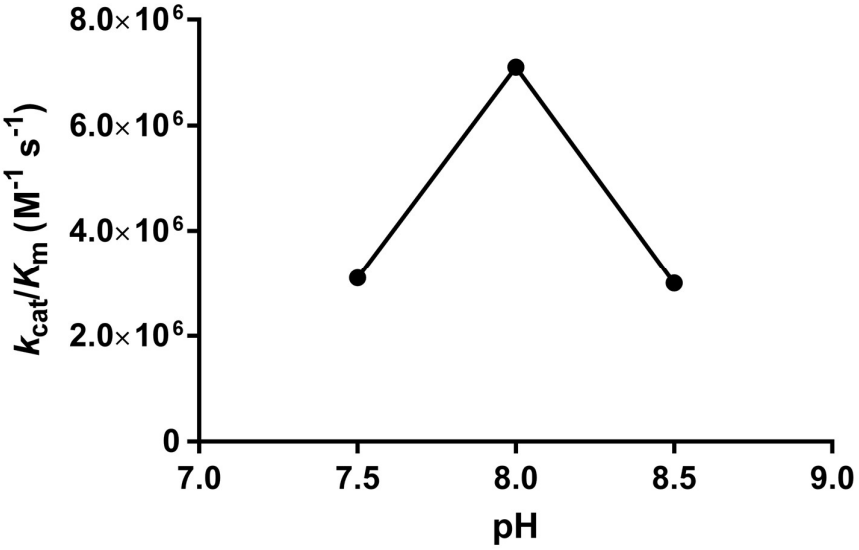

Figure 5.4. Catalytic efficiency of ApeE in pH buffers between 7.5 and 8.5. Purified $ApeE_{25\text{-}385}$ was added to a final concentration of 1 nM to arrays of 4-muH ranging from 0-15 μM in each pH buffer. Each assay contained 2 replicates and buffer only controls. Fluorescence was measured every 2 min for 20 min, and the data represented here show the complete k_{cat}/K_m for each pH buffer tested.

Table 5.1. 4-methylumbelliferyl substrates

Name	Name(full)	Chemical formula	Acyl chain length
4-muH	4-methylumbelliferyl heptanoate	$C_{17}H_{20}O_4$	7
4-muB	4-methylumbelliferyl butyrate	$C_{14}H_{14}O_4$	4
4-muP	4-methylumbelliferyl palmitate	$C_{26}H_{38}O_4$	16
4-muO	4-methylumbelliferyl oleate	$C_{28}H_{37}F_3O_4$	18

(Figure 5.5). No activity was detected with the longer acyl chain substrates, 4-muP and 4-muO (Figure 5.5), even when the substrate concentrations of 4-muO and 4-muP were increased to 1 mM (data not shown). These data suggest that for these experimental conditions, an acyl chain length of C_7 was the most favourable for ApeE lipase activity.

Next, the enzyme kinetics of ApeE against substrates 4-muH and 4-muB were compared. To determine the activity of ApeE against these substrates, concentration arrays between 0-1000 µM of 4-muH and 4-muB were generated and the lipase activity assay was set up as previously described. ApeE has a high k_{cat} value (23.0 s^{-1}) and a low K_m value (3.25 µM) when hydrolysing 4-muH (Figure 5.6A). These data indicate that ApeE displays efficient lipase activity against 4-muH as the protein can bind to and hydrolyse this substrate with high efficiency (k_{cat}/K_m = 7.1x10^6 M^{-1} s^{-1}) (Figure 5.6A).

The efficiency of ApeE-mediated hydrolysis against the 4 carbon substrate, 4-muB, was investigated. The experiment was completed in the same way as previously described. With 4-muB as a substrate, ApeE had a low k_{cat} (9.04 s^{-1}), suggesting low substrate turnover and a high K_m (249.0 µM) suggesting low substrate binding affinity and low catalytic efficiency (k_{cat}/K_m = 3.6x10^4 M^{-1} s^{-1}). Together these data suggest that the lipase activity of ApeE against 4-muB was less efficient than that observed against 4-muH (Figure 5.6B).

5.2.5 Inhibition of ApeE by methyl arachidonyl fluorophosphonate.

There have been no previous reports of inhibtors of ApeE. As methyl arachidonyl fluorophosphonate (MAFP) is known to inhibit other serine lipases with high substrate affinity (Casasanta *et al*., 2017) we sought to establish if MAFP would inhibit ApeE activity. To investigate whether the lipase activity of ApeE was inhibited by MAFP, the IC_{50} was determined; the concentration of inhibitor required to deplete the enzyme

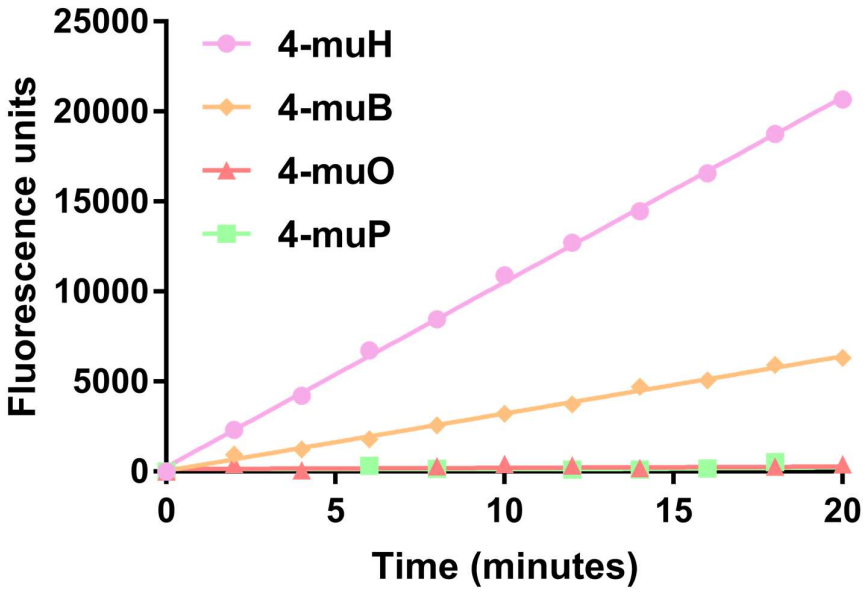

Figure 5.5. Lipase activity of ApeE against fluorescent substrates with varying acyl chain lengths. Fluorescent output of $ApeE_{25\text{-}385}$ lipase activity against 4-muH (pink circles), 4-muB (orange diamonds), 4muP (peach triangles) and 4-muO (green squares). All substrates were tested in pH 8.0 buffer. To initiate the reaction, 1 nM of purified $ApeE_{25\text{-}385}$ was added to 200 μM of substrate, and the fluorescent intensity was measure every 2 min for 20 min at 26°C.

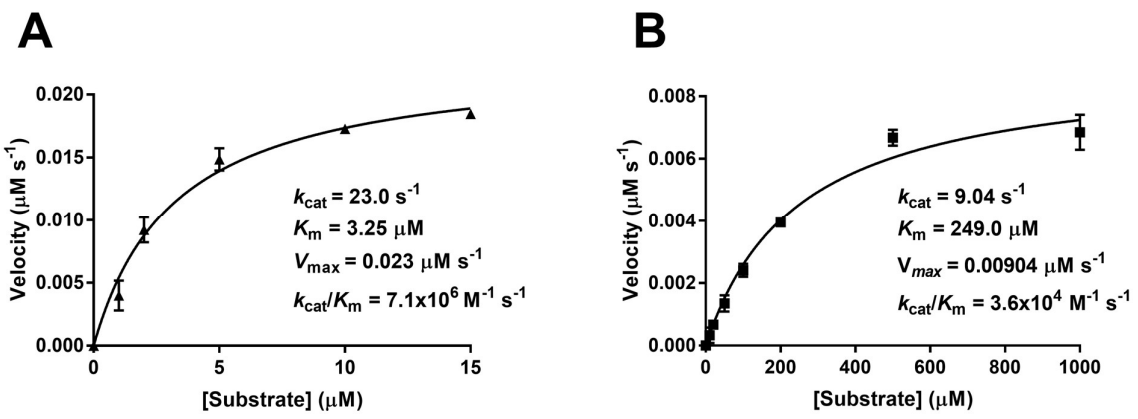

Figure 5.6. Michaelis-Menten kinetics of ApeE against lipase substrates. Enzyme kinetics of ApeE showing turnover of substrate per second for each substrate concentration. An array of 0-15 μM 4-muH or 0-1000 μM 4-muB were generated. To these arrays, either buffer only or 1 nM of purified ApeE was added in duplicate (n=2). The fluorescent output was measured every 2 min for 20 min. The data represented here is a curve showing enzyme velocity over substrate concentration for 4-muH (A) and 4-muB (B).

activity by 50% is known as the IC_{50}. The IC_{50} was calculated by plotting a log(inhibitor) vs. normalised response using variable slope and a least squares (ordinary) fit model. The IC_{50} of MAFP against ApeE was calculated to be 0.53 nM (Figure 5.7). This low IC_{50} value indicates that MAFP is a potent inhibitor of ApeE lipase activity.

To understand the mode of MAFP inhibition against ApeE, ActivX TAMRA-FP was used to label the active site serine of ApeE. TAMRA-FP contains a fluorescent TAMRA molecule connected by a linker to a fluorophosphonate (FP). The FP molecule binds to active site serines and the fluorescence of TAMRA can then be detected. Purified protein (either ApeE or $ApeE_{S35A}$) was incubated with either MAFP or PBS for 20 min at room temperature prior to the addition of TAMRA-FP and a further 20 min incubation at room temperature. The samples were analysed by SDS-PAGE. The gel was imaged using a G:Box XX6 system using the TAMRA fluorescence filter to detect TAMRA fluorescence. Only active ApeE without MAFP showed TAMRA fluorescence (Figure 5.8A). The addition of MAFP resulted in the loss of TAMRA fluorescence (Figure 5.8A). TAMRA fluorescence was not detected in the inactive ApeE ($ApeE_{S35A}$) sample (Figure 5.8A). To ensure the results were not influenced by protein abundance, the same samples were analysed by Western immunoblotting using anti-his tag primary antibodies. The secondary anti-mouse antibody was conjugated to horse radish peroxidase. The blots were incubated with ECL-Plus blotting reagents and subsequently visualised using Lucent Blue X-ray film prior to development on an SRX-101A medical film processor. The blot shows that each sample contained protein and therefore the samples negative for fluorescent TAMRA were not caused by lack of protein in the sample (Figure 5.8B). These data suggest that MAFP is a competitive inhibitor for the active site serine of ApeE.

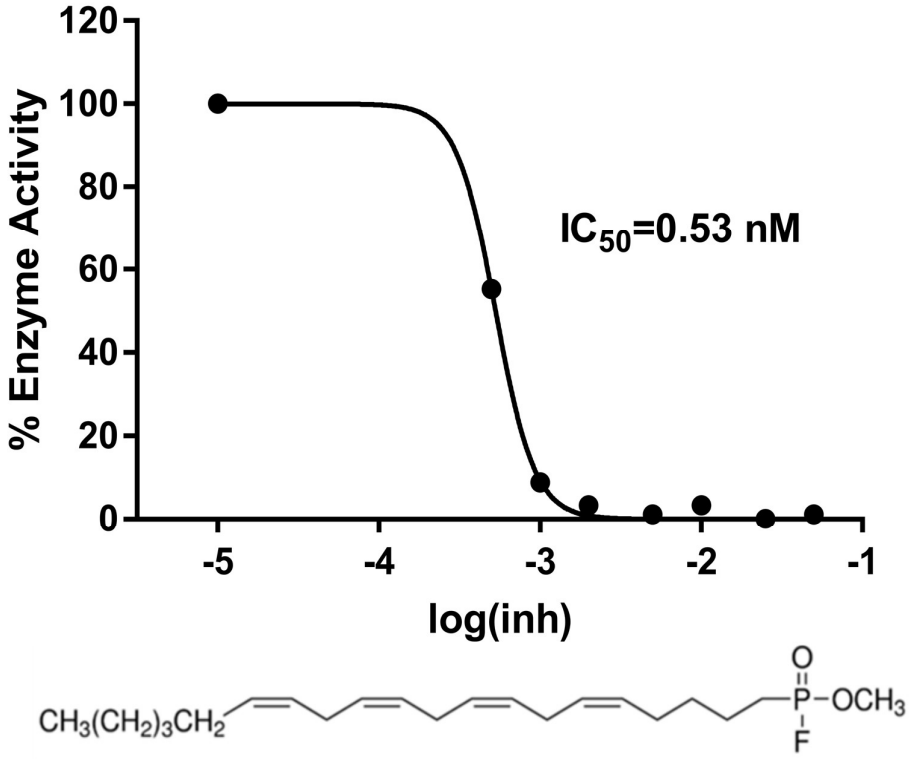

Figure 5.7. IC_{50} of MAFP inhibition of ApeE. The percentage enzyme activity of ApeE in a range of concentrations of MAFP (0-50 nM). The concentrations of MAFP were transformed to a logarithmic scale to show log(inh). The IC_{50} was calculated by fitting the curve to a log(inhibitor) vs normalised response using variable slope and a least squares (ordinary) fit model.

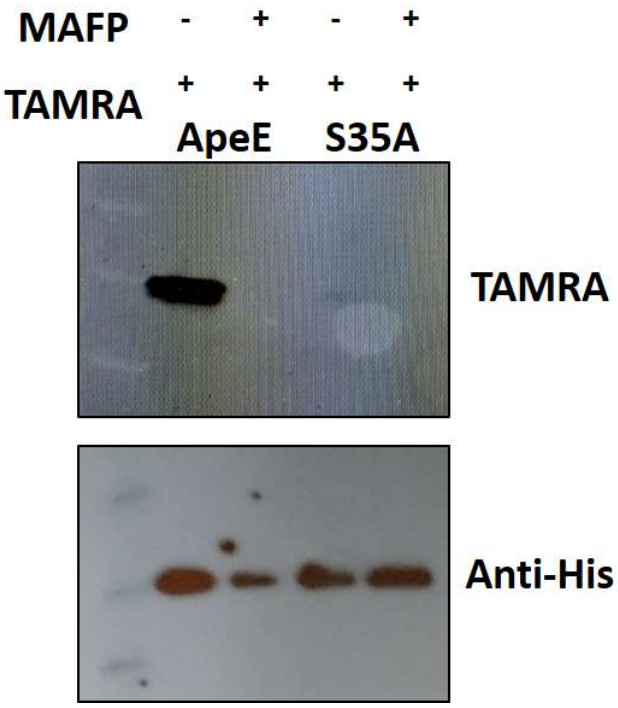

Figure 5.8. TAMRA active site labelling. (A) SDS-PAGE gel visualisation using a G:box XX6 system and the TAMRA fluorescent filter to detect TAMRA-FP bound to active site serine. (B) Western immunoblot using anti-His tag antibodies and detected with the ECL western blotting system.

5.2.6 MAFP inhibition of surface exposed ApeE in *E. coli*.

As MAFP inhibited the action of the purified fragment $ApeE_{25-385}$, its ability to inhibit the full length ApeE was investigated. Thus, overnight cultures of *E. coli* expressing ApeE on the cell surface, which were described in the previous chapter, were incubated with either MAFP or PBS for 1 h. The cells were washed in PBS and resuspended in reaction buffer. For each lipase reaction $2x10^6$ bacterial cells were added to the buffer and the reaction was initiated by the addition of 4-muH or 4-muB. The fluorescence was measured every 2 min for 20 minute at 26°C. Lipase acitivity was detected from the full length ApeE on the surface of *E. coli* cell surface and this activity was not detected when MAFP was also present (Figure 5.9A). In contrast, no lipase activity was detected from the serine mutant or empty vector control (Figure 5.9A). Similarly, lipase activity against 4-muB was detected only in the absence of MAFP (Figure 5.9B). These data suggest that MAFP can inhibit the activity of ApeE exposed on the cell surface and confirm the surface localisation of the active passenger domain described in the previous chapter

5.2.7 Phospholipase characterisation of ApeE.

Other GDSL lipases and indeed autotransporters, have be experimental proven to hydrolyse phospholipids (Casasanta *et al*., 2017). As the multiple autotransporter strain was attenuated in murine gallbladders, and bile phospholipids might be carbon source for *Salmonella in vivo*, the ability of ApeE to hydrolyse artificial phospholipid substrates was investigated. Phospholipases that cleave ester bonds exist in 3 forms; phospholipases A_1, A_2 and B (PLA_1, PLA_2 and PLB respectively). PLA_1 enzymes hydrolyse the ester bond at the sn-1 position on the phospholipid, PLA_2 enzymes cleave the ester bond at the sn-2 position and PLB enzymes are able to cleave both ester bonds.

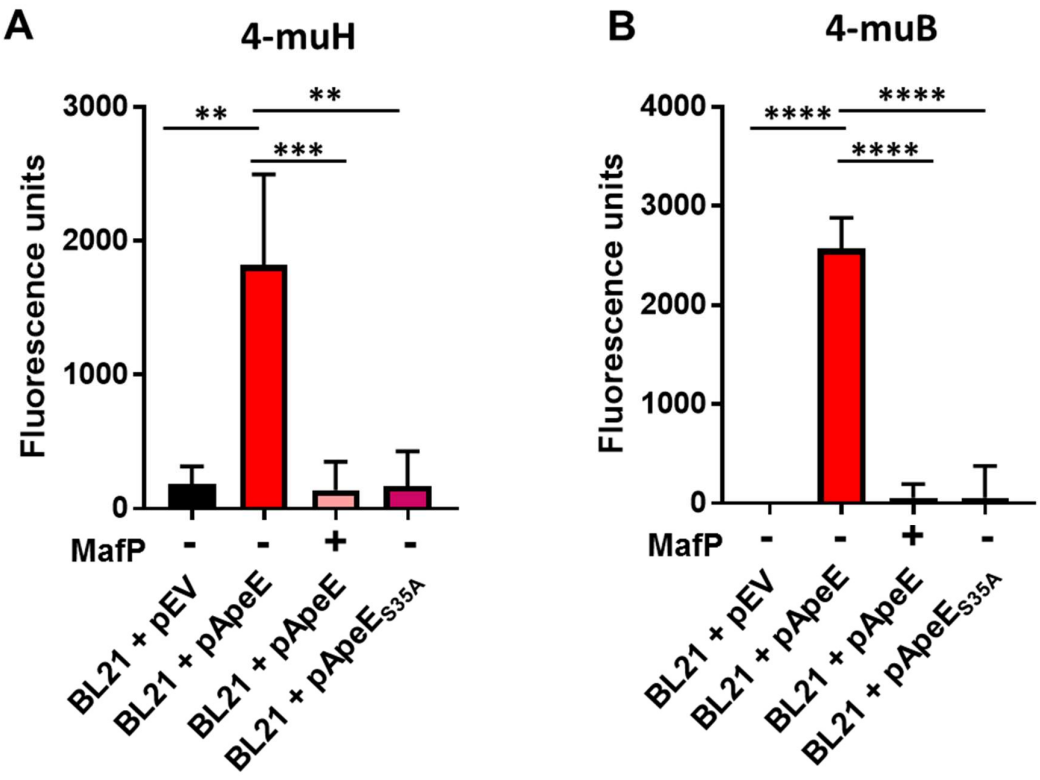

Figure 5.9. Inhibition of ApeE expressed on the surface of *E. coli* BL21. Fluoresence readings represented here are after 20 min of the reaction with n=2. Strains were either incubated with MAFP (+) or PBS (-) prior to reaction initiation. Statistical significance was calculated using a one-way anova test with significance determined as $p<0.05$. (A) Activity of surface exposed ApeE against 4-muH. (B) Activity of surface expressed ApeE against 4-muB.

To classify the phospholipase activity of ApeE, PLA_1 and PLA_2 determination kits were used. These kits each contained a phospholipase substrate and positive A1 or A2 phospholipase control enzymes. The substrates were either PLA_1 or PLA_2 specific such that they will only fluoresce upon cleavage of the ester bond at the sn-1 or sn-2 position respectively. Each substrate was incorporated into liposomes and diluted in reaction buffer to a final concentration of 1.65 μM. For the experiment, the liposome mix for each substrate was incubated with the A1 and A2 control enzymes or purified ApeE at either 10 or 1 μM concentrations. The fluorescence was measured every 2 min for 30 min at 26°C. The fluorescence reported is the final measurements after 30 min incubation. For the PLA_1 specific substrate, the A1 control enzyme, but not the A2 control enzyme, cleaved the substrate to produce fluorescence. Both concentrations of ApeE resulted in high fluorescence, and this was significantly higher than the fluorescence measured for the control A1 enzyme (Figure 5.10A). Similarly, using the PLA_2 specific substrate, the A2 but not the A1 control enzyme cleaved the substrate and both ApeE concentrations showed hydrolysis of the PLA_2 substrate (Figure 5.10B). Therefore, ApeE had PLA_1 and PLA_2 enzyme activity and was classified as a PLB enzyme.

5.2.8 MAFP inhibition of ApeE phospholipase B activity.

In the previous section ApeE was shown to be a phospholipase B (PLB) enzyme, which is capable of cleaving both ester bonds in a phospholipid to release the acyl chains and the head group. As MAFP was shown to inhibit ApeE lipase acvtivity, but not specifically to inhibit phospholipase activity, the effect of MAFP on ApeE PLB activity was investigated. Purified ApeE was incubated with either MAFP or PBS for 30 min at room temperature. The reaction was initiated by the addition of liposomes either PED-A1 (PLA_1) or bis-BODIPY® PC-A2 (PLA_2) substrates. The fluorescence intensity

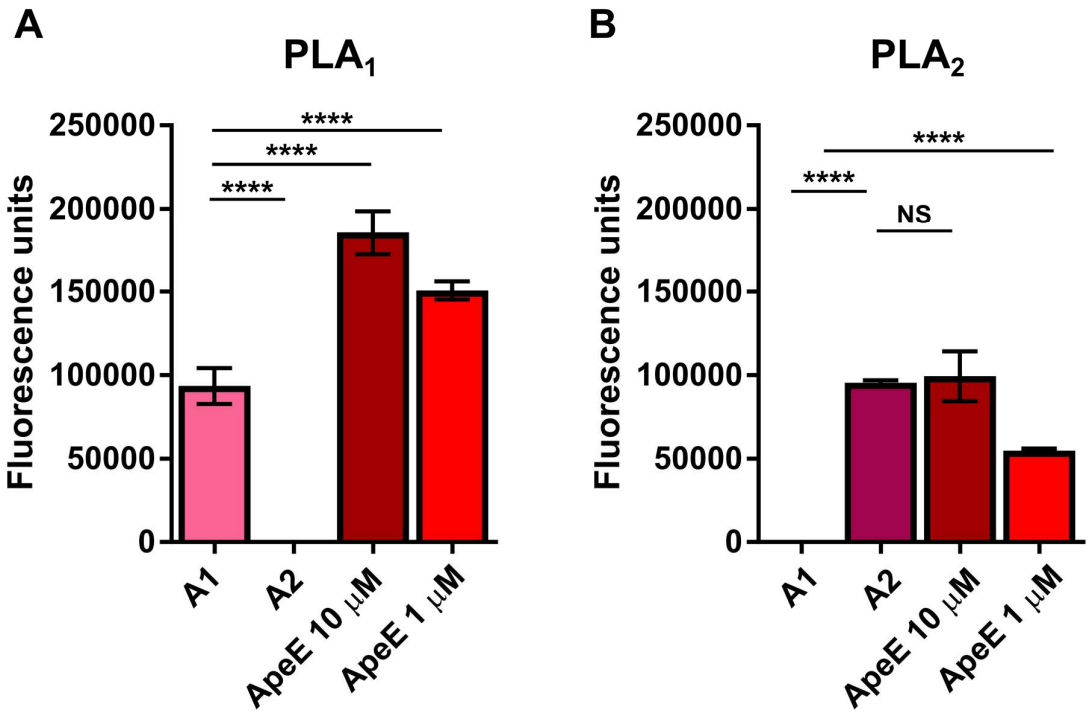

Figure 5.10. Phospholipase characterisation of ApeE. Phospholipase A_1 (PLA_1) and phospholipase A_2 (PLA_2) specific fluorescent substrates (PED-A1 and BODIPY® PC-A2 respectively) were incorporated into liposomes containing dioleoylphosphoglycerol and dioleoylphospahtidylcholine in reaction buffer 50 mM Tris-HCl, 100 mM NaCl, 1 mM $CaCl_2$, pH 8.9. Buffer only control or ApeE was added at 2 concentrations (1 and 10 μM) to initiate the reactions. Each reaction contained a positive A_1 or A_2 control enzyme. The fluorescence was measured (excitation = 505 nm and emission = 460 nm) for 30 minutes at 26°C. The fluorescence was corrected for buffer only background and the data here represented the final fluorescence measurement after 30 minutes for (A) PLA_1 and (B) PLA_2 substrates. Statistical significance ($p<0.05$) was determined using a one-way anova with Dunnet's correction for multiple comparison comparing the test samples to the positive A_1 or A_2 controls.

was measured every 2 min for 20 min. For both PLA_1 and PLA_2 substrates, ApeE was active in the absence of MAFP (Figure 5.11).

5.3 Discussion

In this chapter the lipase activity of ApeE was explored. First, the effect of pH on ApeE activity was investigated. It was determined that the optimum pH for ApeE activity was pH 8.0. At pH 8.0, ApeE had the most efficient catalytic activity and substrate binding. These data might correspond to the environment in which *Salmonella* resides within the host. The pH of the small intestine ranges from 6.0-7.4 (Fallingborg, 1999) and therefore if ApeE were to be expressed there, the catalytic efficiency may be decreased in comparison to other sites of the body. One organ that *Salmonella* can colonise, and persist chronically within, is the gallbladder. Therefore, ApeE might be very catalytically efficient within bile. These data indicate that ApeE would not be as efficient in areas of low pH, such as the stomach or perhaps inside an activated phagosome, which are typically acidic.

ApeE showed enzyme activity against the substrates with acyl chain lengths between C_4 and C_7 (4-muB and 4-muH). This phenomenon was observed previously (Casasanta *et al.*, 2017) whereby the phospholipase A_1 FplA from *F. nucleatum* was able to hydrolyse 4-muH much more efficiently that 4-muB. It could be that the artificial substrates are more unsaturated than natural phospholipid's and the lack of double bonds might result in a rigidity that natural phospholipids do not have. ApeE is known to hydrolyse the chromogenic substrate C_8 substrate methylumbelliferyl caprylate (Carinato *et al*, 1998), has an acyl chain of 8. It might be that ApeE can hydrolyse these longer acyl chain substrates, but the conditions were not optimised during this experiment.

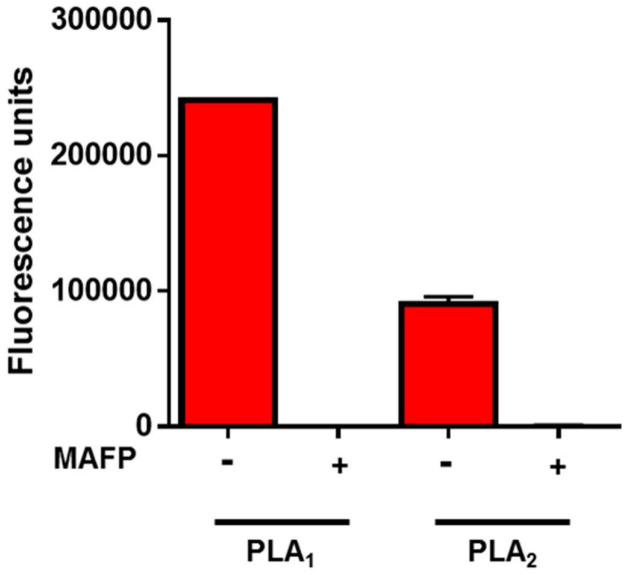

Figure 5.11. MAFP inhibition of phospholipase B activity of ApeE. (A) Activity of ApeE against PLA_1 (PED-A1) and PLA_2 (bis-BODIPY® FL C11-PC) in the presence (+) or absence (-) of MAFP.

It became apparent upon analysis of the kinetic data that the concentration of enzyme used for the experiments (1 nM) was perhaps too high, especially at pH 8.0 with 4-muH as the substrate. Future experiments could look at titrating the enzyme concentration to establish an enzyme concentration that would be low enough to detect activity when the substrates were in excess. It would be interesting to compare the substrate binding affinities of ApeE on a substrate more similar to naturally occurring lipids. Indeed, studies that compare the substrate binding affinities of a serine lipase autotransporter to the lipase substrates 4-muH and PED-A1 found that the enzyme bound the synthetic phospholipase substrate with much higher affinity (Casasanta *et al*, 2017). Due to time limitations, the PLA_1 and PLA_2 enzyme kinetics for ApeE could not be investigated.

In this chapter, an ApeE inhibitor (MAFP) was identified and characterised. MAFP was a competitive inhibitor of ApeE that inhibited lipase activity of the purified protein and full length protein enzyme activity on the surface of *E. coli* with a low IC_{50} value. MAFP has been shown to inhibit other serine lipases (Casasanta *et al*., 2017, Phillips *et al*., 2003). MAFP was initially shown to be an inhibitor of a phospholipase A_2 (PLA_2) enzyme by an irreversible reaction that inhibited enzyme substrate binding (Lio *et al*., 1996). Future work could look at characterising other ApeE inhibitors and potentially ones that could be used to specifically inhibit ApeE activity *in vivo*.

ApeE was shown to be able cleave both ester bonds of a phospholipid, and was therefore characterised as a phospholipase B enzyme. Phospholipases can be important for virulence, by interfering with various host processes such as intracellular signalling (van der Meer-Janssen *et al*., 2010). As ApeE has phospholipase activity, it might be important for *S.* Typhimurium virulence. In the next chapters, results from examining the biological substrates of ApeE are reported.

CHAPTER 6

The interaction of ApeE with glycerophospholipids

6.1 Introduction

Glycerophospholipids are the major lipid species of cellular membranes in *S*. Typhimurium. The membrane phospholipid composition was shown to be ~83% phosphatidylethanolamine (PE), 11% phosphatidylglycerol (PG), 4% cardiolipin (CL) and 2% acyl-PG (Olsen and Ballou, 1971). The lipid composition of eukaryotes is more complex, with additional lipid species present in the membranes. These lipid species include phosphatidylcholine (PC), phosphatidylserine (PS) and Phosphatidylinositol (PI) sphingomyelin (SM). In addition, some eukaryotic lipid species can act as second messenger signals under various conditions (van Meer *et al*., 2008). Phospholipids can also exist in a "Lyso" form. Lyso-phospholipids are derivatives of phospholipids that have been hydrolysed by a phospholipase A_2 enzyme, resulting in a phospholipid head group with one acyl chain.

As shown in earlier chapters, ApeE is a GDSL lipase autotransporter conserved in *Salmonella*. GDSL lipase proteins are known to be promiscuous for substrates, hydrolysing a variety of lipids of varying acyl chain length and head group (Lescic Asler *et al*., 2010). The results of studies into the ability of ApeE to bind, cleave and utilise host and bacterial glycerophospholipids are presented in this Chapter.

6.2 Results

6.2.1 Novel phospholipid substrates of ApeE.

Lipid binding is the first enzymatic step to lipid hydrolysis, therefore the ability of ApeE to bind to a range of phospholipids was tested. To determine the glycerophospholipids to which ApeE is able to bind to, 50 µg/ml of purified $ApeE_{25\text{-}385}$ was incubated with PIP strip membranes (Thermofisher). PIP strips are PVDF

membranes impregnated with 200 pmol of each different glycerophospholipid. After incubation, the strips were washed and anti-ApeE antibody was added. Anti-rabbit IgG AP conjugated antibody was added and the spots were visualised upon addition of the substrate BCIP-NBP. The lipid spots would appear dark if ApeE had bound to it. ApeE bound most glycerophospholipids on the strip, apart from sphingosine-1-phosphate (Figure 6.1). The result suggests ApeE bound phosphatidic acid (PA) and phosphatidylserine (PS) with the highest affinity (Figure 6.1). ApeE also bound both bi- and tri- phosphorylated various phosphatidylinositides (PtdIns).

6.2.2 Lipid profiles of ox-bile exposed to ApeE.

To identify the biological host lipids ApeE might interact with, the ability of ApeE to hydrolyse lipids in host bile was investigated. Purified ApeE was added to a final molar concentration of 2 μM to a solution of 5% ox bile in water (v/v) and incubated for 12 h at 37°C. As a control sample, buffer only was added to 5% bile solution. Lipids were extracted using a Bligh-Dyer method and resuspended in chloroform prior to loading onto Silica coated aluminium Thin Layer Chromatography (TLC) plates. Once the spots had dried, the TLC plate was placed in a humid chamber containing an equilibrated solvent system of chloroform: methanol: water (65:25:4). This solvent system is known to separate phospholipids based on head group polarity. The TLC plates were air dried and stained with phosphomolybdic acid (PMA) once the solvent front reached ~ 1 cm away from the top of the plate. The plates were charred to activate the PMA stain and the intensities of each lipid species were examined. The lipid species within the bile samples resolved in this solvent system and showed good separation. The buffer only controls had comparable levels of all lipid species to the bile only sample. When ApeE was introduced to bile, two lipid species (labelled 1 and

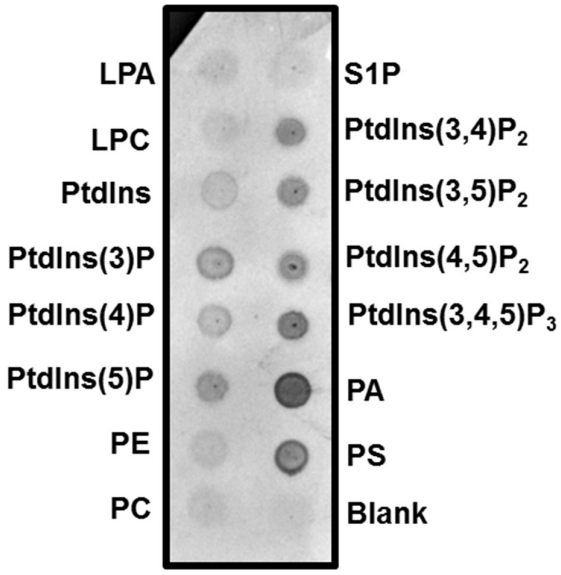

Figure 6.1. Phospholipid binding of ApeE. Different species of phospholipid spotted onto a PVDF membrane at a concentration of 200 pmol. The strips were blocked with 3% BSA prior to the addition of 50 µg/ml of purified ApeE protein. The strips and protein were incubated overnight at 4°C with shaking. The strips were washed and then incubated with anti-ApeE antibodies (1:2,000) for 1 h. The strips were washed and subsequently incubated with anti-rabbit IgG secondary antibody. The spots were detected upon the addition of the AP substrate BCIP-NBP. Abbreviations are; Lyso-phosphatidic acid (LPA), Lyso-phosphatidylcholine (LPC), Phosphatidylinositol (PtdIns), Phosphatidylinositol-3-phosphate (PtdIns(3)p), Phosphatidylinositol-4-phosphate (PtdIns(4)P), Phosphatidylinositol-5-phosphate (PtdIns(5)P), Phosphatidylethanolamine (PE), Phosphatidylcholine (PC), Sphingosin-1-phosphate (S1P), Phosphatidylinositol-3,4-biphosphate (PtdIns(3,4)P_2), Phosphatidylinositol-3,5-bisphosphate (PtdIns(3,5)P_2), Phosphatidylinositol-4,5-bisphosphate (PtdIns(4,5)P_2), Phosphatidylinositol-3,4,5-trisphosphate (PtdIns(3,4,5)P_3), Phosphatidic acid (PA) and Phosphatidylserine (PS).

2) were either reduced or no longer detectable (Figure 6.2). The relative front (rf) values for the lipid species labelled as 2 corresponded to the known migration of Lyso-phosphatidylcholine (Figure 6.2) and the lipid species labelled as 1 corresponded to the known migration of either phosphatidylserine (PS), phosphatidylcholine (PC,) or phosphatidylinositol (PI), therefore this lipid species might be PS, PI, PC or a mixture.

To better resolve the lipid species represented by number 1 in Figure 6.2, an alternative solvent system was used. This solvent system was comprised of chloroform: methanol: ammonium hydroxide (65:25:4). This solvent system can differentiate PC from PI and PS; unlike PC, neither PS nor PI migrate from the origin. Lipid extracts were added to a TLC plate as previously described and placed into a humid chamber with the equilibrated solvent system. The plates were removed and stained as described previously. Bile incubated with purified ApeE showed changes in the abundance of three lipid species, and the complete degradation of one lipid species, which had an rf value of 0.08 (Figure 6.3A). This rf value indicated that the lipid species that was completely degraded by ApeE might have been Lyso-PC, similar to the previous solvent system. To test this hypothesis, a standard of Lyso-PC was used. The Lyso-PC standard was applied to TLC plates and placed in a humid chamber containing the solvent system described above. The Lyso-PC standard appeared to migrate to the same rf as the lipid species that was completely degraded by ApeE (Figure 6.3B). Therefore, the lipid species that ApeE can completely degrade in ox bile was likely to be Lyso-PC. The other lipid species were not formally identified, but the species labelled as number 1 in Figure 6.4A had an rf value of 0.30, which is the known rf value of PC. The lipid species labelled as number 2 in Figure 6.3A had an rf value of 0.12. This rf value might correspond to PS, PI or sphingomyelin (SM).

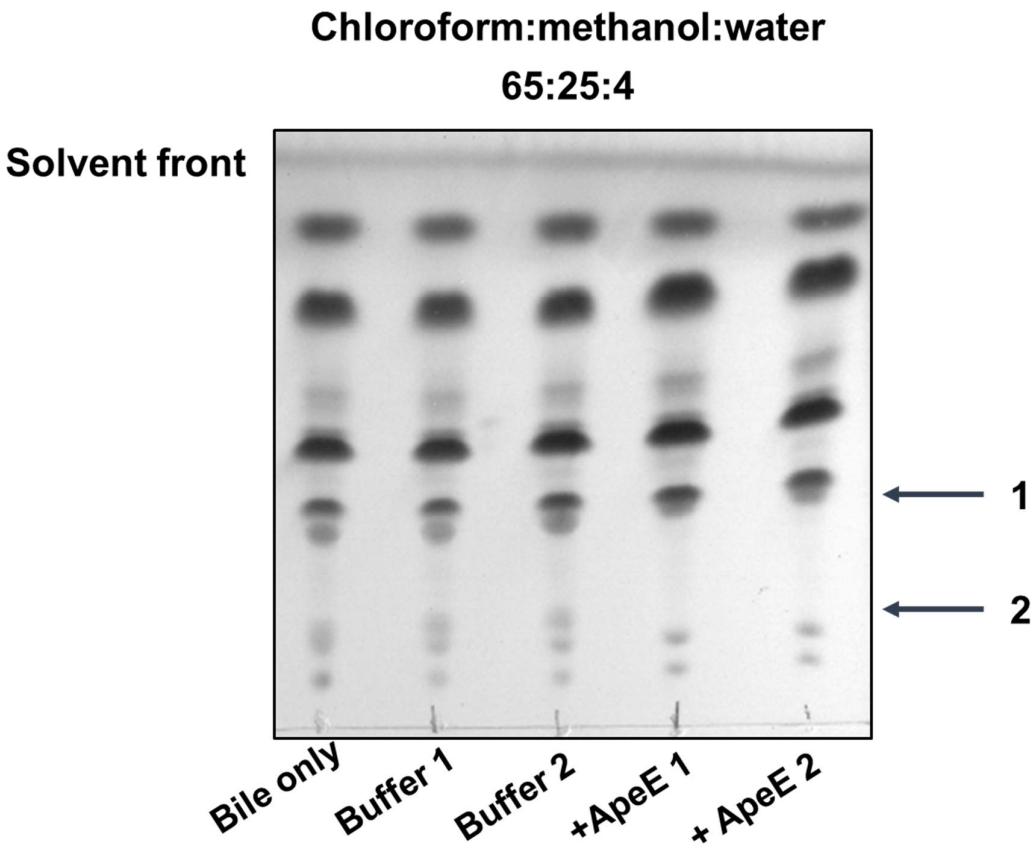

Figure 6.2. One-direction thin layer chromatography analysis of bile lipids after incubation with purified ApeE. Ox bile (5% in water w/v) was incubated with either buffer only or 2 μM of purified ApeE for 12 h at 37°C. 1 mL of liquid was used for lipid extraction. Lipids were extracted using a Bligh-Dyer method and analysed by TLC. Silica TLC plates were cut as 10 cm by 10 cm squares and the lipids were spotted on using glass microcapillary tubes. The solvent system used was chloroform: methanol: water (65:25:5). Plates were air dried and subsequently stained with phosphomolybdic acid (PMA), and charred with a heat gun to reveal lipid species. Numbers 1 and 2 correspond to the lipid species that were altered between buffer only samples and those incubated with ApeE.

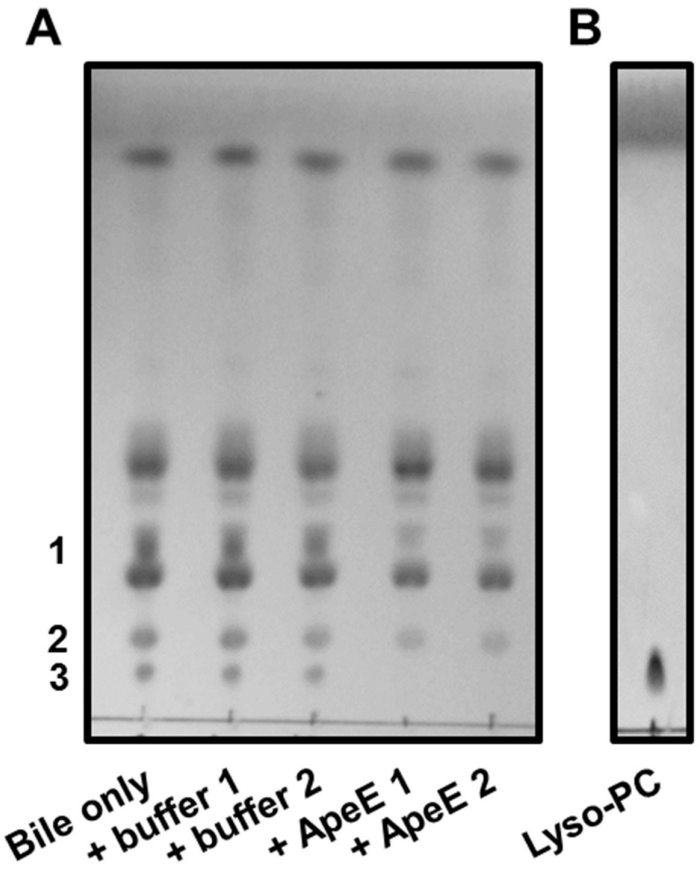

Figure 6.3. One-directional TLC lipid profile of Ox bile incubated with purified ApeE. (A) Lipids extracted from ox bile incubated with either buffer only or purified ApeE were analysed by TLC. Lipids were spotted onto 10 cm by 10 cm silica TLC plates. The lipids were separated by a chloroform: methanol: ammonium hydroxide (65:25:4) solvent system. Plates were air dried and stained with phosphomolybdic acid prior to charring with a heat gun to reveal lipid species. Number 1, 2 and 3 correspond to lipid species altered between samples incubated with purified ApeE or not. (B) TLC analysis of a Lyso-PC standard in the solvent system described above.

6.2.3 *Salmonella* growth using bile phospholipids as sole carbon sources *in vitro*.

Previous work showed that *Salmonella* was able to utilise phospholipids in bile *in vivo* and *in vitro* as a potential carbon source (Antunes *et al*., 2011). As purified ApeE altered the amounts of Lyso PC in ox-bile, the role of ApeE for utilisation of Lyso-PC as a sole carbon source was investigated. Lyso-PC is a derivative of PC that is formed by the action of a phospholipase A_2 enzyme on PC (Figure 6.4A and B). Lyso-PC has one acyl chain and is more water soluble that PC, and can therefore be added to water-based liquid growth medium.

M9 minimal media supplemented with L-Histidine and either glucose or Lyso-PC as sole carbon sources were inoculated with either SL1344, *apeE::aph,* complemented mutant (+pApeE) or serine mutant (+pS35A). The OD_{600nm} was measured using a Clariostar plate reader every 3-6 h, with manual resuspension to ameliorate Lyso-PC settling, for 24 h at 37°C. All strains grew to comparable levels and with similar rates when glucose was provided as the sole carbon source (Figure 6.4B). Only strains expressing active ApeE (Wild-type SL1344, and +pApeE complement) were able to grow utilising Lyso-PC as a sole carbon source and strains not expressing *apeE* (*apeE::aph*) or the inactive serine mutant (+pS35A) showed no growth (Figure 6.4C).

Lyso-PC in solution tended to become insoluble over the course of the experiment, therefore the growth of *S.* Typhimurium SL1344 strains on M9 minimal media agar plates was investigated. Overnight cultures of each strain were washed twice with sterile PBS before being serially diluted 1:10. Each strain was spot plated onto M9 minimal media agar plates supplemented with either glucose or Lyso-PC as a sole carbon source. Similar to liquid growth, all strains grew to comparative levels

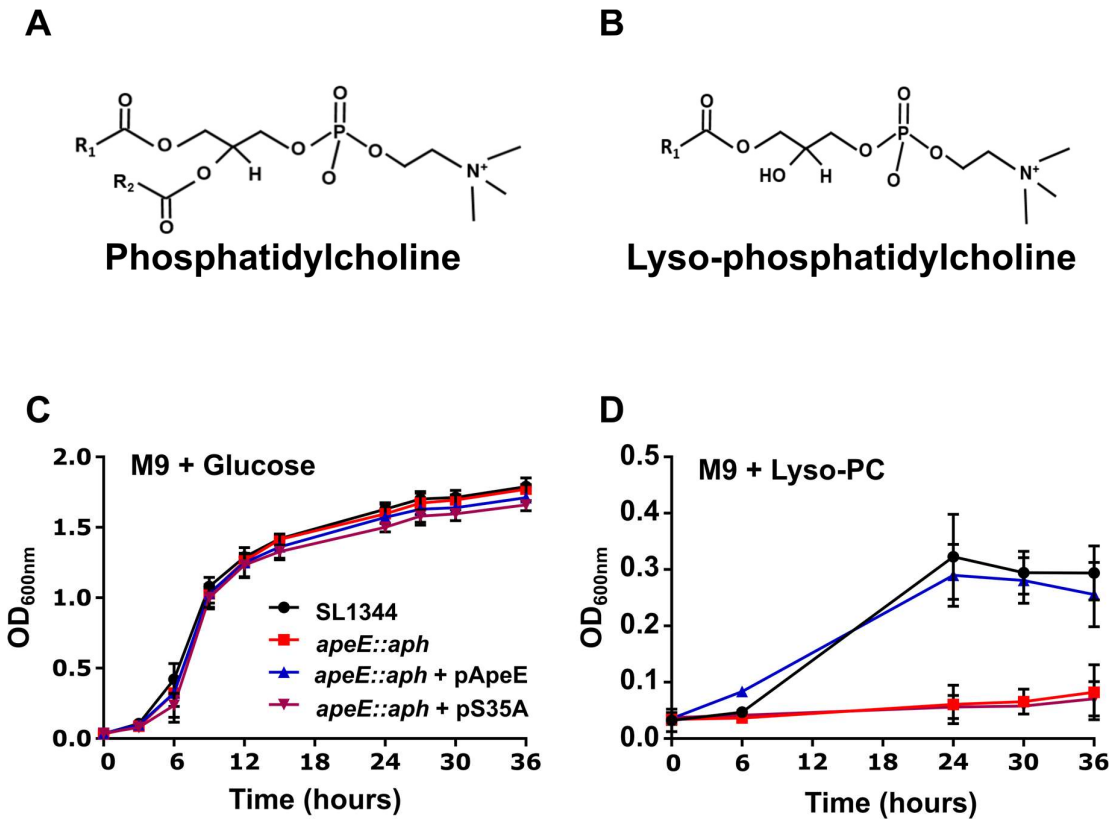

Figure 6.4. Growth of *S.* Typhimurium SL1344 strains in M9 minimal media supplemented with either glucose or Lyso-PC. Chemical structures of phosphatidylcholine (A) and Lyso-phosphatidylcholine (B). (C) Growth of *S.* Typhimurium SL1344 (black), *apeE::aph* (red), *apeE::aph* + pApeE (blue) and *apeE::aph* + pS35A (purple) over 36 h in M9 minimal medium supplemented with 0.4% glucose. (D) Growth of the aforementioned strains in M9 minimal medium supplemented with 1 mg/ml Lyso-PC. Both growth curves were completed in 96 well microtitre plates and the OD_{600nm} measured using a Clariostar plate reader after manual resuspension of the growth medium. The plates were incubated at 37°C for 36 h. Data here represents 3 biological replicates and the error bars show standard error of the mean (SEM).

using glucose as a carbon source and the only strains with active ApeE could grow utilising Lyso-PC as a sole carbon source (Figure 6.5).

To establish whether ApeE was actively breaking down Lyso-PC in the media, wild-type SL1344, *apeE* mutant, pApeE complement and the $ApeE_{S35A}$ mutant were grown in M9 minimal medium containing Lyso-PC as a sole carbon source for 24 h at 37°C. After growth, the bacterial cells were removed via centrifugation and the lipids were extracted and resuspended in chloroform. Lipid samples from each strain were analysed using TLC with a chloroform: methanol: water (65:25:4) solvent system. The TLC plates were stained with PMA before being charred. After 30 h of growth, Lyso-PC can no longer be detected in the media of strains with active ApeE (SL1344 and +pApeE complement), but is detectable in strains that do not express active ApeE (mutant and +p$ApeE_{S35A}$) (Figure 6.6). These data suggest that ApeE enables growth on Lyso-PC as a sole carbon source and this is mediated by the active hydrolysis of Lyso-PC into constituent molecules; head group and fatty acid.

6.2.4 ApeE mediates *E. coli* growth on Lyso-PC as a sole carbon source.

There is no homolog of *apeE* in *E. coli* and therefore to understand whether ApeE was a single factor that could promote hydrolysis of Lyso-PC, an empty vector plasmid or plasmids expressing either full length *apeE* or $apeE_{S35A}$ were transformed into *E. coli* BW25113. Whole cell protein samples from induced overnight cultures were analysed by SDS-PAGE and Western Immunoblotting. Membranes were probed with primary anti-ApeE antibody followed by an anti-rabbit AP conjugated secondary antibody. The blot was developed using the substrate NBP-BCIP. ApeE can be detected from strains expressing either ApeE or $ApeE_{S35A}$ but not the empty vector control (Figure 6.7A). All samples had comparable levels of protein when analysed by SDS-PAGE (Figure 6.7A).

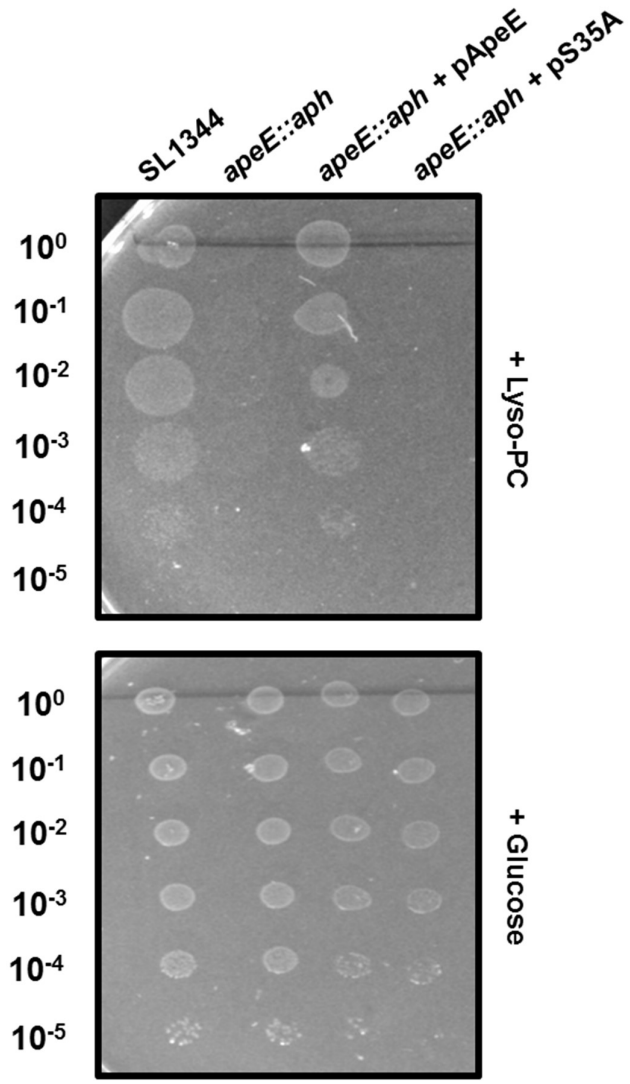

Figure 6.5. Growth of SL1344 strains on M9 minimal agar supplemented with either glucose or Lyso-PC. M9 minimal media plates were supplemented with either 0.4% glucose or 1 mg/ml Lyso-PC. Overnight cultures of SL1344, *apeE::aph*, *apeE::aph* + pApeE and *apeE::aph* + pS35A were washed twice in sterile PBS and serially diluted 1:10. Each dilution was spotted onto the M9 minimal media agar plates and incubated at 37°C for 16 h.

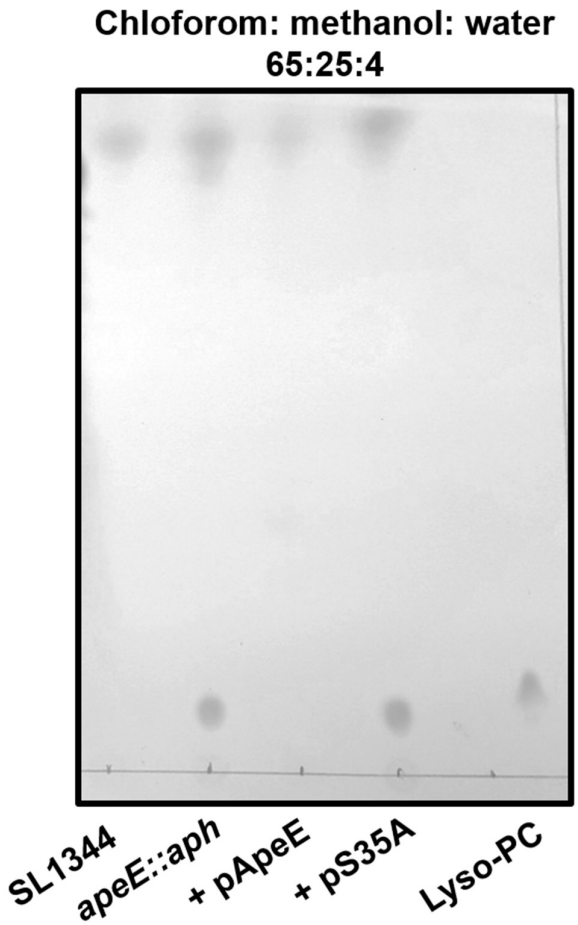

Figure 6.6. TLC analysis of M9 minimal medium supplemented with Lyso-PC after SL1344 growth. Lipids from liquid M9 minimal medium were extracted after SL1344 growth using a Bligh-Dyer method. The lipids were resuspended in chloroform and analysed by TLC. The solvent system used was chloroform: methanol: water (65:25:4) and the plates were stained with phosphomolybdic acid prior to charring with a heat gun.

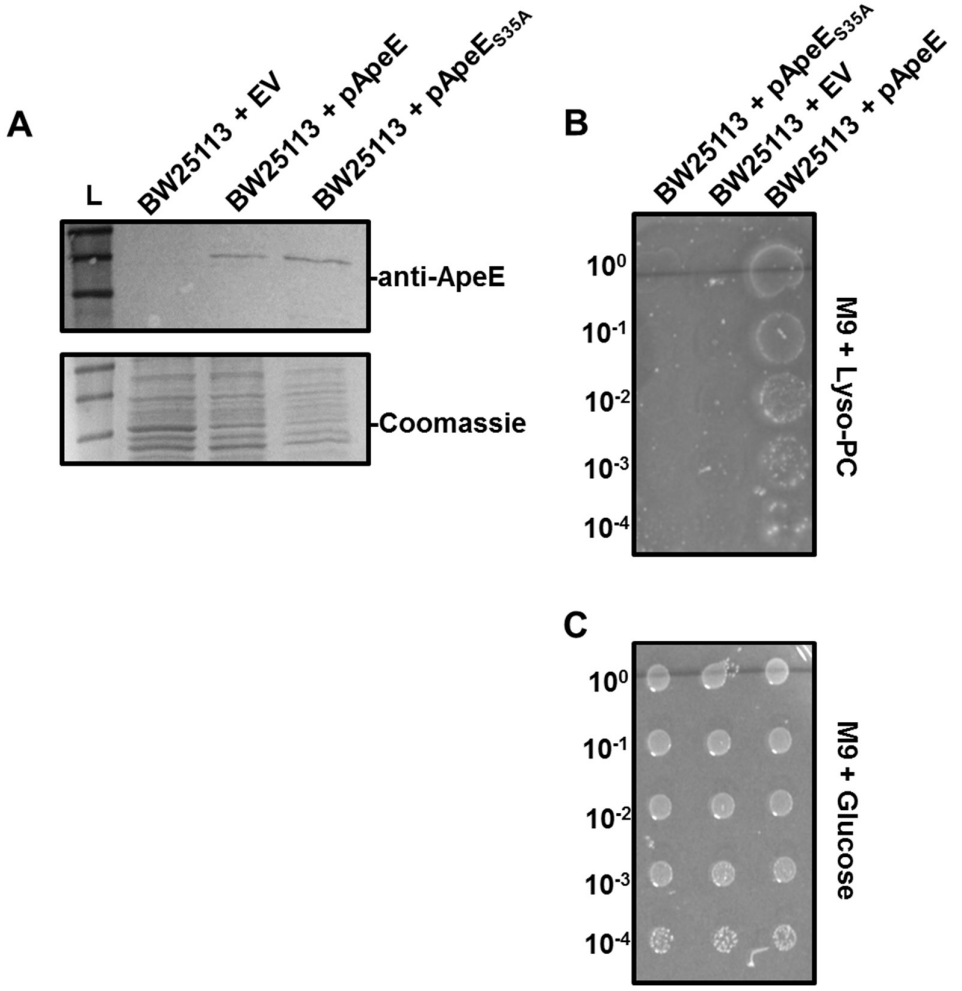

Figure 6.7. ApeE expression and activity in *E. coli* BW25113. (A) Whole cell proteins were isolated from *E. coli* BW25113 that had been transformed with either pQE60 (EV), pQE60-ApeE (pApeE) or pQE60-ApeE$_{S35A}$ (pApeE$_{S35A}$). The protein samples were analysed by SDS-PAGE and Western immunoblot. Western blot analysis used an anti-ApeE primary antibody (1:5,000 dilution), an anti-rabbit IgG raised in goats (1:10,000) secondary antibody and the blots were developed upon addition of the alkaline phosphatase substrate NBP-BCIP. (B) Overnight cultures of *E. coli* BW25113 strains were washed twice in sterile PBS and were serially diluted 1:10. Spots of each dilution were plates onto M9 minimal agar plates supplemented with either 0.4% glucose or 1 mg/ml Lyso-PC. Plates were incubated at 37°C for 16 h.

To determine whether ApeE enabled *E. coli* to grow utilising Lyso-PC as a sole carbon source, overnight cultures of each strain were washed twice in sterile PBS and serially diluted 1:10. The dilution series were plated onto M9 minimal agar containing either glucose or Lyso-PC as a sole carbon source. Neither the empty vector control or +pS35A were able to grow using Lyso-PC as a sole carbon source, but the strain expressing active ApeE could grow (Figure 6.7B). All strains grew at similar rates when glucose was provided as a sole carbon source (Figure 6.7C). These data show that ApeE can mediate the survival of *E. coli* on Lyso-PC as a sole carbon source.

6.2.5 The inhibition of Lyso-PC hydrolysis by MAFP

In chapter 5 of this study, a potent inhibitor (MAFP) of ApeE activity was determined. To investigate whether MAFP inhibits native ApeE from *S.* Typhimurium SL1344, 10^9 bacterial from an overnight culture of SL1344 were washed twice in sterile PBS and resuspended in 1 mL of PBS. MAFP was added to the cells and incubated for 60 min at room temperature. For MAFP negative samples, PBS alone was added to the cells. Each sample was serially diluted 1:10 into sterile PBS prior to being spot plated onto M9 minimal agar supplemented with either 1 mg/ml Lyso-PC or 0.4% glucose. Lyso-PC can be hydrolysed by ApeE and this can enable *Salmonella* to survive utilising Lyso-PC as a sole carbon source. The plates were incubated for 24 h at 37°C. The addition of MAFP inhibited the growth of *S.* Typhimurium SL1344 on plates containing Lyso-PC as a sole carbon source, whereas the SL1344 sample without MAFP was able to grow utilising Lyso-PC (Figure 6.8A). Both samples with and without MAFP grew to comparable levels on M9 medium supplemented with glucose (Figure 6.8B). These data suggest that MAFP can inhibit native ApeE on the surface of *Salmonella* and as the addition of MAFP did not affect growth of *Salmonella* on

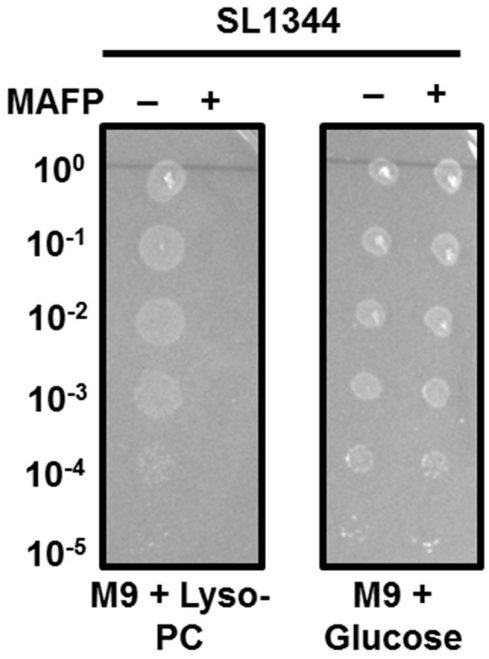

Figure 6.8. MAFP inhibition of ApeE mediated hydrolysis of Lyso-PC. Spot plates of serially diluted *S.* Typhimurium SL1344 either incubated with MAFP (+) or PBS (-) on M9 minimal agar supplemented with either 1 mg/ml Lyso-PC or 0.4% glucose.

glucose. Therefore, the growth defect observed on Lyso-PC medium is unlikely due to toxicity of MAFP to the bacterial cells.

6.2.6 Use of the breakdown products of Lyso-phosphatidylcholine as sole carbon sources.

As ApeE is a PLB enzyme, ApeE might hydrolyse both acyl chains of a phospholipid. In the case Lyso-PC, this hydrolysis would result in the formation of glycerophosphocholine (GPC) ($C_9H_{20}PO_6N$) and free fatty acids (Figure 6.9). In theory, each breakdown product as a sole carbon source would allow an *apeE* mutant to grow. To test the hypothesis, the growth of several *Salmonella* strains in M9 minimal medium supplemented with 0.5 mg/ml GPC was investigated. Cells from overnight cultures of either SL1344, *apeE::aph*, +pApeE and +pS35A were washed twice in sterile PBS and were inoculated into M9 minimal medium containing GPC as a sole carbon source. The OD_{600nm} was measured every hour as described previously. All strains grew similarly using GPC as a sole carbon source (Figure 6.10). These data confirm that the *apeE* mutant is able to import and utilise GPC as a sole carbon source.

6.2.7 Glp and Ugp transport pathway gene deletion constructs in SL1344.

As the hydrolysis of glycerophospholipids would result in the formation of a glycerol-phosphate head group and free fatty acids, the roles of the *sn*-glycerol-3-phosphate (G3P) transport systems (Glp and Ugp) and the fatty acid degradation (fad) systems were investigated during Lyso-PC metabolism.

In *E. coli* and *S*. Typhimurium, the *glp* operon encodes a periplasmic major facilitator transport protein termed GlpT (Elvin *et al*., 1985), which is involved in transporting G3P whilst exporting intracellular P_i (Wong and Kwan, 1992, Hengge *et al*., 1983). In an operon with *glpT* is a gene that encodes for a periplasmic

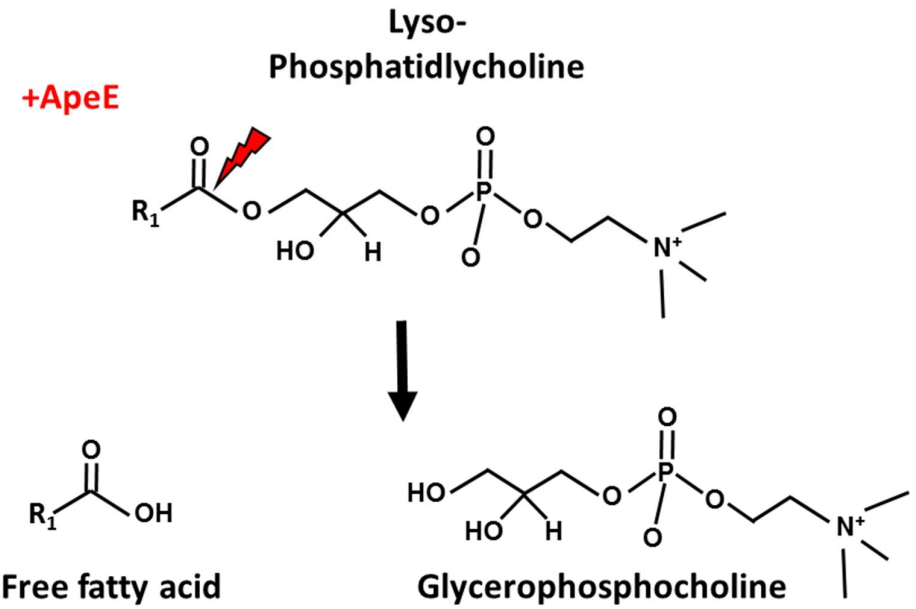

Figure 6.9. ApeE hydrolysis of Lyso-phosphatidylcholine. (A) The addition of ApeE to Lyso-phosphatidylcholine would result in the hydrolysis of the ester bond (red lightning strike). This hydrolysis would generate a free fatty acids and a free glycerophosphocholine head group.

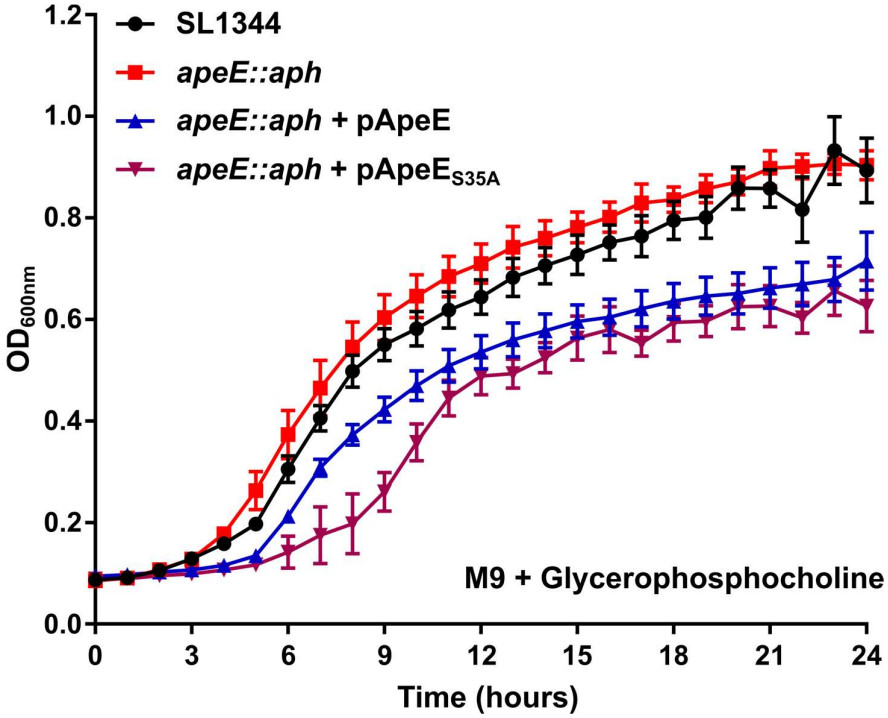

Figure 6.10. *Salmonella* growth on glycerophosphocholine as a sole carbon source. The head group of Lyso-PC and PC is glycerophosphocholine (GPC). Overnight cultures of SL1344 (black), *apeE::aph* (red), *apeE::aph* + pApeE (blue) and *apeE::aph* + pS35A (purple) were washed twice in sterile PBS. The washed cells were inoculated into M9 minimal medium supplemented with 0.5 mg/ml GPC and incubated in 96 well microtitre plates. The OD_{600nm} was measured for 24 h at 37°C in a Clariostar plate reader. The cultures were agitated before OD_{600nm} measurement. Data here represents 3 biological replicates, each with 2 technical replicates, and the error bars show standard error of the mean (SEM).

glycerodiester phosphodiesterase termed GlpQ (Larson *et al*., 1983). Glycerodiester phosphodiesterase have been shown to hydrolyse phospholipid head groups into G3P with an alcohol breakdown product (Larson *et al*., 1983). The Glp system has been shown to utilise G3P as a sole carbon source and the expression of the *glp* operon is repressed by GlpR under phosphate limiting conditions (Wong and Kwan, 1992) and this repression is alleviated upon the presence of G3P (Brzoska *et al*., 1994).

The *ugp* operon is analogous to the *glp* operon but is upregulated under phosphate limiting conditions by PhoBR to utilise G3P as a sole phosphate source (Brzoska *et al*., 1994, Kasahara *et al*., 1991). This system also encodes a glycerodiester phosphodiesterase termed UgpQ, which is located in the cytoplasm (Brzoska *et al*., 1994). The *ugp* operon is responsible for the utilisation of G3P as a sole phosphate source

In order to understand which components of the Glp and the Ugp uptake systems were required for the utilisation of glycerophosphocholine, individual and multiple gene deletions were made. To construct the single gene deletions, primers were designed to anneal ~200 bp up and downstream of the *glpT*, *glpQ* (Figure 6.11A) and *ugpQ* (Figure 6.11B) genes. A gene deletion library in the *S*. Typhimurium strain 14028s was used as a template for PCR whereby the correct mutant was isolated and streaked to single colonies before checking for gene disruption via colony PCR. The PCR checked mutants were used as templates for PCR to generate single gene deletions in SL1344. The resulting PCR fragment contained the kanamycin resistance cassette flanked by ~200 bp of homology to the gene of interest. The PCR fragment was then electroporated into SL1344 electrocompetent cells expressing λ-red recombinase. Mutants were selected for on kanamycin agar plates and confirmed for gene disruption by PCR (Figure 6.11C).

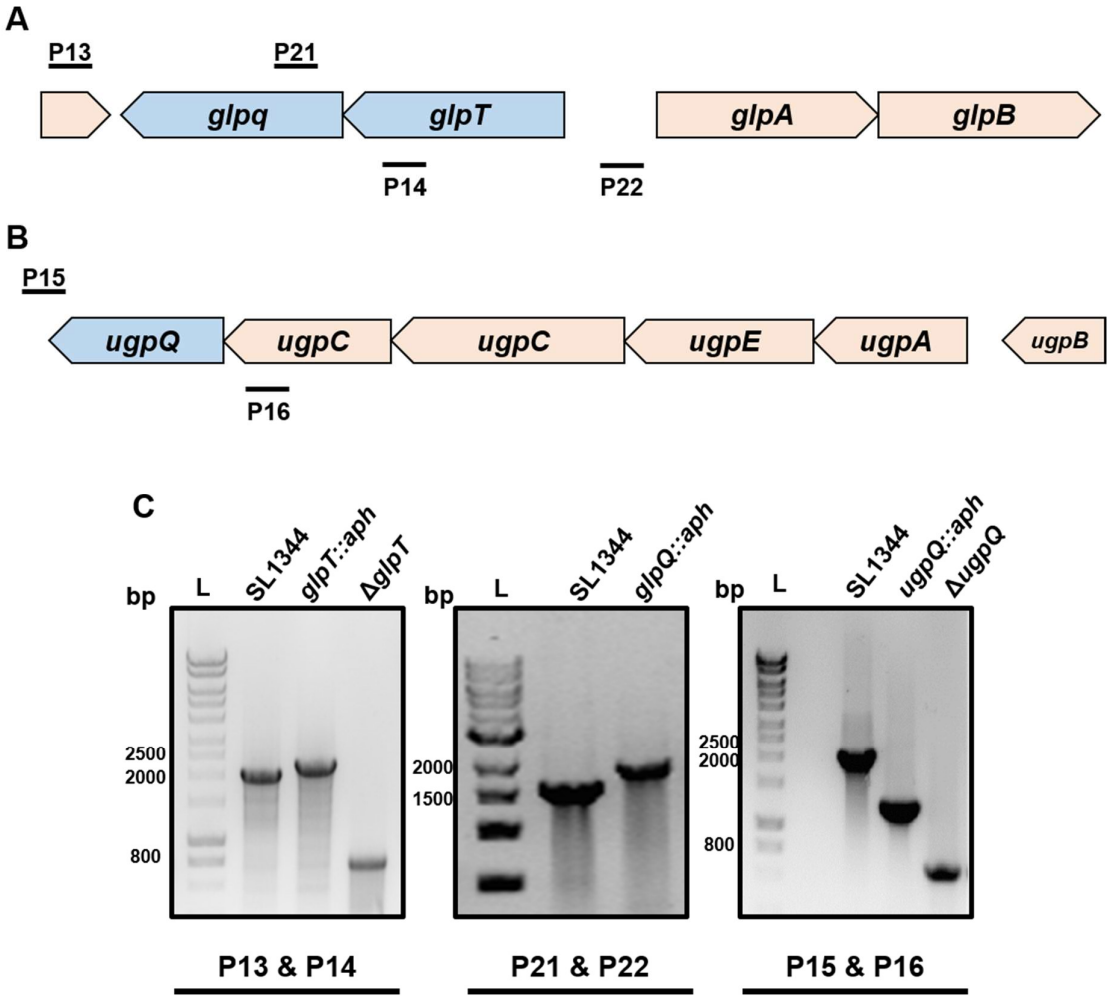

Figure 6.11. *glp* and *ugp* single mutant construction in *S.* Typhimurium SL1344. (A) The genetic locus of the *glp* system with the *glpT* and *glpQ* genes coloured in blue. Primers (P13, P14, P21 and P22) were designed to anneal approximately 200 bp up and downstream of the gene of interest to generate the linear fragment for constructing gene deletions. (B) The genetic locus of the *ugp* system, with the *ugpQ* gene highlighted in blue. Primers for gene deletion were designed as above. (C) Colony PCR of wild-type SL1344 and each mutant: *glpT; glpQ;* and *ugpQ* (left to right).

As there are 2 glycerodiester phosphodiesterases in *S.* Typhimurium, a double gene deletion strain was constructed that had both enzymes deleted from the chromosome. To do this, the kanamycin cassette was removed from *ugpQ::aph* by the action of Flp recombinase encoded for on plasmid pCP20, to generate Δ*ugpQ*. The plasmid encoding the λ-red recombinase gene (pKD46) was transformed into Δ*ugpQ*. The linear DNA fragment encoding the kanamycin resistance cassette flanked by *glpQ* loci homology was electroporated into Δ*ugpQ* expressing λ-recombinase. The kanamycin cassette was removed from the double mutant using the Flp recombinase as previously described. The resulting double mutant was genetically Δ*ugpQ* Δ*glpQ* and confirmed by PCR (Figure 6.12).

To determine the roles of GlpT, GlpQ and UgpQ in the utilisation of GPC as a sole carbon/phosphate source, cells from overnight cultures of SL1344 wild-type, single and double mutants were washed twice with sterile MOPS mix. This MOPS mix did not contain any source of carbon or phosphate. MOPS based media was supplemented with either phosphate (K_2HPO_4) or carbon (glucose) alone, or both, as controls. To test which mutants were required for the utilisation of GPC as a carbon or phosphate source, the MOPS media was supplemented with GPC alone (0.5 mg/ml), or GPC with a phosphate or carbon source. The washed cultures were added to the media to a starting OD_{600nm} 0.02 and the plate was incubated at 37°C for 24 hours and the OD_{600nm} was measured every hour in a Clariostar plate reader.

When GPC was the sole carbon and phosphate source, the SL1344 wild-type and the *ugpQ* mutant showed similar growth (Figure 6.13A). In contrast, the *glpT* mutant had an extremely delayed lag phase and both the *glpQ* and Δ*ugpQ gplQ::aph* strains did not show any growth (Figure 6.13A), suggesting that GlpQ and, to some extent, GlpT are required for utilising GPC as a sole carbon/phosphate source. When

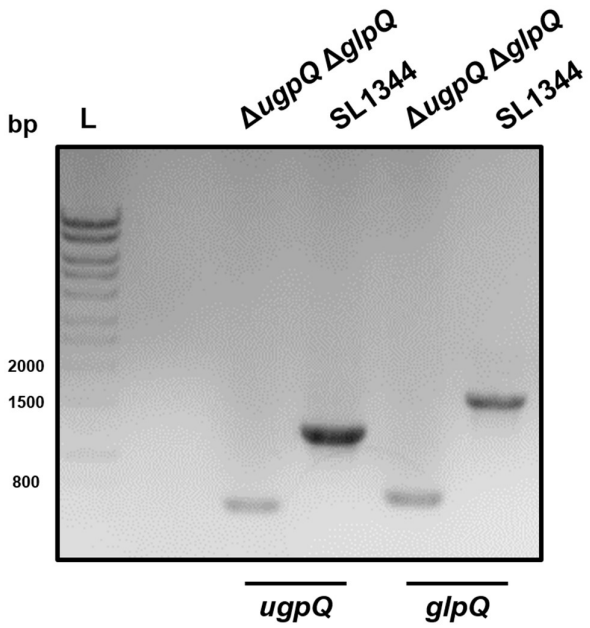

Figure 6.12. PCR check of the Δ*ugpQ* Δ*glpQ* double mutant. A colony of either SL1344 or Δ*ugpQ* Δ*glpQ* was added to sterile water and boiled to be used as a template for colony PCR. Primers that annealed to the *ugpQ* loci and *glpQ* loci were used to determine gene deletion.

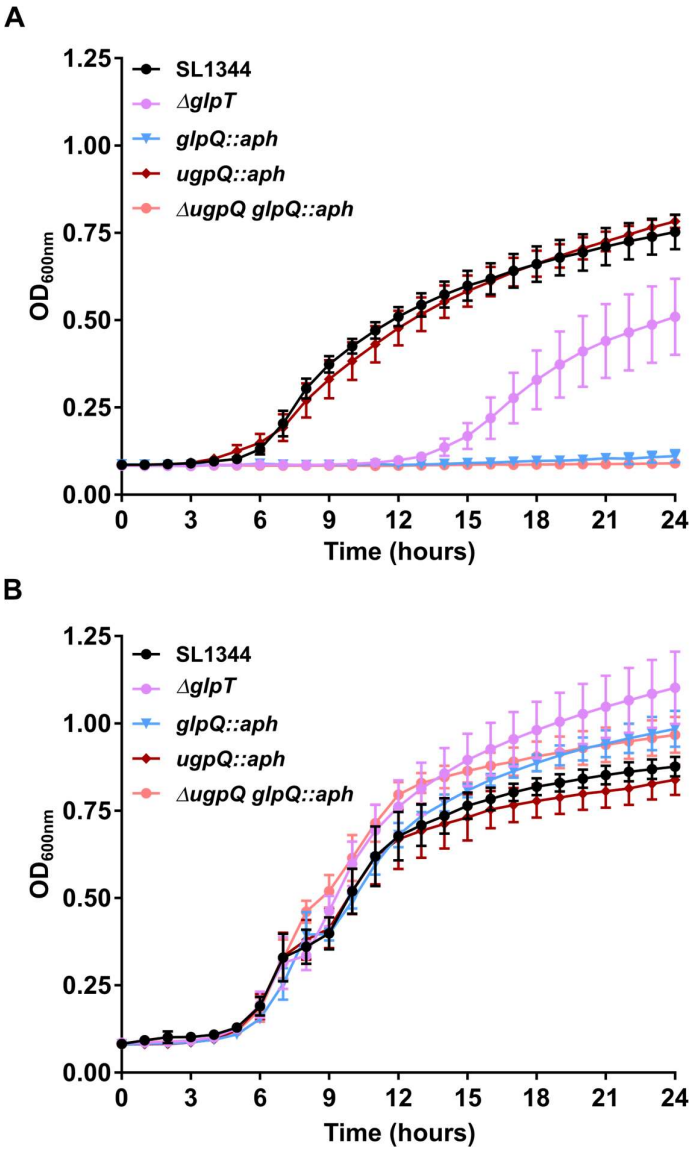

Figure 6.13. Growth of single mutants using Glycerophosphocholine as a sole carbon and phosphate source in MOPS minimal medium. Overnight cultures of SL1344, Δ*glpT*, *glpQ::aph, ugpQ::aph* and Δ*ugpQ* Δ*glpQ* were washed twice in MOPS mix without carbon or phosphate supplementation. Each strain was inoculated into MOPS mix supplemented with either 0.5 mg/ml GPC (A) or 0.4% glucose and K_2HPO_4 (B). The growth was measured every hour for 24 h in a Clariostar plate reader at 37°C. Data here represents 3 biological replicates, each with 2 technical replicates, and the error bars show standard error of the mean (SEM).

the MOPS medium was supplemented with both glucose and K_2HPO_4, all the strains grew comparably (Figure 6.13B).

To determine which proteins were required for the utilisation of GPC as a sole phosphate source, MOPS media was supplemented with GPC and glucose. Therefore the only source of phosphate was GPC. The *glpT*, *glpQ*, and *ugpQ* single mutants all grew to comparable levels as the SL1344 wild-type (Figure 6.14A). However, the Δ*ugpQ glpQ::aph* double mutant was unable to grow in this medium (Figure 6.14A), suggesting both glycerodiester phosphodiesterases are required to utilise GPC as a sole carbon source. In comparison, when the media was supplemented with glucose alone with no phosphate, none of the strains grew (Figure 6.14B), suggesting that the medium contained no source of Pi and therefore the phosphate in GPC was the only source available in the previous media.

In order to investigate which of the proteins involved in the degradation of GPC were required for the utilisation of GPC as a sole carbon source, the MOPS medium was supplemented with GPC and K_2HPO_4. The *ugpQ* single mutant was able to grow similarly to SL1344 wild-type in this media (Figure 6.15A), whereas the *glpQ* and Δ*ugpQ* Δ*glpQ* strains all failed to grow (Figure 6.15A). The single *glpT* mutant had variable growth in this medium, with some replicates showing a delayed lag phase (Figure 4.8A). To determine whether there was no other carbon source in the media, the MOPS media was supplemented with K_2HPO_4 alone. In this medium, none of the strains grew (Figure 6.15B), suggesting there were no other carbon sources in the medium. Therefore, the requirement of each *glp* and *ugp* mutant for growth utilising GPC varies depending on whether it is used as a carbon or phosphate source.

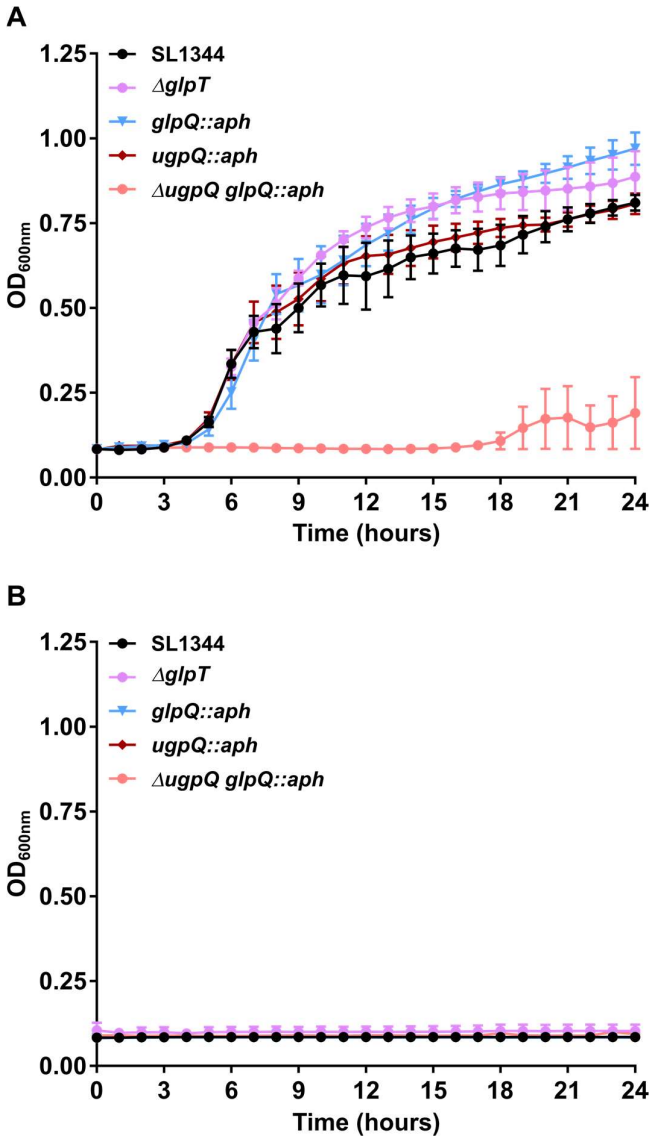

Figure 6.14. Growth of *Salmonella* strains in MOPS minimal medium using GPC as a sole phosphate source. Overnight cultures of SL1344, Δ*glpT*, *glpQ::aph, ugpQ::aph* and Δ*ugpQ* Δ*glpQ* were washed twice in MOPS mix without carbon or phosphate supplementation. Data here represents 3 biological replicates, each with 2 technical replicates, and the error bars show standard error of the mean (SEM). Each strain was inoculated into MOPS mix supplemented with either 0.5 mg/ml GPC and K_2HPO_4 (A) or K_2HPO_4 alone (B). Growth was measured every hour for 24 h in a Clariostar plate reader at 37°C.

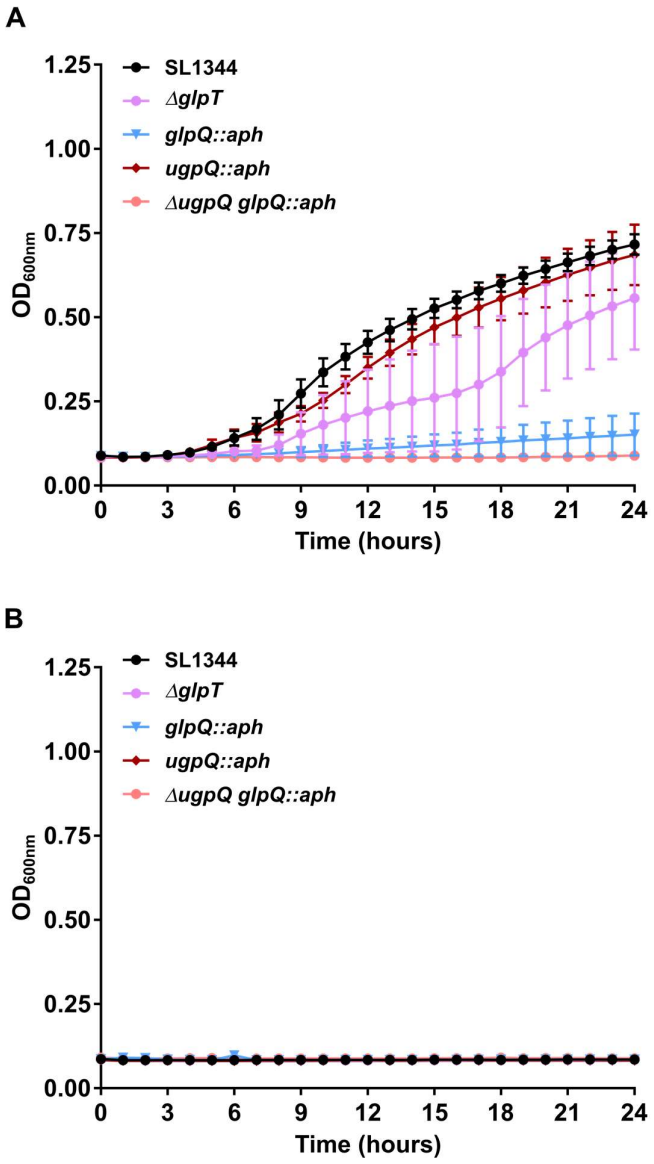

Figure 6.15. Growth of *Salmonella* in MOPS minimal medium with GPC as a sole carbon source. Overnight cultures of SL1344, Δ*glpT*, *glpQ::aph, ugpQ::aph* and Δ*ugpQ* Δ*glpQ* were washed twice in MOPS mix without carbon or phosphate supplementation. Data here represents 3 biological replicates, each with 2 technical replicates, and the error bars show standard error of the mean (SEM). Each strain was inoculated into MOPS mix supplemented with either 0.5 mg/ml GPC 0.4% glucose (A) or glucose alone (B). Growth was measured every hour for 24 h in a Clariostar plate reader at 37°C.

6.2.8 Fatty acid degradation mutant construction

For the import and utilisation of the exogenous long chain fatty acids, *S.* Typhimurium has a dedicated fatty acid degradation (Fad) pathway. FadL is an outer membrane protein responsible for the import of exogenous medium-long chain fatty acids and FadD is an acyl-CoA synthetase that adds an acyl-CoA molecule onto fatty acids as the first step of β-oxidation (Clark and Cronan, 2005).

Single mutants for the fatty acid degradation system were generated as described above with primer annealing for the construction of *fadD* and *fadL* mutants described (Figure 6.16A and B). Mutants were selected for on kanamycin agar plates and confirmed via PCR (Figure 6.16C). The growth of each mutant utilising Tween80 as a sole carbon source was used to test whether the mutants generated had the correct phenotype. Overnight cultures of SL1344 wild-type, *fadD::aph, fadL::aph* and Δ*ugpQ* Δ*glpQ* were washed twice in PBS and diluted 1:10. Each dilution was spot plated onto M9 minimal agar supplemented with either Tween80 or glucose. The plates were incubated at 37°C for 36 hours. Strains defective for fatty acid import (*fadL::aph*) and β-oxidation (*fadD::aph*) showed no growth utilising Tween80 as a sole carbon source, whereas all other strains grew similarly to the SL1344 wild-type (Figure 6.17A). All strains grew comparatively using glucose as a sole carbon source (Figure 6.17B). This experiment confirmed that the *fad* mutants were correct and not able to utilise long chain fatty acids as carbon sources.

6.2.9 Role of the individual mutants in Lyso-PC utilisation

To investigate whether the head group or acyl chain of Lyso-PC was used as a sole carbon source, each single *glp, ugp*, *fad* mutant and double Δ*ugpQ* Δ*glpQ* mutant was tested for growth on M9 agar plates supplemented with Lyso-PC as a sole carbon source. Overnight cultures of each mutant strain and SL1344 wild-type were washed

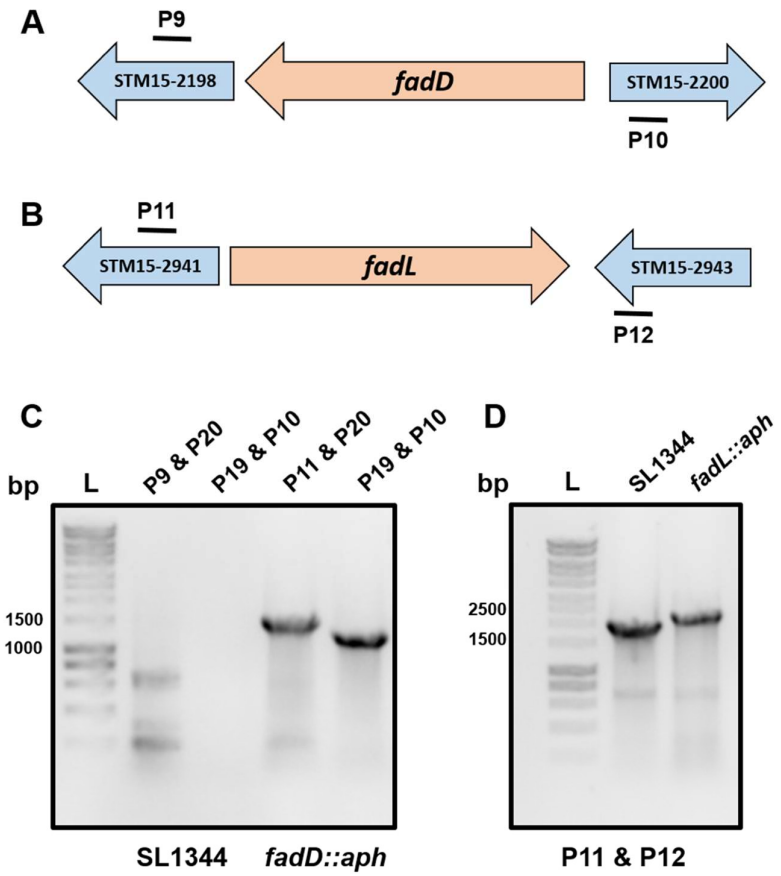

Figure 6.16. Fatty acid degradation mutant construction in SL1344. (A) The genetic loci of the two genes that comprise part of the fatty acid degradation (Fad) system. (A) Primer annealing to generate the single *fadD* mutant and (B) *fadL* mutant. (C) Colony PCR of wild-type SL1344 and *fadD::aph* mutant. As the kanamycin cassette was the same size as the *fadD* gene, deletion was confirmed by colony PCR with primers that annealed internally to the kanamycin cassette (P20 and P19). These primers were paired with *fadD* forward and reverse primers, such that only strains with the kanamycin cassette inserted at the *fadD* loci would produce product. (D) Colony PCR of the *fadL* loci using FadL forward and reverse primers (P11 and P12).

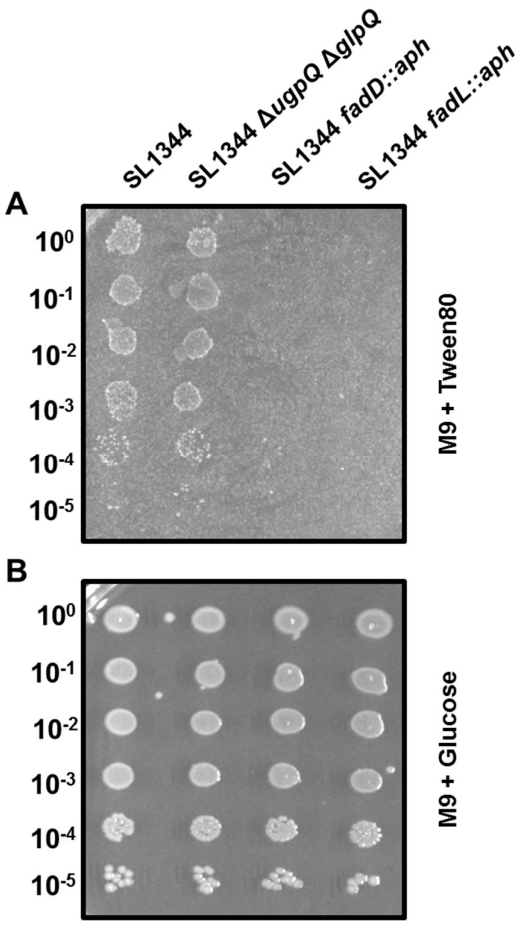

Figure 6.17. Growth of the *fad* mutants on M9 minimal agar plates supplemented with Tween80. Overnight cultures of SL1344, Δ*ugpQ* Δ*glpQ*, *fadD::aph* and *fadL::aph* were washed twice in PBS and serially siluted 1:10 prior to spot plating onto M9 minimal agar plates. The plates were incubated at 37°C for 36 hours. (A) Growth of *S*. Typhimurium strains utilising Tween80 as a sole carbon source. M9 minimal agar was supplemented with 4% Tween80 (v/v). (B) Growth of strains on M9 minimal agar supplemented with 0.4% glucose.

and serially diluted as previously described. The strain dilutions were spotted onto M9 minimal agar supplemented with either Lyso-PC or glucose. The plates were incubated at 37°C for 16 hours. All strains grew at similar rates when grown on Lyso-PC (Figure 6.18A) and glucose (Figure 6.18B). As all strains grew utilising Lyso-PC as a sole carbon source, both the head group and acyl chain can be used as a sole carbon source *in vitro*.

6.2.10 The interaction of ApeE and Lyso-phosphatidylglycerol.

Having shown that ApeE could bind to glycerophospholipids and hydrolyse the eukaryotic derived Lyso-PC, its ability to hydrolyse bacterial glycerophospholipids was investigated using Lyso-phosphatidylglycerol (Lyso-PG) as a substrate. Lyso-PG is a derivative of PG that contains a glycerol-based head group, and one acyl chain (instead of two) connected by an ester bond. To test whether ApeE could hydrolyse Lyso-PG, overnight cultures of SL1344, *apeE::aph,* +pApeE and +pS35A were sub-cultured into the M9 media supplemented with either 0.4% glucose or 1 mg/ml Lyso-PG to a starting OD_{600nm} of around 0.02. The cultures were added to 96 well plates and the OD_{600nm} was measured in a Clariostar plate reader every hour for 24 h. Each strain grew to comparable levels using glucose as a sole carbon source (Figure 6.19A). Only strains with active ApeE (SL1344 or +pApeE) could grow utilising Lyso-PG as a sole carbon source (Figure 6.19B).

Overnight cultures of SL1344, *apeE::aph,* +pApeE and +pS35A were also washed in PBS and serially diluted 1:10 prior to spot plating on M9 minimal agar plates supplemented with either glucose or Lyso-PG. On M9 minimal media agar plates, growth of every strain was similar with glucose as a sole carbon source, but strains lacking ApeE or active ApeE (*apeE::aph* or + pS35A complement) failed to grow on

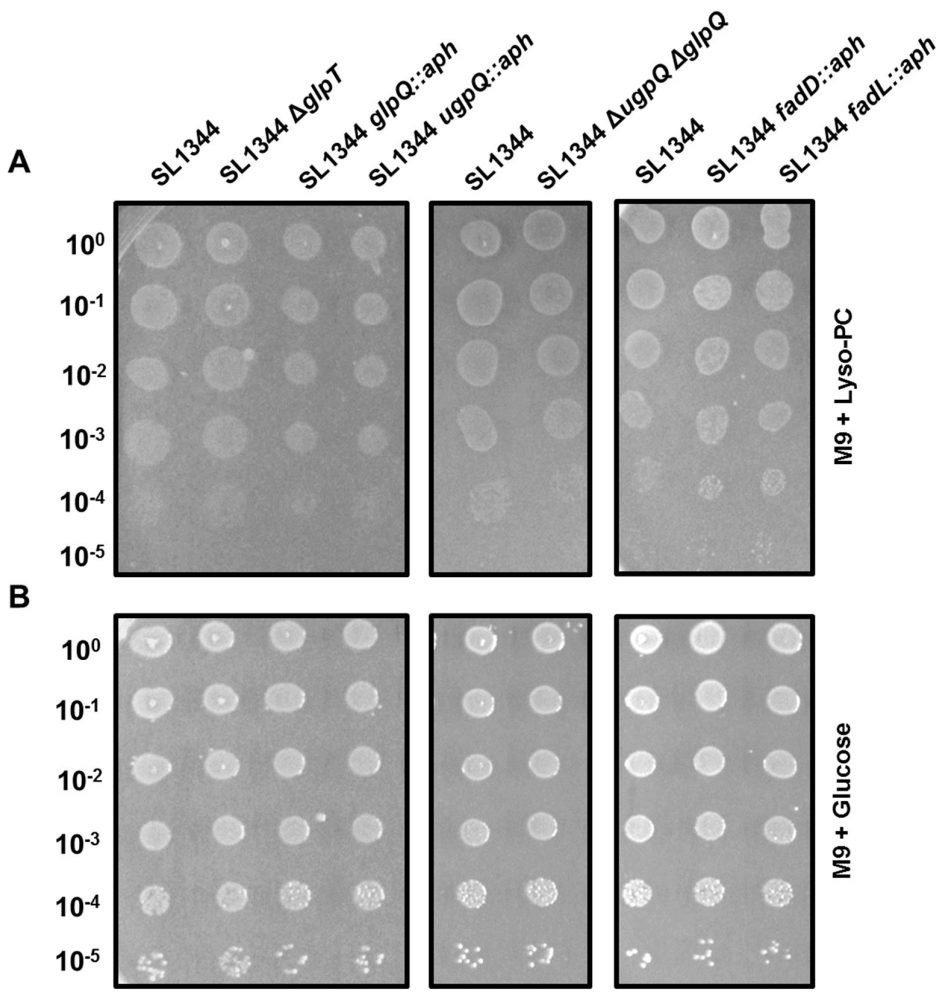

Figure 6.18. Growth of single mutants utilising Lyso-PC as a sole carbon source. Overnight cultures of SL1344 wild-type and each *glp, ugp,* and *fad* mutant were washed twice in PBS and serially diluted 1:10, before spot plating onto M9 minimal agar supplemented with (A) Lyso-PC (1 mg/ml) or (B) glucose (0.4% v/v). Plates were incubated overnight at 37°C.

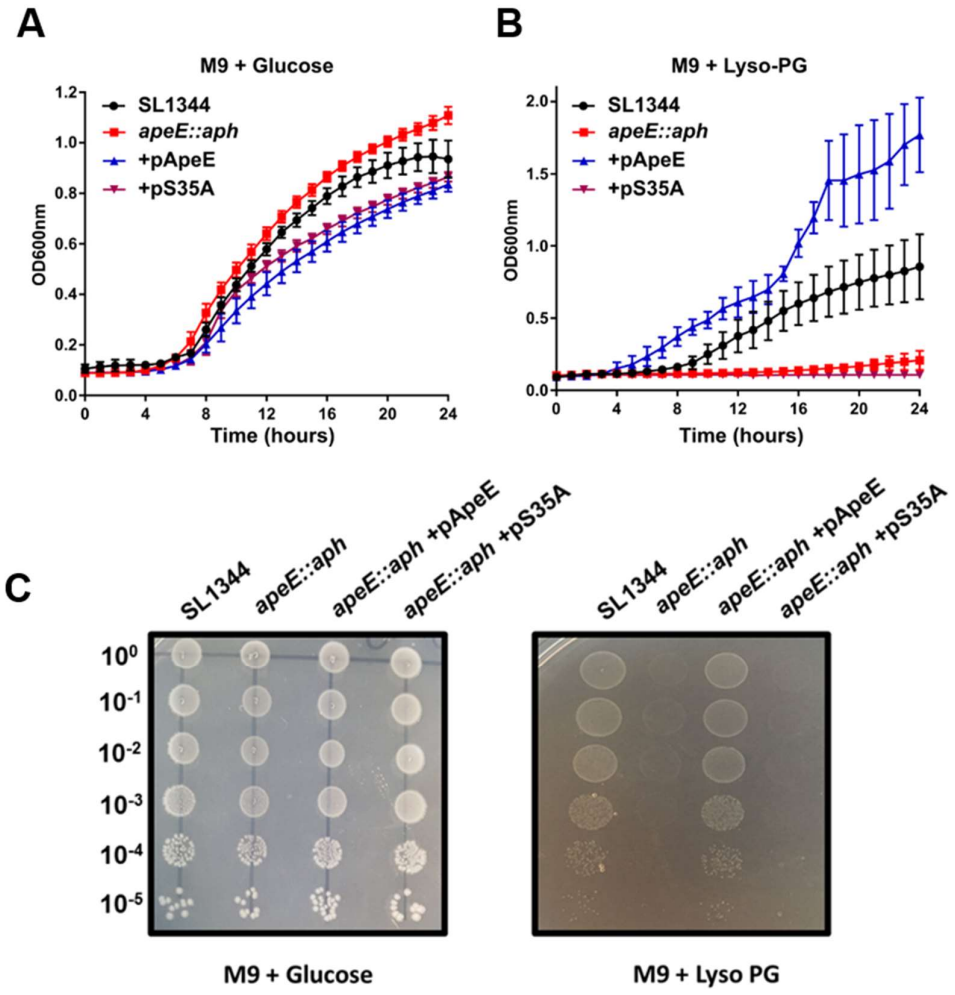

Figure 6.19. Growth of *Salmonella* on Lyso-PG as a sole carbon source. Growth curves of SL1344 wild-type (black), *apeE::aph* (red), +pApeE (blue) and +pS35A (purple) in M9 minimal media supplemented with 0.4% glucose (A) or Lyso-PG (B). Each strain was inoculated in duplicate and the data shown here is a combination of 3 biological replicates with error bars representing the SEM. Strains were incubated at 37°C for 24 h with OD_{600nm} measured every hour in a Clariostar plate reader (A & B). Growth of serially diluted *S*. Typhimurium strains on M9 agar, supplemented with either 4% glucose or Lyso-PG (C). Plates were incubated at 37°C for 16 h.

medium containing Lyso-PG as a sole carbon source (Figure 6.19C). These data suggest that ApeE can hydrolyse Lyso-PG.

To determine whether ApeE was actively hydrolysing Lyso-PG, phospholipids were isolated from the spent media after *Salmonella* growth. The lipids were extracted and separated as above by TLC. For these experiments, the solvent system was chloroform: methanol: water (65:25:4 v/v). Only strains that were able to grow on Lyso-PG as a sole carbon source (SL1344, +pApeE*)* depleted the Lyso-PG from the media (Figure 6.20A). However, only the complemented strain completely degraded all of the Lyso-PG (Figure 6.20A), suggesting that the complemented strain produced more ApeE than the SL1344 wild-type.

To test whether the +pApeE strain was producing more ApeE protein than the wild-type, whole cell protein fractions were isolated from overnight cultures of either SL1344, *apeE::aph,* +pApeE or +pS35A. These protein fractions were separated by SDS-PAGE and then Western immunoblotted using anti-ApeE antibodies. The blots were developed using the AP substrate BCIP-NBP. The amount of ApeE protein was much higher in the strains expressing *apeE* from plasmids (+pApeE or pS35A) than in the SL1344 wild-type (Figure 6.20B). These data confirm that the reason Lyso-PG is completely degraded in the +pApeE complement is because more ApeE is being produced.

6.2.11. The membrane phospholipid ratios of *S.* Typhimurium wild-type and *apeE::aph* mutant.

Phosphatidylglycerol (PG) is a major component of the *S.* Typhimurium outer membrane (Olsen and Ballou, 1971). Lyso-PG is a breakdown product of PG after hydrolysis by a PLA_2 enzyme. Therefore, it was hypothesised that ApeE might be able to cleave bacterial membrane phospholipids altering the lipid profiles of the bacterial

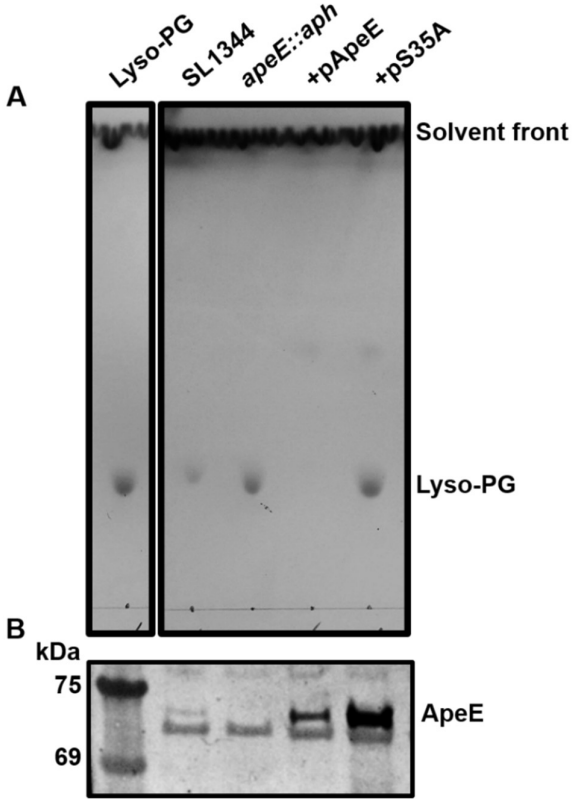

Figure 6.20. Analysis of the effect of ApeE on Lyso-PG in M9-minimal medium. (A) Lipid extraction from M9 minimal medium + Lyso-PG after 24 h of *S*. Typhimurium growth. The lipids were extracted using a Bligh-Dyer method, and the lipid extracts spotted onto silica thin layer chromatography plates. The plates were incubated in a humid chamber containing an equilibrated solvent system of 65:25:4 chloroform: methanol: water (v/v) until the solvent front had migrated about 1 cm from the top of the plate. The plates were air dried prior to staining with phosphomolybdic acid, and charring by a heat gun to reveal the lipid species. (B) Western immunoblot of *S.* Typhimurium whole cell protein extracts separated by SDS-PAGE. The SDS-PAGE gels were transferred to a nitrocellulose membrane. The membrane was probed with anti-ApeE antibody (1:5,000). Blots were developed upon the addition of the substrate BCIP-NBP.

membrane. To test this hypothesis, the membrane phospholipid composition of an *apeE* mutant was compared with that of the SL1344 wild-type. Overnight cultures of either SL1344 or *apeE::aph* were centrifuged and the lipids from the membranes were extracted using a modified Bligh-Dyer method. Once the membrane phospholipids had been isolated, each sample was spotted onto silica TLC plates. Once the spots had dried, the plates were placed in a humid chamber containing an equilibrated solvent system of chloroform: methanol: acetic acid (65:25:10 v/v). This solvent system was known to separate membrane lipids (Rowlett *et al*., 2017). Once the solvent system had migrated about 1 cm from the top of the plate, the plate was removed and air dried prior to staining with phosphomolybdic acid (PMA) and subsequent charring of the plate to reveal the lipid species present. For each sample (wild-type and *apeE* mutant), three lipid species were detected: CL; PG; and PE. The abundance of all the lipid species in the wild-type (SL1344) and the congenic ApeE mutant was comparable (Figure 6.21)

6.2.12. Biofilm formation during growth in Lyso-PG medium.

After growth in M9 + Lyso-PG, SL1344 wild-type and the +pApeE complemented appeared to form aggregates (data not shown). Aggregation is a result of cell to cell adhesion and therefore could indicate biofilm formation. As this was unusual, the ability of this strain to form biofilm was investigated. After 24 h of growth in either M9 + glucose, M9 + Lyso-PG or M9 + Lyso-PC media, the planktonic cells were removed and the plates were incubated in 0.1% crystal violet prior to vigorous washing and de-staining in an ethanol: acetone (80:20 v/v) solution. Biofilm was measured as an increase in $OD_{600nm.}$ Little to no biofilm was detected when the strains were grown in M9 + glucose or M9 + Lyso-PC (Figure 6.22).

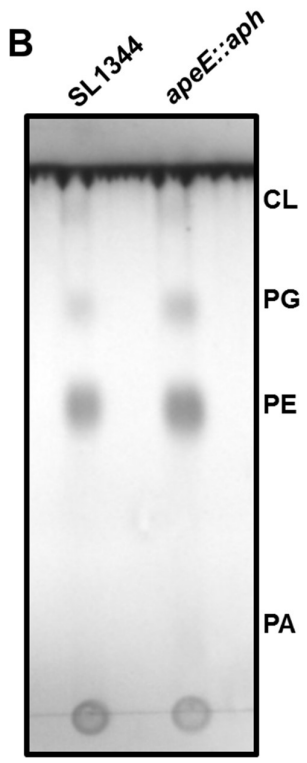

Figure 6.21. TLC analysis of membrane phospholipids in *S.* Typhimurium. Membrane phospholipids were extracted from 5 mL overnight cultures of either SL1344 or *apeE::aph* mutant using a modified Bligh-Dyer method. The lipids were finally dissolved in chloroform. The lipids were spotted onto 10 cmx10 cm silica thin layer chromatography plates. The plates were incubated in a humid chamber with an equilibrated solvent system of chloroform: methanol: acetic acid (65:25:10 v/v). The TLC plate was removed from the chamber once the solvent front reached approximately 1 cm from the top of the plate. The plates were air dried then stained with phosphomolybdic acid. Once the stain had completely dried, the plates were charred with a heat gun to visualise the lipid species. Abbreviations are: cardiolipin (CL); phosphatidylglycerol (PG); phosphatidylethanolamine (PE); and phosphatidic acid (PA).

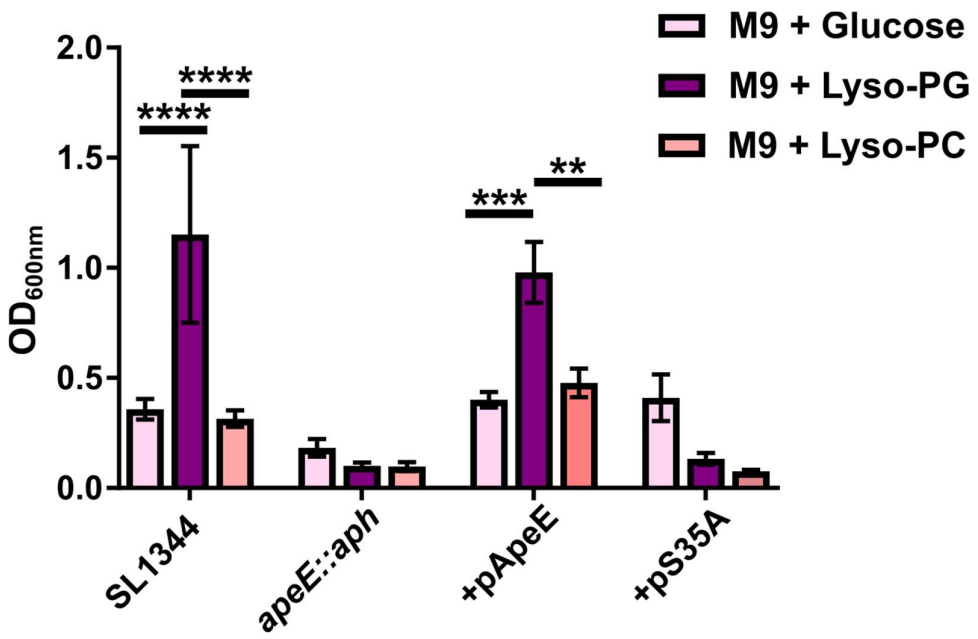

Figure 6.22. Biofilm profiles of *S*. Typhimurium SL1344 derived strains grown in M9 minimal media with varying carbon sources. Biofilm profiles of *S*. Typhimurium strains after growth in M9 minimal media supplemented with either glucose (pink), Lyso-PG (purple) or Lyso-PC (peach). Data represented here is the OD_{600nm} measurement of a crystal violet based microtitre plate biofilm assay after growth for 24 h at 37°C. The values here represent 6 independent biological replicates, and the error bars represent standard deviation (SD). Statistical significance ($p<0.05$) was determined using a 2-way anova using Turkey correction for multiple comparisons using Graphpad prism software. $p<0.05$ (** $p<0.01$, *** $p<0.001$ and **** $p<0.0001$).

In contrast, a clear biofilm was visible in wells inoculated with bacteria that had grown successfully in M9 + Lyso-PG (Figure 6.22). The *apeE* mutant nor the +pS35A mutant grew in M9 + Lyso-PG media and therefore did not form a biofilm in any condition tested (Figure 6.22). These data suggest that a strain that does not usually form a biofilm is able to do so after growth in M9 medium supplemented with Lyso-PG.

6.2.13. Role of Fad and Glp in Lyso-PG utilisation and biofilm formation.

The roles of the fatty acid degradation (Fad) system and the Glp and Ugp systems for *Salmonella* growth in Lyso-PC were previuosly investigated in this study. The main difference between the two phospholipid species is the head group. To understand whether the head group or the acyl chain was the main signalling molecule that initiated the switch from planktonic to biofilm lifecycles, various *fad*, *glp* and *ugp* mutants were tested for their ability to grow using Lyso-PG as a sole carbon source and to induce biofilm formation.

To test the ability of each mutant to grow in the different conditions, *fadD::aph, glpT::aph* and Δ*ugpQ glpQ::aph* mutants, as well as SL1344 wild-type control, were inoculated to a starting OD_{600nm} of 0.02 in microtitre plates containing either M9 + glucose or M9 + Lyso-PG. The strains were incubated at 37°C for 24 h with OD_{600nm} measurements every hour. Each strain grew to comparable levels when grown in M9 supplemented with glucose (Figure 6.23A) and Lyso-PG (Figure 6.23B). These data show that the mutants tested were not defective for growth using Lyso-PG as a sole carbon source.

Each mutatation results in a defect in either the utilisation of the acyl chain or head group of (Lyso)phospholipids. GlpT was shown in this study to be required for efficient import of the head group of Lyso-PC, as the *glpT* mutant showed an extended

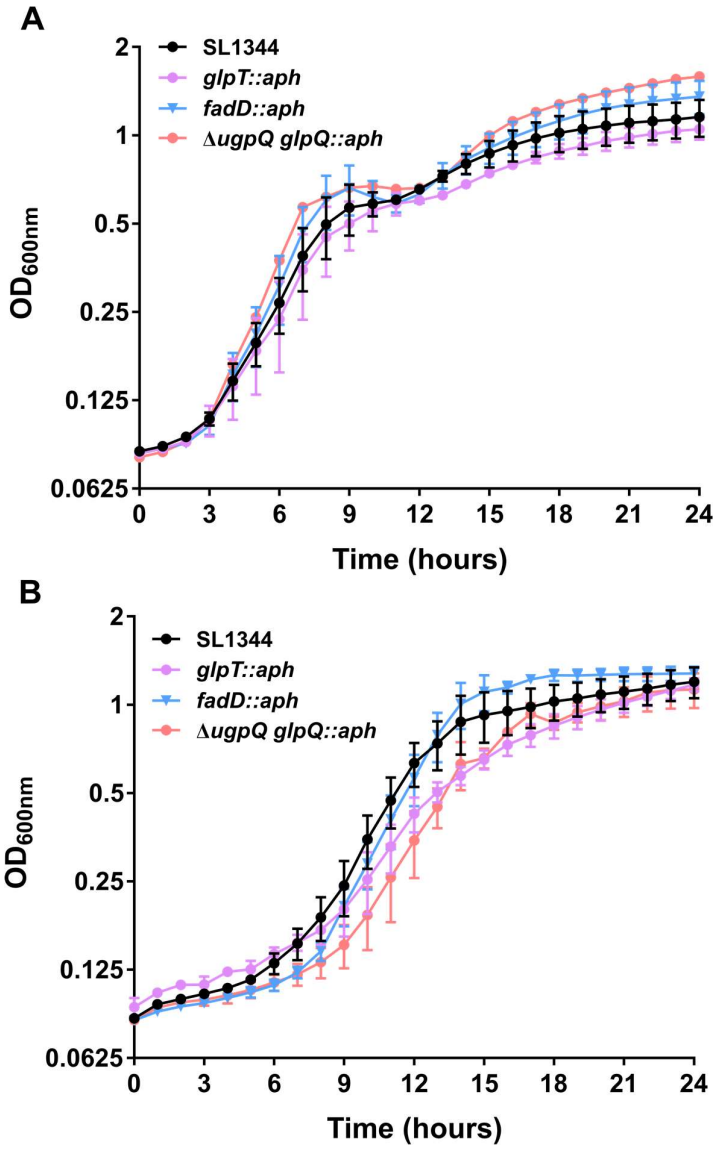

Figure 6.23. Growth of various *Salmonella* mutant strains in M9 + Lyso-PG medium. (A) Growth curve of *S.* Typhimurium SL1344 strains in M9 minimal medium supplemented with glucose. (B) Growth curve of *S.* Typhimurium SL1344 strains in M9 minimal medium supplemented with Lyso-PG. All growth curves were measured in a Clariostar microtritre plate reader with the OD_{600nm} measured every hour for 24 h at 37°C. SL1344 (black), Δ*glpT* (pink), *fadD::aph* (blue) and Δ*ugpQ glpQ::aph* were inoculated in duplicate for each growth curve. Data from 3 independent biological replicates are shown, and the error bars represent the SEM.

lag phase in M9 medium supplemented with glycerophosphocholine as the sole carbon source. UgpQ and GlpQ are glycerophosphodiesterases found in the cytoplasm and periplasm, respectively (Tommassen *et al*., 1991). These proteins are responsible for hydrolysing the head groups of phospholipids into glycerol-3-phosphate and an alcohol. FadD is an acyl Co-A synthetase responsible for the additon of Acyl-CoA onto long chain fatty acids for the first step of β-oxidation (Iram and Cronan, 2006). Therefore testing the ability of each of these mutants to form biofilm when grown in Lyso-PG M9 minimal medium might indicate which part of the phospholipid is important for signalling biofilm formation. After growth in either M9 minimal medium supplemented with glucose or Lyso-PG, the strains were tested for biofilm formation using the microtitre plate biofilm assay. No biofilm was detected when the strains were grown in M9 minimal medium supplemented with glucose (Figure 6.24A), and the biofilm formed by the *fadD* and *glpT* mutants in M9 + Lyso-PG medium was not significantly different than the SL1344 wild-type (Figure 6.24B). However, the biofilm formed by the Δ*ugpQ glpQ::aph* mutant in Lyso-PG medium was significantly different to the biofilms made by the SL1344 wild-type, and was more similar to the glucose control (Figure 6.24B). These data suggest that the hydrolysis of the Lyso-PG headgroup is important for the formation of a biofilm by *S.* Typhimurium.

6.2.14. The role of cellulose biosynthesis regulation in Lyso-PG mediated biofilm formation.

Garcia *et al*., (2004) demonstrated that the strain SL1344 does not form biofilm because the protein, MlrA, that is the positive regulator for the expression of *csgD*, was not transcribed at sufficiently high levels under the conditions tested (Garcia *et al*., 2004). CsgD is a protein that regulates the expression of genes required for cellulose and curli biogenesis (Liu *et al*., 2014). Cellulose has been shown to be an important

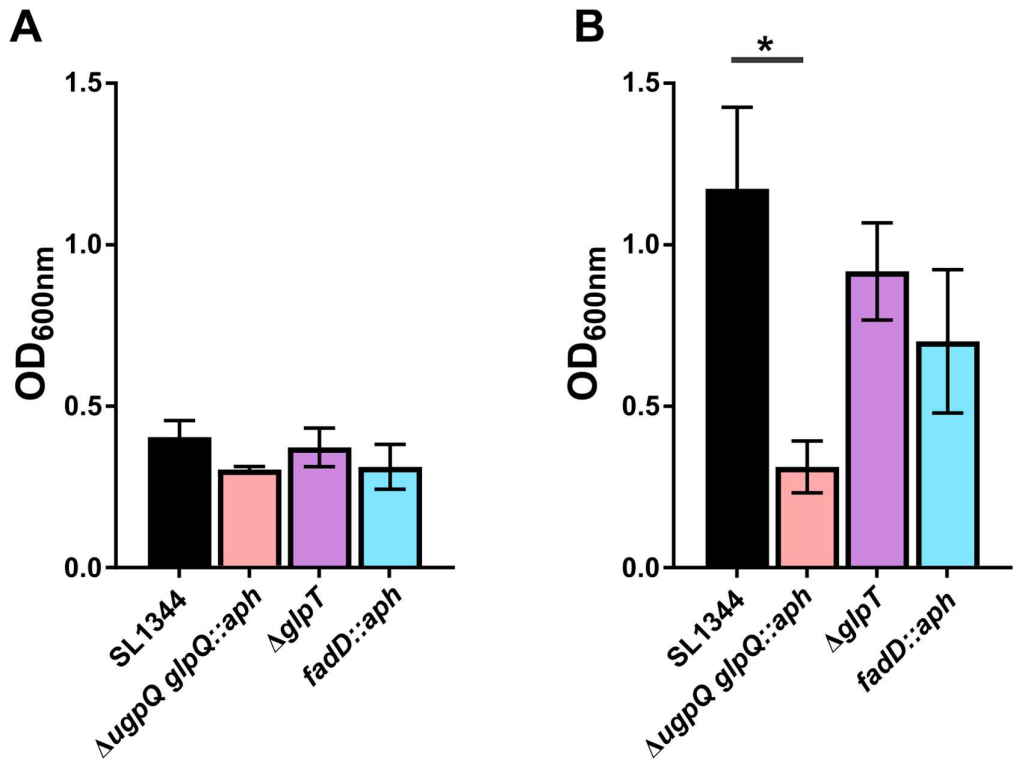

Figure 6.24. Biofilm formation of *Salmonella* strains in M9 media. Biofilm profiles of *S.* Typhimurium SL1344 wild-type (black), *fadD::aph* (blue), Δ*glpT* (purple) and Δ*ugpQ glpQ::aph* (peach) mutant grown in either M9 minimal media supplemented with glucose (A) or Lyso-PG (B). Data here represented 3 biological replicates of a crytstal violet based microtitre plate assay, with error bars showing SD. The biofilm was measured as the OD_{600nm}. Statistical significance ($p<0.05$) was calculated using a one-way anova with Dunnett's correction for mutiple comparison using Graphpad prism software.

component of the extracellular matrix of *S.* Typhimurium and *E. coli* biofilms (Zogaj *et al*., 2001). As SL1344 has all the genes required for the production and regulation of cellulose and curli biogenesis, it was hypothesised that utilising Lyso-PG as a sole carbon source could be inducing the expression of the overall regulator, MlrA.

To test this hypothesis, a deletion mutant of *mlrA* was constructed. Primers were designed to anneal approximately 300 bp up and downstream of the *mlrA* gene (Figure 6.25A). The *mlrA::aph* mutant in the *S.* Typhimurium 14028s deletion library was used as a template for PCR. The linear PCR fragment contained the kanamycin resistance cassette flanked by regions of homology to the *mlrA* locus. This fragment was electroporated into SL1344 cells expressing λ- recombinase. Resulting mutants were selected on kanamycin agar plates and confirmed by PCR (Figure 6.25B).

To determine whether MlrA was important for biofilm formation in the Lyso-PG medium, the *mlrA::aph* mutant and SL1344 wild-type were grown in M9 minimal media supplemented with either Lyso-PG or glucose for 24 h. The OD_{600nm} was measured every hour, and after 24 h, the plates were used for a crystal violet microtitre plate biofilm assay. The *mlrA::aph* mutant was able to grow utilising Lyso-PG as a sole carbon source (Figure 6.26A). Additionally, the *mlrA* mutant did not form biofilm when grown in M9 + glucose (Figure 2.26B) but did form biofilm when grown in Lyso-PG medium (Figure 6.26C). The biofilm formed by the *mlrA* mutant was not significantly different to the biofilm formed by the SL1344 wild-type control (Figure 6.26C). These data suggested that MlrA was not important for the induction of biofilm formation of SL1344 when utilising Lyso-PG as a sole carbon source. Therefore, cellulose and curli production might not be important for biofilm formation under the conditions tested.

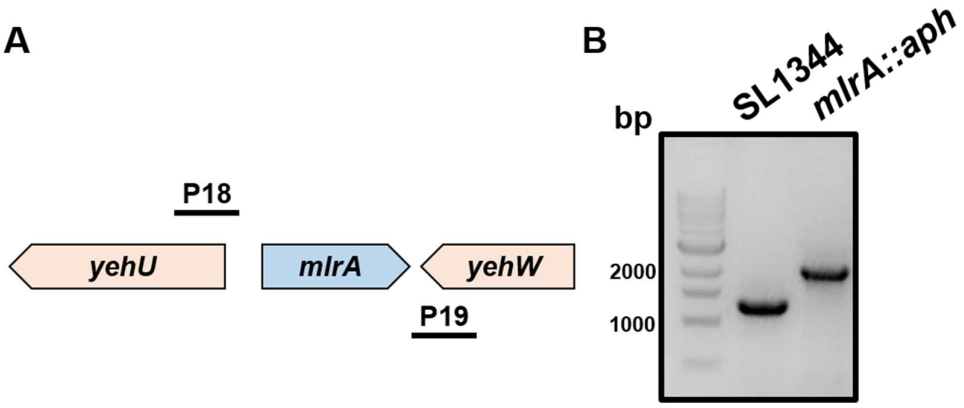

Figure 6.25. PCR check of *mlrA* gene deletion mutant. (A) Primer annealing at the *mlrA* loci to generate PCR fragment for gene deletion. (B) DNA gel showing the PCR product using primers P18 and P19 for the *mlrA* loci in SL1344 wild-type and *mlrA::aph.*

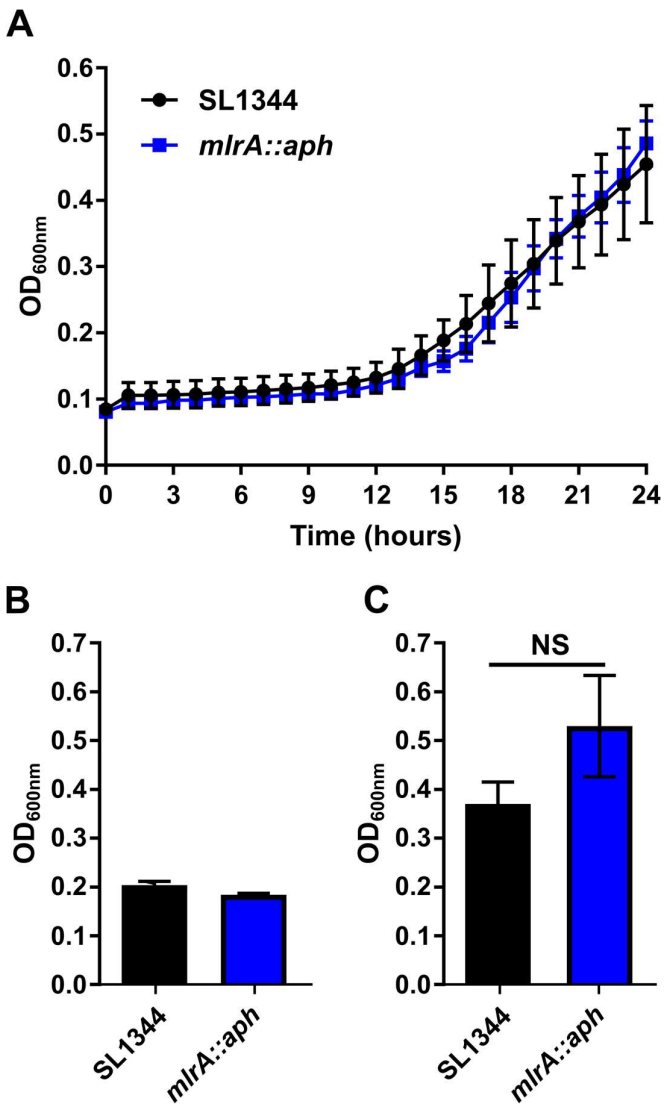

Figure 6.26. Growth and biofilm formation of an *mlrA* mutant in M9 + Lyso-PG medium. (A) Growth curve of SL1344 (black) and *mlrA::aph* (blue) in M9 minimal medium supplemnted with 1 mg/ml Lyso-PG. Growth was measured as OD_{600nm} over 24 h with measurements every hour in a Clariostar plate reader. Error bars represent standard error of the mean (SEM). (B) Crystal violet based biofilm profiles of SL1344 wild-type (black) and *mlrA::aph* (blue) grown in M9 + glucose and (C) M9 + Lyso-PG, error bars represent the SD. Data here is an average of 3 biological replicates. Statistical significance ($p<0.05$) was determined by a parametric 2-tailed Student's t-test using Graphpad prism.

6.2.15. The role of ApeE for biofilm formation in non-aggregating *E. coli* HB101.

No homologue of *apeE* exists in *E. coli*, and previous work in this thesis showed that expression of *apeE* in *E. coli* BW25113 allowed *E. coli* to utilise Lyso-PC as a sole carbon source. As the growth of *S*. Typhimurium SL1344 in Lyso-PG promoted biofilm formation that is dependent upon the presence of active ApeE, the biofilm forming properties of ApeE were investigated. A plasmid expressing *apeE* (pApeE) under an IPTG inducible promoter was transformed into the non-aggregating *E. coli* strain HB101. To test whether *apeE* was expressed in this *E. coli* strain, whole cell protein fractions from overnight cultures of either HB101 + pQE60 (EV) or HB101 + pQE60-ApeE (+pApeE) were isolated. The protein fractions were separated by SDS-PAGE and then transferred to a nitrocellulose membrane. The membrane was used for Western immunoblotting with anti-ApeE primary antibody. The blot shows that ApeE can be detected as a band at approx. 69 kDa only in the sample with pApeE present (Figure 6.27A).

For the subsequent assays, ApeE was required to be folded and functional. Outer membrane proteins are known to migrate differently on SDS-PAGE depending on whether or not they are folded (Reithmeier and Bragg, 1974), therefore a quick test to check the folded state of an outer membrane protein is to analyse boiled (100°C) and non-boiled (25°C) samples by SDS-PAGE. Outer membrane protein samples were isolated from HB101 cultures containing either EV or pApeE using the TritonX-100 extraction method. The outer membrane fractions were mixed with Laemmli sample buffer and either boiled, or not, prior to analysis by SDS-PAGE and Western immunoblotting. The membrane was probed with anti-ApeE antibodies and these bound antibodies identified by the addition of the substrate BCIP-NBP. Samples of

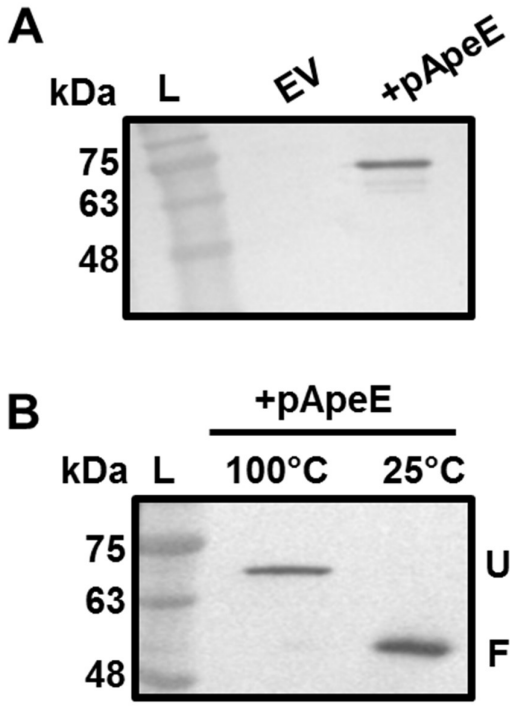

Figure 6.27. Expression and folding of ApeE in *E. coli* HB101. (A) Western immunoblot using anti-ApeE antibodies. Whole cell proteins from *E. coli* HB101 with either pQE60 (EV) or pQE60-ApeE (+pApeE) were separated by SDS-PAGE and transferred to a nitrocellulose membrane. The blots were developed upon addition of the substrate BCIP-NBP. (B) Whole cell protein extracts from HB101 + pQE60-ApeE were either boiled (100°C) or incubated at room temperature (25°C) for 5 min prior to separation by SDS-PAGE and Western immunoblotting with anti-ApeE antibodies.

boiled ApeE did not migrate as far on the gel as the un-boiled sample (Figure 6.27B). These data suggest that ApeE produced in *E. coli* HB101 was folded.

The ability of ApeE to induce biofilm formation in *E. coli* HB101 was investigated. *E. coli* HB101 expressing either empty vector (EV), ApeE (pApeE) or a known biofilm inducing autotransporter, SadA (pSadA), were grown in M9 minimal medium supplemented with 0.4% glucose for 16 h at 37°C without shaking in a microtitre plate. The only strain that formed biofilm under these conditions was *E. coli* HB101 + pSadA (positive control) (Figure 6.28). The strain expressing *apeE* did not form biofilm that was significantly different to the EV control (Figure 6.28). These data suggest that ApeE was not a biofilm promoting factor.

6.2.16. The ability of *E. coli* to grow and form biofilm in Lyso-PG M9 media.

Next, the ability of ApeE to mediate growth of *E. coli* HB101 using Lyso-PG as a sole carbon source was investigated. Overnight cultures of HB101 expressing ApeE (+pApeE) or empty vector (EV) were washed twice in sterile PBS before being inoculated into M9 minimal media supplemented with either glucose or Lyso-PG. Both strains grew at similar rates with glucose as the sole carbon source (Figure 6.29A). Only *E. coli* expressing *apeE* (+pApeE) was able to grow with Lyso-PG as a sole carbon source (Figure 6.29B), suggesting that ectopic expression of *apeE* allowed *E. coli* to utilise Lyso-PG as a sole carbon source.

As growth in M9 minimal medium supplemented with Lyso-PG as a sole carbon source signalled biofilm formation in *Salmonella,* the ability of *E. coli* grown in the presence of Lyso-PG was tested. Similar factors influence biofilm formation by *Salmonella* and *E. coli*, and therefore similar environmental signals might induce similar responses. To test whether ApeE-mediated growth of *E. coli* in M9 + Lyso-PG medium induced biofilm formation, the crystal violet microtitre plate biofilm assay was

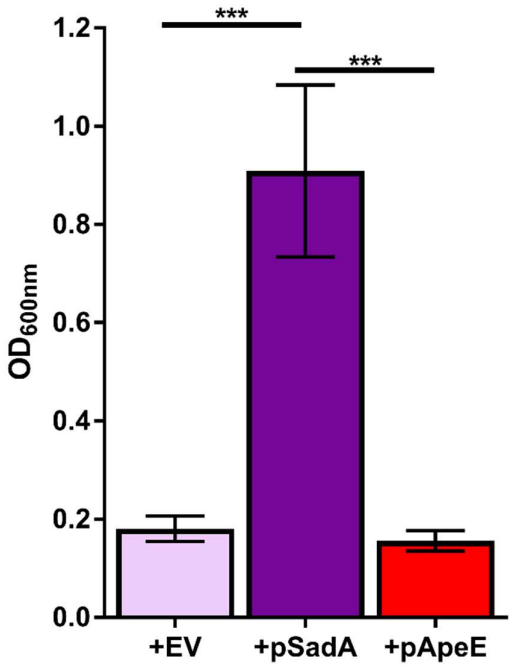

Figure 6.28. Biofilm formation of *E. coli* HB101 strains. Biofilm profiles of HB101 with either +EV (pink), +pSadA (purple) or +pApeE (red) after growth in a microtitre plate statically for 16 h at 37°C. The data presented here are the endpoint OD_{600nm} measurements of 3 biological replicates, and the error bars represent SD. Statistical significance ($p<0.05$) was determine by a one-way anova multiple comparison with Turkey's correction using Graphpad prism (*** $p<0.001$).

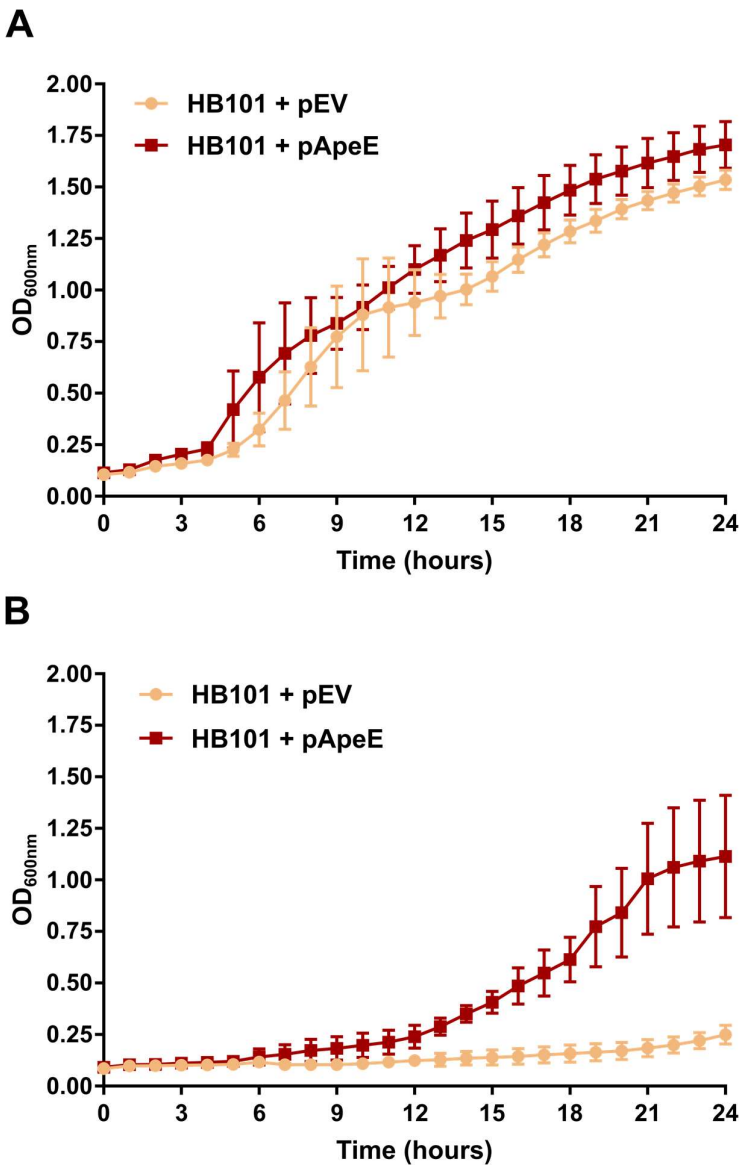

Figure 6.29. Growth of *E. coli* HB101 using Lyso-PG as a sole carbon source. (A) Growth curve of HB101 + pQE60 (yellow) and HB101 + pQE60-ApeE (red) in M9 minmal media supplemented with glucose and (B) Lyso-PG. Data here are the average of 3 biological replicates of OD_{600nm} measurements taken every hour for 24 hours in a Clariostar plate reader. The error bars represent the SEM and plates were incubated at 37°C.

used. When ApeE mediated growth in Lyso-PG medium, *E. coli* HB101 did form significantly more biofilm than when grown in M9 minimal medium supplemented with glucose (Figure 6.30). Therefore, growth on Lyso-PG as a sole carbon source in M9 minimal medium induced biofilm formation in *E. coli* as well as *S.* Typhimurium SL1344

6.3 Discussion.

In this chapter, the phospholipid binding specificity of ApeE was explored, using a PIP strip binding assay. ApeE was shown to bind to most glycerophospholipids including those that make up biological membranes and eukaryotic signalling lipids. Importantly, binding to these lipids does not necessarily prove that ApeE can hydrolyse these lipid species as binding tends to occur at the oxyanion hole and hydrolysis at the active site of the enzyme. To test whether ApeE could actively hydrolyse the lipids that were identified by PIP strip binding, the utilisation of each as a sole carbon source in M9 minimal media/agar could be used. Growth would indicate hydrolysis.

PI, PS and PA make up eukaryotic cellular membranes (van Meer *et al*., 2008). In this chapter, ApeE was shown to bind strongly to all of these lipid species. A previous report showed that *S.* Cholereasuis and *S*. Typhimurium could utilise PS as a sole source of nitrogen and carbon *in vitro* and in murine derived caecal mucus (Krivan *et al*., 1992). Therefore, as ApeE can bind to PS with relatively high affinity, the enzyme might be mediating the hydrolysis of PS. In contrast, ApeE was shown to not alter the membrane phsopholipid composition of *S.* Typhimurium. This is unsurprising given that phospholipid biogenesis occurs in the cytoplasm and the lipase motif of ApeE is surface exposed.

In this study, ApeE was shown to hydrolyse both Lyso-PC and Lyso-PG, allowing *S.* typhimurium to utilise these lipids as sole carbon sources *in vitro*. Bile is a rich source

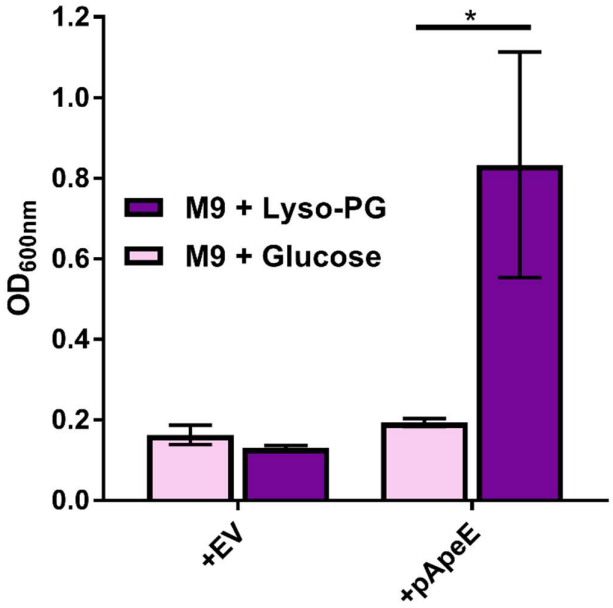

Figure 6.30 Biofilm profiles of *E. coli* HB101 expressing *apeE*. Biofilm profiles of *E. coli* HB101 with either pQE60 (EV) or pQE60-ApeE (+pApeE) after 24 hours growth in M9 minimal media supplemented with either glucose (pink) or Lyso-PG (purple). The biofilm formation was measured as OD_{600nm}. The data here represent 3 biological replicates, with the error bars showing SD. Statistical significance ($p<0.05$) was determined by a 2-way anova with Bonferroni's correction for multiple comparisons.

of phospholipid, whereby 22% of bile content is phospholipid, with the majority being PC (Reshetnyak, 2013). ApeE was able to hydrolyse at least 3 lipid species found in ox-bile. One of these lipid species was likely to be Lyso-PC. The biological relevance for lipid hydrolysis in bile can be speculated. Lyso-PC has been implicated to be an important carbon source for *S*. Typhimurium in bile (Antunes *et al*., 2011). However, the portion of the Lyso-PC that is more important for growth remains unclear. In this study, *S*. Typhimurium was shown to grow on Lyso-PC and Lyso-PG as sole carbon sources in the absence of either the Gglp/Ugp or Fad systems, suggesting that the head group and fatty acid acyl chains can be used as sole carbon sources.

In this study, the role of the Glp and Ugp system for import and degradation of glycerophosphocholine (GPC) was investigated. When GPC was present as a sole carbon and phosphate source, the transporter GlpT and the periplasmic glycerodiester phosphatase, GlpQ, were required for growth. When the medium was supplemented with GPC and a source of P_i, GlpQ and GlpT to some extent, were required for growth. When GPC and a source of carbon was added to the medium, only the double glycerodiester phosphatase mutant strain did not grow, suggesting both are important for the utilisation of GPC as as sole phosphate source. These data fit in with published work that shows that GlpT is not required for utlisation of GPC as a sole source of phosphate (Brzoska *et al*., 1994). The requirement of each system when *S.* Typhimuium is metabolising Lyso-PC, or any ApeE phospholipid substrate, will depend upon the nutrient limitation that the cells are exposed to.

Bile is made up of a mixture of substances, including protein and GPC (Antunes *et al*., 2011). As *S.* Typhimurium was able to utilise GPC as a sole carbon and phosphate source, then the bacteria could utilise this for energy and would not necessary require the fatty acid acyl chains of Lyso-PC for growth. It is plausible that

fatty acid uptake might occur for reasons other than, or in addition to, energy production. For example, LCFA have been shown to inhibit the expression of *hilA* and the utilisation of LCFA as carbon sources did not affect this inhibition (Golubeva *et al*., 2016). Therefore the import of LCFA might not be just for energy production in certain environments. A study comparing the differential expression of genes from *S*. Typhi and *S*. Typhimurium in bile identified that genes involved in the Fad system were universally upregulated (Johnson *et al*., 2018b). Suggesting that the importation of fatty acids in bile is an important process conserved in *S.* Typhi as well as *S.* Typhimurium. Overall, it is hypothesised that utilising phospholipids in additon to other sources of carbon/phosphate for growth might enable more efficient growth and thus be advantageous in certain environments.

One of the major lifestyle changes that bacteria can make in response to external stimuli is the switch from planktonic growth to biofilm formation. Biofilms are complex communities of bacterial cells that are known to contribute to various human diseases (Del Pozo, 2018). Biofilms are known to be more resistant to antibiotics and other environmental stresses such as the host immune system (Gonzalez *et al*., 2018). In this study, the non-biofilm forming strain of *S.* Typhimurium, SL1344, was shown to form biofilm on polystyrene microtitre plates when grown in M9 minimal medium supplemented with Lyso-PG as a sole carbon source. This biofilm was not observed when the cells were grown in Lyso-PC as a sole carbon source, although this might be because the levels of growth in each medium were not comparable. Processing of the Lyso-PG head group was shown to be important for biofilm formation as the *ugpQ glpQ* double mutant was able to grow utlising Lyso-PG as a sole carbon source, but did not form biofilm comparable to the wild-type. One possible explanation is that the PG head group is negatively charged, and if this headgroup was being processed and

incorporated into the bacterial membrane, it might cause the membrane to become more nagatively charged than normal. Lyso-PC is a zwitterionic lipid with an overall neutral charge, and therefore it could be that the reason for no biofilm formation after growth in Lyso-PC might be because the negative charge is important. If that were to be the case, growth utilising other negatively charged phospholipids, such as PA or PS, as sole carbon sources might induce biofilm as well. In *E. coli,* various mutants for phospholipid synthesis have been constructed such that one does not make PE, another PG and the last one CL (Rowlett *et al*., 2017). In each mutant, the bacterial membrane phospholipid ratios altered in comparison with the wild-type, which was typically 75% PE, 25% PG and 5%CL (Rowlett *et al*., 2017). In the PE strain, the membrane phospholipid content was approximately 50% PG and the other 50% CL. This would generate a highly negatively charged membrane and, under some conditions, this strain formed more biofilm than the wild-type (Rowlett *et al*., 2017). Even though the CL^- strain would also be more negatively charged than the wild-type, this did not form as high biofilm under any condition tested, but the number of dead cells increased in this mutant, and therefore lack of biofilm might be attributed to increased cell death (Rowlett *et al*., 2017). Indeed, the overall regulator of the formation of ECM molecules, MlrA, was not required for biofilm formation during growth in Lyso-PG, suggesting that ECM molecules might not be the driving factors for bioiflm formation in these conditions. The fact that ApeE enabled *E. coli* to grow using Lyso-PG as the sole carbon source, and to form a biofilm, suggests a conserved mechanism of biofilm formation. One way to determine the factors responisble for biofilm formation would be to investigate the differential expression of genes in *S.* Typhimurium SL1344 between gluocse and Lyso-PG growth. This might provide some insight into the factors that might be responsible for bifofilm formation. It would also be interesting to

investigate whether the utlilisation of Lyso-PG as a sole phosphate source would also induced biofilm formation.

CHAPTER 7

The role of ApeE during *Salmonella* infection

7.1 Introduction

In chapter 4 of this study, the *S.* Typhimurium autotransporters were shown to be important for chronic infections in a murine host. Subsequently, ApeE was shown to be highly conserved across *Salmonellae* and a potent lipase capable of hydrolysing lipids in ox-bile with an optimum pH of 8.0 for enzyme activity. Other GDSL containing proteins have been shown to be important during infection, such as the *S.* Typhimurium SPI2 effector, SseJ (Kolodziejek and Miller, 2015, Lossi *et al*., 2008, Ruiz-Albert *et al*., 2002). Previous work from our laboratory has shown that ApeE is required for the hydrolysis of the tomato cuticle, which is an area of nutrient limitation. ApeE hydrolysis of the cuticle allowed the *Salmonellae* to access the rich tissue underneath. Therefore, the presence of ApeE provided an advantage to *Salmonella* in the nutrient limited environment of the tomato cuticle.

To date, ApeE has not been characterised during murine infections of *Salmonellosis.* Given the conservation of ApeE, its phospholipase activity and importance during nutrient limited environments, it was hypothesised that ApeE might be important for *Salmonella* virulence. To test this hypothesis, murine models of acute and chronic *Salmonella* infections were used to characterise the role of ApeE during infection.

7.2 Results

7.2.1. The role of ApeE for invasion and replication inside host cells.

One of the first barriers that *S. enterica* must overcome in an infection setting is active invasion into host cells. To test whether an *apeE* mutant was able to invade host epithelial cells, the immortalised HeLa cell line was used. HeLa cells were cultured

under standard laboratrory conditons. $5x10^5$ HeLa cells were seeded and bacteria (either SL1344 or *apeE::aph*) were added to a multiplicity of infection (MOI) of 10. After 2 h of incubation, the HeLa cells were lysed and the bacterial cfu/ml were calculated by plating out serial dilutions. Each experiment included a non-infected to control to ensure the HeLa cells were not contaminated. The *apeE* mutant had comparable cfu/ml as the SL1344 wild-type in HeLa cells (Figure 7.1A). Therefore ApeE is not required for HeLa cell invasion.

The next barrier is replication inside host cells. Epithelial cells are usually permissive to *S.* Typhimurium intracellular replication and therefore to test the veracity of an *apeE::aph* mutant inside host cells, the immortalised murine macrophage (Raw 264.7) cell line was used. These cells were infected with either SL1344 or *apeE::aph.* At 2, 4 and 24 h post infection, the Raw264.7 cells were lysed and the bacterial cfu/ml was caculated. The *apeE* mutant was phagocytosed to the same level as the SL1344 wild-type (2 h timepoint) and survived as well as the wild-type in later timepoints (4 and 24 h timepoints) (Figure 7.1B). Therefore ApeE is not required for replication inside immortalised macrophages.

7.2.2 The role of ApeE in complement killing.

As ApeE did not seem to promote invasion into HeLa cells or survival inside immortalised macrophage cell lines, ApeE might be involved in promoting resistance to complement mediated killing. Other autotransporters are notable for promoting serum resistance (Schindler *et al.*, 2012). To test whether ApeE promoted resistance to complement mediated killing, SL1344 *apeE::aph* and *E. coli* BW25113 were inoculated into whole human serum. The serum and bacteria were incubated at 37°C for either 45, 90 or 180 minutes. At each timepoint the bacterial cfu/ml was calculated and compared to the initial inoculum. At each timepoint tested, the *apeE* mutant was

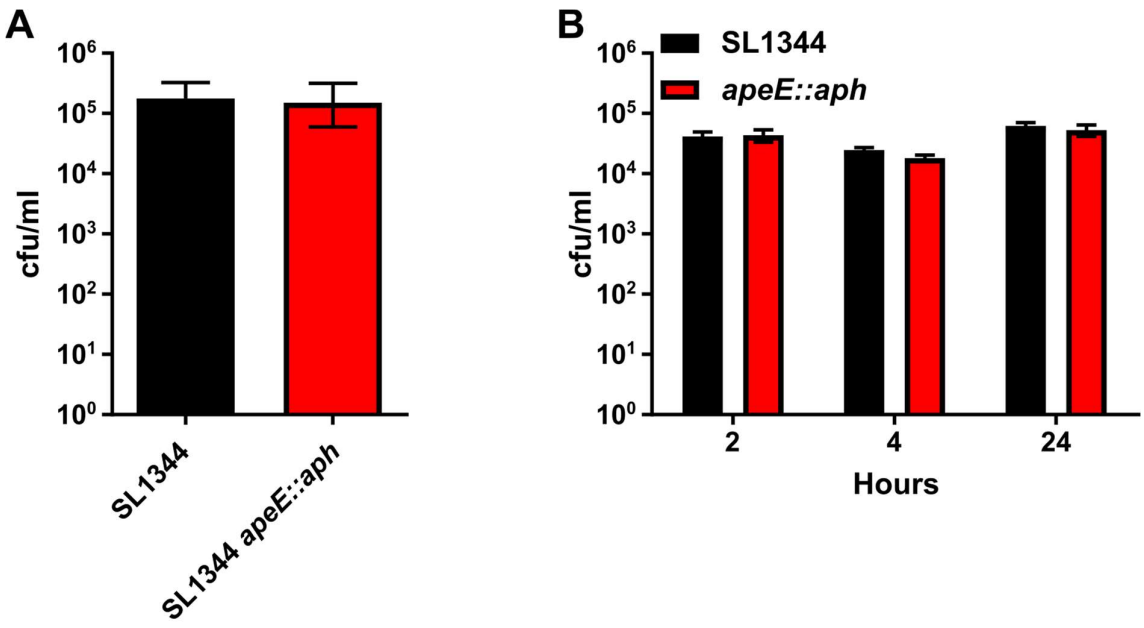

Figure 7.1. Invasion and replication of *S.* Typhimurium inside HeLa and Raw macrophages. (A) HeLa cells were infected with either SL1344 (black) or *apeE::aph* (red) at a multiplicity of infection (MOI) of 10 for 2 hours prior to enumeration of serial dilutions on agar plates to determine cfu/ml. (B) Raw 264.7 macrophage cells were infected with either SL1344 (black) or *apeE::aph* (red) at an MOI of 10 for either 2, 4 or 24 hours. At each time point, the Raw 264.7 cells were lysed and the bacterial numbers calculated as cfu/ml. Data represented here is from 3 biological replicates, and the error bars denote the SD of the geometric mean.

as resistant to serum killing as the SL1344 wild-type (Figure 7.2), suggesting that ApeE does not have a significant impact on serum resistance in *S*. Typhimurium.

7.2.3. The role of ApeE in acute murine infections by *Salmonella* Typhimurium.

In this study, ApeE was shown in this study to hydrolyse lipids. An area that is rich in lipids in the host gallbladder. Given that ApeE was not required for cell invasion, replication or for serum resistance, it was hypothesised that its role might be in specific sites of the mouse host. To understand the contribution of ApeE to colonisation of the different sites in a host, an acute infection model of *S.* Typhimurium was used. The virulent strain *S. enterica* SL1344 was used to infect 6-8 week old C57BL/6 mice (n=5) by oral gavage with 10^7 cfu per dose. Mice were humanely culled on day 5 post infection and the bacterial burdens of the spleen, liver, blood and gallbladders were enumerated by methods described previously. In all organs investigated, there were no significant differences in bacterial burdens between the wild-type and the mutant (Figure 7.3A-D). In the gallbladder, mice infected with the *apeE* mutant had slightly reduced bacterial burdens, but this was not statistically significant (Figure 7.3D). Taken together these data suggest that an *apeE* mutant strain retains the capacity to kill highly sensitive C57BL/6 mice, and thus the role of ApeE at later time points could not investigated.

7.2.4. Generating single mutants in *Salmonella* Typhimurium.

To investigate whether *apeE* played a role in SL3261 in the chronic murine model, a single *apeE* gene deletion on an SL3261 background was required. An *apeE* mutant was generated using a modified Datsenko and Wanner method. Primers (P7 and P8)

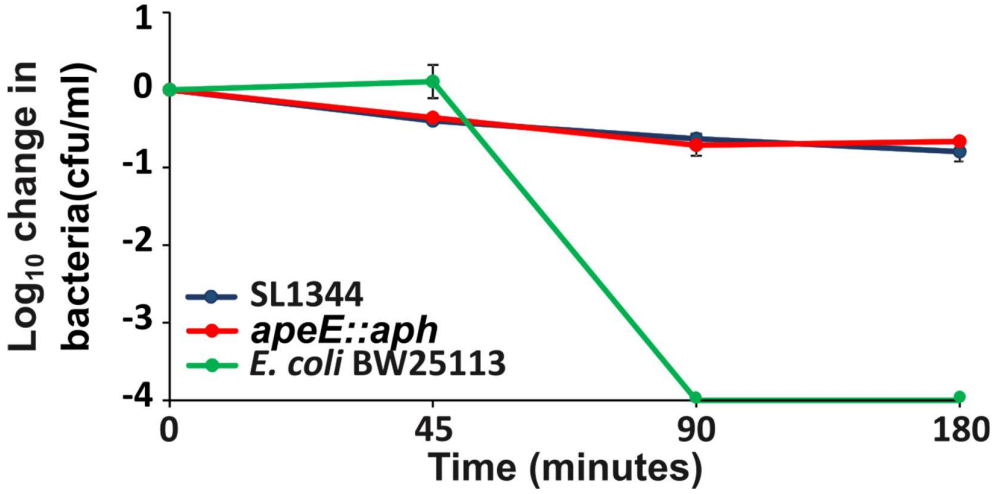

Figure 7.2. Complement mediated killing of *S.* Typhimurium. Killing curve of *S.* Typhimurium SL1344, *apeE::aph* and *E. coli* BW25113 in whole human serum for 180 minutes. The bacteria were incubated with the serum at 37°C and at 45, 90 and 180 minutes, the bacterial cfu/ml were calculated by counting colonies from serial dilutions. The bacterial numbers at each time point were compared to the initial inoculum and the graph shows the Log_{10} change in live bacteria (cfu/ml) in comparison to the initial inoculum over the time of the experiment. *E. coli* BW25115 (O-antigen$^-$) represents an internal control to show the activity of complement. Error bars represent the SD.

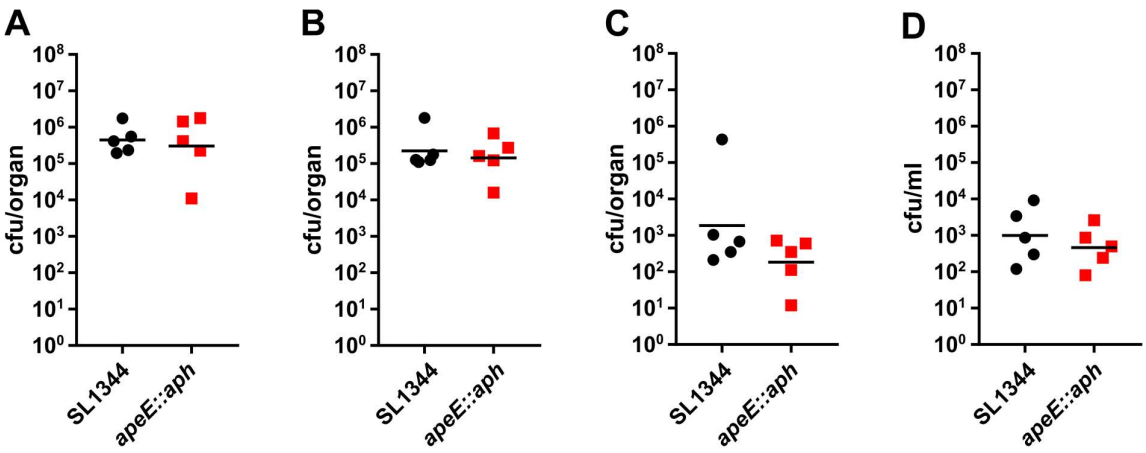

Figure 7.3. The bacterial burdens of mouse organs at day 5 of infection. The bacterial burdens of the spleen (A), liver (B), gallbladder (C) and blood (D) of mice infected orally with either SL1344 (black circles) or SL1344 *apeE::aph* (black squares) from day 5 post infection. Statistical significance ($p<0.05$) was determined using a Mann-Whitney non-parametric U-test.

were designed to anneal ~200 bp up and downstream of the *apeE* gene (Figure 7.4A). The existing SL1344 *apeE::aph* mutant was used as a template for PCR, producing a DNA fragment containing the kanamycin resistance cassette (*aph*) flanked by 200 bp of homology to the *apeE* locus. The linear DNA fragment was electroporated into SL3261 expressing λ recombinase and the resulting mutants selected for on kanamycin agar and gene deletion was confirmed by PCR (Figure 7.4B). Several positive candidates were checked for second site mutations using whole genome sequencing provided for as a service by MicrobesNG (University of Birmingham); none were found. LPS was isolated from SL3261 wild-type and *apeE* mutant by lysing the bacterial cells and degrading cellular proteins using proteinase K as described in Chapter 2. The extracted LPS was analysed by Nu-PAGE followed by silver staining. The *apeE* mutant had the same LPS profile as SL3261 wild-type (Figure 7.4C) and was therefore used for subsequent studies.

7.2.5 Role of ApeE in a chronic infection model of Salmonellosis.

In previous experiments, day 21 was shown to be a critical time point for autotransporter mediated organ colonisation, therefore day 21 was used as an initial time-point to understand the interaction of ApeE with the murine host. C57BL/6 mice were infected with either SL3261 or *apeE* mutant intraperitoneally with ~10^5 cfu's (n=14) and the bacterial burdens of the spleens, livers, and gallbladders were measured by plating serial dilutions of homogenised organs onto selective agar plates. At day 21, no significant differences in bacterial burdens of mice infected with the wild-type or *apeE* mutant were detected in the spleen or liver (Figure 7.5A and B). However, mice infected with the *apeE* mutant had significantly reduced bacterial numbers in the gallbladder in comparison to the wild-type SL3261 at day 21 (Figure 7.5C).

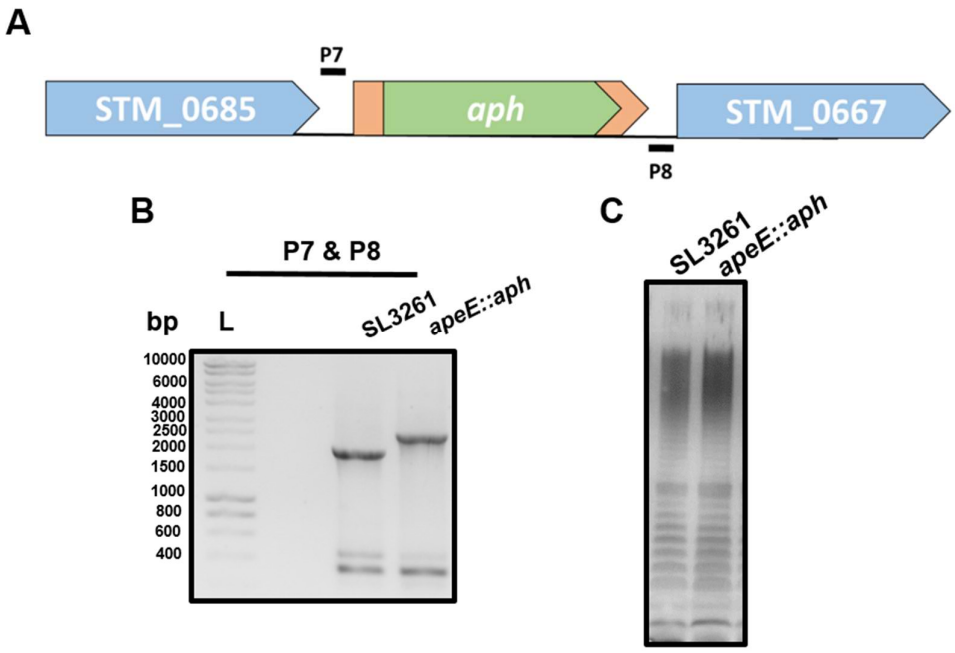

Figure 7.4. PCR amplification of the *apeE* loci in *S.* Typhimurium to generate SL3261 *apeE::aph* via modified Datsenko and Wanner method. (A) The sites of primer binding at the *apeE* loci. (B) Agarose gel analysis of PCR amplification of the SL3261 wild-type and *apeE::aph* mutant. (C) LPS profiles of *apeE::aph* mutant and SL3261 wild-type analysed by Nu-PAGE and silver staining.

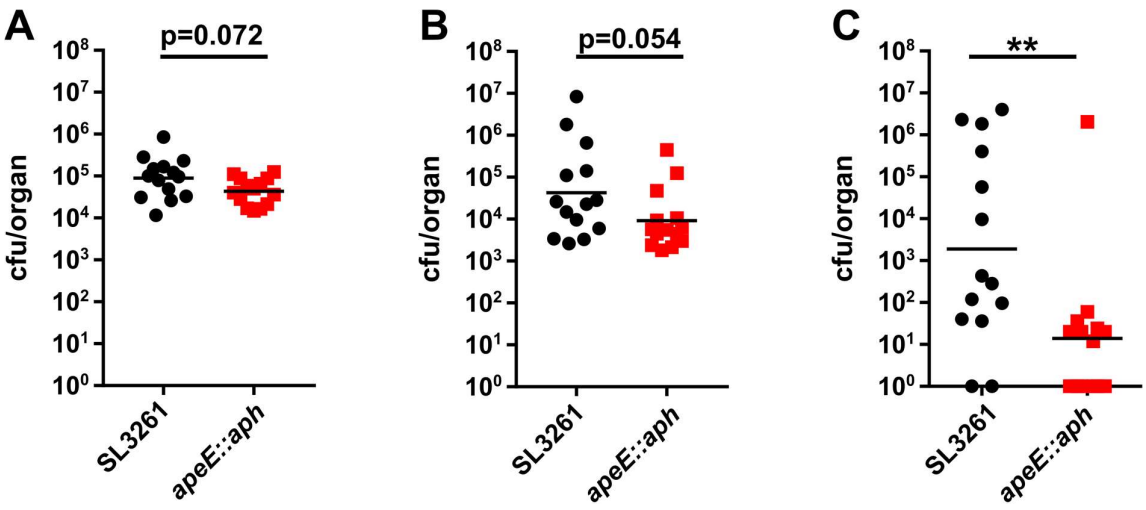

Figure 7.5. Bacterial burdens of mouse organs at day 21 of infection. Bacterial burdens of mice infected with either SL3261 (black circles) or *apeE::aph* mutant (red squares) at day 21 post infection in the spleen (A), liver (B), and gallbladder (C). On day 1 of infection, mice were infected with ~5x10^5 cfu's intraperitoneally. Statistical significance ($p<0.05$) was determined using a Mann-Whitney non-parametric U-test (** $p<0.01$). Data shown here represents 3 independent experiments with 4-5 mice in each group.

To understand the role of ApeE during chronic infections more thoroughly, the impact of an *apeE* mutant on infection at days 7, 14, 21, 28 and 35 were investigated. On day 1, C57BL/6 mice were infected with SL3261 and *apeE::aph* as described previously with each group containing 5 mice. At the time points mentioned, spleens, livers, gallbladders, and blood were harvested and processed to enumerate bacterial burdens. In the spleen there were significant differences between mice infected with SL3261 wild-type and *apeE* mutant on days 7, 21, 28 and 35, although these differences were modest. (Figure 7.6A). In the liver, there was a significant difference in bacterial burdens between groups on day 21, but again, this difference was modest (Figure 7.6B). In the gallbladder and blood, there were significant differences between mice infected with SL3261 and the *apeE* mutant post day 21 of infection (Figure 7.6C and D respectively), suggesting the role of ApeE might be in chronic infections rather than acute ones.

7.2.6. The requirement of ApeE for long-term faecal shedding in mice.

During the infection cycle of *S.* Typhimurium, the bacteria in the gallbladder are secreted into the intestine with gallbladder bile and are then shed out in faeces. As ApeE was required for chronic gallbladder colonisation, it might also play a role in faecal shedding. To test whether ApeE was required for faecal shedding, faeces from mice infected with either SL3261 or *apeE* mutant were obtained every 2 days for 31 days. Faeces were weighed and the cfu/ 100 mg of faeces was determined. Over time, mice infected with the *apeE* mutant tended to have fewer detectable bacteria in their faeces compared those infected with SL3261, although the bacterial burdens tended to vary across groups and days (Figure 7.7A). On each given day, mice infected with the SL3261 wild-type had an average of 3 mice per group of 5 with detectable bacteria in their faeces, whereas mice infected with the *apeE* mutant averaged 1 mouse out of

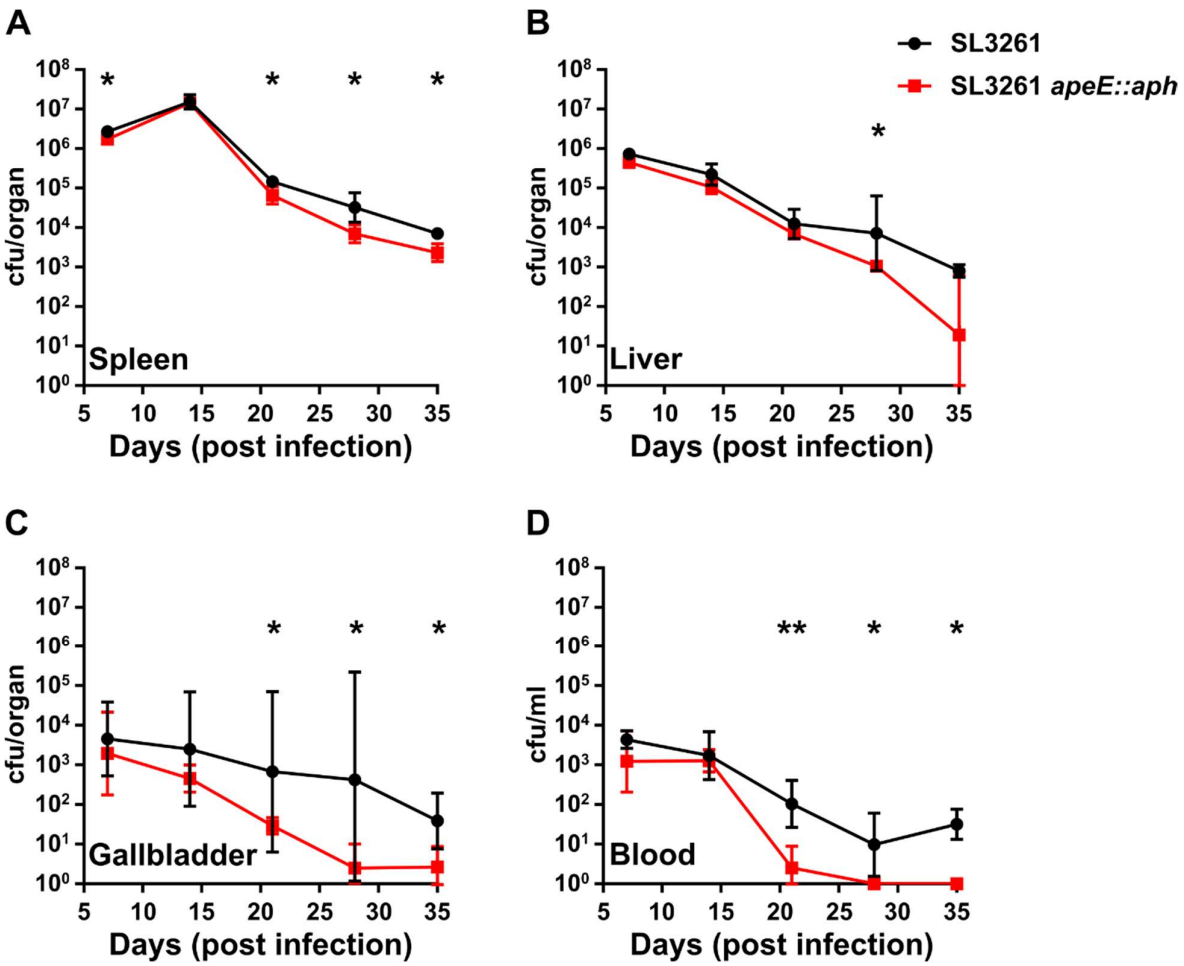

Figure 7.6. Bacterial burdens of the spleens, livers, blood, and gallbladders at days 7, 21 and 35 post infection. Time series of the bacterial burdens of mice infected with either SL3261 (black) or *apeE::aph* (red) over 35 day infection period in the (A) spleen, (B) liver, (C) gallbladder and (D) blood. Statistical significance ($p<0.05$) was determined using a Mann-Whitney non-parametric U-test (*$p<0.05$ and **$p<0.01$). Each group had 5 mice.

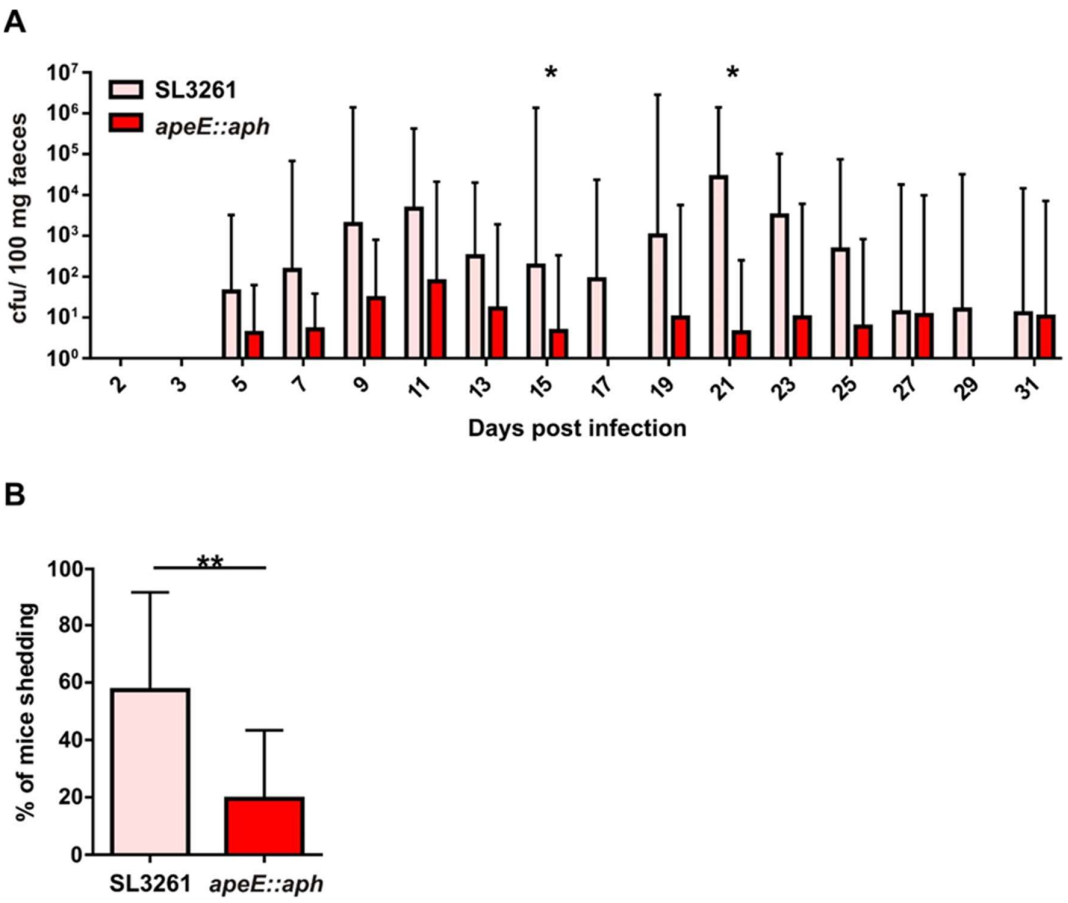

Figure 7.7. Faecal shedding of bacteria over 31 day infection period. (A) Data represents the cfu/ 100 mg of faeces of over a 31 day infection period of mice infected on day 1 with $5x10^5$ cfu of either SL3261 (pink bars) or *apeE::aph* (red bars). Faecal samples were plated on Xylose Lysine Deoxycholate (XLD) agar with appropriate antibiotics to select for *Salmonella.* (B) The percentage of mice with detectable bacteria in their faeces infected with either SL3261 (pink) or *apeE::aph* (red). Statistical significance was determined using a Mann-Whitney non-parametric U-test with significance defined as $p<0.05$ (* $p<0.05$ and ** $p<0.01$). Each group had 5 mice.

5 (Figure 7.7B). These data suggest that *apeE* mutant might have a defect in faecal shedding, although further experiments are required to confirm this hypothesis. For the rest of this study, the mechanism for ApeE mediated gallbladder survival was investigated.

7.2.7. The interaction of ApeE with murine bile

As a single ApeE mutant was attenuated in the gallbladder at day 21 of infection, and ApeE has been characterised as a phospholipase capable of hydrolysing phospholipids in ox-bile, the interaction of ApeE with murine bile was investigated in a liquid-chromatography mass spectrometry (LCMS) experiment. Mice were infected via I.P injection with either SL3261 or *apeE::aph.* Age matched uninfected (naïve) mice were used as a control group. On day 21, spleens, livers and bile were extracted from the mice. The amount of bile extracted successfully varied between mice and was not in sufficient quantity to determine bacteria colonisation of the mouse. The bacterial burdens of the spleens and livers of the infected mice groups were enumerated and compared to previous datasets. Mice infected with either strain for the lipidomics experiment had similar numbers of bacteria per spleen and liver as the previous experiments (Figure 7.8). Therefore, the infection dynamics were likely to be similar.

To determine whether the lipid content of murine bile changed in response to ApeE, bile samples were sent for further investigation. Lipids were extracted from the bile and subsequently analysed by LCMS as a service by Metabolomics Australia, Bio21.The data were analysed by Metabolomics Australia, Bio21 as part of the service. Over 400 lipid species were identified in murine bile (see appendix Tables ii, iii and iv). The abundance of 151 lipid species were significantly different in naïve mice compared to those infected with SL3261 wild-type, 163 were different between the naïve and

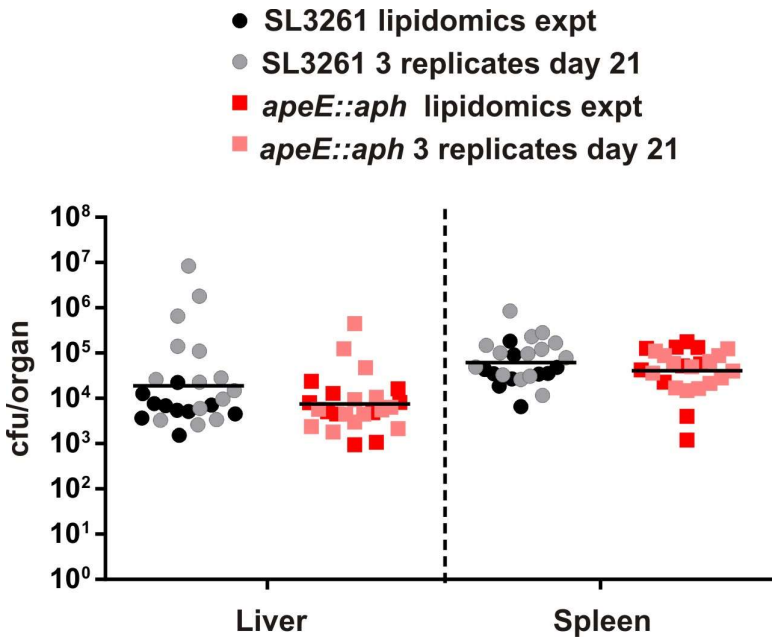

Figure 7.8 Comparing bacterial loads of mice at day 21 of infection. Bacterial burdens of the spleens and livers of mice infected with either SL3261 (black) or *apeE::aph* (red) at day 21 of infection. Block colours represent bacterial burden from previous day 21 experiments, and opaque colours represent the bacterial burdens of the mice used in the lipidomics study.

apeE::aph infected group and 18 were different between mice infected with either SL3261 or *apeE*::*aph* (Table 7.1). The lipids species that were different between SL3261 and *apeE::aph* infected mice included: Acylcarnitine; Cholesterol ester (CE); Lyso-PC (LPC); PE; PI; SM; triacylglycerol (TG); and ubiquinone (Table 7.1). The signal intensities of these 18 lipid species were compared to the uninfected naïve mouse group to determine the fold change of each lipid species following infection with *S.* Typhimurium (Table 7.2). The fold change values gave an indication about the abundancy of each lipid species in relation to the uninfected group and therefore provided a more accurate picture about what was happening *in vivo*. There were lipid species that were less abundant in mice infected with SL3261 including: LPC 22:5 (a/b/c); PE 36:4; PE 40:6; PE (P-18:1/22:5) (a/b); PI 38:3(a/b); and SM 42:2 (a/b) (Table 7.2). However, the other 12 lipid species were in higher abundancies in mice infected with the SL3261 wild-type, and these included four species of PC, three species of ceramide (Cer) and one cholesterol ester (CE) (Table 7.2). From these data, there is evidence that ApeE might be hydrolysing certain lipid species in bile *in vivo*. However, as some of the lipid species decreased in mice infected with the mutant in comparison to those infected with the wild-type, more complex lipid interactions are likely to be occurring in infected murine gallbladders.

7.2.8 Growth of *S*. Typhimurium utilising PC as a sole carbon source.

In the previous section, four species of PC were identified by LCMS as more abundant in the gallbladders of mice infected with the wild-type than those infected with the *apeE::aph* mutant (Table 7.2). It was hypothesised that PC was therefore not a substrate of ApeE. To test this hypothesis, overnight cultures of SL1344 wild-type, *apeE* mutant, complement and serine complement were washed twice in sterile PBS and serially diluted. The dilution series were spot plated onto M9 minimal

Table 7.1 Number of lipids significantly different between the infection groups

Lipid species	Number of lipid species		
	N vs A	N vs S	A vs S
Acylcarnitine	12	11	1
Cholesterol esters (CE)	11	15	1
Ceramides (CER)	9	12	3
Diacylglycerol (DG)	4	9	0
Dihydroxyl ceramides (dhCer)	1	1	0
Hexosylceramide (Hex1Cer)	1	3	0
Lyso phosphatidylcholine (LPC)	21	20	1
Lyso phosphatidylethanolamine (LPE)	5	6	0
Lyso phosphatidylinositol (LPI)	3	3	0
Phosphatidylcholine (PC)	48	29	4
Phosphatidylethanolamine (PE)	18	18	3
Phosphatidylglycerol (PG)	2	1	0
Phosphatidylinositol (PI)	6	1	1
Phosphatidylserine (PS)	1	2	0
Sphingomyelin (SM)	21	18	2
Triacylglycerol (TG)	0	2	1
Total	**163**	**151**	**18**

Mice infected with N = Naïve; S = SL3261; A = *apeE::aph*

Table 7.2 Fold change vs naïve mice of lipids significantly different between wild-type and *apeE::aph* infected mice.

Lipid Species	Mean fold change vs naïve mice	
	SL3261	***apeE::aph***
Acylcarnitine 17:0	0.140 ± 0.023	0.075 ± 0.025
CE 16:0	1.755 ± 0.422	0.612 ± 0.067
Cer(d18:1/26:0)	0.999 ± 0.271	0.435 ± 0.038
Cer (d20:1/24:0)	3.108 ± 1.031	0.839 ± 0.261
Cer (d20:1/24:1)	5.502 ± 1.996	0.729 ± 0.130
LPC 22:5 (a\b\c)*	0.074 ± 0.030	0.310 ± 0.128
PC 30:0	1.228 ± 0.283	0.503 ± 0.53
PC 36:0	0.549 ± 0.267	0.273 ± 0.066
PC 38:3	0.860 ± 0.241	0.426 ± 0.110
PC (O-32:1)	3.800 ± 0.773	2.077 ± 0.369
PE 36:4*	0.379 ± 0.079	0.546 ± 0.109
PE 40:6*	0.439 ± 0.249	0.669 ± 0.174
PE (P-18:1/22:5)(a\b)*	0.462 ± 0.197	1.203 ± 0.271
PI 38:3 (a\b)*	0.556 ± 0.170	1.588 ± 0.321
SM 42:2 (a\b)*	0.190 ± 0.083	0.413 ± 0.143
SM 44:3 (a\b)	1.883 ± 0.559	0.729 ± 0.130
TG 14:1 18:1 18:1	0.561 ± 0.124	0.407 ± 0.076
Ubiquinone	1.478 ± 0.594	0.405 ± 0.042

Bold* signify lipids that are less abundant in mice infected with SL3261 wild-type

agar supplemented with either glucose or PC. The plates were incubated at 37°C for 36 hours. All strains grew comparably utilising glucose as a sole carbon source, but no growth was detected for any strain using PC as a sole carbon source (Figure 7.9). Therefore PC cannot be utilised by *S.* Typhimurium as a sole carbon source and was unlikely to be a substrate of ApeE under the conditions tested.

7.2.9 Growth of *S.* Typhimurium in M9 minimal media with multiple carbon sources.

It was hypothesised that ApeE mediated long term survival in murine gallbladders by hydrolysing phospholipid substrates in bile, such as Lyso-PC, and this might confer a growth advantage over time. To test this hypothesis, SL3261 wild-type, *apeE* mutant, *apeE* complement (+pApeE) and the site directed mutant $ApeE_{S35A}$ (+$pApeE_{S35A}$) were grown in M9 minimal media supplemented with casamino acids (CAA) and either glucose, Lyso-PC or no additional carbon source. The plates were incubated for 42 hours and at regular intervals, the cultures were manually resuspended and the OD_{600nm} measured at regular intervals. Each strain grew to comparative levels with glucose as the sole carbon source (Figure 7.10A). When Lyso-PC was added to the medium, SL3261 wild-type and pApeE complement grew significantly better than the mutant or +$pApeE_{S35A}$ complement (Figure 7.10B). The addition of casamino acids as a sole carbon source promoted comparable growth in all strains (Figure 7.10C). The growth of the *apeE* mutant and serine mutant in medium supplemented with both Lyso-PC and CAA was no different to the growth in CAA medium alone (Figure 7.10D). These findings show that hydrolysis of Lyso-PC can confer a growth advantage when multiple carbon sources are present, providing active ApeE is present.

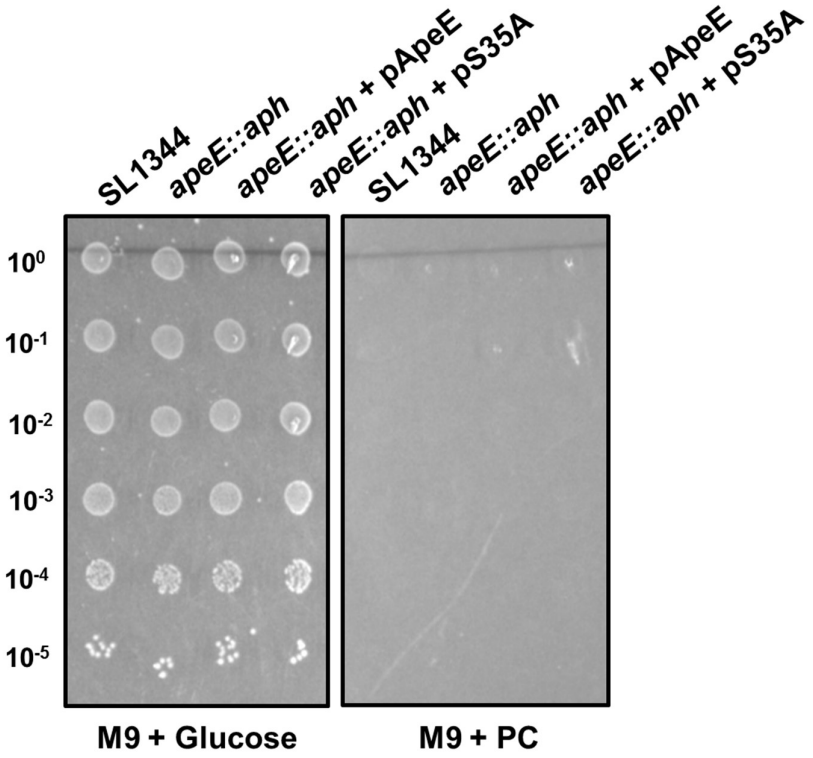

Figure 7.9. Growth of *S*. Typhimurium on M9 minimal agar supplemented with either glucose or phosphatidylcholine. Overnight cultures of either SL1334, *apeE::aph, apeE::aph* + pApeE or *apeE::aph* +pS35A were washed twice in sterile PBS and serially diluted 1:10. The dilution series for each strain was spot plated on M9 minimal agar supplemented with either 0.4% glucose or 1 mg/ml phosphatidylcholine (PC).

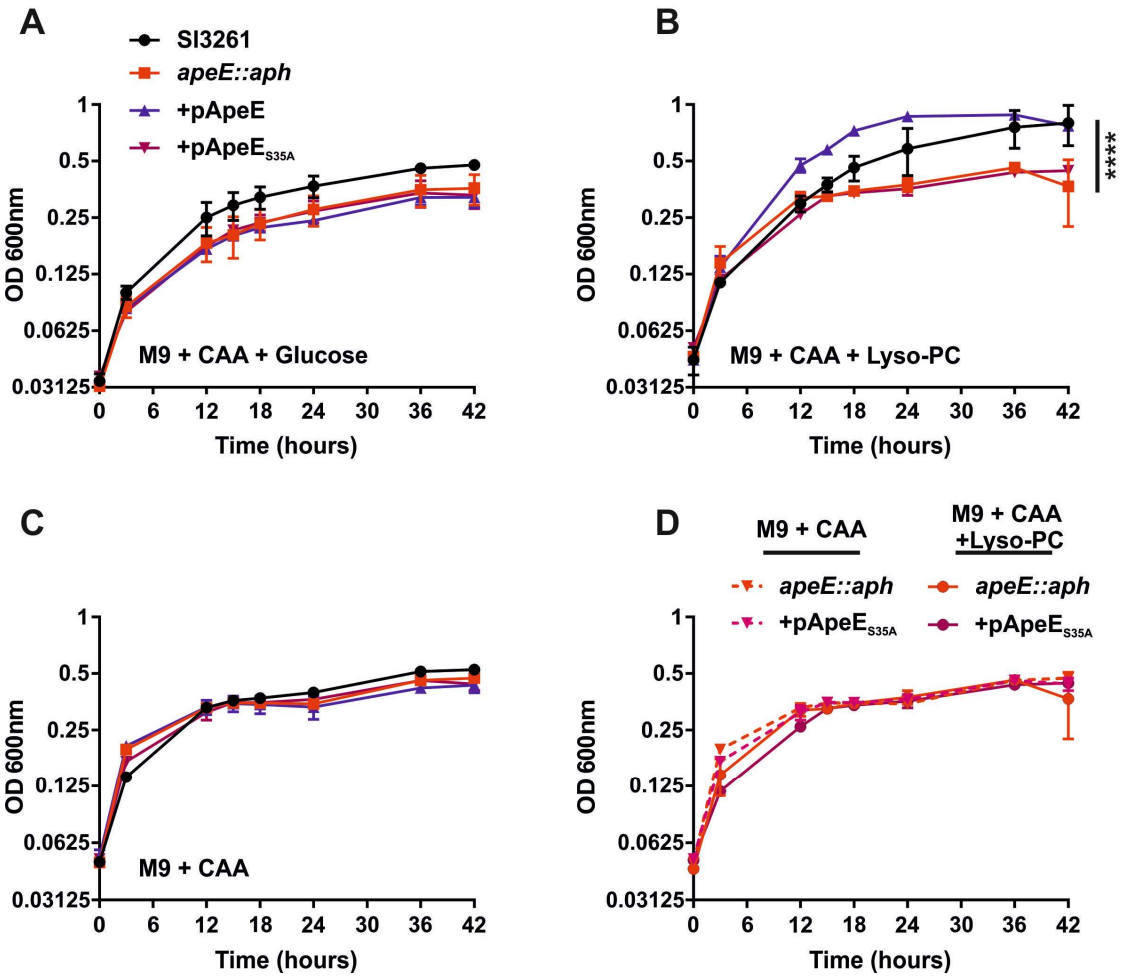

Figure 7.10. Growth of SL3261 strains using Lyso-PC as a carbon source *in vitro*. Growth of SL3261 (black circles), *apeE::aph* (red squares), *apeE::aph* + pApeE (blue triangles) and *apeE::aph* + pApeE$_{S35A}$ (purple triangles) in M9 minimal media supplemented with casamino acids (CAA) and (A) glucose, (B) Lyso-PC, (C) CAA only. (D) Comparison of the *apeE::aph* and *apeE::aph* + pApeE$_{S35A}$ growth in M9 minimal media supplemented with CAA only (lines) or CAA and Lyso-PC (dashed line). All growth was at 37°C for 42 hours with manual resuspension prior to OD_{600nm} measurement. Statistical significance ($p<0.05$) was determined using a Two-way anova with Turkeys correction for multiple comparison (****$p<0.0001$).

7.3 Discussion

In this chapter, the role of ApeE during infection was explored using *in vitro* and *in vivo* techniques. ApeE was shown not to be required for host cell invasion or replication, or for acute infections in a murine host. ApeE was, however, required for gallbladder colonisation (post day 21) and potentially for faecal shedding in more long-term murine infections. This data corroborates the infection data from mice infected with the multiple autotransporter knockout strains (SLATs) as this strain also showed attenuation in murine gallbladders in comparison to the wild-type (Figure 4.2). The SLATs strain was highly attenuated in all organs, on every day tested. This overall attenuation was not observed in the single *apeE* mutant and therefore the attenuation observed by the SLATs strain cannot be attributed to loss of ApeE alone.

Loss of ApeE resulted in an inability to colonise murine gallbladders post day 21 of infection. To explore the mechanism of gallbladder attenuation, the interaction of SL3261 with the lipids in murine bile *in vivo* were investigated. Lipid profiles of murine bile between the different infection groups were compared and 18 lipid species were identified as being significantly different between mice infected with the wild-type and those infected with an *apeE* mutant. Some of the lipid species identified were decreased upon infection with the wild-type in comparison to the *apeE* mutant, and some were increased. Similar lipids are reduced in bile upon wild-type *Salmonella* infection as identified in a previous studies (Antunes *et al*., 2011) (Appendix Table i), suggesting that the data are robust and reproducible. It is worth noting that as this is a different infection model and a different infecting strain of *S*. Typhimurium. As a result, there are likely to be differences in the lipids identified between the two studies.

Of interest were the lipid species that had decreased upon infection with the SL3261 wild-type but not decreased, or decreased less, in mice infected with the

apeE::aph mutant. Lipids that followed this pattern might be ApeE substrates in bile, and might provide insight into the mechanism of ApeE mediated gallbladder survival. Lipids that followed this pattern included a species of Lyso-PC, PE and PI. Lyso-PC has previously been characterised as a substrate of ApeE and in this chapter, growth on Lyso-PC in addition to another carbon source (Casamino acids) conferred a significant growth advantage *in vitro* and it is possible that this advantage might exist *in vivo* as well. As bile is replenished regularly (Jazrawi *et al*., 1995), it might be possible that depletion of certain lipid species might not be detected when using *in vivo* models. It would be interesting to compare the lipid species in bile that are affected by SL3261 and *apeE::aph* mutant growth *in vitro* as this would overcome the issues of bile turnover inside hosts, and host metabolite concentration variation.

Lyso-PC, in the host, is a secondary signalling molecule that has been implicated in monocyte and T lymphocyte recruitment (Quinn *et al*., 1988, McMurray *et al*., 1993). If *S*. Typhimurium hydrolyses Lyso-PC in the host, and Lyso-PC is a chemoattractant for $CD4^+$ T cells, ApeE hydrolysis of Lyso-PC might impact recruitment of T lymphocytes. It has been shown in a chronic model of *Salmonellosis* that at day 21, the proportion of $CD4^+$ T cells in spleens increase and this results in initiating bacterial clearance (Johanns *et al*., 2010). Therefore, it is possible that interferring with signalling molecules might disrupt immune cell recruitment and impact the ability of the immune response to control infections. These hypotheses would need to be tested further as in the current experiments investigating ApeE mediated gallbladder survival have not extensively characterised the immune response to infection.

One of the lipids that was reduced upon infected with the SL3261 wild-type but increased in mice infected with the mutant was PI 38:3 (a/b). Previous lipid binding assays showed that ApeE could bind to PI and also to bi and tri phosphorylated PtdIns

(Figure 6.1). PtdIns are important eukaryotic signalling molecules that are involved in vesicle trafficking (Roth and Sternweis, 1997). Intracellular pathogens are known to interfere with PtdIns signalling to enable survival inside host cells (Gaspar and Machner, 2014). Here, ApeE was not required for HeLa cell entry or survival in Raw264.7 macrophages *in vitro*. Therefore ApeE was not an important factor for efficient survival inside the host cells tested. Although other studies have identified ApeE as a protein that increases in number after 6 h growth inside HeLa cells (Liu *et al*., 2015) and *apeE* is upregulated 2-fold inside of macrophages (Srikumar *et al*., 2015). Taken together, perhaps there is a role for ApeE inside of host cells, but it was not identified under the conditions tested in this study. As primary and immortalised macrophage cell lines have been shown to have very different transcriptional profiles upon infection (Andreu *et al*., 2017), it is plausible that there might be a role for ApeE following ingestion by activated macrophages or primary macrophages isolated from murine bone marrow.

Another body site that was consistently differentially infected with SL3261 and autotransporter mutants was murine blood. In Chapter 3, the SLATs strain had fewer bacterial cfus detected in blood compared to the SL3261 wild-type and the same phenotype was observed for the single *apeE* mutant. In this chapter, the susceptibility of *S.* Typhimurium lacking ApeE to human complement was tested, and it was determined that ApeE was not involved in resistance to complement mediated killing. It is unlikely that the SLATs and *apeE* mutant are susceptible to murine complement, especially because murine complement has been shown to be less able to kill *Salmonella* than human complement (Siggins *et al*., 2011). Another possibility, is that ApeE is interacting with lipids in murine blood. Lyso-PC is also present in blood

(Phillips, 1957) and therefore ApeE might be interacting with lipids in blood. It would be interesting to repeat the lipidomics analysis but on the serum as well as bile.

There were another subset of lipids that changed in abundancy between mice infected with the wild-type and those with the *apeE* mutant, but these lipids showed an increase when infected with the wild-type in relation to the mutant. These lipid species included CE, CER and PC. CE are formed by the transfer of an acyl chain from PC to cholesterol (Buckley, 1982). Enzymes that do this are termed Glycerophospholipid: Cholesterol Acyl Transferases (GCAT) enzymes. In the lipidomics data, CE were present in higher numbers in mice infected with SL3261 than mice infected with the mutant (see Appendices). It could be that ApeE has GCAT activity and is capable of transferring an acyl chain from a phospholipid onto cholesterol. Indeed, another *S*. Typhimurium GDSL lipase, SseJ, has GCAT activity in a RhoA GTPase dependent manner (Lossi *et al*., 2008, Christen *et al*., 2009). Therefore, if ApeE were mediating transfer of an acyl chain to cholesterol to generate CE, this would be a novel function for ApeE.

PC did not appear to be a substrate of ApeE. In the lipidomics study, PC species tended to decrease upon infection with the *apeE* mutant, and this was not observed in mice infected with the SL3261 wild-type (Table 7.2). During *in vitro* growth assays, *S.* Typhimurium SL1344 did not grow on M9 minimal agar supplemented with PC as a sole carbon source (Figure 7.9). PC is the most abundant phospholipid in bile and it seems counterintuitive that this predominant eukaryotic lipid, might not be an ApeE substrate. The role of PC in bile has been extensively studied, and it is proposed to form mixed micelles with bile salts, that surround cholesterol, thereby enabling cholesterol to stay in solution (Carey and Small, 1978). There are also reports that suggest PC shields gallbladder epithelial cells from the damaging properties of bile

salts (Dial *et al*., 2015). It could be that if *Salmonella* were to hydrolyse PC, it might also increase the susceptibility of *S*. Typhimurium to bile salt damages. The overall contribution of *S.* Typhimurium interaction with PC is not fully understood. However, as the abundancies of many PC species changed when infected with *S.* Typhimurium (Table 7.1), there was obviously interaction between biliary PC and *Salmonella*. Further experiments are required to understand this interaction more fully.

The central dogma of *Salmonella* life cycle inside hosts is that bacteria in the gallbladder are secreted back into the intestines with normal bile secretions, and then leave the host during faecal shedding. In this study, the SL3261 wild-type infected mice overall had more detectable bacteria in their faeces in comparison to mice infected with the *apeE::aph* mutant. The faecal shedding for all groups was quite variable but the data, overall, suggested that ApeE was important for faecal shedding. This role of ApeE in faecal shedding might be linked directly to its role in gallbladder survival, as fewer bacteria in the gallbladder will also mean fewer are secreted back into the intestine. It would be interesting to investigate whether the defect in faecal shedding still exists where the bacteria are administered orally.

CHAPTER 8

General Discussion

8.1. Summary

In this study, the role of the *S.* Typhimurium autotransporters for virulence in mice was investigated. In particular, the role of the GDSL lipase autotransporter ApeE was investigated for interaction with host derived lipids. ApeE was shown to be a phospholipase B enzyme capable of binding to, and hydrolysing some eukaryotic lipids. ApeE mediated growth utilising Lyso-PC and Lyso-PG as a sole carbon sources. Growth in Lyso-PG induced biofilm formation in *S.* Typhimurium and *E. coli* suggesting a conserved mechanism. During *in vivo* murine infections, ApeE was required for long term colonisation of the blood, gallbladder and faeces of mice post day 21 of infection. Finally, ApeE was shown to change the abundance of lipids in murine bile by a LCMS experiment, indicating that this interaction between ApeE and murine biliary lipids might be important for *S.* Typhimurium inside the host.

8.2. The biological substrates of ApeE.

Prior to this study, a role for ApeE during infection had not been elucidated. In fact, the first paper that characterised the regulation of *apeE* suggested that ApeE likely did not have a role during infection as *phoBR* mutants did not have any observable virulence defects. The paper concluded it was therefore unlikely that genes under the transcriptional control of PhoBR would not be important for *Salmonella* virulence (Conlin *et al*., 2001). With time, this observation was shown to be incorrect, as some PhoBR regulated genes are upregulated inside HeLa cells, including genes that form the *ugp* operon (Liu *et al*., 2015), suggesting that there are roles for proteins that are produced in response to phosphate limitation inside the host. There is an argument that the induction of *apeE* expression might not be just under phosphate limiting conditions, as *apeE* was expressed when SL1344 was grown in M9 minimal media

supplemented with Lyso-phospholipids (Figure 6.20). M9 minimal medium is rich in P_i and as a result, there might be another mechanism of *apeE* regulation that has not yet been investigated.

In this study ApeE was shown to bind to and cleave various phospholipids. These lipids included eukaryotic derived Lyso-PC, PE, and PI. Lipids in the host can be involved in maintaining structural integrity of membranes, for energy storage or for signalling (van Meer *et al*., 2008). The hydrolysis of host lipids by pathogens is an important virulence function for many intracellular organisms (van der Meer-Janssen *et al*., 2010). Many pathogens have proteins that disable or hijack host signalling by lipids for their benefit (Gaspar and Machner, 2014, Niebuhr *et al*., 2002). *Salmonella* also have mechanisms to interfere with host PtdIns signalling to re-arrange the host cytoskeleton during host cell invasion (Perrett and Zhou, 2013a). In this study, ApeE bound to various PtdIns, and might hydrolyse a species of PI in bile, which might indicate a role for ApeE in mediating efficient host cell replication/survival. *S.* Typhimurium is hypothesised to hydrolyse phospholipids in bile for use as carbon sources (Antunes *et al*., 2011). In this study, ApeE was shown to hydrolyse Lyso-PC in bile *in vivo* and *in vitro* and is most catalytic active at pH 8.0, which falls within the normal pH range of bile (Crawford and Brooke, 1955), suggesting that ApeE might be highly efficient at lipid hydrolysis in the gallbladder.

8.3. Hypothesised mechanism of ApeE mediated gallbladder survival.

Evidence from this study suggests that ApeE hydrolysis of Lyso-PC might confer a growth advantage over time. Hydrolysis of Lyso-PC in bile by ApeE would generate free fatty acids and a glycerophosphocholine (GPC) head group. The head

group can be imported into the cell. If the phospholipid was to be used as a source of phosphate, GlpQ and UgpQ would break apart the head group into glycerol-3-posphate (G3P), and this would be used solely as a phosphate source. If the phospholipid was to be utilised as a carbon source, the head group would be processed by GlpQ only, and the G3P would be imported by GlpT and then enter glycolysis (Tommassen *et al*., 1991). The acyl chains would be imported into the cell by FadL, and if they are to be used for energy, they would be processed by FadD, which would add an acyl-CoA molecule onto the fatty acid as the first step in β-oxidation (Clark and Cronan, 2005). However, the exact role for these fatty acids is unclear, as in this study, it was determined that GPC could be used a phosphate and carbon source *in vitro*, thereby suggesting that the acyl chains might not be required simply for energy production. This would concur with other studies, which determined that long chain fatty acid import in bile was not for energy production, but was instead to repress expression of SPI1 and thus active host cell invasion (Golubeva *et al*., 2016, Prouty and Gunn, 2000). The overall result of ApeE mediated phospholipid hydrolysis would be that *Salmonella* growth was increased and therefore in the absence of ApeE, this growth would not occur and the bacterial burdens of the gallbladder would be reduced (Figure 8.1).

The next step in the model is that as *S.* Typhimurium replicate inside the gallbladder utilising Lyso-PC for energy production, the bacteria would be transported into the intestines alongside bile. Therefore, an increased bacterial burden in the gallbladder might cause increased bacterial numbers detected in faeces. Inefficient growth in bile by an *apeE* mutant might lead to decreased bacteria in the faeces. Of course, the relevance of this is that if ApeE is indirectly mediating efficient faecal

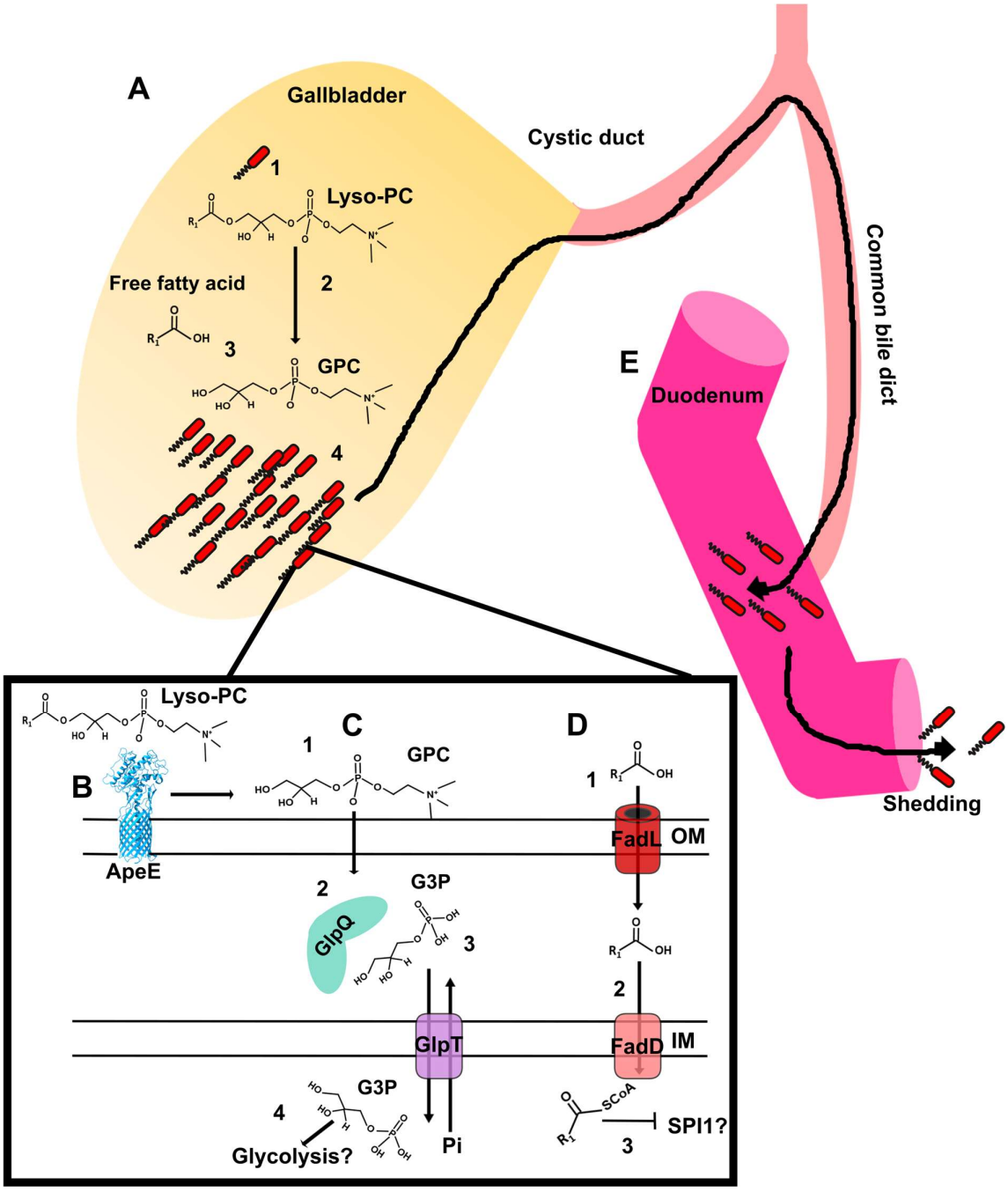

Figure 8.1. Hypothesised mechanism of ApeE mediated gallbladder survival. (A) *S.* Typhimurium in the gallbladder (1) utilise Lyso-PC in bile to generate glycerophosphocholine (GPC) (2) and free fatty acids (3). This allows the bacteria to grow efficiently in bile (4). (B) ApeE in the outer membrane (OM) of *S.* Typhimurium hydrolyses Lyso-PC into its constituent parts. (C). GPC diffuses across the OM (1) and

is picked up by GlpQ (2), which breaks apart GPC into glycerol-3-phsophate (G3P) and an alcohol. G3P is transported across the inner membrane (IM) by GlpT against the antiport of P_i (3). G3P can then be used as a carbon source in glycolysis (4). (D) The free fatty acid generated from ApeE hydrolysis of Lyso-PC crosses the OM via the transporter FadL (1) and an Acyl-CoA molecule is added at the IM by FadD (2). The fatty acid might inhibit expression of Spi1 (3) or be used for β-oxidation. (E) Efficient growth mediate by ApeE hydrolysis of Lyso-PC in the gallbladder permits more bacteria to pass into the duodenum with bile secretion and thus more bacteria are shed in the faeces.

shedding, it is plausible to assume that *S.* Typhimurium lacking ApeE would be less able to transmit from an infected host to an uninfected one.

8.4 The role of ApeE and the chronic carrier state.

Approximately 1-4% of typhoid patients develop asymptomatic chronic carriage, which has frequently been linked with chronic gallbladder colonisation and faecal shedding (Gunn and Keddie, 1972). This phenomenon is not only found in humans with systemic *Salmonella* infections, it is also observed in chronic infections of chickens with serovar Gallinarum (Sadeyen *et al*., 2004) and non-susceptible mouse strains with serovar Typhimurium (Crawford *et al*., 2010). Therefore, chronic carriage of *Salmonella* inside a host seems to be a fairly conserved mechanism to enable spread and dissemination of this pathogen. As ApeE seems to be required for survival in murine gallbladders post infection, it might be that ApeE is an important *Salmonella* factor for long term survival in gallbladders, and this could have implications for the carrier state. The animal model used in this study typically clears systemic bacteria by 12 weeks post infection, and actually, colonisation of the gallbladder was starting to clear by week 5 (Figure 3.2 and Figure 7.6). To understand whether ApeE contributes towards the carrier state in murine infections, non-susceptible mouse strains (such as CD1 mice) could be used as an infection model. These mice can be infected with the virulent *S.* Typhimurium strain SL1344 and can be chronically infected with *Salmonella* (Prouty *et al*., 2002, Crawford *et al*., 2010). These mice might prove a very powerful model to try to understand whether ApeE contributes to the carrier state or not. Furthermore, these resistant mouse breeds can be fed a lithogenic diet to induce gallstone formation (Crawford *et al*., 2010). In chapter 6 of this study, ApeE hydrolysis of the anionic Lyso-PG in M9 minimal medium resulted in significantly higher biofilm

formation than when the strains were grown in M9 glucose or Lyso-PC media (Figure 6.22). Cholesterol gallstones have been widely implicated to be a scaffold for *Salmonella* biofilms *in vivo* (Prouty *et al*., 2002, Crawford *et al*., 2010, Gonzalez-Escobedo *et al*., 2011), and that to form efficient biofilms on gallstones *in vitro*, bile needs to present (Prouty *et al*., 2002), demonstrating that cholesterol might not be the important signal that *Salmonella* can detect to induce biofilm formation. It might be possible that ApeE mediated hydrolysis of certain phospholipid species in bile might induce biofilm formation with cholesterol gallstones.

8.5 The future prospects of research into the role of ApeE during infection

There are still outstanding questions in this model. First, which was discussed above is, what are the roles, if any, for the free fatty acids generated by hydrolysis of phospholipids? One way to address this question might be to use an RNA-seq experiment to observe what genes are differentially expressed when *S.* Typhimurium utilising phospholipids/free fatty acids as sole carbon-phosphate sources *in vitro*. The next question is what are the consequence of ApeE hydrolysis of PtdIns? ApeE was shown to bind to PtdIns, and bi and tri phosphorylated PtdIns. In the lipidomics study, PI 38:0 was identified as a lipid species that was decreased upon infection with the wild-type but not with the *apeE* mutant. Therefore, it is plausible that ApeE can bind to and hydrolyse PtdIns, but the role for this hydrolysis is currently unknown. One method to confirm whether ApeE can hydrolyse PtdIns would be to use them as sole carbon sources in M9 minimal media for growth, but this would not answer the fundamental question about the role of this hydrolysis *in vivo.*

8.6 Concluding remarks

In this study, the role of ApeE for chronic gallbladder colonisation was established. Interaction of ApeE with host derived lipids might mediate this colonisation by providing extra nutrients for growth in bile. Further studies are required to determine the effect that loss of ApeE has on the carrier state in murine models of infection. However, the importance of the work in this study is that the interaction of ApeE with host lipids might be an important process for efficient and long term gallbladder colonisation in mice.

Appendix

Appendix Table i. Comparison of lipid species reduced in bile by *Salmonella*

	Fold change of lipid species abundance naïve: infected with wild-type *S.* Typhimurium	
Lipid	**(Antunes *et al*., 2011)**	**Metabolomics Australia**
LPC 16:1	1:0.47	1:0.1
LPC 18:1	1:0.31	1:0.07
LPC 20:4	1:0.29	1:0.04
LPC 20:5	1:0	1:0.07
LPC 22:6	1:0.32	1:0.04
LPE 18:2	1:0.27	1:0.07
LPE 22:6	1:0.45	1:0.07
PC 30:0	1:0	1:1.61
PC 35:4	1:0	1:0.49
PC 38:4	1:0	1:0.48
PC 40:8	1:0	1:0.36

Appendix Table ii. Signal intensity for lipids detected from mice infected with *apeE::Aph*

Name	ApeE-1	ApeE-2	ApeE-3	ApeE-4	ApeE-5	ApeE-6	ApeE-7
AcylCarnitine 12:0	21175	37080	190150	9407	89998	8738	10252
AcylCarnitine 13:0	2819	5940	26433	1299	15884	1275	1915
AcylCarnitine 14:0	36762	128251	324841	29540	125616	32100	17462
AcylCarnitine 14:1	78745	97560	707887	25210	303986	27650	26099
AcylCarnitine 14:2	26234	28127	210502	9195	105196	8537	9493
AcylCarnitine 15:0	4235	11931	38752	4435	16073	4274	1773
AcylCarnitine 16:0	166517	364493	991503	234107	285620	198992	81547
AcylCarnitine 16:1	44331	168392	447220	39199	226255	49189	18598
AcylCarnitine 17:0	3525.247	6618.915	21639.32	3847.798	10793.61	5138.288	2509.038
AcylCarnitine 18:0	22696	47782	168817	49411	50690	31881	21681
AcylCarnitine 18:1	139225	407049	940687	167022	465244	180160	60133
AcylCarnitine 18:2	44167	167392	483858	60381	159774	67816	16425
CE 16:0	548	361	670	351	452	346	344
CE 16:1	1213	1037	1055	910	657	934	1047
CE 16:2	87	78	78	41	83	79	47
CE 18:0	575	247	775	605	393	665	365
CE 18:1	10176	3013	6457	5041	5785	5458	4669
CE 18:2	55933	3704	12346	11645	9668	6753	19580
CE 18:3	2460	664	1161	1145	1407	1673	1636
CE 20:0	1339	1203	1220	535	1080	1001	1250
CE 20:1	1337	878	2679	1345	1278	1666	1438
CE 20:2	2199	520	4664	1390	487	2115	1397
CE 20:3	3912	408	3626	1537	688	1352	2118
CE 20:4	74887	2965	15296	12811	4601	5030	24408
CE 20:5	5703	77	1488	1278	1017	694	2855
CE 22:0	570	473	575	642	637	609	579
CE 22:1	1282	880	1910	1271	1314	1539	1273
CE 22:4	5134	116	9347	3661	206	6469	6715
CE 22:5(a\b)	7468	518	13711	4127	1106	6321	10709
CE 22:6	53572	4297	31681	17162	8292	12073	26291
CE 24:0	1118	942	847	1022	1085	1068	1198
CE 24:1	3226	1945	5279	3120	2215	3748	2943
CE 24:4	8641	546	31981	8107	1115	13408	11303
CE 24:5	634	76	2376	798	23	1113	1883
CE 24:6	563	47	1056	537	206	487	701
Cer(d16:1/24:1)	637	2645	619	1067	2544	1058	492

Cer(d17:1/16:0)	10101	26732	7472	33780	12437	14416	5622
Cer(d17:1/18:0)	512	357	421	413	505	280	426
Cer(d17:1/20:0)	50	311		130	219	17	
Cer(d18:1/14:0)	339	60	79	1097	84	1554	90
Cer(d18:1/16:0)	3779	378	683	6673	412	2641	772
Cer(d18:1/18:0)	475	60	408	113	3640	401	3938
Cer(d18:1/20:0)	4087	13777	5670	11558	10211	6705	3268
Cer(d18:1/22:0)	43248	140786	28937	93862	111914	56438	15166
Cer(d18:1/24:0)	121148	211426	84537	293776	145203	149756	49158
Cer(d18:1/24:1)	192571	176163	113311	372274	127471	261239	59344
Cer(d18:1/26:0)	1072	1286	1126	1665	1143	1897	1224
Cer(d18:2/16:0)	12514	21405	5271	49533	3995	23756	9666
Cer(d18:2/18:0)	2197	10852	4166	7828	6957	3431	1302
Cer(d18:2/20:0)	97	841	371	602	542	343	138
Cer(d18:2/22:0)	1394	12577	2448	4923	9311	2395	1248
Cer(d18:2/26:0)	1982	1953	1817	1833	1741	1181	1804
Cer(d19:1/20:0)	174	920	258	913	832	117	731
Cer(d19:1/24:0)	388	480	496	1012	469	698	589
Cer(d19:1/26:0)	454	401	486	447	348	466	446
Cer(d20:1/22:0)	3655	4024	4991	9114	3091	5751	2319
Cer(d20:1/24:0)	981	872	4285	5866	762	4477	1159
Cer(d20:1/24:1)	1545	1702	6289	9012	1102	5564	1878
Cer(d20:1/26:0)	2093	1825	2365	2875	1561	2672	2101
DG 30:0 -(14:0)	47278	47950	42528	48911	49431	58204	58453
DG 32:0 -(16:0)	1289311	1308291	1274177	1185994	1234263	1201174	1240851
DG 34:1 -(18:1)	25477	21896	19725	99749	141311	30169	24677
DG 34:2 -(18:2)	5724	3175	4489	27397	71581	10489	3675
DG 36:1 -(18:1)	12986	11154	9089	18311	35012	12744	12530
DG 36:2 -(18:2)	7464	2259	3898	15317	34038	4175	3564
DG 36:3 -(18:2)	9471	5227	6334	24107	178039	10844	6877
DG 36:4 -(18:2)	6133	2026	3779	29868	265994	8648	3502
DG 36:4 -(18:3)	1932	1113	1398	6664	44186	2311	1374
DG 36:4 -(20:4)	2907	152	341	4728	446	927	2210
DG 38:4 -(20:4)	18950	222	5611	34457	2563	11903	15666
DG 38:5 -(20:4)	1865	240	211	2953	7102	1096	1462
DG 38:5 -(22:5)	13296	13156	11125	16389	17211	14890	14888
DG 38:6 -(20:4)	2116	311	934	5011	22775	1512	1190
DG 38:6 -(22:6)	2161	257	452	5167	2491	1119	980
DG-D5 (IS)	53147	51484	57947	47603	63977	55381	64673
dhCer 24:0	1238	2391	2204	2699	1876	1842	758
dhCer 24:1	3923	3145	1574	3949	2617	4102	272
GM1(d18:1/16:0)	1398	2030	1504	1390	1705	1375	1143
GM3(d18:1/16:0)	2051	785	1275	4360	1101	2269	579
Hex1Cer(d16:1/20:0)	820	770	4	814	846	835	807
Hex1Cer(d18:1/18:0)	1889	903	889	4715	1333	2072	914

Hex1Cer(d18:1/20:0)	1040	1155	1535	2225	3591	1635	484
Hex1Cer(d18:1/22:0)	1972	2419	2518	5660	7254	2543	897
Hex1Cer(d18:1/24:0)	7744	4574	7234	14167	7034	9137	2162
Hex1Cer(d18:1/24:1)	14437	2839	15079	25412	7466	18306	4231
Hex2Cer(d18:1/24:0)	1207	1128	1041	2356	1171	961	303
Hex2Cer(d18:1/24:1)	5	16	92	270	46	71	9
LPC 14:0	9190	37377	85372	22927	30164	15325	7517
LPC 15:0	7928	57125	93786	20782	53421	14182	8906
LPC 16:0	1778624	8409841	13749331	3185551	6704142	2027146	1576369
LPC 16:1	64884	935546	1512263	290629	1170442	202079	51564
LPC 18:0	610149	1338742	1942185	884405	1558368	489826	535580
LPC 18:1	294206	2025984	3334154	636366	13688617	509373	226877
LPC 18:2	466916	6645410	15813979	1033029	5245981 4	517103	315839
LPC 18:3	8690	584713	461445	112356	1142494	53497	13248
LPC 18:3(104)	43186	351924	504808	120975	276111	56818	36096
LPC 20:0	5943	56506	24512	9485	55325	5958	5810
LPC 20:1	7997	40310	38895	18065	37470	16650	7551
LPC 20:2	13447	56627	100750	43771	94049	36196	12420
LPC 20:3	62417	858263	759673	263499	1802431	192738	46543
LPC 20:4	332937	7042006	3479303	1404215	16754958	704719	155075
LPC 20:5	14953	346537	298453	95237	962339	47426	11937
LPC 22:0	2315	5941	7197	2548	4858	1560	2088
LPC 22:1	1130	4986	3858	2400	3778	1298	1323
LPC 22:4	6737	33020	28386	33828	22917	18396	4755
LPC 22:5(104)	8545	53874	50066	22900	103931	13012	5408
LPC 22:5(a\b\c)	30219	318192	325832	113764	711291	75019	16437
LPC 22:6	169202	3032051	2178815	637101	7989076	319325	67114
LPC 24:0	2831	6443	8728	5275	4232	2762	3307
LPC(O-16:0)	26189	34021	809382	55010	29133	33389	24085
LPC(O-18:0)	17101	14303	234061	23230	21369	15171	12535
LPC(O-18:1)	23610	22381	205105	76188	21367	38397	15546
LPC(O-20:0)	33211	71590	71724	36759	86300	30820	33767
LPC(O-20:1)	1126	3857	7059	2610	3640	2713	1306
LPC(O-22:0)	457	1940	1645	495	1975	398	482
LPC(O-24:0)	445	916	1482	662	787	369	516
LPC(O-24:1)	256	424	497	298	238	266	271
LPC(O-24:2)	280	179	1077	376	158	247	213

LPC(P-16:0)	300	1157	8685	1493	1136	736	542
LPC(P-18:0)	21748	19886	193805	64098	17868	32958	13781
LPE 16:0	35035	351083	190552	98207	263766	53769	24175
LPE 18:0	21886	228625	95445	79270	147635	36675	21347
LPE 18:1	15014	192595	109947	44189	143913	36294	12767
LPE 18:2	11982	146796	153719	50575	491218	30922	7049
LPE 20:4	14339	424984	89658	80335	373362	44746	9615
LPE 22:6	14931	431029	136926	65013	511662	36991	7331
LPE(P-16:0)	2157	8515	27297	5067	1651	1842	1136
LPE(P-18:0)	2291	7563	31413	4362	2369	2391	1371
LPE(P-18:1)	489	2768	8464	1535	507	652	354
LPE(P-20:0)	304	539	1478	428	201	331	235
LPI 18:0	2107	1946	2106	3387	5813	1785	1084
LPI 18:1	546	1308	1999	1173	1492	864	646
LPI 18:2	1017	2718	4772	1636	4386	997	1197
LPI 20:4	9455	22975	31932	19544	43005	13595	9369
oxCE 18:2 +2O NH4	1894	1505	1365	1624	1535	1964	1871
PC 30:0	170615	223963	790003	252621	400923	115107	122466
PC 31:1	23485	25817	31743	50726	28790	38994	16950
PC 32:0	4662831	6163572	12142686	8071482	8312004	3983012	3308744
PC 32:1	12434969	14286715	37581651	12975676	18378400	8612846	22620305
PC 32:2	657646	997304	3095184	420819	2532268	251283	627879
PC 34:0	8519675	9324118	13000721	6413458	1300651	3729961	9107571
PC 34:1	13082489	12552344	15084349	7914476	15729860	6273354	13040892
PC 34:2	##########	##########	##########	85479507	##########	62916921	##########
PC 34:3(a\b\c)	10265810	24087037	43205207	5549534	65526050	2485684	9650970
PC 34:4	301349	503694	814152	160243	1193489	59352	204710
PC 34:5	6871	12005	10795	5158	35904	2889	8448
PC 35:4	254134	515318	768784	177981	1586591	78977	242379
PC 35:5	18839	25631	64957	12028	92755	7195	35826
PC 36:0	214998	297955	554195	225805	709780	116403	225858
PC 36:1	2388584	3171403	5326369	2513142	7854710	1185204	2238360
PC 36:2(a\b)	29237723	43485926	64805603	23970997	87390360	8699936	20259805
PC 36:3(a\b\c)	33853844	39108866	76397358	23473193	83164689	16039331	30564673
PC 36:4(a\b)	30957943	27860501	31619537	31154583	35703220	16115784	23788301
PC 36:5(a\b)	1800004	4257404	8419459	1769719	14615807	743556	3034840

PC 36:6	28992	40122	54617	20946	120765	11390	23306
PC 37:6	82409	77536	224606	45861	489562	21808	45171
PC 38:2	305615	560010	571395	474325	417473	307874	174080
PC 38:3	459396	923874	672856	694970	157294 6	204941	251422
PC 38:4(a\b\c)	493308 1	807505 0	853781 8	610672 5	129317 18	202377 5	242685 6
PC 38:5(a\b)	810943 1	991598 9	928025 4	864036 7	121668 95	584204 6	664367 4
PC 38:6(a\b)	189693 56	221057 81	196426 82	139297 38	486637 84	805455 0	150611 01
PC 38:7(a\b\c)	173831	275357	642721	202207	170583 1	105574	206415
PC 39:5	20402	47342	32045	22143	61440	9001	11773
PC 40:4(a\b)	40155	69245	92173	94496	116392	57828	27027
PC 40:5(a\b)	513331	997510	565754	971877	136698 6	450161	316630
PC 40:6	312349	294968	324845	390297	178842	308245	217468
PC 40:7(a\b\c)	821877	970380	860611	112208 0	115438 5	839684	738034
PC 40:8	220205	696988	445703	355558	195742 6	142421	159260
PC(19:0/19:0)(IS)	47281	99843	88070	53505	121133	42132	55998
PC(O-32:0)	59472	74247	112120	133188	172109	109198	29856
PC(O-32:1)	23606	29975	14829	42875	19523	38994	10499
PC(O-32:2)	4971	7739	9173	9350	4175	6077	2637
PC(O-34:1)	327185 7	486546 4	890280 1	237527 4	690679 4	135650 3	409250 8
PC(O-34:2)	133665 9	267859 9	460202 0	669459	639784 7	316603	106968 5
PC(O-35:4)	301349	503694	814152	160243	119348 9	90311	278261
PC(O-36:1)	474619	766516	160660 0	372699	241624 7	179184	512259
PC(O-36:2)(a\b)	173072 2	337313 5	730347 0	105537 9	126381 96	625258	207936 7
PC(O-36:3)(a\b)	157557 4	299056 8	326649 6	857862	501828 7	547315	172854 0
PC(O-36:4)	386547	856190	151571 3	260850	279856 7	119876	365772
PC(O-36:5)	26083	38436	64957	12028	92755	12764	35826
PC(O-38:5)	184656	175307	150052	650873	120961	329780	98104
PC(O-38:6)	82409	77536	224606	45861	489562	21808	45171
PC(O-40:5)	20402	40111	2475	22143	61440	305	2352
PC(O-40:6)	26393	28969	36119	25920	21867	33859	12481
PC(O-40:7)(a\b)	13364	13874	31759	20233	36804	105740	61811
PC(P-30:0)	10458	9915	19436	15657	34095	8298	5952
PC(P-32:0)	20733	25817	14829	42875	19523	38994	10499
PC(P-32:1)	3973	4114	9173	9350	4175	6077	2637
PC(P-34:0)	327185 7	486546 4	890280 1	237527 4	690679 4	135650 3	409250 8

PC(P-34:1)	1336659	2678599	4602020	669459	6397847	295068	1048402
PC(P-34:2)	3394	1748	3736	2786	681	4807	1356
PC(P-34:3)	661	2544	2845	343	947	2696	281
PC(P-36:2)(a\b)	1575574	2990568	3266496	857862	5018287	547315	1728540
PC(P-36:3)	253177	488540	907902	176675	1542090	69798	181770
PC(P-36:4)	26083	38436	64957	12028	92755	12764	35826
PC(P-36:5)	33	789	4922	172	702	172	85
PC(P-38:4)	184656	186398	96582	650873	120961	329780	98104
PC(P-38:5)(a\b)	82409	126770	224606	45861	489562	21808	45171
PC(P-38:6)	214998	297955	554195	225805	709780	116403	225858
PC(P-40:4)	20402	40111	2475	22143	61440	305	2352
PC(P-40:5)(a\b)	32324	33712	36119	25920	21867	17242	12481
PC(P-40:6)	55655	57511	31759	20233	36804	105740	61811
PC(P-40:7)	32024	12165	5599	30386	8171	84145	33477
PE 32:0	11427	9443	13507	20822	8456	13356	10224
PE 32:1	40234	32099	109039	90987	26161	61649	88072
PE 34:1	590764	641004	2404806	729326	825799	408821	797076
PE 34:2	979055	1513872	2231050	117688	1870025	608199	1040459
PE 34:3(a\b\c)	80964	149577	232026	118792	219228	58144	99216
PE 36:0	5361	3358	1185	1651	806	1664	3852
PE 36:1	38236	75556	102879	80010	101415	62366	38110
PE 36:2(a\b)	410420	976574	917079	645157	2031952	331571	256995
PE 36:3(a\b)	288183	839195	799515	479062	1733022	256792	213087
PE 36:4	34046	102169	50476	57281	109237	37961	33411
PE 36:5(a\b)	35159	143410	113084	89380	293677	40626	38532
PE 38:3(a\b)	135961	494868	211867	369653	960647	124455	67116
PE 38:4	1246950	4394924	1661390	3204008	7773937	1060956	534550
PE 38:5(a\b)	657727	1828917	1090722	1384788	2659898	764924	457839
PE 38:6	915637	1251765	450880	1816066	985780	1144006	434844
PE 40:4	26467	36765	56731	82214	34171	33446	11423
PE 40:5(a\b)	32999	84580	58347	84431	184590	13358	19564
PE 40:6	13883	35606	32271	31062	76932	15892	16694
PE 40:7	211897	457096	203776	453473	521018	282115	103838
PE(O-34:2)	2263	7617	6178	6032	7995	4071	1804
PE(O-36:3)(a\b)	604	2718	1612	1935	1151	1244	508
PE(O-36:4)	9755	58571	53089	47269	40966	42220	19358
PE(O-36:5)	166	444	912	41	1265	762	159
PE(O-38:4)(a\b)	6868	34672	40041	25879	39853	21016	11166
PE(O-38:5)(a\b)	29024	48073	45124	48018	43145	36252	27634
PE(O-38:6)	1021866	1093302	872589	106291	1010835	114560	974406

PE(O-40:5)	11040	17581	16389	16033	21639	11212	8417
PE(O-40:6)	10217	20241	24173	19713	24160	12158	7794
PE(P-16:0/18:1)	8687	41307	25526	25738	44731	15114	8719
PE(P-16:0/18:2)	5853	12014	6551	17801	9687	11674	3000
PE(P-16:0/20:4)	101385	272727	121803	332422	99774	165366	65276
PE(P-16:0/20:5)	642	1995	201	2902	530	1639	319
PE(P-16:0/22:4)	16993	56384	49697	50278	50489	31097	10222
PE(P-16:0/22:5)(a\b)	18819	63353	47383	93209	50432	46705	17386
PE(P-16:0/22:6)	70729	161856	283200	211291	172996	80436	47815
PE(P-18:0/18:1)	2385	5638	5147	3845	6238	2788	935
PE(P-18:0/18:2)	2638	6167	4406	7055	8355	5192	1498
PE(P-18:0/20:3)	2181	8212	6999	8489	6880	5197	1606
PE(P-18:0/20:4)	34428	120390	95737	112752	94704	59438	25481
PE(P-18:0/22:4)	848	3609	2968	3803	1865	2286	499
PE(P-18:0/22:5)(a\b)	3264	14625	10469	12481	12147	6438	2844
PE(P-18:0/22:6)	20593	57660	75577	57469	63256	29393	14638
PE(P-18:1/18:1)	2601	10503	7557	5953	12455	4109	2142
PE(P-18:1/18:2)	1819	5070	3248	5097	4789	3025	1009
PE(P-18:1/18:3)	1285	1245	1392	228	1399	1322	1049
PE(P-18:1/20:4)	35076	102603	62100	132593	67293	56455	29046
PE(P-18:1/22:4)	7425	24253	23406	25970	20696	12134	3887
PE(P-18:1/22:5)(a\b)	4078	14296	13115	15478	8607	4918	2395
PE(P-18:1/22:6)(a\b)	19362	38264	43494	54988	22801	23667	10173
PE(P-20:0/18:2)	1001	237	1132	246	1201	1203	993
PE(P-20:0/20:4)	999	2719	1590	2971	2307	1146	316
PE(P-20:0/22:6)	208	885	449	500	766	125	55
PG 17:0 17:0 (IS)	4593348	2857294	2265388	4064278	3094570	5076893	4460304
PG 34:1	25373	107241	39566	86430	86984	42310	16017
PG 34:2	4805	20020	6151	19596	35633	9310	4546
PG 36:1	2679	4545	1023	6377	2434	2928	931
PG 36:2	10521	17815	6498	25584	11996	6403	2146
PI 32:0	547	1456	2211	1171	2195	1146	459
PI 32:1	1315	4383	1532	7001	3260	4442	1032
PI 34:0	1333	1712	838	3208	659	3979	1132
PI 34:1	14513	29890	15739	42739	24971	26837	8418
PI 36:1	1858	2613	1404	9218	1518	11091	1649
PI 36:2	46584	100111	51100	112138	81303	59021	18133
PI 36:3(a\b\c)	53947	125098	56196	162452	258627	99191	23036
PI 36:4	160874	321784	151496	451283	595823	261247	72265
PI 38:2	21203	37564	3313	33737	25815	35605	9277
PI 38:3(a\b)	235656	541898	129627	495164	471054	365096	105876
PI 38:4	1014643	3050072	1239363	2203295	3042932	1019655	4206204
PI 38:5(a\b)	68781	169157	99243	201620	357822	147317	38521

PI 38:6	12800	17337	8410	39136	41125	15473	4787
PI 40:5(a\b)	26441	29551	12257	58151	21634	54955	9933
PI 40:6	24633	44848	20855	41812	90367	13391	7064
PS 36:1	81065	236691	223311	232453	209938	137303	80174
PS 36:2	38675	47650	16567	145161	12310	52306	22739
PS 38:3	8392	14446	11248	23956	55316	23576	8726
PS 38:4	429593	868695	320836	1120188	887344	583561	224899
PS 40:5	42381	51444	35483	114714	52959	83296	21700
PS 40:6	169854	405898	223281	478239	645904	191175	58551
SM 30:1	358	622	1943	227	1238	193	290
SM 31:1	266	552	931	236	963	133	248
SM 32:0	973	1920	2527	1290	2914	733	687
SM 32:1	10591	20911	25134	13285	32356	7306	7736
SM 32:2	227	779	1037	215	1301	167	250
SM 33:1	31326	54031	62776	46926	109031	25485	20408
SM 34:0	222572	211629	251350	649196	133721	490088	133438
SM 34:1	3692351	5049979	9818031	9209649	5828890	3493022	1630799
SM 34:2	31746	95420	76445	54338	86448	22232	20146
SM 36:1	211225	771614	495023	431385	755359	244332	156413
SM 36:2	24651	113825	38158	60707	67349	31515	21174
SM 36:3	31	151	475	304	230	95	58
SM 37:1	609742	1190388	1890419	256871	3224490	163101	540997
SM 37:2	4273	2555	14328	3285	3665	3043	11295
SM 38:1	66872437	58779501	80921021	41999056	66784921	32857501	59786578
SM 38:2	5830030	9483907	23610057	2456791	31914242	1216463	4628532
SM 38:3 (a\b)	173713	272820	401350	92951	737605	48306	140837
SM 39:1	1535399	2470944	4487438	762168	8132492	392884	1191201
SM 40:0	1236371	1527680	2782493	1183504	4020713	724416	1256994
SM 40:1	16975168	25731182	41085838	11758165	53750731	4524745	13820401
SM 40:2 (a\b)	17510100	24689557	52474426	14023953	56361465	9994782	20405900
SM 40:3 (a\b\c)	13609629	17723774	13112407	14248140	20729973	8433945	9856599
SM 41:0	2903	7476	15021	5104	22807	2030	5367
SM 41:1	63620	174156	189683	71784	532155	55845	59570
SM 41:2(a\b)	102011	61758	195150	85008	247166	75882	103925
SM 42:1	115082	151296	223423	145022	266834	120742	55974
SM 42:2 (a\b)	497676	703517	1413563	677030	2904612	392017	393474
SM 44:2	1904	8849	2320	4474	7295	1223	611
SM 44:3 (a\b)	17025	34113	41259	33034	53776	23290	11789
TG 14:0 16:0 18:2	38358	40442	39970	50664	112647	54069	62160

TG 14:0 16:1 18:1	45650	20959	44335	45988	63692	40600	48787
TG 14:0 16:1 18:2	37113	30998	30576	37648	69571	36927	39129
TG 14:0 18:0 18:1	7114	6070	5423	5938	12206	7220	7205
TG 14:0 18:2 18:2	7928	2485	4916	10154	59394	5730	5964
TG 14:1 16:0 18:1	11087	12045	11183	10826	14295	12644	13651
TG 14:1 16:1 18:0	133085	151092	146946	146524	151685	186575	230888
TG 14:1 18:0 18:2	2270	2115	1434	2092	1926	2231	1095
TG 14:1 18:1 18:1	31826	19475	26940	34412	76392	31008	44462
TG 15:0 18:1 16:0	28244	28409	25561	25950	27216	31310	34271
TG 15:0 18:1 18:1	8156	5309	7277	7640	15833	8850	8543
TG 16:0 16:0 16:0	360924	326328	284222	350613	475779	345983	398283
TG 16:0 16:0 18:0	115286	99675	85903	98375	142513	120827	115989
TG 16:0 16:0 18:1	185564	110641	157385	223412	638697	155176	198247
TG 16:0 16:0 18:2	89392	31242	75082	124081	517107	84385	92771
TG 16:0 16:1 18:1	242499	136617	187900	251408	585935	266637	345843
TG 16:0 18:0 18:1	47918	26945	47198	66304	230104	45947	55603
TG 16:0 18:1 18:1	372186	68865	213211	379285	1007107	240917	323584
TG 16:0 18:1 18:2	467250	40148	228381	386111	1357607	235785	258309
TG 16:0 18:2 18:2	72977	7575	35601	67988	219787	43407	39982
TG 16:1 16:1 16:1	164081	150083	155889	155444	172094	158819	192867
TG 16:1 16:1 18:0	10516	8690	9666	10495	25097	10620	12709
TG 16:1 16:1 18:1	74636	45295	64150	81820	120274	78110	105569
TG 16:1 18:1 18:1	87215	31318	65463	107889	259651	78273	108801
TG 16:1 18:1 18:2	39098	8859	23098	46008	173805	27018	37072
TG 17:0 16:0 16:1	133613	141329	111312	114916	102848	132337	146586
TG 17:0 16:0 18:0	11338	13681	15165	16349	19597	10915	12149
TG 17:0 17:0 17:0 (IS)	5903	5077	2676	3898	1319	3423	4502

TG 17:0 18:1 14:0	53725	49535	43926	41614	36774	65106	60145
TG 17:0 18:1 16:0	21204	15089	15868	16827	27524	20950	16490
TG 17:0 18:1 16:1	40106	32134	28743	41020	60493	43975	44232
TG 17:0 18:1 18:1	5962	3497	5362	7526	23323	5947	6030
TG 17:0 18:2 16:0	29818	17791	21013	29296	69151	29241	32572
TG 18:0 18:0 18:0	105205	82021	62531	99695	93246	116500	103772
TG 18:0 18:0 18:1	20869	13903	16437	24206	70613	20337	20568
TG 18:0 18:1 18:1	13789	14923	5579	50977	202314	18633	26770
TG 18:0 18:2 18:2	11351	1706	8783	17820	52288	11904	7200
TG 18:1 14:0 16:0	128896	126692	123427	136509	238021	147967	157287
TG 18:1 18:1 18:1	438757	249868	502200	502276	1789775	383948	441561
TG 18:1 18:1 18:2	48336	10953	34158	63043	185956	35434	28596
TG 18:1 18:1 20:4	38311	114	13506	25589	29587	17056	10883
TG 18:1 18:1 22:6	9994	39	4728	6532	15792	4383	2615
TG 18:1 18:2 18:2	104855	33300	67315	126574	382138	77022	68463
TG 18:2 18:2 18:2	79606	23475	66460	120658	295678	80042	43952
TG 18:2 18:2 20:4	19961	28	7320	12307	16021	7972	5114
TG(O-50:1)	129258	121469	111312	114916	102848	132337	146586
TG(O-52:0)	8840	11275	12745	14039	16268	9005	8927
TG(O-52:2)	29818	17791	21013	29296	69151	29241	32572
Ubiquinone	722	920	870	1030	672	1324	631

Appendix Table iii. Signal intensities for lipid species detected in uninfected mice

Name	Naive-1	Naive-2	Naive-3	Naive-4	Naive-5	Naive-6
AcylCarnitine 12:0	280576	322031	281591	287291	196183	334449
AcylCarnitine 13:0	33168	39934	37354	45480	32570	85646
AcylCarnitine 14:0	543808	575756	459503	454838	613963	913195
AcylCarnitine 14:1	989046	1074856	933850	1048843	933941	1877194
AcylCarnitine 14:2	354326	403797	305097	410169	232055	631016
AcylCarnitine 15:0	29588	31784	26182	47634	39663	99864
AcylCarnitine 16:0	1899692	1548682	1128951	1089223	1332728	1368887
AcylCarnitine 16:1	974155	1034044	834185	855775	1139650	1864040
AcylCarnitine 17:0	34941.31	28200.21	20018.95	29061.56	284645.1	223057.9
AcylCarnitine 18:0	193153	195016	72843	129088	332986	204811
AcylCarnitine 18:1	1638467	1658989	1200036	1865378	2365567	4108625
AcylCarnitine 18:2	253910	296058	159582	871217	517631	1314380
CE 16:0	134	539	385	32	1489	1721
CE 16:1	700	934	578	517	1986	1637
CE 16:2	109	82	49	37	76	182
CE 18:0	279	359	338	291	644	900
CE 18:1	2410	5046	2439	1114	17982	21524
CE 18:2	3510	6599	4196	1672	17830	17327
CE 18:3	769	1472	907	96	2779	3740
CE 20:0	1536	1496	693	1118	1847	1362
CE 20:1	733	1176	896	617	1653	1688
CE 20:2	231	276	326	383	1303	1461
CE 20:3	213	317	136	160	1528	1030
CE 20:4	1624	2444	2442	440	17128	12468
CE 20:5	285	455	418	35	1793	1397
CE 22:0	632	705	465	487	1163	1079
CE 22:1	1085	1169	785	730	2273	1808
CE 22:4	47	49	137	125	183	401
CE 22:5(a\b)	486	263	698	62	852	921
CE 22:6	2778	3475	3770	741	10713	15600
CE 24:0	921	1212	764	819	2028	1501
CE 24:1	2077	2319	1501	1598	3653	3322
CE 24:4	1091	555	1032	1196	1449	1313
CE 24:5	12	51	47	11	224	192
CE 24:6	82	113	172	25	118	83
Cer(d16:1/24:1)	1134	1141	1429	1283	8260	4351
Cer(d17:1/16:0)	8131	7141	6846	5947	8771	3260
Cer(d17:1/18:0)	104	483	391	522	439	515
Cer(d17:1/20:0)	77	258	224	155	2455	1064
Cer(d18:1/14:0)	73	17	28	30	103	10
Cer(d18:1/16:0)	96	99	30	17	15	14
Cer(d18:1/18:0)	197	263	332	3585	684	744
Cer(d18:1/20:0)	8572	6020	5134	6468	63252	27973
Cer(d18:1/22:0)	66312	76230	81228	45621	224945	190153
Cer(d18:1/24:0)	88998	114084	123779	68957	99871	76274
Cer(d18:1/24:1)	83390	75956	84942	61927	293375	179273

Cer(d18:1/26:0)	1172	612	483	1194	9314	5784
Cer(d18:2/16:0)	4398	1879	2670	2009	6147	1598
Cer(d18:2/18:0)	5959	5751	2794	4353	22525	2816
Cer(d18:2/20:0)	426	365	188	505	8336	2546
Cer(d18:2/22:0)	6538	6485	7803	4538	43903	27922
Cer(d18:2/26:0)	1827	1873	1713	1852	257	133
Cer(d19:1/20:0)	88	852	25	548	308	850
Cer(d19:1/24:0)	387	341	302	365	839	667
Cer(d19:1/26:0)	440	576	636	448	963	1199
Cer(d20:1/22:0)	2415	3657	3231	3787	963	552
Cer(d20:1/24:0)	1132	758	633	1421	11677	3172
Cer(d20:1/24:1)	1288	1213	866	1613	4129	1048
Cer(d20:1/26:0)	2145	2160	1733	2162	2967	3502
DG 30:0 -(14:0)	46352	43501	45959	49212	21685	20518
DG 32:0 -(16:0)	1316153	1186371	1252406	1348625	1111569	1096046
DG 34:1 -(18:1)	10423	19353	17001	17698	68067	53117
DG 34:2 -(18:2)	1616	4783	1622	4464	23314	30458
DG 36:1 -(18:1)	10084	9669	10534	12912	86002	71895
DG 36:2 -(18:2)	1895	2160	2610	2620	11187	12478
DG 36:3 -(18:2)	4334	8209	5558	1955	42950	34853
DG 36:4 -(18:2)	1892	6463	2544	3494	10757	12816
DG 36:4 -(18:3)	1179	1582	628	930	3848	2856
DG 36:4 -(20:4)	700	314	109	1042	1160	1037
DG 38:4 -(20:4)	287	192	487	974	3056	2109
DG 38:5 -(20:4)	17	190	274	501	2721	1207
DG 38:5 -(22:5)	15498	13829	13600	13996	5036	4481
DG 38:6 -(20:4)	64	487	252	208	921	555
DG 38:6 -(22:6)	1553	2333	274	167	1533	777
DG-D5 (IS)	59773	54045	40284	47097	205691	193860
dhCer 24:0	1528	1653	1404	991	3137	1527
dhCer 24:1	1716	2191	2039	2185	3414	2164
GM1(d18:1/16:0)	1256	1875	1787	1228	14	11
GM3(d18:1/16:0)	1460	782	417	305	2331	186
Hex1Cer(d16:1/20:0)	825	829	849	794	847	685
Hex1Cer(d18:1/18:0)	1254	530	531	331	1214	1030
Hex1Cer(d18:1/20:0)	2889	1963	2299	932	5560	2799
Hex1Cer(d18:1/22:0)	3076	3594	3746	2120	27992	16986
Hex1Cer(d18:1/24:0)	4223	3602	5562	2335	11785	11013
Hex1Cer(d18:1/24:1)	3925	3856	3888	3175	27869	11732
Hex2Cer(d18:1/24:0)	890	587	524	186	2615	1110
Hex2Cer(d18:1/24:1)	143	82	74	99	364	3
LPC 14:0	163790	171873	160867	34335	52916	38549

LPC 15:0	188407	219455	211471	78729	57438	84690
LPC 16:0	31463129	32746821	34000553	10295087	13509624	13591334
LPC 16:1	6973691	7032941	6277661	645650	1212921	1058965
LPC 18:0	3242677	3189553	3134956	1837760	5423812	2967122
LPC 18:1	72995771	59060735	73918125	5319572	9516869	9653295
LPC 18:2	########	########	########	19586820	24046257	36932718
LPC 18:3	7542613	7693695	8166525	492397	504903	906067
LPC 18:3(104)	433783	559102	346653	333191	574595	564634
LPC 20:0	71113	113106	67589	60143	155865	139533
LPC 20:1	122168	96902	110421	26010	79245	49560
LPC 20:2	580439	292387	581230	26521	57856	38808
LPC 20:3	11099675	7749268	11479882	442064	874686	886991
LPC 20:4	58410403	49346088	53382102	4537843	7910177	7484816
LPC 20:5	3434069	2582513	4097535	207762	389308	432041
LPC 22:0	6966	8047	6250	6245	21029	16319
LPC 22:1	5473	8949	3738	3965	12361	7311
LPC 22:4	98350	67902	117699	6879	17323	9264
LPC 22:5(104)	427413	433681	604924	123779	77250	84674
LPC 22:5(a\b\c)	605571	1711592	1558807	103046	267021	157019
LPC 22:6	33625450	26491615	30458001	1925923	3310288	3910978
LPC 24:0	6275	6568	4116	4302	12572	5026
LPC(O-16:0)	41489	49792	42812	34972	89445	48746
LPC(O-18:0)	25341	30848	28323	21552	45379	33390
LPC(O-18:1)	13671	12284	13956	10774	21866	11762
LPC(O-20:0)	103530	118374	104196	232717	154801	116899
LPC(O-20:1)	12619	11243	17504	4998	5296	4231
LPC(O-22:0)	2226	2656	1991	2287	4903	4943
LPC(O-24:0)	1033	988	845	701	2489	1259
LPC(O-24:1)	566	362	357	368	919	543
LPC(O-24:2)	146	172	193	190	513	390
LPC(P-16:0)	3809	4105	3082	1249	6186	4234
LPC(P-18:0)	11702	12606	12231	10429	19177	10177
LPE 16:0	621939	809657	869902	207338	224075	274084
LPE 18:0	317673	346438	398423	114613	173049	168746
LPE 18:1	416354	412378	461620	117667	134220	124707
LPE 18:2	1420338	1504426	1516697	169885	198897	323937
LPE 20:4	889544	892048	746477	95145	212573	164840
LPE 22:6	1106234	1123459	862003	114375	252428	250287
LPE(P-16:0)	5652	5685	3041	2082	3603	1275
LPE(P-18:0)	5583	4684	3060	2813	2832	1275
LPE(P-18:1)	1360	1355	879	695	1173	330
LPE(P-20:0)	404	363	426	216	550	414
LPI 18:0	1015	1489	1149	1203	2589	2486

LPI 18:1	464	643	397	839	2545	1986
LPI 18:2	5189	6540	3710	3036	9460	11824
LPI 20:4	42416	56571	36503	24069	113996	86599
oxCE 18:2 +2O NH4	1510	1900	1356	1327	1999	3009
PC 30:0	403232	577843	476709	403969	1218644	458596
PC 31:1	33970	18356	11140	8769	9207	2778
PC 32:0	8666401	7821640	9001057	5497771	16970395	6896440
PC 32:1	15317359	23513374	14185421	14456726	36613842	22283707
PC 32:2	2061960	4271660	1832469	3401324	15858941	10435703
PC 34:0	12626697	15139142	13011452	13987614	16753134	17764941
PC 34:1	14959804	17693595	13996224	16375193	15845142	15502871
PC 34:2	########	########	########	########	########	########
PC 34:3(a\b\c)	59560386	########	58320047	90845441	########	########
PC 34:4	1087604	1939726	885889	1962608	4725706	6244920
PC 34:5	16079	33640	21298	36332	79652	74643
PC 35:4	2019650	1706998	2106111	2364060	2802718	2278344
PC 35:5	55785	82258	82004	115498	234787	445894
PC 36:0	657107	735121	582349	731116	2564764	2109269
PC 36:1	62030983	79858934	56637835	73864484	27045683	25044874
PC 36:2(a\b)	72917202	86743195	87172695	90332257	########	########
PC 36:3(a\b\c)	75198635	81238517	75021722	86133684	########	########
PC 36:4(a\b)	26226109	36070646	33596519	30849459	40740428	25981045
PC 36:5(a\b)	84577464	44690003	10539163	12230971	18213968	14133422
PC 36:6	90643	126477	77173	149815	517651	412896
PC 37:6	347978	433188	370342	552629	432609	724070
PC 38:2	669304	651785	582201	442838	2315424	1411131
PC 38:3	1736516	1688551	1665365	1514250	1701025	1306363
PC 38:4(a\b\c)	13233397	13655164	13399641	12606839	16072746	10878510
PC 38:5(a\b)	11597397	12825660	11764861	12702784	13798038	11552633
PC 38:6(a\b)	46650341	39144713	32370542	42049187	55152972	47436063
PC 38:7(a\b\c)	1229564	1536217	1084158	2296488	7134552	5990931
PC 39:5	46447	22933	65292	43501	17696	58968
PC 40:4(a\b)	119243	89145	55105	78041	339742	190596
PC 40:5(a\b)	1004496	822127	751571	682274	1108126	632593
PC 40:6	139381	192498	97457	374516	102193	23721
PC 40:7(a\b\c)	798962	600271	650213	597620	887216	607264

PC 40:8	1414390	1366024	1376061	1917798	1145976	2333659
PC(19:0/19:0)(IS)	133702	139450	134263	330669	212547	170486
PC(O-32:0)	149356	105774	115033	73512	279688	99343
PC(O-32:1)	24179	18356	11127	8769	9207	2778
PC(O-32:2)	7033	7348	6700	3425	6268	6624
PC(O-34:1)	5568129	8901023	6618535	6853028	8081706	10686659
PC(O-34:2)	6592506	9340445	7638845	8694719	9303061	15070444
PC(O-35:4)	1087604	1939726	885889	1962608	4725706	6321684
PC(O-36:1)	1510876	2106187	1949630	1664731	3663796	5131188
PC(O-36:2)(a\b)	9087238	11601596	12869445	13343161	14290534	24452637
PC(O-36:3)(a\b)	5108401	6253415	4769016	5983952	5564047	9801539
PC(O-36:4)	3019851	2521008	2221934	3471658	3753811	3456294
PC(O-36:5)	55785	82258	82004	115498	234787	445894
PC(O-38:5)	139256	72050	59869	64634	79416	18952
PC(O-38:6)	347978	433188	370342	552629	432609	724070
PC(O-40:5)	46447	22933	65292	43501	17696	58968
PC(O-40:6)	24258	20058	11587	14719	16710	6524
PC(O-40:7)(a\b)	37602	19160	43160	25359	24469	25347
PC(P-30:0)	30598	29781	28910	28774	103215	53999
PC(P-32:0)	24179	18356	3533	8769	9207	2778
PC(P-32:1)	2552	7348	2818	3425	6268	7555
PC(P-34:0)	5568129	8901023	6618535	6853028	8081706	10686659
PC(P-34:1)	6592506	9340445	7638845	8694719	9303061	15070444
PC(P-34:2)	1156	290	579	472	985	477
PC(P-34:3)	1099	1102	1446	871	1049	2315
PC(P-36:2)(a\b)	5108401	6253415	4769016	5983952	5564047	9801539
PC(P-36:3)	1737507	2242594	1788070	1374107	2619104	2526893
PC(P-36:4)	55785	82258	82004	115498	234787	445894
PC(P-36:5)	1696	3595	674	2384	4614	647
PC(P-38:4)	139256	66562	57998	64634	79416	12647
PC(P-38:5)(a\b)	347978	433188	370342	552629	432609	724070
PC(P-38:6)	657107	735121	582349	731116	2564764	2109269
PC(P-40:4)	46447	22933	65292	43501	17696	58968
PC(P-40:5)(a\b)	15503	20058	11587	14719	16710	6524
PC(P-40:6)	37602	19160	43160	25359	24469	25347
PC(P-40:7)	10313	10989	4467	2335	4357	9409
PE 32:0	6342	5328	5004	3642	10269	2300
PE 32:1	7130	12601	7191	5338	21614	12021
PE 34:1	486894	714637	508336	674164	1090700	1031325
PE 34:2	1245786	1801320	1749895	2038640	2202879	3426318
PE 34:3(a\b\c)	118245	200423	130116	209704	443413	445586
PE 36:0	780	773	2038	465	59	528
PE 36:1	138490	120312	61857	81580	342876	150508
PE 36:2(a\b)	1239384	1245936	1368635	1553567	3156867	3551615

PE 36:3(a\b)	1054919	1141128	1100086	1347423	1806203	2275143
PE 36:4	90049	82637	95433	130870	87354	180001
PE 36:5(a\b)	156859	193911	198908	189927	547388	354836
PE 38:3(a\b)	703434	629698	757450	433201	988191	697311
PE 38:4	6544564	5404757	6195227	3629007	7991939	5461055
PE 38:5(a\b)	2246372	2111808	2475133	1606016	2914854	1755168
PE 38:6	585816	465076	533886	411312	778758	565903
PE 40:4	66136	51619	26220	34479	106387	28316
PE 40:5(a\b)	128282	117134	121410	70444	175891	144015
PE 40:6	40904	39121	46494	29314	87239	41817
PE 40:7	395041	353425	446146	245396	437710	355685
PE(O-34:2)	23074	17973	4352	8490	38488	4246
PE(O-36:3)(a\b)	4771	3739	1032	2463	7426	284
PE(O-36:4)	94152	77530	29600	45806	131478	9852
PE(O-36:5)	1552	134	311	28	66	140
PE(O-38:4)(a\b)	69863	60875	22349	33596	196653	15447
PE(O-38:5)(a\b)	55347	35715	27512	29819	37487	18441
PE(O-38:6)	1096283	875007	806433	761135	946810	784275
PE(O-40:5)	23663	15751	14515	14989	34737	23459
PE(O-40:6)	28625	18288	14388	14265	53160	17035
PE(P-16:0/18:1)	123310	89530	25043	50143	205914	21729
PE(P-16:0/18:2)	12720	11767	8656	6210	10198	7157
PE(P-16:0/20:4)	366441	206000	78804	113567	149695	14024
PE(P-16:0/20:5)	522	1103	370	387	843	107
PE(P-16:0/22:4)	109089	89530	32113	51558	160763	17974
PE(P-16:0/22:5)(a\b)	84825	71352	30146	39468	75006	13894
PE(P-16:0/22:6)	313299	248837	106619	151837	313318	81520
PE(P-18:0/18:1)	8542	8302	3254	5692	59912	11135
PE(P-18:0/18:2)	6962	8048	6993	6335	12152	10084
PE(P-18:0/20:3)	17580	11535	4456	7735	31793	4158
PE(P-18:0/20:4)	262668	173391	67999	101031	391096	45558
PE(P-18:0/22:4)	5301	4502	1917	2955	28214	3064
PE(P-18:0/22:5)(a\b)	17335	18850	7973	9611	35942	5798
PE(P-18:0/22:6)	91230	71424	43359	38045	124962	37422
PE(P-18:1/18:1)	22659	16756	8485	11424	43354	8075
PE(P-18:1/18:2)	6301	4714	4339	2771	4857	2017
PE(P-18:1/18:3)	279	145	22	1256	1406	1274
PE(P-18:1/20:4)	152804	112515	50875	72538	125517	16282
PE(P-18:1/22:4)	37727	28918	17180	19245	62523	9704
PE(P-18:1/22:5)(a\b)	14836	9040	4236	5864	9416	1407
PE(P-18:1/22:6)(a\b)	45619	29083	17570	20016	30278	3025
PE(P-20:0/18:2)	181	224	1158	1133	863	720
PE(P-20:0/20:4)	4502	3681	2329	2040	10376	2939
PE(P-20:0/22:6)	1033	691	890	377	2491	2189
PG 17:0 17:0 (IS)	2368566	1739906	1889266	1671774	2362171	1611665

PG 34:1	59137	43734	53015	18936	36563	13965
PG 34:2	18286	17362	23158	12195	28288	17825
PG 36:1	2177	2030	1044	1020	1315	838
PG 36:2	12584	9519	8941	3194	2164	2522
PI 32:0	2325	2322	1731	1625	8538	1185
PI 32:1	1661	1808	1475	656	3219	707
PI 34:0	714	541	690	422	433	4
PI 34:1	17742	18501	8859	12824	37145	9925
PI 36:1	1579	1087	757	1245	1941	412
PI 36:2	55620	49181	45975	26795	32567	18259
PI 36:3(a\b\c)	121024	108505	135808	58740	142655	118607
PI 36:4	265606	279174	330831	107847	362743	195446
PI 38:2	16702	9865	16389	3210	3581	3754
PI 38:3(a\b)	364593	234038	369237	92194	128481	77137
PI 38:4	2906160	1806911	2728707	753571	1217786	664276
PI 38:5(a\b)	238403	193201	230082	98172	281522	120944
PI 38:6	16901	13922	16389	6063	11060	11912
PI 40:5(a\b)	16868	8363	7076	2591	6246	2427
PI 40:6	54014	31352	58818	14388	11390	11605
PS 36:1	715908	448756	130176	256169	654860	57048
PS 36:2	17765	21226	12815	11629	68149	11444
PS 38:3	60218	42535	35232	17766	58876	16253
PS 38:4	1038783	707333	642406	306940	838669	247139
PS 40:5	37549	52416	22474	20613	49083	11719
PS 40:6	577463	304190	354275	143332	283229	122405
SM 30:1	1415	1609	1336	1079	7543	4723
SM 31:1	1053	1402	1038	899	4148	2383
SM 32:0	2579	2980	2939	2384	7250	3656
SM 32:1	30454	32501	28936	23751	72624	35324
SM 32:2	1517	1754	1802	1151	4558	1767
SM 33:1	97096	94693	84860	83082	295196	172386
SM 34:0	164266	74655	67461	59336	57625	20939
SM 34:1	8207908	7179796	5385055	3501400	8665844	2010867
SM 34:2	148653	134965	93691	86310	278140	92376
SM 36:1	2070556	1281280	483767	630744	1745520	178996
SM 36:2	192165	159922	53346	85413	215780	18650
SM 36:3	140	356	90	1657	472	564
SM 37:1	2973170	4111502	3386327	3902695	4151564	7668731
SM 37:2	3267	3533	552	302	6813	906
SM 38:1	73369992	83499536	72872857	80615472	67231145	77201263
SM 38:2	32579961	38635183	18028484	35763348	44528166	62159226
SM 38:3 (a\b)	486444	999914	595393	851826	2859215	2908602
SM 39:1	6683749	8165515	7286663	9371973	10420079	16661756
SM 40:0	3716412	4202012	2739218	3749770	14210574	12616671

SM 40:1	47760870	55671921	53377979	58448291	73074408	73850854
SM 40:2 (a\b)	49019899	52591066	46559790	42534534	74783196	60245198
SM 40:3 (a\b\c)	46457819	47933103	46676538	48204406	54100478	66485925
SM 41:0	6777	19361	16783	19662	93228	88626
SM 41:1	286882	357012	422685	362291	766987	1061556
SM 41:2(a\b)	123783	147025	176795	174469	225146	248651
SM 42:1	264476	279068	209258	160990	281	1198245
SM 42:2 (a\b)	979177	1451421	1656959	1604292	4820237	3982708
SM 44:2	4181	8141	3651	3868	32545	25208
SM 44:3 (a\b)	58147	39473	27450	38499	77632	10628
TG 14:0 16:0 18:2	37395	44836	33757	47494	208018	135215
TG 14:0 16:1 18:1	27923	48835	26760	49981	140549	150690
TG 14:0 16:1 18:2	29908	32044	29675	37469	44699	41590
TG 14:0 18:0 18:1	6321	7242	5558	7671	13676	13204
TG 14:0 18:2 18:2	2552	2901	2376	6198	18281	17240
TG 14:1 16:0 18:1	9738	11705	8886	12641	28418	31662
TG 14:1 16:1 18:0	140769	159578	120581	176411	556203	452042
TG 14:1 18:0 18:2	2210	2043	1569	1221	10070	9417
TG 14:1 18:1 18:1	19278	14198	16522	26807	297337	183372
TG 15:0 18:1 16:0	28504	33423	20340	23848	57375	61160
TG 15:0 18:1 18:1	5951	6409	5660	9068	28092	34035
TG 16:0 16:0 16:0	358014	387776	295198	414322	569285	597313
TG 16:0 16:0 18:0	107418	105068	117291	132113	425390	337025
TG 16:0 16:0 18:1	107255	126817	61494	158759	739284	469054
TG 16:0 16:0 18:2	39339	47343	28024	72029	240483	211468
TG 16:0 16:1 18:1	168955	184633	142346	186178	1128634	593219
TG 16:0 18:0 18:1	33899	38445	19537	46569	295500	217614
TG 16:0 18:1 18:1	61364	88869	58456	281677	2551680	1616471
TG 16:0 18:1 18:2	40012	53654	34258	434650	2245463	2113555
TG 16:0 18:2 18:2	7633	10007	5715	71135	628887	663484
TG 16:1 16:1 16:1	152818	161242	138606	162393	189827	181110
TG 16:1 16:1 18:0	8575	11179	7635	11801	19459	17606
TG 16:1 16:1 18:1	49677	66203	41950	76215	743127	415076
TG 16:1 18:1 18:1	35439	38198	28328	70637	659516	369126
TG 16:1 18:1 18:2	10355	11606	6982	36744	596174	495494
TG 17:0 16:0 16:1	79844	150363	102291	138224	206800	224408
TG 17:0 16:0 18:0	18347	19293	7796	12904	81514	65334
TG 17:0 17:0 17:0 (IS)	4014	4492	2612	5868	32783	25337
TG 17:0 18:1 14:0	52168	39892	40168	60433	82570	89839
TG 17:0 18:1 16:0	16002	20963	15143	18392	49267	52532
TG 17:0 18:1 16:1	30418	36963	28047	43162	157044	151684
TG 17:0 18:1 18:1	4129	3776	2988	6223	27911	29210
TG 17:0 18:2 16:0	18113	21169	15842	26403	144306	105708
TG 18:0 18:0 18:0	79364	65791	113539	94475	1801192	1550653
TG 18:0 18:0 18:1	16851	15800	13093	18672	61366	46541

TG 18:0 18:1 18:1	9099	10537	10148	16533	137176	64771
TG 18:0 18:2 18:2	2827	3025	1956	7700	32571	38755
TG 18:1 14:0 16:0	114813	134208	105782	126652	211225	194538
TG 18:1 18:1 18:1	223434	287642	220552	485888	2211949	2286707
TG 18:1 18:1 18:2	10243	15150	10548	41058	162224	196315
TG 18:1 18:1 20:4	509	559	524	8243	64938	51374
TG 18:1 18:1 22:6	32	52	45	6752	49115	78160
TG 18:1 18:2 18:2	30875	36224	28151	91083	427315	565694
TG 18:2 18:2 18:2	25161	25805	22041	74397	142319	207997
TG 18:2 18:2 20:4	276	220	122	3653	14755	17879
TG(O-50:1)	79844	150363	102291	138224	206800	224408
TG(O-52:0)	15134	16168	6985	8710	76100	59664
TG(O-52:2)	18113	21169	15842	26403	144306	105708
Ubiquinone	696	1318	660	729	8144	1501

Appendix Table iv. Signal intensities for lipids detected from mice infected with SL3261

Name	WT_1	WT_2	WT_3	WT_4	WT_5	WT_6	WT_7
AcylCarnitine 12:0	20562	15997	43170	136359	26085	158943	24607
AcylCarnitine 13:0	2909	1096	7859	17759	2161	26644	2895
AcylCarnitine 14:0	37010	42097	109409	170337	68130	233374	47697
AcylCarnitine 14:1	58773	35872	134832	352885	71344	593473	64624
AcylCarnitine 14:2	28375	13305	54339	122295	24188	231235	22400
AcylCarnitine 15:0	4870	4954	15733	18092	6716	29165	5338
AcylCarnitine 16:0	176261	235852	639696	587370	238463	612112	204166
AcylCarnitine 16:1	46376	38886	145236	151656	88140	296200	47948
AcylCarnitine 17:0	7068.832	7121.301	18600.14	18962.09	10424.73	22266.78	17046.08
AcylCarnitine 18:0	32485	54945	156842	210366	26820	177069	42699
AcylCarnitine 18:1	137796	159705	480441	539159	209829	779408	158019
AcylCarnitine 18:2	60362	58443	223123	194538	95132	212050	52298
CE 16:0	658	1596	694	2092	488	2498	779
CE 16:1	1436	1310	1118	3290	603	4162	849
CE 16:2	82	28	106	624	12	546	43
CE 18:0	518	1086	940	1123	346	1119	394
CE 18:1	7747	14172	11726	8271	1919	10673	7679
CE 18:2	23575	44368	17158	9140	3650	8522	15325
CE 18:3	1412	3150	2342	2758	518	2009	1504
CE 20:0	1057	1739	934	2888	1455	2102	1127
CE 20:1	1468	2656	1932	2294	1025	2304	1290
CE 20:2	2215	4200	2638	3533	892	2449	1719
CE 20:3	1846	3572	2378	2218	605	1363	1168
CE 20:4	19493	55594	10221	25317	3372	5281	16985
CE 20:5	1605	3177	1421	1095	295	192	1741
CE 22:0	633	671	517	1217	472	1307	516
CE 22:1	1384	2055	1485	2198	879	2415	1105
CE 22:4	6293	22287	6543	16567	2000	7885	5645
CE 22:5(a\b)	6296	22226	9598	20448	2369	6964	4715
CE 22:6	24176	63040	24896	43289	6480	7815	21128
CE 24:0	1261	913	879	2038	901	2212	908
CE 24:1	3895	4591	3662	4103	2203	4368	2886
CE 24:4	10235	39842	13073	12082	6265	4679	9909
CE 24:5	1381	4311	1369	3912	485	1665	823
CE 24:6	576	1491	715	1783	294	244	285
Cer(d16:1/24:1)	690	1243	2977	1055	354	745	344

Cer(d17:1/16:0)	11620	32683	34938	4644	6062	5775	7465
Cer(d17:1/18:0)	402	447	230	471	401	273	345
Cer(d17:1/20:0)	64	163	134	300	29	148	70
Cer(d18:1/14:0)	460	1176	1286	25	295	34	327
Cer(d18:1/16:0)	3481	4726	4828	62	875	204	2545
Cer(d18:1/18:0)	394	675	683	140	206	585	653
Cer(d18:1/20:0)	4141	13896	16538	23284	2877	8610	5591
Cer(d18:1/22:0)	37360	108602	163341	100653	12372	41950	36111
Cer(d18:1/24:0)	107514	326004	453176	87349	38715	74420	105488
Cer(d18:1/24:1)	169430	418972	775430	325048	30575	135237	154453
Cer(d18:1/26:0)	1277	2289	2947	7323	1699	4726	1361
Cer(d18:2/16:0)	12920	41680	30843	5594	8798	2270	21362
Cer(d18:2/18:0)	2210	11745	13849	5529	1629	1875	5140
Cer(d18:2/20:0)		567	160	1260	82	1003	82
Cer(d18:2/22:0)	2099	6294	5359	8467	703	2223	2018
Cer(d18:2/26:0)	1709	1865	1856	2067	2034	1384	1763
Cer(d19:1/20:0)	844	796	936	632	804	76	126
Cer(d19:1/24:0)	443	1200	2221	613	738	964	497
Cer(d19:1/26:0)	640	523	440	1021	1087	867	620
Cer(d20:1/22:0)	3565	2754	3714	170	3278	4243	3468
Cer(d20:1/24:0)	2392	4565	23895	14925	2625	16172	3570
Cer(d20:1/24:1)	4455	8711	29231	4895	4451	7819	5636
Cer(d20:1/26:0)	2030	2764	5101	3298	4779	2271	2245
DG 30:0 -(14:0)	55061	54805	48675	3923	63564	6889	71320
DG 32:0 -(16:0)	1325649	131538 4	140412 2	30341	135335 3	44587	134727 7
DG 34:1 -(18:1)	23623	37149	52119	53387	19444	54086	28431
DG 34:2 -(18:2)	9626	17374	16572	15600	4490	16361	6221
DG 36:1 -(18:1)	12796	12960	14532	13132	13681	9824	13863
DG 36:2 -(18:2)	9399	17579	17124	3579	2646	4870	8405
DG 36:3 -(18:2)	9126	13326	10707	18585	7472	24209	7728
DG 36:4 -(18:2)	8345	11639	11510	4472	5578	7027	7205
DG 36:4 -(18:3)	2335	3536	2679	2387	1955	3272	2354
DG 36:4 -(20:4)	4025	14102	6735	440	327	1364	4324
DG 38:4 -(20:4)	26522	113383	43895	3621	1505	11060	35360
DG 38:5 -(20:4)	4778	7750	3902	169	764	1021	3145
DG 38:5 -(22:5)	13531	13684	17476	542	15110	1181	16924
DG 38:6 -(20:4)	4921	8700	7398	107	2706	172	3075
DG 38:6 -(22:6)	5349	11959	8005	316	357	1719	3970
DG-D5 (IS)	52349	51312	54715	148210	55318	184470	55127
dhCer 24:0	1167	2753	3469	1366	1128	1183	1234
dhCer 24:1	2834	6625	7951	2038	1446	807	3224
GM1(d18:1/16:0)	1594	1014	2101	45	1737	16	1966
GM3(d18:1/16:0)	2657	4637	11565	852	403	444	2015
Hex1Cer(d16:1/20:0)	838	685	814	709	819	806	806
Hex1Cer(d18:1/18:0)	2177	4254	3943	416	717	385	804

Hex1Cer(d18:1/20:0)	1365	3218	4130	790	473	974	1527
Hex1Cer(d18:1/22:0)	2034	4509	11187	5057	800	3030	2052
Hex1Cer(d18:1/24:0)	6496	11900	29321	10045	2544	3037	4901
Hex1Cer(d18:1/24:1)	15206	19087	46359	18164	2520	11124	7321
Hex2Cer(d18:1/24:0)	965	4673	3642	1862	530	599	1054
Hex2Cer(d18:1/24:1)	3	356	697	13	32	23	35
LPC 14:0	10620	12538	39681	54052	26132	31855	10276
LPC 15:0	9203	10697	39277	68014	25002	38847	10847
LPC 16:0	1841462	2471999	6848490	15246783	3343458	7520563	1837866
LPC 16:1	69707	118615	519164	724767	458537	226058	128035
LPC 18:0	589760	769291	1598830	5654096	888828	2474932	523075
LPC 18:1	5461438	1098703	3603223	6374993	2797991	1749317	877329
LPC 18:2	1091342	1905743	5677976	15273559	5076528	2763206	1243295
LPC 18:3	16997	40310	112460	536725	171872	62413	28483
LPC 18:3(104)	41199	63671	245259	676748	139013	362507	44817
LPC 20:0	7193	7680	25032	36218	8322	22842	6906
LPC 20:1	14402	11277	44750	36488	12805	29066	9807
LPC 20:2	23047	22166	86940	59949	34628	37145	16744
LPC 20:3	75308	102330	390988	577237	212866	145272	68377
LPC 20:4	3009785	5776771	1446883	4061488	1252020	580473	323591
LPC 20:5	15581	29177	93318	497893	114672	51992	22701
LPC 22:0	2119	2596	8637	11456	2082	7924	2242
LPC 22:1	1501	1634	6144	4870	1323	3603	1484
LPC 22:4	7414	16166	36554	21038	21177	8267	8058
LPC 22:5(104)	4089	8507	12652	125983	27867	17589	3689
LPC 22:5(a\b\c)	13844	29764	76937	173812	48879	18061	16675
LPC 22:6	1401702	2432560	6259085	2754720	5735360	3029210	1330880
LPC 24:0	2845	4824	21169	14203	2829	8934	4042
LPC(O-16:0)	31385	35807	108889	131011	33736	77803	24118
LPC(O-18:0)	19683	19765	65682	43931	17550	25044	13623
LPC(O-18:1)	34964	33941	96872	41941	32956	27743	20873
LPC(O-20:0)	34126	34153	68291	67245	40583	50412	32171
LPC(O-20:1)	1929	2122	5304	5885	2856	3965	1439
LPC(O-22:0)	502	527	1563	1096	437	887	448
LPC(O-24:0)	409	757	1993	1997	407	1034	545
LPC(O-24:1)	267	425	767	384	202	255	272
LPC(O-24:2)	279	284	941	1336	230	883	225
LPC(P-16:0)	1917	1417	1565	4183	2244	3568	7934
LPC(P-18:0)	30543	32122	89652	38227	32828	24182	20129

LPE 16:0	41942	62676	173985	305413	93442	88141	27459
LPE 18:0	35836	56568	126833	140416	52758	62885	21688
LPE 18:1	23462	29872	95685	114870	41870	44526	15876
LPE 18:2	14969	19361	75223	190253	41080	28604	10385
LPE 20:4	17102	34475	98740	104230	36525	15112	16078
LPE 22:6	11795	24483	61708	127443	29387	15011	10970
LPE(P-16:0)	2688	4972	7173	3568	4242	3077	2029
LPE(P-18:0)	2934	5001	10016	2271	3765	1828	2033
LPE(P-18:1)	773	1386	1768	821	1030	602	581
LPE(P-20:0)	444	415	977	264	239	230	148
LPI 18:0	3008	3895	8128	1221	584	862	1563
LPI 18:1	1274	824	3788	2128	405	1448	959
LPI 18:2	879	955	3143	5096	898	3579	1473
LPI 20:4	10458	10492	35860	41529	8218	23533	12698
oxCE 18:2 +2O NH4	1997	1773	1653	3612	1142	3720	2039
PC 30:0	410924	765891	1226054	1378427	299986	722324	267178
PC 31:1	35505	85310	87246	7236	22186	27707	48007
PC 32:0	4679264	8943671	23021960	10796590	2652490	6345510	4344131
PC 32:1	13296793	11617079	33457364	30164991	17352499	33204988	22334918
PC 32:2	640292	419328	2711207	7211698	468423	3787237	853361
PC 34:0	6556136	6600807	11171340	16662736	6663325	15357396	9004136
PC 34:1	11150711	9004788	12310600	16703475	9787911	15610399	11320201
PC 34:2	98779479	90756927	##########	##########	##########	##########	##########
PC 34:3(a\b\c)	6564430	5968815	35221013	##########	5050848	5951154	8415332
PC 34:4	323086	315903	1253062	4537113	289770	1993648	457896
PC 34:5	4871	5372	22864	71079	4427	31768	8583
PC 35:4	271098	301274	1076832	2967044	161666	1133466	288936
PC 35:5	20942	18520	59307	267102	16805	93113	25439
PC 36:0	161789	229494	694249	2558328	149332	755174	181843
PC 36:1	1661578	2491311	6477229	25974880	1731294	8390163	2038724
PC 36:2(a\b)	16785932	14135132	61547937	##########	14321983	73868031	16257579
PC 36:3(a\b\c)	29823382	17161310	55858143	##########	13966072	89241915	24530678
PC 36:4(a\b)	25979311	33279956	35308130	32171364	24686485	30114168	29584249
PC 36:5(a\b)	1867348	2373677	7419790	39283978	1654555	11096415	2414126
PC 36:6	46630	40744	192044	524397	30126	235030	58573

PC 37:6	49369	56750	185786	776428	20514	309517	51446
PC 38:2	374788	611270	1276606	2279701	184142	1049551	331206
PC 38:3	782141	1229704	3248627	1277550	384461	2198809	526520
PC 38:4(a\b\c)	2327875	5853630	10273757	10317937	1675505	5943612	2338012
PC 38:5(a\b)	7651338	10039746	14608964	17067264	4891009	9990763	7826438
PC 38:6(a\b)	16156131	19950934	26667469	49571807	9494884	28078307	11947776
PC 38:7(a\b\c)	241038	212810	837126	3167648	126339	1139433	239380
PC 39:5	7751	43516	46923	56714	11972	12087	14788
PC 40:4(a\b)	56578	135815	96206	126753	35811	40272	26008
PC 40:5(a\b)	571015	1180392	1378731	758521	302761	495333	407096
PC 40:6	117209	254177	632540	360522	16678	420066	105090
PC 40:7(a\b\c)	1098887	1385950	2167969	927524	399458	1078331	769116
PC 40:8	225958	374252	1037543	1317727	79571	527483	139972
PC(19:0/19:0)(IS)	48709	51869	86478	105246	66916	79107	47803
PC(O-32:0)	77015	148330	574531	90942	63351	68399	121025
PC(O-32:1)	35505	85310	78810	40485	21521	23439	44847
PC(O-32:2)	3988	8552	22768	2292	5001	6129	6791
PC(O-34:1)	2520243	2395012	7036022	11205114	2589231	10250333	4540800
PC(O-34:2)	870650	672627	3174103	9269204	566721	6222777	917772
PC(O-35:4)	337130	320563	1303010	4417461	295467	1993648	457896
PC(O-36:1)	187795	169092	960522	1990941	84384	765665	235370
PC(O-36:2)(a\b)	852990	831682	3201170	11506467	683526	5016560	889977
PC(O-36:3)(a\b)	1347177	822803	2082090	3471804	756333	4737219	1322470
PC(O-36:4)	330425	341226	1336993	4580115	163229	2238280	381363
PC(O-36:5)	20942	18520	59307	267102	16805	93113	25439
PC(O-38:5)	276592	517664	435801	10263	159010	35335	165031
PC(O-38:6)	49369	56750	187620	776428	20514	309517	51446
PC(O-40:5)	7751	43516	46923	24281	2187	12087	14788
PC(O-40:6)	15281	54019	68257	7830	14854	11643	14341
PC(O-40:7)(a\b)	29918	46267	26101	24302	46869	39680	44448
PC(P-30:0)	10381	15519	40033	35285	5912	14070	10048
PC(P-32:0)	35505	85310	54627	7236	11450	3313	33988
PC(P-32:1)	3988	8552	22768	3862	5001	6129	6791
PC(P-34:0)	2520243	2395012	7036022	11205114	2589231	10250333	4540800

PC(P-34:1)	617662	553036	2569677	9269204	357346	5418103	769444
PC(P-34:2)	5135	6549	9500	418	1014	1207	4844
PC(P-34:3)	599	4769	12700	150	1218	1038	262
PC(P-36:2)(a\b)	1347177	822803	2082090	3471804	756333	4737219	1344798
PC(P-36:3)	205731	212652	896611	2792682	115208	1049996	187351
PC(P-36:4)	20942	18520	59307	267102	16805	93113	25439
PC(P-36:5)	78	531	4272	3330	29	4801	205
PC(P-38:4)	282195	517664	481560	31787	169089	35335	165031
PC(P-38:5)(a\b)	49369	56750	187620	776428	20514	309517	51446
PC(P-38:6)	161789	229494	694249	2558328	149332	755174	181843
PC(P-40:4)	7751	43516	46923	24281	2187	12087	14788
PC(P-40:5)(a\b)	39456	54019	68257	7830	14854	11643	14341
PC(P-40:6)	29918	46267	26101	24302	46869	39680	44448
PC(P-40:7)	73522	42404	7086	4685	55346	6613	65539
PE 32:0	14212	24539	21897	10855	6839	4932	9618
PE 32:1	81293	62224	195671	71501	42480	88407	68201
PE 34:1	848603	646335	3018503	3329883	319212	2301652	516989
PE 34:2	1020373	984372	2514269	5046384	435646	1806451	642091
PE 34:3(a\b\c)	83738	79843	340341	704005	37506	251993	60880
PE 36:0	3544	2099	208	125	9957	56	3816
PE 36:1	52299	113206	304518	214496	23130	112512	66079
PE 36:2(a\b)	466911	623306	2121275	2517204	143466	826904	281651
PE 36:3(a\b)	420335	372248	1657052	1353468	65907	870091	205969
PE 36:4	55367	43309	81096	50265	10326	30071	24172
PE 36:5(a\b)	41055	71500	349612	360798	11912	114132	31137
PE 38:3(a\b)	104487	300967	668944	298060	31658	108263	95444
PE 38:4	1159303	3373259	7017999	3396992	314226	1106493	999249
PE 38:5(a\b)	726514	1030358	3260923	1265452	134016	785896	580366
PE 38:6	1076384	1810332	2098322	607545	275595	421784	575890
PE 40:4	27008	70572	94188	26451	15952	13253	17618
PE 40:5(a\b)	23520	80795	217788	91726	8999	26066	20882
PE 40:6	1437	12409	88406	27106	927	14141	1529
PE 40:7	301408	386778	702250	157596	43257	103641	137470
PE(O-34:2)	2917	8110	15088	4858	1272	2732	3552
PE(O-36:3)(a\b)	1097	1234	11574	1936	796	878	3575
PE(O-36:4)	21806	89459	205375	47986	19923	39474	79853
PE(O-36:5)	44	217	880	111	1254	1109	331
PE(O-38:4)(a\b)	11547	52211	94581	45320	7503	24551	35278
PE(O-38:5)(a\b)	32932	54771	94935	22054	26748	33175	31947

PE(O-38:6)	1037048	1001903	991453	799284	891774	869894	935140
PE(O-40:5)	11466	15279	26126	18659	7590	15926	8529
PE(O-40:6)	7383	16653	34022	14392	7297	10885	10666
PE(P-16:0/18:1)	10260	39127	49408	24347	5681	13542	16654
PE(P-16:0/18:2)	8781	13676	11394	2823	6292	4417	8825
PE(P-16:0/20:4)	150017	378219	348745	31891	70433	33104	109326
PE(P-16:0/20:5)	1384	1179	2715	216	320	140	483
PE(P-16:0/22:4)	22669	60088	128885	19907	11415	9561	14934
PE(P-16:0/22:5)(a\b)	31459	72232	70913	9437	12653	8811	21078
PE(P-16:0/22:6)	79276	219690	358829	122255	38156	71234	84563
PE(P-18:0/18:1)	2010	4721	8104	9582	1044	9195	3311
PE(P-18:0/18:2)	3403	6100	19510	4668	2948	4978	4560
PE(P-18:0/20:3)	2355	8074	13041	4625	1354	2431	2926
PE(P-18:0/20:4)	51852	138550	220466	55337	25410	34541	49287
PE(P-18:0/22:4)	1065	4656	4467	2843	565	1640	618
PE(P-18:0/22:5)(a\b)	4677	13322	15497	4445	2318	2782	3659
PE(P-18:0/22:6)	28693	70786	107745	35425	11733	18566	20467
PE(P-18:1/18:1)	3132	8150	14410	1518	776	805	3378
PE(P-18:1/18:2)	2066	4328	9701	1295	456	1102	2332
PE(P-18:1/18:3)	1203	1534	543	1169	1144	1080	1372
PE(P-18:1/20:4)	52081	123400	156647	29859	18881	16629	44433
PE(P-18:1/22:4)	10227	16212	50855	5069	1847	2237	6511
PE(P-18:1/22:5)(a\b)	3484	2870	12000	1397	849	1223	2342
PE(P-18:1/22:6)(a\b)	25710	59656	62303	11482	8254	10137	21856
PE(P-20:0/18:2)	1016	1114	570	238	919	1041	1076
PE(P-20:0/20:4)	1395	2554	5309	2411	316	1366	273
PE(P-20:0/22:6)	152	520	538	606	146	266	159
PG 17:0 17:0 (IS)	3931252	4396753	3535938	2146553	5156265	2012544	4422801
PG 34:1	38256	105456	179979	10405	11799	12264	41917
PG 34:2	7869	20891	45253	9757	2231	3576	11241
PG 36:1	2890	5937	3418	497	1536	354	2891
PG 36:2	14735	22299	29985	1951	4389	1134	4866
PI 32:0	615	2900	8797	2054	804	1133	1527
PI 32:1	2222	4086	22479	622	1457	361	2516
PI 34:0	2484	6158	2535	69	3259	301	2496
PI 34:1	19801	39488	187546	14143	9076	7701	20802
PI 36:1	4101	10065	14921	571	4040	1155	5835
PI 36:2	45607	86428	268701	11298	17732	19210	35206
PI 36:3(a\b\c)	73148	116257	457392	23314	16962	14230	52379
PI 36:4	241201	369849	1337848	79886	59531	44720	155066
PI 38:2	25346	32100	31512	321	8452	815	14360
PI 38:3(a\b)	177948	228367	220899	3616	67576	8489	114565

PI 38:4	1240279	2701369	4475015	282974	361600	372122	899301
PI 38:5(a\b)	149308	194063	685105	40393	24652	28351	75338
PI 38:6	14815	28570	61318	5136	4545	2114	11049
PI 40:5(a\b)	32211	52562	58181	2212	9722	3051	20105
PI 40:6	14360	36583	102132	5808	6036	3720	15580
PS 36:1	120309	405184	999936	172408	68398	152800	255582
PS 36:2	162920	27889	390921	29889	63162	30482	109949
PS 38:3	12138	20549	35706	9652	2839	8676	11229
PS 38:4	575171	1242400	1664603	244371	155513	152727	530836
PS 40:5	54616	86020	134132	6500	15923	9325	30950
PS 40:6	435235	863878	1756759	273187	99882	100506	307893
SM 30:1	289	219	676	1516	438	1209	193
SM 31:1	214	179	650	1331	174	940	161
SM 32:0	787	1095	3664	3632	559	1793	776
SM 32:1	8606	11909	38805	39404	7312	20107	9194
SM 32:2	220	199	443	1770	267	890	275
SM 33:1	34293	48561	118436	102378	20924	45324	32636
SM 34:0	356464	880331	398444	43403	298367	57109	346864
SM 34:1	3827012	10126174	24165739	7280336	2191783	4094721	4045291
SM 34:2	24927	53908	81892	72645	34906	34776	37296
SM 36:1	218415	949903	1158186	289170	126621	328735	399487
SM 36:2	23920	76671	56634	31020	27120	23174	44817
SM 36:3	7577	334	1039	296	747	116	
SM 37:1	289532	231145	1227519	4170211	178699	2797485	377238
SM 37:2	3307	3735	12510	8023	9275	16574	11770
SM 38:1	53878963	43933728	71062096	73475002	48574533	86653512	51059991
SM 38:2	1655365	2315509	7033679	15012577	6980064	20104145	2815380
SM 38:3 (a\b)	106175	111984	435658	1577600	100976	558155	159084
SM 39:1	257909	535700	1776748	6833792	451468	3208315	677520
SM 40:0	762686	1349313	3849002	14919543	944205	4648416	1122730
SM 40:1	12135086	12557368	36315914	76577845	7867455	50609883	10079887
SM 40:2 (a\b)	21642883	12146994	47923518	74762582	8638514	58080241	17727390
SM 40:3 (a\b\c)	16261649	18210675	22230255	45330558	11922053	23469940	14742878
SM 41:0	2628	5147	12547	78375	4169	34765	4546
SM 41:1	44140	45718	116979	328111	25420	119981	33678
SM 41:2(a\b)	134216	94529	222397	290185	52024	278017	100122
SM 42:1	29599	47626	154200	396941	16935	218111	26951

SM 42:2 (a\b)	304209	69227	1602205	527648	121530	448006	140891
SM 44:2	3004	4387	6819	6547	1186	5450	1343
SM 44:3 (a\b)	41378	111179	208514	98222	27069	39634	27142
TG 14:0 16:0 18:2	45351	280656	54636	109198	37270	99748	56708
TG 14:0 16:1 18:1	40925	82617	42717	99978	41822	85248	29516
TG 14:0 16:1 18:2	36367	64529	37687	30132	29606	26145	38082
TG 14:0 18:0 18:1	10901	11541	9225	25984	8402	23884	11071
TG 14:0 18:2 18:2	8972	14741	10249	3139	2977	2046	11391
TG 14:1 16:0 18:1	1073	9960	1078	23543	6118	22455	10753
TG 14:1 16:1 18:0	145187	394806	164868	416507	141344	395661	153915
TG 14:1 18:0 18:2	2208	3714	1604	7971	1998	5147	4325
TG 14:1 18:1 18:1	36758	113044	36638	68448	21652	48023	40086
TG 15:0 18:1 16:0	27417	32293	21522	69038	24465	62719	27771
TG 15:0 18:1 18:1	7916	9374	8300	18446	6739	16545	9554
TG 16:0 16:0 16:0	354302	651881	323094	594029	381494	537906	384126
TG 16:0 16:0 18:0	96122	152292	64669	80389	114630	81492	135376
TG 16:0 16:0 18:1	229233	497726	234730	333723	117811	392545	252434
TG 16:0 16:0 18:2	96659	214137	105548	77572	35872	69346	103839
TG 16:0 16:1 18:1	299803	728780	405311	307185	166277	292536	357944
TG 16:0 18:0 18:1	58989	102577	57085	104020	29634	90757	70835
TG 16:0 18:1 18:1	332529	556921	411839	240491	78873	258876	383208
TG 16:0 18:1 18:2	395508	584570	429499	136642	65454	45068	395449
TG 16:0 18:2 18:2	64004	63884	69310	27730	8782	19305	63362
TG 16:1 16:1 16:1	164642	400462	154423	157679	152070	122381	159168
TG 16:1 16:1 18:0	10687	18602	9738	20306	9233	18134	10688
TG 16:1 16:1 18:1	83060	10132	18753	192152	47306	133877	63614
TG 16:1 18:1 18:1	102956	268326	147716	86050	41236	81911	106998
TG 16:1 18:1 18:2	36649	88935	43745	28950	8079	17474	43963

TG 17:0 16:0 16:1	126010	138956	99039	323630	58948	275491	128171
TG 17:0 16:0 18:0	17495	10412	8625	25787	6706	24399	9065
TG 17:0 17:0 17:0 (IS)	4026	4902	2241	11817	3847	13608	6767
TG 17:0 18:1 14:0	45500	40472	27919	121820	54496	115035	53661
TG 17:0 18:1 16:0	15423	20553	16020	43925	18317	56173	15820
TG 17:0 18:1 16:1	42875	44401	33898	105085	31791	90302	43910
TG 17:0 18:1 18:1	6037	8825	5393	12113	3303	12862	7322
TG 17:0 18:2 16:0	30213	43219	30118	55489	18516	52911	32235
TG 18:0 18:0 18:0	126333	109061	84782	25877	105777	26279	136170
TG 18:0 18:0 18:1	27594	28487	26235	43267	14976	41378	26043
TG 18:0 18:1 18:1	52359	49239	34986	85921	25143	87877	40204
TG 18:0 18:2 18:2	17267	18101	15701	10920	4015	10145	18701
TG 18:1 14:0 16:0	134572	165325	130447	214477	107872	177317	121058
TG 18:1 18:1 18:1	547882	621063	369173	737655	262566	771171	579090
TG 18:1 18:1 18:2	54318	53396	45926	31891	14839	29643	57156
TG 18:1 18:1 20:4	41614	64227	75259	2114	1803	1315	33749
TG 18:1 18:1 22:6	13811	21949	17073	1136	564	486	10540
TG 18:1 18:2 18:2	125054	135171	103443	86337	36634	61232	123221
TG 18:2 18:2 18:2	94435	80861	91217	32517	28325	22246	124334
TG 18:2 18:2 20:4	20088	33705	33587	1089	985	367	15725
TG(O-50:1)	126010	138956	99039	323630	116450	275491	128171
TG(O-52:0)	17495	10412	8625	25787	6706	24399	9065
TG(O-52:2)	30213	43219	30118	55489	18516	52911	32235
Ubiquinone	1334	2179	2446	10380	401	4509	1245

Bibliography

AKOH, C. C., LEE, G. C., LIAW, Y. C., HUANG, T. H. & SHAW, J. F. 2004. GDSL family of serine esterases/lipases. *Prog Lipid Res,* 43**,** 534-52.

ALBRECHT, R., SCHUTZ, M., OBERHETTINGER, P., FAULSTICH, M., BERMEJO, I., RUDEL, T., DIEDERICHS, K. & ZETH, K. 2014. Structure of BamA, an essential factor in outer membrane protein biogenesis. *Acta Crystallogr D Biol Crystallogr,* 70**,** 1779-89.

ALVAREZ-MARTINEZ, C. E. & CHRISTIE, P. J. 2009. Biological diversity of prokaryotic type IV secretion systems. *Microbiol Mol Biol Rev,* 73**,** 775-808.

ANDERSEN, K. R., LEKSA, N. C. & SCHWARTZ, T. U. 2013. Optimized *E. coli* expression strain LOBSTR eliminates common contaminants from His-tag purification. *Proteins,* 81**,** 1857-61.

ANDREU, N., PHELAN, J., DE SESSIONS, P. F., CLIFF, J. M., CLARK, T. G. & HIBBERD, M. L. 2017. Primary macrophages and J774 cells respond differently to infection with *Mycobacterium tuberculosis*. *Sci Rep,* 7**,** 42225.

ANTUNES, L. C., ANDERSEN, S. K., MENENDEZ, A., ARENA, E. T., HAN, J., FERREIRA, R. B., BORCHERS, C. H. & FINLAY, B. B. 2011. Metabolomics reveals phospholipids as important nutrient sources during *Salmonella* growth in bile *in vitro* and *in vivo*. *J Bacteriol,* 193**,** 4719-25.

AO, T. T., FEASEY, N. A., GORDON, M. A., KEDDY, K. H., ANGULO, F. J. & CRUMP, J. A. 2015. Global burden of invasive nontyphoidal *Salmonella* disease, 2010(1). *Emerg Infect Dis,* 21.

BABA, T., ARA, T., HASEGAWA, M., TAKAI, Y., OKUMURA, Y., BABA, M., DATSENKO, K. A., TOMITA, M., WANNER, B. L. & MORI, H. 2006. Construction of *Escherichia coli* K-12 in-frame, single-gene knockout mutants: the Keio collection. *Mol Syst Biol,* 2**,** 2006 0008.

BAKER, S. & DOUGAN, G. 2007. The genome of *Salmonella enterica* serovar Typhi. *Clin Infect Dis,* 45 Suppl 1**,** S29-33.

BAKOWSKI, M. A., BRAUN, V., LAM, G. Y., YEUNG, T., HEO, W. D., MEYER, T., FINLAY, B. B., GRINSTEIN, S. & BRUMELL, J. H. 2010. The phosphoinositide phosphatase SopB manipulates membrane surface charge and trafficking of the *Salmonella*-containing vacuole. *Cell Host Microbe,* 7**,** 453-62.

BARNARD, T. J., DAUTIN, N., LUKACIK, P., BERNSTEIN, H. D. & BUCHANAN, S. K. 2007. Autotransporter structure reveals intra-barrel cleavage followed by conformational changes. *Nat Struct Mol Biol,* 14**,** 1214-20.

BECHTLUFT, P., NOUWEN, N., TANS, S. J. & DRIESSEN, A. J. 2010. SecB--a chaperone dedicated to protein translocation. *Mol Biosyst,* 6**,** 620-7.

BERGSBAKEN, T., FINK, S. L. & COOKSON, B. T. 2009. Pyroptosis: host cell death and inflammation. *Nat Rev Microbiol,* 7**,** 99-109.

BIRGE, R. B., BOELTZ, S., KUMAR, S., CARLSON, J., WANDERLEY, J., CALIANESE, D., BARCINSKI, M., BREKKEN, R. A., HUANG, X., HUTCHINS, J. T., FREIMARK, B., EMPIG, C., MERCER, J., SCHROIT, A. J., SCHETT, G. & HERRMANN, M. 2016. Phosphatidylserine is a global immunosuppressive signal in efferocytosis, infectious disease, and cancer. *Cell Death Differ,* 23**,** 962-78.

BODELON, G., MARIN, E. & FERNANDEZ, L. A. 2009. Role of periplasmic chaperones and BamA (YaeT/Omp85) in folding and secretion of intimin from enteropathogenic *Escherichia coli* strains. *J Bacteriol,* 191**,** 5169-79.

BOYEN, F., PASMANS, F., DONNE, E., VAN IMMERSEEL, F., MORGAN, E., ADRIAENSEN, C., HERNALSTEENS, J. P., WALLIS, T. S., DUCATELLE, R. & HAESEBROUCK, F. 2006. The fibronectin binding protein ShdA is not a prerequisite for long term faecal shedding of *Salmonella* typhimurium in pigs. *Vet Microbiol,* 115**,** 284-90.

BOYER, H. W. & ROULLAND-DUSSOIX, D. 1969. A complementation analysis of the restriction and modification of DNA in *Escherichia coli*. *J Mol Biol,* 41**,** 459-72.

BOYER, J. L. 2013. Bile formation and secretion. *Compr Physiol,* 3**,** 1035-78.

BRZOSKA, P., RIMMELE, M., BRZOSTEK, K. & BOOS, W. 1994. The pho regulon-dependent Ugp uptake system for glycerol-3-phosphate in *Escherichia coli* is trans inhibited by Pi. *J Bacteriol,* 176**,** 15-20.

BUCKLE, G. C., WALKER, C. L. & BLACK, R. E. 2012. Typhoid fever and paratyphoid fever: Systematic review to estimate global morbidity and mortality for 2010. *J Glob Health,* 2**,** 010401.

BUCKLEY, J. T. 1982. Substrate specificity of bacterial glycerophospholipid:cholesterol acyltransferase. *Biochemistry,* 21**,** 6699-703.

CAI, X., WANG, W., LIN, L., HE, D., HUANG, G., SHEN, Y., WEI, W. & WEI, D. 2017. Autotransporter domain-dependent enzymatic analysis of a novel extremely thermostable carboxylesterase with high biodegradability towards pyrethroid pesticides. *Sci Rep,* 7**,** 3461.

CAREY, M. C. & SMALL, D. M. 1978. The physical chemistry of cholesterol solubility in bile. Relationship to gallstone formation and dissolution in man. *J Clin Invest,* 61**,** 998-1026.

CARINATO, M. E., COLLIN-OSDOBY, P., YANG, X., KNOX, T. M., CONLIN, C. A. & MILLER, C. G. 1998. The *apeE* gene of *Salmonella typhimurium* encodes an outer membrane esterase not present in *Escherichia coli*. *J Bacteriol,* 180**,** 3517-21.

CAROFF, M. & KARIBIAN, D. 2003. Structure of bacterial lipopolysaccharides. *Carbohydr Res,* 338**,** 2431-47.

CASASANTA, M. A., YOO, C. C., SMITH, H. B., DUNCAN, A. J., COCHRANE, K., VARANO, A. C., ALLEN-VERCOE, E. & SLADE, D. J. 2017. A chemical and biological toolbox for Type Vd secretion: Characterization of the phospholipase A1 autotransporter FplA from *Fusobacterium nucleatum*. *J Biol Chem,* 292**,** 20240-20254.

CHARLSON, E. S., WERNER, J. N. & MISRA, R. 2006. Differential effects of *yfgL* mutation on *Escherichia coli* outer membrane proteins and lipopolysaccharide. *J Bacteriol,* 188**,** 7186-94.

CHAUDHURI, R. R., MORGAN, E., PETERS, S. E., PLEASANCE, S. J., HUDSON, D. L., DAVIES, H. M., WANG, J., VAN DIEMEN, P. M., BUCKLEY, A. M., BOWEN, A. J., PULLINGER, G. D., TURNER, D. J., LANGRIDGE, G. C., TURNER, A. K., PARKHILL, J., CHARLES, I. G., MASKELL, D. J. & STEVENS, M. P. 2013. Comprehensive assignment of roles for *Salmonella typhimurium* genes in intestinal colonization of food-producing animals. *PLoS Genet,* 9**,** e1003456.

CHEMINAY, C., MOHLENBRINK, A. & HENSEL, M. 2005. Intracellular *Salmonella* inhibit antigen presentation by dendritic cells. *J Immunol,* 174**,** 2892-9.

CHIU, C. H., SU, L. H. & CHU, C. 2004. *Salmonella enterica* serotype Choleraesuis: epidemiology, pathogenesis, clinical disease, and treatment. *Clin Microbiol Rev,* 17**,** 311-22.

CHOU, M. M. & KENDALL, D. A. 1990. Polymeric sequences reveal a functional interrelationship between hydrophobicity and length of signal peptides. *J Biol Chem,* 265**,** 2873-80.

CHRISTEN, M., COYE, L. H., HONTZ, J. S., LAROCK, D. L., PFUETZNER, R. A., MEGHA & MILLER, S. I. 2009. Activation of a bacterial virulence protein by the GTPase RhoA. *Sci Signal,* 2**,** ra71.

CHUA, C. E., LIM, Y. S. & TANG, B. L. 2010. Rab35--a vesicular traffic-regulating small GTPase with actin modulating roles. *FEBS Lett,* 584**,** 1-6.

CLANTIN, B., DELATTRE, A. S., RUCKTOOA, P., SAINT, N., MELI, A. C., LOCHT, C., JACOB-DUBUISSON, F. & VILLERET, V. 2007. Structure of the membrane protein FhaC: a member of the Omp85-TpsB transporter superfamily. *Science,* 317**,** 957-61.

CLARK, D. P. & CRONAN, J. E. 2005. Two-Carbon Compounds and Fatty Acids as Carbon Sources. *EcoSal Plus,* 1.

COBURN, B., SEKIROV, I. & FINLAY, B. B. 2007. Type III secretion systems and disease. *Clin Microbiol Rev,* 20**,** 535-49.

COLEMAN, J. J. 2016. The *Fusarium solani* species complex: ubiquitous pathogens of agricultural importance. *Mol Plant Pathol,* 17**,** 146-58.

CONLIN, C. A., TAN, S. L., HU, H. & SEGAR, T. 2001. The *apeE* gene of *Salmonella enterica* serovar Typhimurium is induced by phosphate limitation and regulated by phoBR. *J Bacteriol,* 183**,** 1784-6.

COSTA, T. R., FELISBERTO-RODRIGUES, C., MEIR, A., PREVOST, M. S., REDZEJ, A., TROKTER, M. & WAKSMAN, G. 2015. Secretion systems in Gram-negative bacteria: structural and mechanistic insights. *Nat Rev Microbiol,* 13**,** 343-59.

COTTER, S. E., SURANA, N. K. & ST GEME, J. W., 3RD 2005. Trimeric autotransporters: a distinct subfamily of autotransporter proteins. *Trends Microbiol,* 13**,** 199-205.

CRAWFORD, N. & BROOKE, B. N. 1955. The pH and buffering power of human bile. *Lancet,* 268**,** 1096-7.

CRAWFORD, R. W., ROSALES-REYES, R., RAMIREZ-AGUILAR MDE, L., CHAPA-AZUELA, O., ALPUCHE-ARANDA, C. & GUNN, J. S. 2010. Gallstones play a significant role in *Salmonella* spp. gallbladder colonization and carriage. *Proc Natl Acad Sci U S A,* 107**,** 4353-8.

DA MATA MADEIRA, P. V., ZOUHIR, S., BASSO, P., NEVES, D., LAUBIER, A., SALACHA, R., BLEVES, S., FAUDRY, E., CONTRERAS-MARTEL, C. & DESSEN, A. 2016. Structural Basis of Lipid Targeting and Destruction by the Type V Secretion System of *Pseudomonas aeruginosa*. *J Mol Biol,* 428**,** 1790-803.

DALBEY, R. E., LIVELY, M. O., BRON, S. & VAN DIJL, J. M. 1997. The chemistry and enzymology of the type I signal peptidases. *Protein Sci,* 6**,** 1129-38.

DATSENKO, K. A. & WANNER, B. L. 2000. One-step inactivation of chromosomal genes in *Escherichia coli* K-12 using PCR products. *Proc Natl Acad Sci U S A,* 97**,** 6640-5.

DE JONG, H. K., PARRY, C. M., VAN DER POLL, T. & WIERSINGA, W. J. 2012. Host-pathogen interaction in invasive Salmonellosis. *PLoS Pathog,* 8**,** e1002933.

DE MATTEIS, M. A. & GODI, A. 2004. PI-loting membrane traffic. *Nat Cell Biol,* 6**,** 487-92.

DEL POZO, J. L. 2018. Biofilm-related disease. *Expert Rev Anti Infect Ther,* 16**,** 51-65.

DELCOUR, A. H. 2009. Outer membrane permeability and antibiotic resistance. *Biochim Biophys Acta,* 1794**,** 808-16.

DEPLUVEREZ, S., DEVOS, S. & DEVREESE, B. 2016. The Role of Bacterial Secretion Systems in the Virulence of Gram-Negative Airway Pathogens Associated with Cystic Fibrosis. *Front Microbiol,* 7**,** 1336.

DESVAUX, M., PARHAM, N. J. & HENDERSON, I. R. 2004. The autotransporter secretion system. *Res Microbiol,* 155**,** 53-60.

DEVINNEY, R., STEIN, M., REINSCHEID, D., ABE, A., RUSCHKOWSKI, S. & FINLAY, B. B. 1999. Enterohemorrhagic *Escherichia coli* O157:H7 produces Tir, which is translocated to the host cell membrane but is not tyrosine phosphorylated. *Infect Immun,* 67**,** 2389-98.

DIAL, E. J., DAWSON, P. A. & LICHTENBERGER, L. M. 2015. *In vitro* evidence that phosphatidylcholine protects against indomethacin/bile acid-induced injury to cells. *Am J Physiol Gastrointest Liver Physiol,* 308**,** G217-22.

DONG, C., YANG, X., HOU, H. F., SHEN, Y. Q. & DONG, Y. H. 2012. Structure of *Escherichia coli* BamB and its interaction with POTRA domains of BamA. *Acta Crystallogr D Biol Crystallogr,* 68**,** 1134-9.

DORRELL, N., MARTINO, M. C., STABLER, R. A., WARD, S. J., ZHANG, Z. W., MCCOLM, A. A., FARTHING, M. J. & WREN, B. W. 1999. Characterization of *Helicobacter pylori* PldA, a phospholipase with a role in colonization of the gastric mucosa. *Gastroenterology,* 117**,** 1098-104.

DORSEY, C. W., LAARAKKER, M. C., HUMPHRIES, A. D., WEENING, E. H. & BAUMLER, A. J. 2005. *Salmonella enterica* serotype Typhimurium MisL is an intestinal colonization factor that binds fibronectin. *Mol Microbiol,* 57**,** 196-211.

DU PLESSIS, D. J., BERRELKAMP, G., NOUWEN, N. & DRIESSEN, A. J. 2009. The lateral gate of SecYEG opens during protein translocation. *J Biol Chem,* 284**,** 15805-14.

EHRBAR, K., MIROLD, S., FRIEBEL, A., STENDER, S. & HARDT, W. D. 2002. Characterization of effector proteins translocated via the SPI1 type III secretion system of *Salmonella* typhimurium. *Int J Med Microbiol,* 291**,** 479-85.

ELVIN, C. M., HARDY, C. M. & ROSENBERG, H. 1985. Pi exchange mediated by the GlpT-dependent sn-glycerol-3-phosphate transport system in *Escherichia coli*. *J Bacteriol,* 161**,** 1054-8.

FALLINGBORG, J. 1999. Intraluminal pH of the human gastrointestinal tract. *Dan Med Bull,* 46**,** 183-96.

FIERER, J. & GUINEY, D. G. 2001. Diverse virulence traits underlying different clinical outcomes of *Salmonella* infection. *J Clin Invest,* 107**,** 775-80.

GALAN, J. E. 1999. Interaction of Salmonella with host cells through the centisome 63 type III secretion system. *Curr Opin Microbiol,* 2**,** 46-50.

GARCIA, B., LATASA, C., SOLANO, C., GARCIA-DEL PORTILLO, F., GAMAZO, C. & LASA, I. 2004. Role of the GGDEF protein family in *Salmonella* cellulose biosynthesis and biofilm formation. *Mol Microbiol,* 54**,** 264-77.

GASPAR, A. H. & MACHNER, M. P. 2014. VipD is a Rab5-activated phospholipase A1 that protects *Legionella pneumophila* from endosomal fusion. *Proc Natl Acad Sci U S A,* 111**,** 4560-5.

GIRARD, A. L., MOUNET, F., LEMAIRE-CHAMLEY, M., GAILLARD, C., ELMORJANI, K., VIVANCOS, J., RUNAVOT, J. L., QUEMENER, B., PETIT, J., GERMAIN, V., ROTHAN, C., MARION, D. & BAKAN, B. 2012. Tomato GDSL1 is required for cutin deposition in the fruit cuticle. *Plant Cell,* 24**,** 3119-34.

GOLUBEVA, Y. A., ELLERMEIER, J. R., COTT CHUBIZ, J. E. & SLAUCH, J. M. 2016. Intestinal Long-Chain Fatty Acids Act as a Direct Signal To Modulate Expression of the *Salmonella* Pathogenicity Island 1 Type III Secretion System. *MBio,* 7**,** e02170-15.

GONZALEZ-ESCOBEDO, G. & GUNN, J. S. 2013. Gallbladder epithelium as a niche for chronic *Salmonella* carriage. *Infect Immun,* 81**,** 2920-30.

GONZALEZ-ESCOBEDO, G., MARSHALL, J. M. & GUNN, J. S. 2011. Chronic and acute infection of the gall bladder by *Salmonella* Typhi: understanding the carrier state. *Nat Rev Microbiol,* 9**,** 9-14.

GONZALEZ, J. F., ALBERTS, H., LEE, J., DOOLITTLE, L. & GUNN, J. S. 2018. Biofilm Formation Protects *Salmonella* from the Antibiotic Ciprofloxacin *In Vitro* and *In Vivo* in the Mouse Model of chronic Carriage. *Sci Rep,* 8**,** 222.

GORDON, M. A. 2008. *Salmonella* infections in immunocompromised adults. *J Infect,* 56**,** 413-22.

GOVONI, G. & GROS, P. 1998. Macrophage NRAMP1 and its role in resistance to microbial infections. *Inflamm Res,* 47**,** 277-84.

GRIN, I., HARTMANN, M. D., SAUER, G., HERNANDEZ ALVAREZ, B., SCHUTZ, M., WAGNER, S., MADLUNG, J., MACEK, B., FELIPE-LOPEZ, A., HENSEL, M., LUPAS, A. & LINKE, D. 2014. A trimeric lipoprotein assists in trimeric autotransporter biogenesis in enterobacteria. *J Biol Chem,* 289**,** 7388-98.

GROISMAN, E. A. 2001. The Pleiotropic Two-Component Regulatory System PhoP-PhoQ. *Journal of Bacteriology*.

GROSSKINSKY, U., SCHUTZ, M., FRITZ, M., SCHMID, Y., LAMPARTER, M. C., SZCZESNY, P., LUPAS, A. N., AUTENRIETH, I. B. & LINKE, D. 2007. A conserved glycine residue of trimeric autotransporter domains plays a key role in *Yersinia* adhesin A autotransport. *J Bacteriol,* 189**,** 9011-9.

GUNN, A. & KEDDIE, N. 1972. Some clinical observations on patients with gallstones. *Lancet,* 2**,** 239-41.

GUNN, J. S., MARSHALL, J. M., BAKER, S., DONGOL, S., CHARLES, R. C. & RYAN, E. T. 2014. *Salmonella* chronic carriage: epidemiology, diagnosis, and gallbladder persistence. *Trends Microbiol,* 22**,** 648-55.

HAGAN, C. L., KIM, S. & KAHNE, D. 2010. Reconstitution of outer membrane protein assembly from purified components. *Science,* 328**,** 890-2.

HALPERN, Z., MOSHKOWITZ, M., LAUFER, H., PELED, Y. & GILAT, T. 1993. Effect of phospholipids and their molecular species on cholesterol solubility and nucleation in human and model biles. *Gut,* 34**,** 110-5.

HAN, L., ZHENG, J., WANG, Y., YANG, X., LIU, Y., SUN, C., CAO, B., ZHOU, H., NI, D., LOU, J., ZHAO, Y. & HUANG, Y. 2016. Structure of the BAM complex and its implications for biogenesis of outer-membrane proteins. *Nat Struct Mol Biol,* 23**,** 192-6.

HARTMANN, M. D., GRIN, I., DUNIN-HORKAWICZ, S., DEISS, S., LINKE, D., LUPAS, A. N. & HERNANDEZ ALVAREZ, B. 2012. Complete fiber structures of complex trimeric autotransporter adhesins conserved in enterobacteria. *Proc Natl Acad Sci U S A,* 109**,** 20907-12.

HAYASHI, F., SMITH, K. D., OZINSKY, A., HAWN, T. R., YI, E. C., GOODLETT, D. R., ENG, J. K., AKIRA, S., UNDERHILL, D. M. & ADEREM, A. 2001. The innate immune response to bacterial flagellin is mediated by Toll-like receptor 5. *Nature,* 410**,** 1099-103.

HEGDE, R. S. & BERNSTEIN, H. D. 2006. The surprising complexity of signal sequences. *Trends Biochem Sci,* 31**,** 563-71.

HEINZ, E. & LITHGOW, T. 2014. A comprehensive analysis of the Omp85/TpsB protein superfamily structural diversity, taxonomic occurrence, and evolution. *Front Microbiol,* 5**,** 370.

HELFER, S. 2014. Rust fungi and global change. *New Phytol,* 201**,** 770-80.

HENDERSON, I. R., CZECZULIN, J., ESLAVA, C., NORIEGA, F. & NATARO, J. P. 1999. Characterization of *pic*, a secreted protease of *Shigella flexneri* and enteroaggregative *Escherichia coli*. *Infect Immun,* 67**,** 5587-96.

HENDERSON, I. R., MEEHAN, M. & OWEN, P. 1997. Antigen 43, a phase-variable bipartite outer membrane protein, determines colony morphology and autoaggregation in *Escherichia coli* K-12. *FEMS Microbiol Lett,* 149**,** 115-20.

HENDERSON, I. R., NAVARRO-GARCIA, F., DESVAUX, M., FERNANDEZ, R. C. & ALA'ALDEEN, D. 2004. Type V protein secretion pathway: the autotransporter story. *Microbiol Mol Biol Rev,* 68**,** 692-744.

HENGGE, R., LARSON, T. J. & BOOS, W. 1983. sn-Glycerol-3-phosphate transport in *Salmonella typhimurium*. *J Bacteriol,* 155**,** 186-95.

HERNANDEZ ALVAREZ, B., HARTMANN, M. D., ALBRECHT, R., LUPAS, A. N., ZETH, K. & LINKE, D. 2008. A new expression system for protein crystallization using trimeric coiled-coil adaptors. *Protein Eng Des Sel,* 21**,** 11-8.

HERNANDEZ, L. D., HUEFFER, K., WENK, M. R. & GALAN, J. E. 2004. *Salmonella* modulates vesicular traffic by altering phosphoinositide metabolism. *Science,* 304**,** 1805-7.

HERNANDEZ, S. B., COTA, I., DUCRET, A., AUSSEL, L. & CASADESUS, J. 2012. Adaptation and preadaptation of *Salmonella enterica* to Bile. *PLoS Genet,* 8**,** e1002459.

HOISETH, S. K. & STOCKER, B. A. 1981. Aromatic-dependent *Salmonella* typhimurium are non-virulent and effective as live vaccines. *Nature,* 291**,** 238-9.

IADANZA, M. G., HIGGINS, A. J., SCHIFFRIN, B., CALABRESE, A. N., BROCKWELL, D. J., ASHCROFT, A. E., RADFORD, S. E. & RANSON, N. A. 2016. Lateral opening

in the intact beta-barrel assembly machinery captured by cryo-EM. *Nat Commun,* 7**,** 12865.

IBARRA, J. A. & STEELE-MORTIMER, O. 2009. *Salmonella*--the ultimate insider. *Salmonella* virulence factors that modulate intracellular survival. *Cell Microbiol,* 11**,** 1579-86.

IRAM, S. H. & CRONAN, J. E. 2006. The beta-oxidation systems of *Escherichia coli* and *Salmonella enterica* are not functionally equivalent. *J Bacteriol,* 188**,** 599-608.

JACOB-DUBUISSON, F., LOCHT, C. & ANTOINE, R. 2001. Two-partner secretion in Gram-negative bacteria: a thrifty, specific pathway for large virulence proteins. *Mol Microbiol,* 40**,** 306-13.

JAIN, S. & GOLDBERG, M. B. 2007. Requirement for YaeT in the outer membrane assembly of autotransporter proteins. *J Bacteriol,* 189**,** 5393-8.

JAZRAWI, R. P., PAZZI, P., PETRONI, M. L., PRANDINI, N., PAUL, C., ADAM, J. A., GULLINI, S. & NORTHFIELD, T. C. 1995. Postprandial gallbladder motor function: refilling and turnover of bile in health and in cholelithiasis. *Gastroenterology,* 109**,** 582-91.

JEPSON, M. A. & CLARK, M. A. 2001. The role of M cells in *Salmonella* infection. *Microbes Infect,* 3**,** 1183-90.

JERSE, A. E., YU, J., TALL, B. D. & KAPER, J. B. 1990. A genetic locus of enteropathogenic *Escherichia coli* necessary for the production of attaching and effacing lesions on tissue culture cells. *Proc Natl Acad Sci U S A,* 87**,** 7839-43.

JIANG, J., YU ID, K., QI, L., LIU, Y., CHENG, S., WU, M., WANG, Z., FU, J. & XIAOYUN, L. 2018. A Proteomic View of *Salmonella* Typhimurium in Response to Phosphate Limitation. *Proteome,* 6.

JOHANNS, T. M., ERTELT, J. M., ROWE, J. H. & WAY, S. S. 2010. Regulatory T cell suppressive potency dictates the balance between bacterial proliferation and clearance during persistent *Salmonella* infection. *PLoS Pathog,* 6**,** e1001043.

JOHNSON, R., MYLONA, E. & FRANKEL, G. 2018a. Typhoidal *Salmonella*: Distinctive virulence factors and pathogenesis. *Cell Microbiol,* 20**,** e12939.

JOHNSON, R., RAVENHALL, M., PICKARD, D., DOUGAN, G., BYRNE, A. & FRANKEL, G. 2018b. Comparison of *Salmonella enterica* Serovars Typhi and Typhimurium Reveals Typhoidal Serovar-Specific Responses to Bile. *Infect Immun,* 86.

JOMAA, A., BOEHRINGER, D., LEIBUNDGUT, M. & BAN, N. 2016. Structures of the *E. coli* translating ribosome with SRP and its receptor and with the translocon. *Nat Commun,* 7**,** 10471.

KASAHARA, M., MAKINO, K., AMEMURA, M., NAKATA, A. & SHINAGAWA, H. 1991. Dual regulation of the *ugp* operon by phosphate and carbon starvation at two interspaced promoters. *J Bacteriol,* 173**,** 549-58.

KELLEY, L. 2015. The Phyre2 web portal for protein modeling, prediction and analysis. *Nature Protocols*, 845-858.

KHAN, S., MIAN, H. S., SANDERCOCK, L. E., CHIRGADZE, N. Y. & PAI, E. F. 2011. Crystal structure of the passenger domain of the *Escherichia coli* autotransporter EspP. *J Mol Biol,* 413, 985-1000.

KINGSLEY, R. A., SANTOS, R. L., KEESTRA, A. M., ADAMS, L. G. & BAUMLER, A. J. 2002. *Salmonella enterica* serotype Typhimurium ShdA is an outer membrane fibronectin-binding protein that is expressed in the intestine. *Mol Microbiol,* 43, 895-905.

KINGSLEY, R. A., VAN AMSTERDAM, K., KRAMER, N. & BAUMLER, A. J. 2000. The *shdA* gene is restricted to serotypes of *Salmonella enterica* subspecies I and contributes to efficient and prolonged fecal shedding. *Infect Immun,* 68, 2720-7.

KNOWLES, T. J., BROWNING, D. F., JEEVES, M., MADERBOCUS, R., RAJESH, S., SRIDHAR, P., MANOLI, E., EMERY, D., SOMMER, U., SPENCER, A., LEYTON, D. L., SQUIRE, D., CHAUDHURI, R. R., VIANT, M. R., CUNNINGHAM, A. F., HENDERSON, I. R. & OVERDUIN, M. 2011. Structure and function of BamE within the outer membrane and the beta-barrel assembly machine. *EMBO Rep,* 12, 123-8.

KNOWLES, T. J., JEEVES, M., BOBAT, S., DANCEA, F., MCCLELLAND, D., PALMER, T., OVERDUIN, M. & HENDERSON, I. R. 2008. Fold and function of polypeptide transport-associated domains responsible for delivering unfolded proteins to membranes. *Mol Microbiol,* 68, 1216-27.

KNOWLES, T. J., SCOTT-TUCKER, A., OVERDUIN, M. & HENDERSON, I. R. 2009. Membrane protein architects: the role of the BAM complex in outer membrane protein assembly. *Nat Rev Microbiol,* 7, 206-14.

KOLODZIEJEK, A. M. & MILLER, S. I. 2015. *Salmonella* modulation of the phagosome membrane, role of SseJ. *Cell Microbiol,* 17, 333-41.

KOSHIOL, J., WOZNIAK, A., COOK, P., ADANIEL, C., ACEVEDO, J., AZOCAR, L., HSING, A. W., ROA, J. C., PASETTI, M. F., MIQUEL, J. F., LEVINE, M. M., FERRECCIO, C. & GALLBLADDER CANCER CHILE WORKING, G. 2016. *Salmonella enterica* serovar Typhi and gallbladder cancer: a case-control study and meta-analysis. *Cancer Med,* 5, 3310-3235.

KRIVAN, H. C., FRANKLIN, D. P., WANG, W., LAUX, D. C. & COHEN, P. S. 1992. Phosphatidylserine found in intestinal mucus serves as a sole source of carbon and nitrogen for salmonellae and *Escherichia coli*. *Infect Immun,* 60, 3943-6.

KUBORI, T., MATSUSHIMA, Y., NAKAMURA, D., URALIL, J., LARA-TEJERO, M., SUKHAN, A., GALAN, J. E. & AIZAWA, S. I. 1998. Supramolecular structure of the *Salmonella typhimurium* type III protein secretion system. *Science,* 280, 602-5.

KUDVA, R., DENKS, K., KUHN, P., VOGT, A., MULLER, M. & KOCH, H. G. 2013. Protein translocation across the inner membrane of Gram-negative bacteria: the Sec and Tat dependent protein transport pathways. *Res Microbiol,* 164, 505-34.

KUPZ, A., BEDOUI, S. & STRUGNELL, R. A. 2014a. Cellular requirements for systemic control of *Salmonella enterica* serovar Typhimurium infections in mice. *Infect Immun,* 82**,** 4997-5004.

KUPZ, A., CURTISS, R., 3RD, BEDOUI, S. & STRUGNELL, R. A. 2014b. In vivo IFN-gamma secretion by NK cells in response to *Salmonella typhimurium* requires NLRC4 inflammasomes. *PLoS One,* 9**,** e97418.

LAI, Y., ROSENSHINE, I., LEONG, J. M. & FRANKEL, G. 2013. Intimate host attachment: enteropathogenic and enterohaemorrhagic *Escherichia coli*. *Cell Microbiol,* 15**,** 1796-808.

LARSON, T. J., EHRMANN, M. & BOOS, W. 1983. Periplasmic glycerophosphodiester phosphodiesterase of *Escherichia coli*, a new enzyme of the *glp* regulon. *J Biol Chem,* 258**,** 5428-32.

LAZAR, S. W. & KOLTER, R. 1996. SurA assists the folding of *Escherichia coli* outer membrane proteins. *J Bacteriol,* 178**,** 1770-3.

LEHR, U., SCHUTZ, M., OBERHETTINGER, P., RUIZ-PEREZ, F., DONALD, J. W., PALMER, T., LINKE, D., HENDERSON, I. R. & AUTENRIETH, I. B. 2010. C-terminal amino acid residues of the trimeric autotransporter adhesin YadA of *Yersinia enterocolitica* are decisive for its recognition and assembly by BamA. *Mol Microbiol,* 78**,** 932-46.

LELOUARD, H., FALLET, M., DE BOVIS, B., MERESSE, S. & GORVEL, J. P. 2012. Peyer's patch dendritic cells sample antigens by extending dendrites through M cell-specific transcellular pores. *Gastroenterology,* 142**,** 592-601 e3.

LEO, J. C., ELOVAARA, H., BIHAN, D., PUGH, N., KILPINEN, S. K., RAYNAL, N., SKURNIK, M., FARNDALE, R. W. & GOLDMAN, A. 2010. First analysis of a bacterial collagen-binding protein with collagen Toolkits: promiscuous binding of YadA to collagens may explain how YadA interferes with host processes. *Infect Immun,* 78**,** 3226-36.

LEO, J. C., GRIN, I. & LINKE, D. 2012. Type V secretion: mechanism(s) of autotransport through the bacterial outer membrane. *Philos Trans R Soc Lond B Biol Sci,* 367**,** 1088-101.

LEO, J. C., OBERHETTINGER, P., SCHUTZ, M. & LINKE, D. 2014. The inverse autotransporter family: Intimin, invasin and related proteins. *Int J Med Microbiol*.

LESCIC ASLER, I., IVIC, N., KOVACIC, F., SCHELL, S., KNORR, J., KRAUSS, U., WILHELM, S., KOJIC-PRODIC, B. & JAEGER, K. E. 2010. Probing enzyme promiscuity of SGNH hydrolases. *Chembiochem,* 11**,** 2158-67.

LEVENTIS, P. A. & GRINSTEIN, S. 2010. The distribution and function of phosphatidylserine in cellular membranes. *Annu Rev Biophys,* 39**,** 407-27.

LEYTON, D. L., ROSSITER, A. E. & HENDERSON, I. R. 2012. From self sufficiency to dependence: mechanisms and factors important for autotransporter biogenesis. *Nat Rev Microbiol,* 10**,** 213-25.

LEYTON, D. L., SEVASTSYANOVICH, Y. R., BROWNING, D. F., ROSSITER, A. E., WELLS, T. J., FITZPATRICK, R. E., OVERDUIN, M., CUNNINGHAM, A. F. & HENDERSON, I. R. 2011. Size and conformation limits to secretion of disulfide-bonded loops in autotransporter proteins. *J Biol Chem,* 286**,** 42283-91.

LINKE, D., RIESS, T., AUTENRIETH, I. B., LUPAS, A. & KEMPF, V. A. 2006. Trimeric autotransporter adhesins: variable structure, common function. *Trends Microbiol,* 14**,** 264-70.

LIO, Y. C., REYNOLDS, L. J., BALSINDE, J. & DENNIS, E. A. 1996. Irreversible inhibition of Ca(2+)-independent phospholipase A2 by methyl arachidonyl fluorophosphonate. *Biochim Biophys Acta,* 1302**,** 55-60.

LIU, Y., ZHANG, Q., HU, M., YU, K., FU, J., ZHOU, F. & LIU, X. 2015. Proteomic Analyses of Intracellular *Salmonella enterica* Serovar Typhimurium Reveal Extensive Bacterial Adaptations to Infected Host Epithelial Cells. *Infect Immun,* 83**,** 2897-906.

LIU, Z., NIU, H., WU, S. & HUANG, R. 2014. CsgD regulatory network in a bacterial trait-altering biofilm formation. *Emerg Microbes Infect,* 3**,** e1.

LOSSI, N. S., ROLHION, N., MAGEE, A. I., BOYLE, C. & HOLDEN, D. W. 2008. The *Salmonella* SPI-2 effector SseJ exhibits eukaryotic activator-dependent phospholipase A and glycerophospholipid : cholesterol acyltransferase activity. *Microbiology,* 154**,** 2680-8.

LUIRINK, J. & SINNING, I. 2004. SRP-mediated protein targeting: structure and function revisited. *Biochim Biophys Acta,* 1694**,** 17-35.

MACLENNAN, C. A., GILCHRIST, J. J., GORDON, M. A., CUNNINGHAM, A. F., COBBOLD, M., GOODALL, M., KINGSLEY, R. A., VAN OOSTERHOUT, J. J., MSEFULA, C. L., MANDALA, W. L., LEYTON, D. L., MARSHALL, J. L., GONDWE, E. N., BOBAT, S., LOPEZ-MACIAS, C., DOFFINGER, R., HENDERSON, I. R., ZIJLSTRA, E. E., DOUGAN, G., DRAYSON, M. T., MACLENNAN, I. C. & MOLYNEUX, M. E. 2010. Dysregulated humoral immunity to nontyphoidal *Salmonella* in HIV-infected African adults. *Science,* 328**,** 508-12.

MALINVERNI, J. C., WERNER, J., KIM, S., SKLAR, J. G., KAHNE, D., MISRA, R. & SILHAVY, T. J. 2006. YfiO stabilizes the YaeT complex and is essential for outer membrane protein assembly in *Escherichia coli*. *Mol Microbiol,* 61**,** 151-64.

MALLO, G. V., ESPINA, M., SMITH, A. C., TEREBIZNIK, M. R., ALEMAN, A., FINLAY, B. B., RAMEH, L. E., GRINSTEIN, S. & BRUMELL, J. H. 2008. SopB promotes phosphatidylinositol 3-phosphate formation on *Salmonella* vacuoles by recruiting Rab5 and Vps34. *J Cell Biol,* 182**,** 741-52.

MARINELI, F., TSOUCALAS, G., KARAMANOU, M. & ANDROUTSOS, G. 2013. Mary Mallon (1869-1938) and the history of typhoid fever. *Ann Gastroenterol,* 26**,** 132-134.

MCCLELLAND, M., SANDERSON, K. E., CLIFTON, S. W., LATREILLE, P., PORWOLLIK, S., SABO, A., MEYER, R., BIERI, T., OZERSKY, P., MCLELLAN, M., HARKINS, C. R., WANG, C., NGUYEN, C., BERGHOFF, A., ELLIOTT, G., KOHLBERG, S., STRONG, C., DU, F., CARTER, J., KREMIZKI, C., LAYMAN, D.,

LEONARD, S., SUN, H., FULTON, L., NASH, W., MINER, T., MINX, P., DELEHAUNTY, K., FRONICK, C., MAGRINI, V., NHAN, M., WARREN, W., FLOREA, L., SPIETH, J. & WILSON, R. K. 2004. Comparison of genome degradation in Paratyphi A and Typhi, human-restricted serovars of *Salmonella enterica* that cause typhoid. *Nat Genet,* 36**,** 1268-74.

MCCORMICK, B. A., HOFMAN, P. M., KIM, J., CARNES, D. K., MILLER, S. I. & MADARA, J. L. 1995. Surface attachment of *Salmonella typhimurium* to intestinal epithelia imprints the subepithelial matrix with gradients chemotactic for neutrophils. *J Cell Biol,* 131**,** 1599-608.

MCINTOSH, A., MEIKLE, L. M., ORMSBY, M. J., MCCORMICK, B. A., CHRISTIE, J. M., BREWER, J. M., ROBERTS, M. & WALL, D. M. 2017. SipA Activation of Caspase-3 Is a Decisive Mediator of Host Cell Survival at Early Stages of *Salmonella enterica* Serovar Typhimurium Infection. *Infect Immun,* 85.

MCMURRAY, H. F., PARTHASARATHY, S. & STEINBERG, D. 1993. Oxidatively modified low density lipoprotein is a chemoattractant for human T lymphocytes. *J Clin Invest,* 92**,** 1004-8.

MEDZHITOV, R. 2001. Toll-like receptors and innate immunity. *Nat Rev Immunol,* 1**,** 135-45.

MENENDEZ, A., ARENA, E. T., GUTTMAN, J. A., THORSON, L., VALLANCE, B. A., VOGL, W. & FINLAY, B. B. 2009. *Salmonella* infection of gallbladder epithelial cells drives local inflammation and injury in a model of acute typhoid fever. *J Infect Dis,* 200**,** 1703-13.

MERESSE, S., UNSWORTH, K. E., HABERMANN, A., GRIFFITHS, G., FANG, F., MARTINEZ-LORENZO, M. J., WATERMAN, S. R., GORVEL, J. P. & HOLDEN, D. W. 2001. Remodelling of the actin cytoskeleton is essential for replication of intravacuolar *Salmonella*. *Cell Microbiol,* 3**,** 567-77.

MERRITT, M. E. & DONALDSON, J. R. 2009. Effect of bile salts on the DNA and membrane integrity of enteric bacteria. *J Med Microbiol,* 58**,** 1533-41.

MILLER, S. I., KUKRAL, A. M. & MEKALANOS, J. J. 1989. A two-component regulatory system (*phoP phoQ*) controls *Salmonella typhimurium* virulence. *Proc Natl Acad Sci U S A,* 86**,** 5054-8.

MORRIS, F. C. 2013. *The role of outer membrane homeostasis in the virlunce of Gram-negative bacteria.* Doctor of Philosophy, University of Birmingham.

NIEBUHR, K., GIURIATO, S., PEDRON, T., PHILPOTT, D. J., GAITS, F., SABLE, J., SHEETZ, M. P., PARSOT, C., SANSONETTI, P. J. & PAYRASTRE, B. 2002. Conversion of PtdIns(4,5)P(2) into PtdIns(5)P by the *S.flexneri* effector IpgD reorganizes host cell morphology. *EMBO J,* 21**,** 5069-78.

NIVASKUMAR, M. & FRANCETIC, O. 2014. Type II secretion system: a magic beanstalk or a protein escalator. *Biochim Biophys Acta,* 1843**,** 1568-77.

NOINAJ, N., FAIRMAN, J. W. & BUCHANAN, S. K. 2011. The crystal structure of BamB suggests interactions with BamA and its role within the BAM complex. *J Mol Biol,* 407**,** 248-60.

NUMMELIN, H., MERCKEL, M. C., LEO, J. C., LANKINEN, H., SKURNIK, M. & GOLDMAN, A. 2004. The *Yersinia* adhesin YadA collagen-binding domain structure is a novel left-handed parallel beta-roll. *EMBO J,* 23**,** 701-11.

OLSEN, R. W. & BALLOU, C. E. 1971. Acyl phosphatidylglycerol. A new phospholipid from *Salmonella typhimurium*. *J Biol Chem,* 246**,** 3305-13.

PARHAM, N. J., SRINIVASAN, U., DESVAUX, M., FOXMAN, B., MARRS, C. F. & HENDERSON, I. R. 2004. PicU, a second serine protease autotransporter of uropathogenic *Escherichia col*i. *FEMS Microbiol Lett,* 230**,** 73-83.

PARKHILL, J., DOUGAN, G., JAMES, K. D., THOMSON, N. R., PICKARD, D., WAIN, J., CHURCHER, C., MUNGALL, K. L., BENTLEY, S. D., HOLDEN, M. T., SEBAIHIA, M., BAKER, S., BASHAM, D., BROOKS, K., CHILLINGWORTH, T., CONNERTON, P., CRONIN, A., DAVIS, P., DAVIES, R. M., DOWD, L., WHITE, N., FARRAR, J., FELTWELL, T., HAMLIN, N., HAQUE, A., HIEN, T. T., HOLROYD, S., JAGELS, K., KROGH, A., LARSEN, T. S., LEATHER, S., MOULE, S., O'GAORA, P., PARRY, C., QUAIL, M., RUTHERFORD, K., SIMMONDS, M., SKELTON, J., STEVENS, K., WHITEHEAD, S. & BARRELL, B. G. 2001. Complete genome sequence of a multiple drug resistant *Salmonella enterica* serovar Typhi CT18. *Nature,* 413**,** 848-52.

PEPE, J. C., WACHTEL, M. R., WAGAR, E. & MILLER, V. L. 1995. Pathogenesis of defined invasion mutants of *Yersinia enterocolitica* in a BALB/c mouse model of infection. *Infect Immun,* 63**,** 4837-48.

PERRETT, C. A. & ZHOU, D. 2013a. Erratum: *Salmonella* type III effector SopB modulates host cell exocytosis. *Emerg Microbes Infect,* 2**,** e39.

PERRETT, C. A. & ZHOU, D. 2013b. *Salmonella* type III effector SopB modulates host cell exocytosis. *Emerg Microbes Infect,* 2**,** e32.

PHILLIPS, G. B. 1957. The Isolation of Lysolecithin from Human Serum. *Proc Natl Acad Sci U S A,* 43**,** 566-70.

PHILLIPS, R. M., SIX, D. A., DENNIS, E. A. & GHOSH, P. 2003. *In vivo* phospholipase activity of the *Pseudomonas aeruginosa* cytotoxin ExoU and protection of mammalian cells with phospholipase A2 inhibitors. *J Biol Chem,* 278**,** 41326-32.

PLANT, J. & GLYNN, A. A. 1974. Natural resistance to *Salmonella* infection, delayed hypersensitivity and Ir genes in different strains of mice. *Nature,* 248**,** 345-7.

POHLNER, J., HALTER, R., BEYREUTHER, K. & MEYER, T. F. 1987. Gene structure and extracellular secretion of *Neisseria gonorrhoeae* IgA protease. *Nature,* 325**,** 458-62.

PORWOLLIK, S., SANTIVIAGO, C. A., CHENG, P., LONG, F., DESAI, P., FREDLUND, J., SRIKUMAR, S., SILVA, C. A., CHU, W., CHEN, X., CANALS, R., REYNOLDS, M. M., BOGOMOLNAYA, L., SHIELDS, C., CUI, P., GUO, J., ZHENG,

Y., ENDICOTT-YAZDANI, T., YANG, H. J., MAPLE, A., RAGOZA, Y., BLONDEL, C. J., VALENZUELA, C., ANDREWS-POLYMENIS, H. & MCCLELLAND, M. 2014. Defined single-gene and multi-gene deletion mutant collections in *Salmonella enterica* sv Typhimurium. *PLoS One,* 9**,** e99820.

PROUTY, A. M. & GUNN, J. S. 2000. *Salmonella enterica* serovar typhimurium invasion is repressed in the presence of bile. *Infect Immun,* 68**,** 6763-9.

PROUTY, A. M., SCHWESINGER, W. H. & GUNN, J. S. 2002. Biofilm formation and interaction with the surfaces of gallstones by *Salmonella* spp. *Infect Immun,* 70**,** 2640-9.

QUINN, M. T., PARTHASARATHY, S. & STEINBERG, D. 1988. Lysophosphatidylcholine: a chemotactic factor for human monocytes and its potential role in atherogenesis. *Proc Natl Acad Sci U S A,* 85**,** 2805-9.

QUINTELA, J. C., DE PEDRO, M. A., ZOLLNER, P., ALLMAIER, G. & GARCIA-DEL PORTILLO, F. 1997. Peptidoglycan structure of *Salmonella typhimurium* growing within cultured mammalian cells. *Mol Microbiol,* 23**,** 693-704.

RAGHUNATHAN, D., WELLS, T. J., MORRIS, F. C., SHAW, R. K., BOBAT, S., PETERS, S. E., PATERSON, G. K., JENSEN, K. T., LEYTON, D. L., BLAIR, J. M., BROWNING, D. F., PRAVIN, J., FLORES-LANGARICA, A., HITCHCOCK, J. R., MORAES, C. T., PIAZZA, R. M., MASKELL, D. J., WEBBER, M. A., MAY, R. C., MACLENNAN, C. A., PIDDOCK, L. J., CUNNINGHAM, A. F. & HENDERSON, I. R. 2011. SadA, a trimeric autotransporter from *Salmonella enterica* serovar Typhimurium, can promote biofilm formation and provides limited protection against infection. *Infect Immun,* 79**,** 4342-52.

RAVINDRAN, R., FOLEY, J., STOKLASEK, T., GLIMCHER, L. H. & MCSORLEY, S. J. 2005. Expression of T-bet by CD4 T cells is essential for resistance to *Salmonella* infection. *J Immunol,* 175**,** 4603-10.

REITHMEIER, R. A. & BRAGG, P. D. 1974. Purification and characterization of heat-modifiable protein from the outer membrane of *Escherichia coli*. *FEBS Lett,* 41**,** 195-8.

RESHETNYAK, V. I. 2013. Physiological and molecular biochemical mechanisms of bile formation. *World J Gastroenterol,* 19**,** 7341-60.

ROBERTS, M., CHATFIELD, S., PICKARD, D., LI, J. & BACON, A. 2000. Comparison of abilities of *Salmonella enterica* serovar typhimurium *aroA aroD* and *aroA htrA* mutants to act as live vectors. *Infect Immun,* 68**,** 6041-3.

ROGGENKAMP, A., RUCKDESCHEL, K., LEITRITZ, L., SCHMITT, R. & HEESEMANN, J. 1996. Deletion of amino acids 29 to 81 in adhesion protein YadA of *Yersinia enterocolitica* serotype O:8 results in selective abrogation of adherence to neutrophils. *Infect Immun,* 64**,** 2506-14.

ROSS, N. T. & MILLER, B. L. 2007. Characterization of the binding surface of the translocated intimin receptor, an essential protein for EPEC and EHEC cell adhesion. *Protein Sci,* 16**,** 2677-83.

ROSSITER, A. E., LEYTON, D. L., TVEEN-JENSEN, K., BROWNING, D. F., SEVASTSYANOVICH, Y., KNOWLES, T. J., NICHOLS, K. B., CUNNINGHAM, A. F., OVERDUIN, M., SCHEMBRI, M. A. & HENDERSON, I. R. 2011. The essential beta-barrel assembly machinery complex components BamD and BamA are required for autotransporter biogenesis. *J Bacteriol,* 193**,** 4250-3.

ROTH, M. G. & STERNWEIS, P. C. 1997. The role of lipid signaling in constitutive membrane traffic. *Curr Opin Cell Biol,* 9**,** 519-26.

ROWLETT, V. W., MALLAMPALLI, V., KARLSTAEDT, A., DOWHAN, W., TAEGTMEYER, H., MARGOLIN, W. & VITRAC, H. 2017. Impact of Membrane Phospholipid Alterations in *Escherichia coli* on Cellular Function and Bacterial Stress Adaptation. *J Bacteriol,* 199.

ROYLE, M. C., TOTEMEYER, S., ALLDRIDGE, L. C., MASKELL, D. J. & BRYANT, C. E. 2003. Stimulation of Toll-like receptor 4 by lipopolysaccharide during cellular invasion by live *Salmonella typhimurium* is a critical but not exclusive event leading to macrophage responses. *J Immunol,* 170**,** 5445-54.

RUIZ-ALBERT, J., YU, X. J., BEUZON, C. R., BLAKEY, A. N., GALYOV, E. E. & HOLDEN, D. W. 2002. Complementary activities of SseJ and SifA regulate dynamics of the *Salmonella typhimurium* vacuolar membrane. *Mol Microbiol,* 44**,** 645-61.

RUIZ-PEREZ, F., HENDERSON, I. R., LEYTON, D. L., ROSSITER, A. E., ZHANG, Y. & NATARO, J. P. 2009. Roles of periplasmic chaperone proteins in the biogenesis of serine protease autotransporters of Enterobacteriaceae. *J Bacteriol,* 191**,** 6571-83.

RUTHERFORD, N. & MOUREZ, M. 2006. Surface display of proteins by gram-negative bacterial autotransporters. *Microb Cell Fact,* 5**,** 22.

SABBAGH, S. C., FOREST, C. G., LEPAGE, C., LECLERC, J. M. & DAIGLE, F. 2010. So similar, yet so different: uncovering distinctive features in the genomes of *Salmonella enterica* serovars Typhimurium and Typhi. *FEMS Microbiol Lett,* 305**,** 1-13.

SACHELARU, I., WINTER, L., KNYAZEV, D. G., ZIMMERMANN, M., VOGT, A., KUTTNER, R., OLLINGER, N., SILIGAN, C., POHL, P. & KOCH, H. G. 2017. YidC and SecYEG form a heterotetrameric protein translocation channel. *Sci Rep,* 7**,** 101.

SADEYEN, J. R., TROTEREAU, J., VELGE, P., MARLY, J., BEAUMONT, C., BARROW, P. A., BUMSTEAD, N. & LALMANACH, A. C. 2004. *Salmonella* carrier state in chicken: comparison of expression of immune response genes between susceptible and resistant animals. *Microbes Infect,* 6**,** 1278-86.

SALACHA, R., KOVACIC, F., BROCHIER-ARMANET, C., WILHELM, S., TOMMASSEN, J., FILLOUX, A., VOULHOUX, R. & BLEVES, S. 2010. The *Pseudomonas aeruginosa* patatin-like protein PlpD is the archetype of a novel Type V secretion system. *Environ Microbiol,* 12**,** 1498-512.

SANTOS-BENEIT, F. 2015. The Pho regulon: a huge regulatory network in bacteria. *Front Microbiol,* 6**,** 402.

SANTOS, R. L., ZHANG, S., TSOLIS, R. M., KINGSLEY, R. A., ADAMS, L. G. & BAUMLER, A. J. 2001. Animal models of *Salmonella* infections: enteritis versus typhoid fever. *Microbes Infect,* 3**,** 1335-44.

SATO, H., FRANK, D. W., HILLARD, C. J., FEIX, J. B., PANKHANIYA, R. R., MORIYAMA, K., FINCK-BARBANCON, V., BUCHAKLIAN, A., LEI, M., LONG, R. M., WIENER-KRONISH, J. & SAWA, T. 2003. The mechanism of action of the *Pseudomonas aeruginosa*-encoded type III cytotoxin, ExoU. *EMBO J,* 22**,** 2959-69.

SCHINDLER, M. K., SCHUTZ, M. S., MUHLENKAMP, M. C., ROOIJAKKERS, S. H., HALLSTROM, T., ZIPFEL, P. F. & AUTENRIETH, I. B. 2012. *Yersinia enterocolitica* YadA mediates complement evasion by recruitment and inactivation of C3 products. *J Immunol,* 189**,** 4900-8.

SCHULTHEISS, E., WEISS, S., WINTERER, E., MAAS, R., HEINZLE, E. & JOSE, J. 2008. Esterase autodisplay: enzyme engineering and whole-cell activity determination in microplates with pH sensors. *Appl Environ Microbiol,* 74**,** 4782-91.

SELKRIG, J., MOSBAHI, K., WEBB, C. T., BELOUSOFF, M. J., PERRY, A. J., WELLS, T. J., MORRIS, F., LEYTON, D. L., TOTSIKA, M., PHAN, M. D., CELIK, N., KELLY, M., OATES, C., HARTLAND, E. L., ROBINS-BROWNE, R. M., RAMARATHINAM, S. H., PURCELL, A. W., SCHEMBRI, M. A., STRUGNELL, R. A., HENDERSON, I. R., WALKER, D. & LITHGOW, T. 2012. Discovery of an archetypal protein transport system in bacterial outer membranes. *Nat Struct Mol Biol,* 19**,** 506-10, S1.

SHANNON, P., MARKIEL, A., OZIER, O., BALIGA, N. S., WANG, J. T., RAMAGE, D., AMIN, N., SCHWIKOWSKI, B. & IDEKER, T. 2003. Cytoscape: a software environment for integrated models of biomolecular interaction networks. *Genome Res,* 13**,** 2498-504.

SHARMA, A. & QADRI, A. 2004. Vi polysaccharide of *Salmonella* typhi targets the prohibitin family of molecules in intestinal epithelial cells and suppresses early inflammatory responses. *Proc Natl Acad Sci U S A,* 101**,** 17492-7.

SHAW, R. K., DANIELL, S., FRANKEL, G. & KNUTTON, S. 2002. Enteropathogenic *Escherichia coli* translocate Tir and form an intimin-Tir intimate attachment to red blood cell membranes. *Microbiology,* 148**,** 1355-65.

SIGGINS, M. K., CUNNINGHAM, A. F., MARSHALL, J. L., CHAMBERLAIN, J. L., HENDERSON, I. R. & MACLENNAN, C. A. 2011. Absent bactericidal activity of mouse serum against invasive African nontyphoidal *Salmonella* results from impaired complement function but not a lack of antibody. *J Immunol,* 186**,** 2365-71.

SIMONSEN, A., LIPPE, R., CHRISTOFORIDIS, S., GAULLIER, J. M., BRECH, A., CALLAGHAN, J., TOH, B. H., MURPHY, C., ZERIAL, M. & STENMARK, H. 1998. EEA1 links PI(3)K function to Rab5 regulation of endosome fusion. *Nature,* 394**,** 494-8.

SINNOTT, C. R. & TEALL, A. J. 1987. Persistent gallbladder carriage of *Salmonella* typhi. *Lancet,* 1**,** 976.

SKLAR, J. G., WU, T., GRONENBERG, L. S., MALINVERNI, J. C., KAHNE, D. & SILHAVY, T. J. 2007a. Lipoprotein SmpA is a component of the YaeT complex that assembles outer membrane proteins in *Escherichia coli*. *Proc Natl Acad Sci U S A,* 104**,** 6400-5.

SKLAR, J. G., WU, T., KAHNE, D. & SILHAVY, T. J. 2007b. Defining the roles of the periplasmic chaperones SurA, Skp, and DegP in *Escherichia coli*. *Genes Dev,* 21**,** 2473-84.

SOHLENKAMP, C. & GEIGER, O. 2016. Bacterial membrane lipids: diversity in structures and pathways. *FEMS Microbiol Rev,* 40**,** 133-59.

SRIKUMAR, S., KROGER, C., HEBRARD, M., COLGAN, A., OWEN, S. V., SIVASANKARAN, S. K., CAMERON, A. D., HOKAMP, K. & HINTON, J. C. 2015. RNA-seq Brings New Insights to the Intra-Macrophage Transcriptome of *Salmonella* Typhimurium. *PLoS Pathog,* 11**,** e1005262.

STRUGNELL, R. A., SCOTT, T. A., WANG, N., YANG, C., PERES, N., BEDOUI, S. & KUPZ, A. 2014. *Salmonella* vaccines: lessons from the mouse model or bad teaching? *Curr Opin Microbiol,* 17**,** 99-105.

STUBENRAUCH, C., BELOUSOFF, M. J., HAY, I. D., SHEN, H. H., LILLINGTON, J., TUCK, K. L., PETERS, K. M., PHAN, M. D., LO, A. W., SCHEMBRI, M. A., STRUGNELL, R. A., WAKSMAN, G. & LITHGOW, T. 2016. Effective assembly of fimbriae in *Escherichia coli* depends on the translocation assembly module nanomachine. *Nat Microbiol,* 1**,** 16064.

SUNDIN, G. W., CASTIBLANCO, L. F., YUAN, X., ZENG, Q. & YANG, C. H. 2016. Bacterial disease management: challenges, experience, innovation and future prospects: Challenges in Bacterial Molecular Plant Pathology. *Mol Plant Pathol,* 17**,** 1506-1518.

THANABALU, T., KORONAKIS, E., HUGHES, C. & KORONAKIS, V. 1998. Substrate-induced assembly of a contiguous channel for protein export from *E.coli*: reversible bridging of an inner-membrane translocase to an outer membrane exit pore. *EMBO J,* 17**,** 6487-96.

THOMPSON, J. D., GIBSON, T. J., PLEWNIAK, F., JEANMOUGIN, F. & HIGGINS, D. G. 1997. The CLUSTAL_X windows interface: flexible strategies for multiple sequence alignment aided by quality analysis tools. *Nucleic Acids Res,* 25**,** 4876-82.

TIMME, R. E., PETTENGILL, J. B., ALLARD, M. W., STRAIN, E., BARRANGOU, R., WEHNES, C., VAN KESSEL, J. S., KARNS, J. S., MUSSER, S. M. & BROWN, E. W. 2013. Phylogenetic diversity of the enteric pathogen *Salmonella enterica* subsp. enterica inferred from genome-wide reference-free SNP characters. *Genome Biol Evol,* 5**,** 2109-23.

TOMMASSEN, J., EIGLMEIER, K., COLE, S. T., OVERDUIN, P., LARSON, T. J. & BOOS, W. 1991. Characterization of two genes, *glpQ* and *ugpQ*, encoding glycerophosphoryl diester phosphodiesterases of *Escherichia coli*. *Mol Gen Genet,* 226**,** 321-7.

TOTSIKA, M., WELLS, T. J., BELOIN, C., VALLE, J., ALLSOPP, L. P., KING, N. P., GHIGO, J. M. & SCHEMBRI, M. A. 2012. Molecular characterization of the EhaG and UpaG trimeric autotransporter proteins from pathogenic *Escherichia coli*. *Appl Environ Microbiol,* 78**,** 2179-89.

TSOLIS, R. M., XAVIER, M. N., SANTOS, R. L. & BAUMLER, A. J. 2011. How to become a top model: impact of animal experimentation on human *Salmonella* disease research. *Infect Immun,* 79**,** 1806-14.

UPTON, C. & BUCKLEY, J. T. 1995. A new family of lipolytic enzymes? *Trends Biochem Sci,* 20**,** 178-9.

VAN BERGE HENEGOUWEN, G. P., VAN DER WERF, S. D. & RUBEN, A. T. 1987. Fatty acid composition of phospholipids in bile in man: promoting effect of deoxycholate on arachidonate. *Clin Chim Acta,* 165**,** 27-37.

VAN DEN BERG, B. 2010. Crystal structure of a full-length autotransporter. *J Mol Biol,* 396**,** 627-33.

VAN DER MEER-JANSSEN, Y. P., VAN GALEN, J., BATENBURG, J. J. & HELMS, J. B. 2010. Lipids in host-pathogen interactions: pathogens exploit the complexity of the host cell lipidome. *Prog Lipid Res,* 49**,** 1-26.

VAN MEER, G., VOELKER, D. R. & FEIGENSON, G. W. 2008. Membrane lipids: where they are and how they behave. *Nat Rev Mol Cell Biol,* 9**,** 112-24.

VAZQUEZ-TORRES, A., JONES-CARSON, J., BAUMLER, A. J., FALKOW, S., VALDIVIA, R., BROWN, W., LE, M., BERGGREN, R., PARKS, W. T. & FANG, F. C. 1999. Extraintestinal dissemination of *Salmonella* by CD18-expressing phagocytes. *Nature,* 401**,** 804-8.

VERGNE, I., CHUA, J., LEE, H. H., LUCAS, M., BELISLE, J. & DERETIC, V. 2005. Mechanism of phagolysosome biogenesis block by viable *Mycobacterium tuberculosis*. *Proc Natl Acad Sci U S A,* 102**,** 4033-8.

VOLOKHINA, E. B., BECKERS, F., TOMMASSEN, J. & BOS, M. P. 2009. The beta-barrel outer membrane protein assembly complex of *Neisseria meningitidis*. *J Bacteriol,* 191**,** 7074-85.

VOLOKITA, M., ROSILIO-BRAMI, T., RIVKIN, N. & ZIK, M. 2011. Combining comparative sequence and genomic data to ascertain phylogenetic relationships and explore the evolution of the large GDSL-lipase family in land plants. *Mol Biol Evol,* 28**,** 551-65.

VONAESCH, P., SELLIN, M. E., CARDINI, S., SINGH, V., BARTHEL, M. & HARDT, W. D. 2014. The *Salmonella* Typhimurium effector protein SopE transiently localizes to the early SCV and contributes to intracellular replication. *Cell Microbiol,* 16**,** 1723-35.

VOULHOUX, R., BOS, M. P., GEURTSEN, J., MOLS, M. & TOMMASSEN, J. 2003. Role of a highly conserved bacterial protein in outer membrane protein assembly. *Science,* 299**,** 262-5.

WATSON, K. G. & HOLDEN, D. W. 2010. Dynamics of growth and dissemination of *Salmonella in vivo*. *Cell Microbiol,* 12**,** 1389-97.

WEISS, D. S., RAUPACH, B., TAKEDA, K., AKIRA, S. & ZYCHLINSKY, A. 2004. Toll-like receptors are temporally involved in host defense. *J Immunol,* 172**,** 4463-9.

WELLS, T. J., TOTSIKA, M. & SCHEMBRI, M. A. 2010. Autotransporters of *Escherichia coli*: a sequence-based characterization. *Microbiology,* 156**,** 2459-69.

WELLS, T. J., TREE, J. J., ULETT, G. C. & SCHEMBRI, M. A. 2007. Autotransporter proteins: novel targets at the bacterial cell surface. *FEMS Microbiol Lett,* 274**,** 163-72.

WERNER, J. & MISRA, R. 2005. YaeT (Omp85) affects the assembly of lipid-dependent and lipid-independent outer membrane proteins of *Escherichia coli*. *Mol Microbiol,* 57**,** 1450-9.

WILHELM, S., ROSENAU, F., KOLMAR, H. & JAEGER, K. E. 2011. Autotransporters with GDSL passenger domains: molecular physiology and biotechnological applications. *Chembiochem,* 12**,** 1476-85.

WILHELM, S., TOMMASSEN, J. & JAEGER, K. E. 1999. A novel lipolytic enzyme located in the outer membrane of *Pseudomonas aeruginosa*. *J Bacteriol,* 181**,** 6977-86.

WONG, K. K. & KWAN, H. S. 1992. Transcription of *glpT* of *Escherichia coli* K12 is regulated by anaerobiosis and fnr. *FEMS Microbiol Lett,* 73**,** 15-8.

WORLEY, J., MENG, J., ALLARD, M. W., BROWN, E. W. & TIMME, R. E. 2018. *Salmonella enterica* Phylogeny Based on Whole-Genome Sequencing Reveals Two New Clades and Novel Patterns of Horizontally Acquired Genetic Elements. *MBio,* 9.

WRAY, C. & SOJKA, W. J. 1978. Experimental *Salmonella typhimurium* infection in calves. *Res Vet Sci,* 25**,** 139-43.

WU, T., MALINVERNI, J., RUIZ, N., KIM, S., SILHAVY, T. J. & KAHNE, D. 2005. Identification of a multicomponent complex required for outer membrane biogenesis in *Escherichia coli*. *Cell,* 121**,** 235-45.

YAMAJI-HASEGAWA, A. & TSUJIMOTO, M. 2006. Asymmetric distribution of phospholipids in biomembranes. *Biol Pharm Bull,* 29**,** 1547-53.

ZHANG, H., GAO, Z. Q., HOU, H. F., XU, J. H., LI, L. F., SU, X. D. & DONG, Y. H. 2011. High-resolution structure of a new crystal form of BamA POTRA4-5 from *Escherichia coli*. *Acta Crystallogr Sect F Struct Biol Cryst Commun,* 67**,** 734-8.

ZHANG, S., KINGSLEY, R. A., SANTOS, R. L., ANDREWS-POLYMENIS, H., RAFFATELLU, M., FIGUEIREDO, J., NUNES, J., TSOLIS, R. M., ADAMS, L. G. & BAUMLER, A. J. 2003. Molecular pathogenesis of *Salmonella enterica* serotype typhimurium-induced diarrhea. *Infect Immun,* 71**,** 1-12.

ZOGAJ, X., NIMTZ, M., ROHDE, M., BOKRANZ, W. & ROMLING, U. 2001. The multicellular morphotypes of *Salmonella* typhimurium and *Escherichia coli* produce

cellulose as the second component of the extracellular matrix. *Mol Microbiol,* 39**,** 1452-63.

ZOUED, A., BRUNET, Y. R., DURAND, E., ASCHTGEN, M. S., LOGGER, L., DOUZI, B., JOURNET, L., CAMBILLAU, C. & CASCALES, E. 2014. Architecture and assembly of the Type VI secretion system. *Biochim Biophys Acta,* 1843**,** 1664-73.